**ISTC Project No. A1058**

# Development of a Prototype Detector System for Space Weather Monitoring and Forecasting World-Wide Network.

## Final Project Technical Report

**on the work performed from**
**1 April 2004 – to 31 August 2007**

Yerevan Physics Institute
Alikhanyan Brothers st. 2, Yerevan 36, Armenia

**Project Manager** **Ashot Chilingarian**
Doctor of science

**Director** **Hrachia Asatryan**
Doctor of science

| | |
|---|---|
| Title of the Project: | Development of a Prototype Detector System for Space Weather Monitoring and Forecasting World-Wide Network. |
| Commencement Date: | 1 April 2004 |
| Duration: | 41 months |
| Project Manager | Ashot Chilingarian |
| phone number: | 37410344736 |
| fax number: | 37410344736 |
| e-mail address: | chilli@crdlx5.yerphi.am |
| Leading Institute: | Yerevan Physics Institute<br>Slikhanyan Brother st. 2, Yerevan 36, Armenia<br>37410350015<br>hrachia@yerphi.am<br>http://yerphi.am |
| Foreign Collaborators: | Hartmut Gemmeke<br>Forschungszentrum Karlsruhe, Institute for Data Processing and Electronics, Hermann-von-Helmholtz Platz 1, Eggstein-Leopoldshafen, GE<br>+7247 82 5594<br>gemmeke@ipe.fzk.de<br><br>Vahe Petrossian<br>Stanford University, Varian room 302c, Stanford, 94305-4060, CA, USA<br>+1-415-723-136<br>vahe@astronomy.stanford.edu<br><br>Joseph Kunches<br>Space Environmental Center, NOAA, USA<br>325 Broadway, Boulder, CO, USA<br>+1-303-497-5275<br>Joseph.Kunches@noaa.gov |

Keywords: Cosmic Rays, Space Weather, Solar physics, Particle detectors

# Table of Contents

# 1. Brief description of the work plan: objective, expected results, technical approach

Unpredictable bursts of *Solar Energetic Particles (SEP),* peaking in 11 year cycles are one of the major constraints on the operation of space systems and further technological utilization of near-Earth space (Tylka, 2001). The US National Security Space Architect finds that during the preceding 20 years about one or two satellites per year have suffered either total or partial mission loss due to dangerous space conditions (Space Studies Board, 1999). Since our lives depend so heavily on the satellite based technologies, not to mention the value of protecting humans in space and in aircraft, it is becoming increasingly important to have an accurate and reliable forewarning about the situation in near-Earth space, so that mitigating action can be taken if necessary. The new scientific discipline aimed to investigate and forewarn dangerous space conditions get name "Space Weather":

*Space weather is the physical and phenomenological state of natural space environments. The associated discipline aims, through observation, monitoring, analysis and modeling, at understanding and predicting the state of the sun, the interplanetary and planetary environments, and the solar and non-solar driven perturbations that affect them; and also at forecasting and now-casting the possible impacts on biological and technological systems (COST724 SW definition, 2007).*

Presently Space Weather forecast capability is rather limited due to both lacks in understanding the fundamental physics and in the measurements of the important parameters of solar wind. Timely warning operators of satellites and surface technological system on upcoming sever radiation storm and Geomagnetic storm (GMS) are key ingredients of the scientific and technological progress in 21$^{st}$ century, expected to come mostly from the Space.

Numerous important measurements of the physical parameters connected with violent solar activity, like soft X-ray, hard X-ray, and gamma radiation; fluxes of the low and middle energy protons (KeV-100MeV), ions and electrons; solar wind velocity, density and speed of solar wind, maps of magnetograms and radio-bursts, strength and direction of the "frozen" magnetic fields; solar images taken by coronagraphs are posted on the Internet in real-time and other.

The networks of particle detectors measuring fluxes of secondary particles corresponding to the primaries with energies above 1 GeV also started to post data in real-time. Multidimensional multidetector information from space-borne and ground-based detectors provide good basis for creation of the interplanetary Space Weather services.

The main objective of the project was to *develop, fabricate and test new type of particle detectors providing enlarged possibilities in simultaneous detection of many components of the secondary cosmic* rays and prepare a design of new world-wide network of particle detectors for research in solar physics and for Space Weather forecasting.

To achieve this main goal if framework of project following tasks were performed:

- Development of concept of the hybrid particle detectors measuring both charged and neutron particle fluxes simultaneously; Development of the concept SEVAN worldwide particle detector network.
- Uninterruptable operation of particle detectors of Aragats Space Environmental Center (ASEC) during fall of the 23$^{rd}$ cycle of solar activity. Measurement of most severe solar events by the neutron monitors and new launched hybrid particle detectors;
- Development of the advanced data processing and multiple data visualization software. Establishing of the Internet portal with MSQL data bases equipped with fast access modes.
- Installation of the new servers and networking equipment allowing wireless connections with high altitude research stations;

- Simulations of the particle transport in the magnetosphere and in the atmosphere, as well as calculation of detector response to different species of cosmic rays;
- Development of the CPLD and FPGA based Data Acquisition (DAQ) electronics. Designing and producing of printed circuit boards, high voltage power supplies and analog-to-digital converters;
- Correlation analysis of ASEC monitors data with space detectors registering low-middle energy particle, X-ray and gamma ray flux from the sun. Calculations of the significance of simultaneous peak detection, estimation of the false alarm rate and alert efficiency.
- Fabrication of the working prototype of the SEVAN basic detector. Preparations of charts of mechanical parts and electronics. Calculations of the detector response, various tests of detector. Testing of the new detector design with scintillators equipped by fiber-glass light-shifters.
- Negotiations with possible partners and collaborators. Preparing documentations and rules for scientific and business partnership. Signing Memorandums of understanding (MOU). Preparing certificates and all legal documents for exporting of equipment and materials from Armenia.

Project was fulfilled using facilities of the Aragats Space Environmental Center (ASEC, Chilingarian et al., 2003) consisting of two high altitude stations on Mt. Aragats in Armenia (Geographic coordinates: 40°30'N, 44°10'E. Vertical cutoff rigidity: ~7.1 GV, altitude 3200 and 2000 m.).

We take as prototype 2 particle detectors operating at ASEC: the Solar Neutron Telescope at the Aragats station (ASNT, see details in Matsubara et.al., 1999, Tsuchiya et.al., 2001) and Nor-Amberd Muon Multidirectional Monitor (NAMMM, see detailes in Chilingarian et al., 2005). The ASNT consists of four 1 $m^2$, 60 cm thick scintillation blocks with anti-coincidence shielding above to veto the near vertical charged flux. Incoming neutrons are converted to protons in nuclear interactions inside the thick scintillator target. The energy deposited due to ionization by recoil protons is measured by photomultipliers over the scintillators. ASNT can measure both charged and neutral fluxes. We perform detailed investigation of detector response and reveal many interesting features of detector (Chilingarian et.al., 2007b).

Another candidate for basic detector, the Nor-Amberd Muon Multidirectional Monitor (NAMMM) consists of two layers of 6 plastic scintillators with 0.81 $m^2$ area each, placed above and below one of the three sections of the Nor Amberd Neutron Monotor (NANM, Morall et al., 2000). The lead (Pb) filter of the NANM absorbs the electrons and low energy muons. The threshold energy of the detected muons is estimated to be 250 MeV. New data acquisition system of the NAMMM can register all coincidences of detector signals from the upper and lower layers, thus, enabling measurement of the arrival of the muons from different directions. Therefore, it is possible to register 3 species of the cosmic rays: high energy muons; neutrons; and charged component of cosmic rays.

After analysis of data from both detectors we come to concept of compact particle detector of new generation and to concept of new worldwide network SEVAN (Space Environmental Viewing and Analysis Network). Several prototype detectors were fabricated and tested. Simulations of detector response were performed with program packages CORSIKA, JEANT3, JEANT4 and ANI. Several methods of multivariate data analysis were developed and applied to extreme solar events of 23$^{rd}$ solar activity cycle.

## 2. Particle detectors in Solar physics research and Space Weather forecasting

The sun influences earth in different ways by emissions of electromagnetic radiation, plasma and high energy particles and ions. Although the entire energy of the high energy particles comprises very small fraction of the visible light energy, nonetheless the study of these particles gives clues about fundamental and universal processes of particle acceleration, and provides timely information about the consequences of the huge solar explosions affecting the near-earth environment, space born and surface technologies, i.e. so called Space Weather issues (Lilensten & Bornarel, 2006).

During billions of years of its evolution, the earth was bombarded by the protons and fully stripped ions accelerated in the Galaxy during tremendous explosions of the supernovae and by other exotic stellar sources. This flux was changed during the passage of the sun through the four galactic arms during its path around the center of Galaxy and, may be, was affected several times by huge explosions of nearby stars. Nonetheless, on the shorter time scales the GeV galactic cosmic ray flux is rather stable. In turn, our nearest star – the sun is a tremendously variable object, capable of changing radiation and particle flux intensities by 3-4 orders of magnitude in the span of a few minutes. Because of the sun's closeness, the effects of the changing fluxes have major influence on earth, including climate, safety and other issues (see for example, Carslaw et al, 2002, Daglis, 2003).

The influence of sun on the near earth particle population can be described as modulation of the stable galactic cosmic ray "background" by the sun activity. The sun "modulates" the low energy Galactic Cosmic Rays (GCR) in several ways. The most energetic flaring process in the solar system releases up to $10^{33}$ erg of energy during few minutes. Along with broad-band electromagnetic radiation, the explosive flaring process usually results in ejection of huge amounts of solar plasma and in acceleration of the copious electrons and ions (Solar Energetic Particle events – SEP). Particles can be generated either directly in the coronal flare site with subsequent escape into interplanetary space, or they can be accelerated in CME associated shocks that propagate through corona and interplanetary space (Aschwanden, 2005). These particles, along with neutrons, produced by the accelerated protons and ions in collisions with dense solar plasma, constitute the so called, Solar Cosmic Rays (SCR). If energetic enough to traverse magnetosphere, reaching the Earth atmosphere they initiate cascades of secondary elementary particles. Highest energy particles (above ~1 GeV/nucleon) generate showers capable of reaching the Earth surface and being detected by the surface particle detectors, causing the so called Ground Level Enhancement (GLE). Low energy SCR (up to ~1 GeV/nucleon) are effectively registered by the particle spectrometers on board of space stations (SOHO, ACE) and satellites (GOES, CORONAS).

Only few of the SEP events (usually not more than a dozen during solar activity cycle of ~11 years) can be detected by surface particle detectors. The latitudinal dependence of the geomagnetic field provides the possibility to use the dispersed world-wide network of the Neutron Monitors (NM, Morall et al, 2000) as a spectrometer registering GCR in the rigidity range from 0.5 to ~ 10 GV. This shows huge importance of high energy data obtained by surface detectors because GLEs represent particle acceleration at extreme Solar conditions and are providing tests of particle acceleration in their upper limits.

The spectra of GCR can be approximated by the power law - $dJ_p/dE$ (GCR) ~ $E^{\gamma}$ , $\gamma \sim -2.7$ till ~$3 \cdot 10^{15}$ eV, and $\gamma \sim -3$ for higher energies. SCR flux (mostly protons) at GeV energies usually is very weak ($\gamma > -6$), only at some events, such as at 23 February 1956, 20 January 2005, the spectra of SCR is considerably "hard": $\gamma \sim -4$ - -5 at GeV energies).

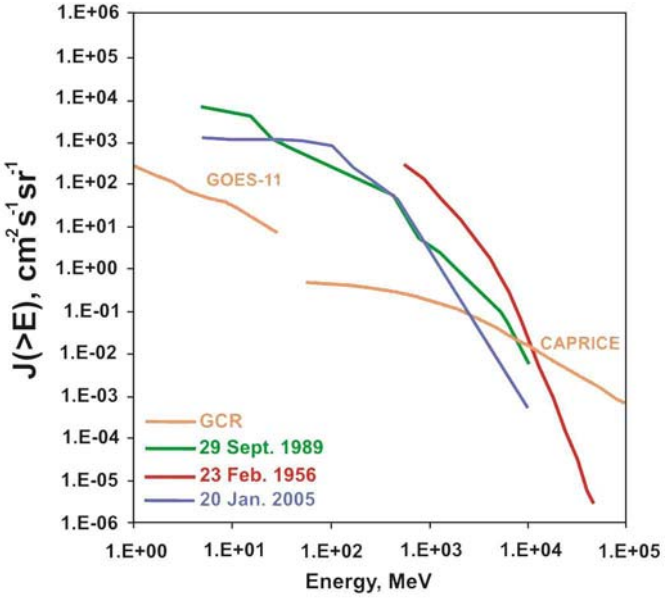


**Figure 1 Galactic and Solar Cosmic Rays**

Surface particle detectors measure the number of the secondary particles incident on the detector surface in a fixed time span. These measurements (usually not more detailed as one minute time series) are the basis for the physical inference on the solar modulation effects. There is absolutely no possibility to distinguish SCR and GCR on event-by-event basis. The solar modulation effects are detected as non-random changes in the time series. And, if at high latitudes, where secondary particles are produced by abundant low energy SCR, modulation effects can reach 1000% and more, at low latitudes the enhancements due to SCR is very small, usually not more than 1-2%. If we take into account that for energies greater than 10 GeV the intensity of the GCR becomes increasingly higher than the intensity of the largest known SEP events (see Figure 1), we confront a very complicated problem of detecting a small signal of the SCR against the huge "background" of the GCR. Low statistics experiments often demonstrate fake peaks with high significances. Some remedies to avoid erroneous inference on existence of signal are discussed in (Chilingarian et al., 2006).

Existing networks of particle detectors are unable to reliably research SCR of highest energies (>10 GeV); therefore we still cannot determine the maximal energy $E_{max}$ of solar accelerators. The common adopted opinions put $E_{max}$ at ~ 20 GeV, although several underground muon detectors report incident solar ion energies above 100 GeV (see review in Miroshnichenko, 2001).

The direct measurement of highest energy cosmic rays by space-born spectrometers or balloons is not feasible yet due to payload and time-of-flight limitations. Therefore, recently some large surface arrays intended to register GCR with energies higher that $10^5$ - $10^6$ GeV (in the region of the so called all particle energy spectra "knee" region) are used for detecting SCR (Chilingarian et al., 2003, Karpov et al., 2005, Poirier & D'Andrea, 2002). The experimental technique used for these arrays i.e. registration of the Extensive Air Showers (EAS) is very similar to the techniques used for detection of SCR. The difference is that PeV particles generate millions and millions of secondary particles in the atmosphere, large portion of which reach the earth's surface (in contrast, only a few particles generated by SCR can reach the earth's surface). To detect and measure the energy (and type) of PeV particles, hundred square meters of particle detectors are used. Usually there are plastic scintillators overviewed by photomultipliers.

Arrays are triggered by checking special conditions (array trigger – usually consisting in registering more than fixed number of particles in several particle detectors, see for example Cilingarian et al, 2007), provided by fast Data Acquisition (DAQ) electronics and rejecting low energy primary particles. However, by established methods of alternative DAQ, it is possible to simultaneously register time series of the secondary particles incident on each of EAS detectors. In

this way, due to large sizes of EAS detectors, the signal-to-noise ratio for detecting low fluxes of SCR is significantly enlarged and the unexplored energy region of >10 GeV becomes attainable for research. For example, in (Wang & Wang, 2006) the use of the L3 detector at the CERN electron-positron collider , LEP, was proposed for the measurement of SCR with energies up to 40 GeV (Adriani et al., 2002).

However, in addition to relevant experimental techniques we need also the particle "beams" from the sun, hard enough to provide sufficient intensities in the GeV region. The Solar Extreme Events (SEE), which occurred in October 2003, and especially in January 2005, provided such "beams" and, fortunately, the secondary neutrons and muons were detected by several EAS arrays. Obtained experimental information from large particle detector arrays proves possibility of measuring SCR spectra up to 20-30 GeV (Karpov et al, 2005, Dziomba, 2005, Bostanjyan et al., 2006, Chilingarian et al., 2007).

Other solar modulation effects also influence the intensity of the cosmic rays in the vicinity of Earth. The strong solar wind during especially in years of active sun "blows out" lowest energy GCR from the solar system, thus changing the GCR intensity and spectrum in heliosphere.

## 1. Introduction

Huge magnetized plasma clouds and shocks initiated by Coronal Mass Ejections (CME) travel in the interplanetary space with velocities up to 2000 Km/sec (so called Interplanetary Coronal Mass Ejection (ICME), are known as major drivers of severe space weather effects. On its way to Earth ICME disturb the Interplanetary Electrical and Magnetic Field (IMF). These disturbances "modulate" flux of Galactic Cosmic Ray (GCR) introducing anisotropy and changing energy (rigidity) spectra (Dvornikov et al., 1988) of protons and nuclei. Changes of rather stable flux of GCR are detected by space-born spectrometers (rigidities up to ~1GV) and by world-wide networks of particle detectors (rigidities up to ~100GV) located at different latitudes, longitudes and altitudes. Therefore, abrupt changes of CR fluxes (so called precursors) can be used for forewarning on upcoming ICME and, consequently on expected Geomagnetic Storm (GMS).
Most geoeffective types of ICMEs, so called magnetic clouds (cylindrical flux rope structures with helical magnetic field lines, see for details Mulligan and Russell, 2001) are directly connected to the flaring region of Sun where Solar Cosmic Rays (SCR) are accelerated. This can explain the "collisionless" transport of Solar Cosmic Rays (SCR) via "highways" inside the magnetic system connected Sun with ICME (see for details Valtonen, 2006 and references herein). The cascade particles generated by these SCR with GV rigidities can be registered by surface detectors comprising, so called, Ground Level Enhancement (GLE) and alerting on upcoming abundant SCR flux dangerous for satellite electronics and surface industries.
Thus, ICME is major modulating agent, forming depletion and enhancement regions of GCR, manifested themselves as peaks and deeps in time series of surface particle detectors. Both GCR and SCR can be used for "probing" ICME, providing highly cost-effective information on the key characteristics of the interplanetary disturbances (ICMEs). Because cosmic rays are fast and have large scattering mean free paths in the solar wind, this information travels rapidly and may prove useful for space weather forecasting (Leerungnavarat et al., 2003).
Size and strength of the "frozen" magnetic field in an ICME are correlated with the modulation effects ICME poses on the ambient population of the galactic cosmic rays during its propagation up to 1 AU. In the same time the presence of strong and long duration southward magnetic field is the primary requirement of ICME geoeffectiveness (Valtonen, 2006). Thus, strong southward magnet field ($B_z$) "frozen" in ICME is both modulation agent of GCR and driver of GMS.

The strong southward magnetic field found in the magnetic cloud of ICME has a well-formed flux-rope structure (see Koskinen and Huttunen, 2006, also see cross-section of the magnetic "rope" (a twisted bundle of magnetic fields) connecting Earth's upper atmosphere directly to the Sun, observed by the THEMIS satellites on May 20, 2007, NASA science, 20.03.08). At 20 November

2003 magnetic cloud was directly connected with solar eruptive region and southward magnetic field was enhanced by an order of magnitude (~ -50 nT).

Sure, there is no uniquely dependence between variations of the GCR and strength of GMS and furthermore besides IMCEs, there exist other drivers of storms and modulation agents of GCR. However, large $B_z$ value associated with approaching ICME is best known diagnostics of GMS strength. Therefore, as was mentioned in the statistical study (Kudela & Storini, 2006) appropriate parameters of the primary and secondary cosmic rays can be a proxy of $B_z$ value long before IMCE reach libration point at 1.5 mln. km from Earth where $B_z$ can be directly measured.
Direct detection of the Energetic Storm Particles (ESP) by the Electron, Proton, and Alpha Monitor (EPAM) instrument on board the Advanced Composition Explorer (ACE) space station (Gold, 1998) can alerts hours prior to the approaching interplanetary shock and plasma cloud (ACE news, 2003). Another space station located in libration point 1.5 mln kilometers from Earth - Solar and Heliospheric Observatory (SOHO) - detected relativistic electrons by its Comprehensive Suprathermal and Energetic Particle Analyzer (COSTEP) instrument. Enhancements in the electron flux also can point on approaching ICME. The modulation effects posed by ICME on the particles of higher energies, not assessable to space-born facilities due to very weak fluxes, are detected by the world-wide networks of Neutron Monitors (NM, responding to GCR energies ≥ 10 GeV) and Muon Telescopes (MT, responding to GCR energies ≥ 50 GeV) well before the onset of a major geomagnetic storm (Belov et al., 2003, Munakata et al., 2000).
To conclude, magnetic clouds dominate intense storm occurrences and simultaneously they are correlated with variations of spectra of particles and nuclei in the interplanetary space, ranging from subtermal solar wind ions till GeV energy galactic cosmic rays. How this abundant information can be used for forewarning of upcoming geoeffective ICME we'll demonstrate on the example of strongest geomagnetic storm of 20 November 2003.

Upon arrival at the magnetosphere, the overall depletion of the GCR triggered by the interplanetary shock and plasma cloud, manifest itself as a decrease in the secondary cosmic rays detected by the networks of particle detectors on the Earth's surface. The relative decrease of the count rate at the particle monitors is well pronounced at high latitudes. Due to low magnetic cutoff rigidity at high latitudes the primary protons and ions, responsible for the greater part of count rate, have considerably low energy (~1 GeV) and are strongly depleted by the disturbances of the IMF. The count rates of the particle monitors at middle to low latitudes are formed by the primaries with energies much higher >5 GeV. Therefore, the relative depletion of higher energies, and consequently depletion of the count rates of low latitude monitors will be less compared to high latitude particle monitors.

Visa-verse geomagnetic storms, appearing as sudden change of the Earth's magnetic field can magnify the relative change of the count rates of middle and low latitude particle detectors, without any corresponding notable alteration in the count rates of the high latitude detectors. If the magnetic field of ICME is directed southwards, it reduces the cutoff rigidity. Therefore, GCRs of lower energies, usually effectively declined by the magnetosphere, penetrate the atmosphere and generate additional secondary particles, thus enlarging the count rate of the monitors located at middle and low latitudes. At high latitudes, cutoff rigidity is very low and the count rates of particle detectors are determined mostly by the attenuation of the cascades in the atmosphere and the decrease of the cutoff rigidity does not significantly magnify the number of secondary particles reaching the detectors at high latitudes. Because, as we already mention, the same southward magnetic field is main trigger of geomagnetic storms, the enhancement of count rates of particle detectors located at middle latitudes perfectly correlates with growing strength of the geomagnetic storm.

Figure 2 compare the famous 2003 Halloween events detected by Oulu NM (the vertical cutoff rigidity ~0.8 GV, bold black curves) and Aragats NM (vertical cutoff rigidity ~7.1 GV, gray curves). The picture shows that the amplitude of Ground Level Enhancement (GLE) is much bigger at high latitudes (~ 6% at Ouly and ~2% on Aragats); Forbush decrease (FD) is also "deeper" at

high latitudes; however the Geomagnetic storm (GMS) is much more pronounced at middle latitudes. The precursors of GSM also start much earlier at middle latitudes.

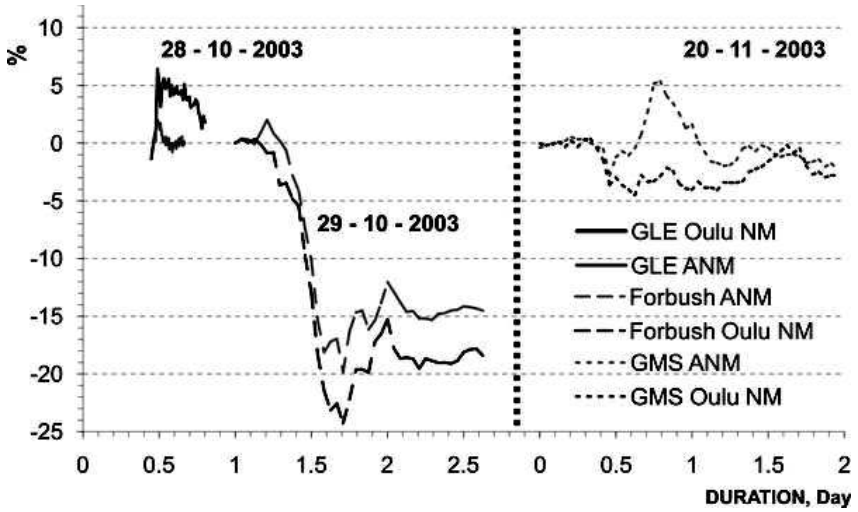


**Figure 2. 2003 Halloween events detected by particle detectors located at high latitude (Oulu NM, vertical cutoff rigidity ~0.8 GV, bold black curves) and middle latitude (Aragats NM (vertical cutoff rigidity ~7.1 GV, gray curves)**

Because the flux of high-energy ions is weak, and because the most violent particle events are usually highly anisotropic, a network of large area particle detectors, located at low latitudes and high mountain altitudes, is necessary for the reliable detection of these particles. The information about primary ion type and energy is mostly smeared during particles successive interactions with the atmospheric nuclei. Thus, only coherent measurement of all secondary fluxes (neutrons, muons, and electrons), along with their correlations, can help to make unambiguous forecasts and estimates of the energy spectra of the dangerous flux that follows. Hybrid particle detectors of Aragats Space Environmental Center (Chilingarian et al., 2005) measuring both charged and neutral components of secondary cosmic rays provide good coverage of Solar Extremely Events (SEE) of the 23rd solar cycle. First results of the physical analysis of these events are presented in this report.

The structure of this chapter of the report is as following:

In the second section we give brief description of the particle detectors measuring neutral and charged fluxes of secondary cosmic rays.

In the third section the spectra of the primary protons responsible for the detected fluxes by ASEC monitors are derived from simulations of─nucleic-electromagnetic cascades in the atmosphere followed by the detector response function calculation.

The forth section presents the largest GLE of the satellite era, which occurred on 20 January 2005, along with a new technique to derive the spectral index of the SCR at highest energies;

Section 5 is devoted to introducing to techniques of alerting of severe radiation storms;

Section 6 – to discuss techniques of forecasting of severe geomagnetic storms;

Section 7 demonstrates drawbacks of spaceborn facilities in detecting and alerting on most severe storms and in Section 8 we discuss place of surface particle detectors in planetary system of Space Weather forecasting.

### 2.1 Networks of particle detectors

Solar modulation effects in general are not global, i.e. their influences do not uniformly and isotropically affect the Earth as a whole. Therefore, a network of particle detectors is necessary for providing coverage of the whole earth, as much as possible - as many latitudes and longitudes as possible. The best coverage up until now has been provided by the network of neutron monitor

instruments located at ~50 locations, some of which are taking data for ~50 years (Shea, Smart 2000).

Charged particles travel and reach the Earth by way of the "best magnetic connection paths", which is not a straight line between their birthplace and the earth. The solar neutrons on the other hand, not influenced by solar and interplanetary magnetic fields, reach earth directly from their place of birth on the solar disc. The special network aimed at detecting very rare neutron events from the Sun includes seven particle detectors on high mountains around the world (Tsuchiya et al., 2001).

The muon detector network (Munakata et al., 2000) (Japan, USA, Brazil, Australia) recently was enlarged by adding new facilities located in Kuwait. Each of the mentioned world-wide networks of particle detectors are intended to measure only one type of secondary particles generated by the primary GCR or SCR. To overcome several limitations on the physical inference, specially for the primaries of highest energies, additional networks are needed to complement these two.

The large variety of solar modulation effects and the stringent limitations of space and surface based facilities require new ideas for developing experimental techniques for measuring the changing fluxes of all the secondary particles. New type of particle detectors with enhanced flexibility to precisely and simultaneously measure changing fluxes of different secondary particles with different energy thresholds will be a key to better understanding of the sun. Establishing a new world-wide network of such detectors, at low to mid latitudes will give the possibility to measure solar proton and ion energy spectra up to 50 GeV, as well as, provide cost-effective possibilities for Space Weather research.

The energy distributions of the primary protons which give rise to charged and neutral particles as secondaries in the atmosphere are shifted from each other. Thus, by measuring fluxes of different particles with various energy thresholds, we can estimate the energy spectra of the highest energy solar ions. To do this we have to understand the detector response function on different particles. For each of the detector channels, we have to determine the efficiency and purity of the detected particles (neutrons, protons, mesons, electrons, muons, gammas). We use the GEANT3 (CERN, 1993) and CORSIKA (Heck & Knapp, 1998) simulation codes for modeling the traversal of particles in the detector and atmosphere respectively.

The Aragats Space Environmental Center (ASEC) provides monitoring of different species of secondary cosmic rays and consists of two high altitude research stations on Mt. Aragats in Armenia. Geographic coordinates: 40°30'N, 44°10'E, cutoff rigidity: ~7.6 GV. The characteristics of the main ASEC particle detectors are depicted in table 1 (Detailed description of the ASEC monitors is published in the (Chilingarian et al., 2005). Data from all ASEC monitors is available on-line from http://crdlx5.yerphi.am/DVIN3/

The Data Visualisation Interactive Network for the Aragats Space-environmental Center (DVIN for ASEC) provides wide possibilities to display physical inference from the multiple time-series of particle fluxes. DVIN enables sending warnings and alerts to users, gives opportunity to remote groups to share the process of analyzing and exchanging data analysis methods and schemes, preparing joint publications, and maintaining networks of particle detectors (Eghikyan & Chilingarian, 2006).

Starting from 1996 we have been developing various detectors, to measure fluxes of different components of secondary cosmic rays at the Aragats research stations of Alikhanian Physics Institute in Armenia. In 1996 we restarted our first detector - the Nor Amberd Neutron Monitor 18NM64 (2000m above sea level). A similar detector was commissioned and started to take data at the Aragats research station (3200m above sea level) in 2000. Solar Neutron Telescope (SNT) is in operation at the Aragats station since 1997, as part of the worldwide network coordinated by the Solar-Terrestrial laboratory of the Nagoya University (Tsuchiya et al., 2001). In addition to the primary goal of detecting the direct neutron flux from the Sun, the SNT also has the possibility to detect charged fluxes (mostly muons and electrons) and roughly measure the direction of the incident muons. Another monitoring system is based on the scintillation detectors of the Extensive

Air Shower (EAS) surface arrays, MAKET-ANI and GAMMA, located on Mt. Aragats at 3200 m above sea level. Charged component monitoring system on Nor Amberd research station started operation in 2002. Data Acquisition (DAQ) system was modernized in 2005. Flexible microcontroller based electronics is designed to support the combined neutron-muon detector system and utilize the correlated information from cosmic ray secondary fluxes, including measurement of the environmental parameters (temperature, pressure, magnetic field). Microcontroller based DAQ systems and high precision time synchronization of the remote installations via Global Positioning System (GPS) receivers are crucial ingredients of the new facilities on Mt. Aragats.

**Table 1 Characteristics of ASEC Monitors**

| Detector | Altitude *m* | Surface $m^2$ | Threshold(s) *MeV* | Operation since | Count rate ($min^{-1}$) |
|---|---|---|---|---|---|
| NANM (18NM64) | 2000 | 18 | 50 | 1996 | $2.7\times10^4$ |
| ANM (18NM64) | 3200 | 18 | 50 | 2000 | $6.1\times10^4$ |
| ASNT<br>8channels | 3200 | 4 (5cm thick)<br>4 (60cm thick) | 7<br>85, 172, 256, 382 | 1998 | $1.2\times10^5$<br>$5.2\times10^{4*}$ |
| NAMMM<br>24 channels | 2000 | 10 – upper<br>10 – down | 7<br>250 | 2006 | $1.8\times10^5$<br>$1.1\times10^5$ |
| AMMM | 3200 | 100 | 5000 | 2002 | $3\times10^5$ |
| MAKET-ANI<br>6 channels | 3200 | 6 | 7 | 1996 | $1.5\times10^5$ |

*Count rate for the first threshold; near vertical charged particles are excluded

Simultaneous detection of variations in low energy charged particles, neutron, and high energy muon fluxes by the ASEC monitors will provide new possibilities for investigating the transient solar events and will allow us to classify Geoeffective events according to their physical nature and magnitude.

### 2.2 Determination of the probable energies of primary protons responsible for the secondary fluxes measured by ASEC particle detectors

The world-wide network of Neutron Monitors located at different latitudes act as a distributed magnetic spectrometer, measuring primary rigidities from 1 to ~10 GV (Ryan et. al., 2000). The current knowledge about solar particles of highest energies is limited by the maximum detectable momentum of this "spectrometer" and by the scarcity of data from solar cosmic rays of highest energies. Furthermore, due to very weak fluxes of GeV particles and vast background of GCR, the energy region of 5-10 GeV is also very poorly investigated by the low latitude NM and there are not many attempts to obtain energy spectra of SCR above 5 GeV in any detail. Usually the energy spectra well above satellite energies are shown in the figures by wide shaded areas or extrapolated dotted lines because of the uncertainty in measurement techniques.

Thus, it is vitally important to acquire data on the SCR above 5 GeV to better define this range of the spectrum. The network of muon monitors is not yet well developed, and moreover extremely rare GLE events initiated by SCR with energies above 5 GeV are very anisotropic. Therefore, for the estimating of the energy spectra of SCR above 5 GeV, it is crucial to perform multiple measurements at the same location. ASEC monitors provide excellent possibilities for the research

of highest energy SCR by measuring muon and neutron content of secondary cosmic rays at the same latitude and 2 altitudes (in 2007 we plan to add additional particle detectors located at 1000 m a.s.l. to complement those already existing at the research stations at 2000 and 3200 m a.s.l.).

To outline the energy range of the primary particles, which can be investigated by the ASEC monitors, we perform simulation of the cascade development initiated by primary protons by the CORSIKA code (Heck & Knapp, 1998) along with the detectors response simulation with the GEANT3 code (CERN, 1993). The primary proton spectra was adopted from (Boezio et.al.,2003). The details of the simulations are available from (Zazyan & Chilingarian, 2005).

In Figure 3 we present the spectra "selected" by different ASEC monitors from proton spectrum incident on the terrestrial atmosphere. Each ASEC detector registers secondary particles, corresponding to parent protons with different energy spectra. As we can see from Figure 2, if protons just above rigidity cutoff of 7.6 GV effectively generate neutrons detected at 3200 m., the most probable energy of the low energy charged particles "parents" is above 10 GeV. 5 GeV muons are effectively generated by the primary protons with energies of 25-30 GeV.

For the SCR, we have to consider much softer energy spectra of primaries compared to the GCR. In Figure 4 we assume power index of $\gamma$= -4 and, as we can expect, the most probable energies of the "parent" protons are shifted to the lower values. Mode of the distribution of the low energy component is shifted to ~ 8-9 GeV, and of 5 GeV muons to 15-25 GeV. Nonetheless, ASEC monitors provide several independent measurements of the secondary particle fluxes corresponding to the primary energies of up to ~ 25 GeV. We measure fluxes of neutrons and low energy charged particles with neutron monitors and plastic scintillators at 2000 and 3200 m a.s.l. and - 5 GeV muons by scintillators located under 14 meters of concrete and soil (detailed description of the ASEC detectors is given in Chilingarian et al., 2005). Newly installed Advanced Data Acquisition System (ADAS, S. Chilingarian, 2006) enables a number of software controlled triggers, thus selecting secondary cosmic rays of specific energies coming from a range of directions.

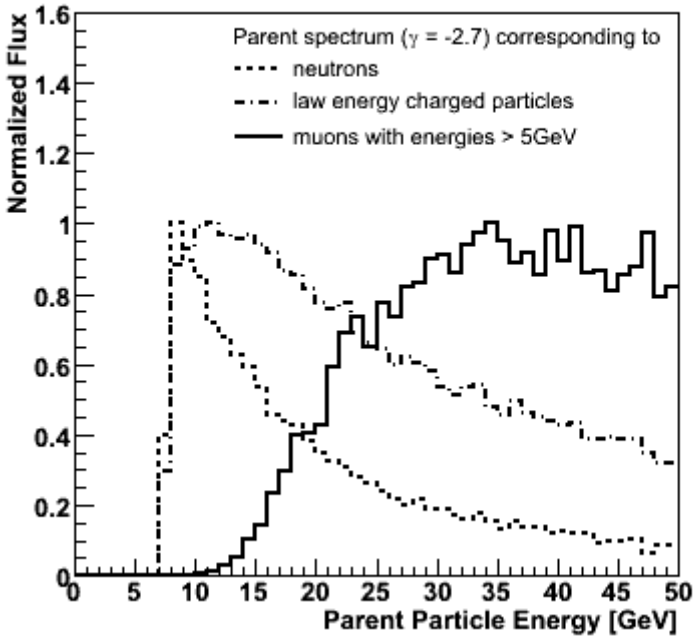


**Figure 3 Simulation of the "Parent" energy spectra of secondary particles initiated by the GCR (spectral slop equals -2.7), "selected" by the ASEC monitors at 3200 m**

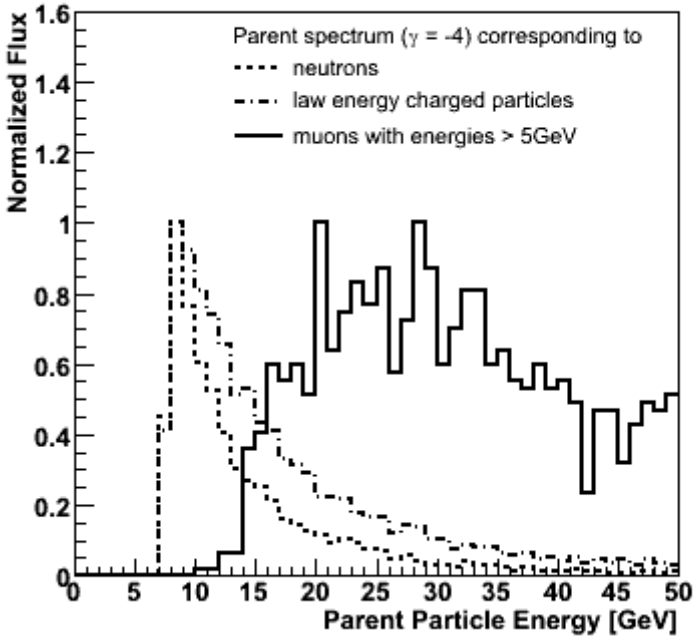


**Figure 4 Simulation of the "Parent" energy spectra of secondary particles initiated by the SCR (spectral slop equals -4), "selected" by the ASEC monitors at 3200 m.**

The highest energy detector is, of course, AMMM, with probable primary energy of ~20-25 GeV for the SCR and rather large detecting surface (44 m2, to be enlarged to 100 m2 in 2007).

### 2.3 Highest energy particles detected on 20 January 2005

On 20 January 2005, during the recovery phase of the Forbush decrease a long lasting X-ray burst occurred near the west limb of the Sun (helio-coordinates: 14N, 67 W). The start of X7.1 solar flare was at 06:36 and maximum of the X-ray flux at 7:01. The fastest (relative to X-ray start time) SEP/GLE event of 23-cycle was detected by space-born and surface particle detectors few minutes after the flare onset. The start of GLE was placed at 6:48; the maximal amplitude of 5000% recorded by NM at the South Pole is the largest increase ever recorded by neutron monitors. The event was highly anisotropic (Belov et al., 2006, Vashenuk et al., 2005a and 2005b) and the hardest of the 23-rd solar cycle.

As we can see in the Figure 5 on 20 January 2005, ASEC monitors detected significant excess of count rates at 7:00 – 8:00 UT. From 7:02 to 7:04 UT, AMMM detected a peak with significance *~4σ*. It was the first time that we detected a significant enhancement of the >5 GeV muons coinciding with the GLE detected by the world-wide networks of Neutron Monitors. Detailed statistical analysis of the peak (Bostannjyan et al, 2006) proves the non-random nature of the detected enhancement. This short enhancement (denoted in Figure 5 by the solid curve with open circles) at 7:02-7:05 exactly coincides in time with peaks from Tibet NM (Miyasaka et al., 2005), Tibet SNT (Zhu et. al., 2005) and Baksan array (Karpov et al., 2005). The solid line in Figure 5 denotes the time series of the low energy charged component and the dashed line indicates the Aragats neutron Monitor time series.

Although peak signal from the other ASEC monitors do not coincide in time with the 5 GeV muons flux peak, and low energy charged particles (mostly electrons and muons) peak, they also demonstrate enhancement at 7:02-7:05, thus providing possibility to extend the energy spectrum measured by the proton channels of GOES 11 satellite up to 20 GeV (presented in Figure 6). The differential energy spectra of the SCR protons at 7:02 – 7:05 UT measured by the space born

spectrometers and surface particle detectors covers more than 3 orders of magnitude from 10 MeV to 20 GeV and demonstrates very sharp "turn-over" at 700-800 MeV.

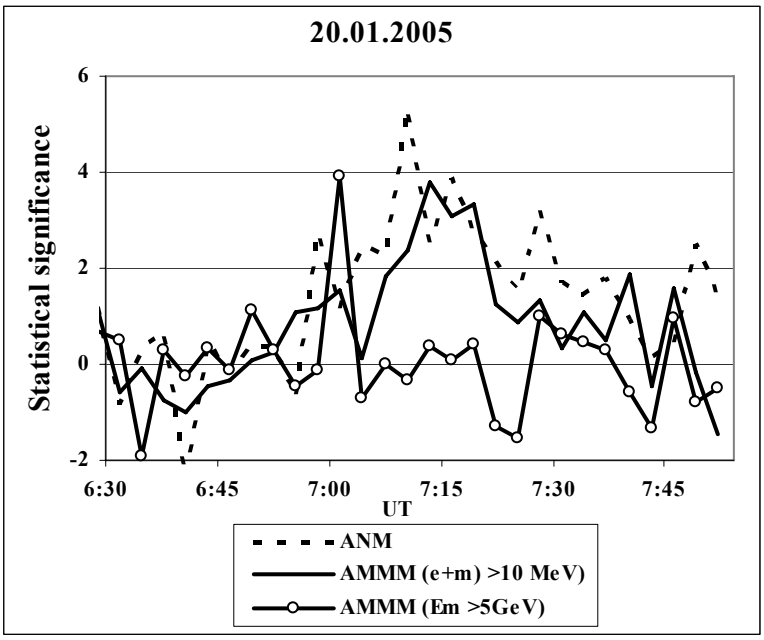


**Figure 5 Detection of the GLE from 20 January 2005 by ASEC monitors**

The energy spectrum remains very hard up to ~ 800 MeV (with power index ~ -1) and prolongs till tens of GeV with power index ~ -4 to -5. This signifies that acceleration at GeV energies probably have a different nature than at MeV energies.

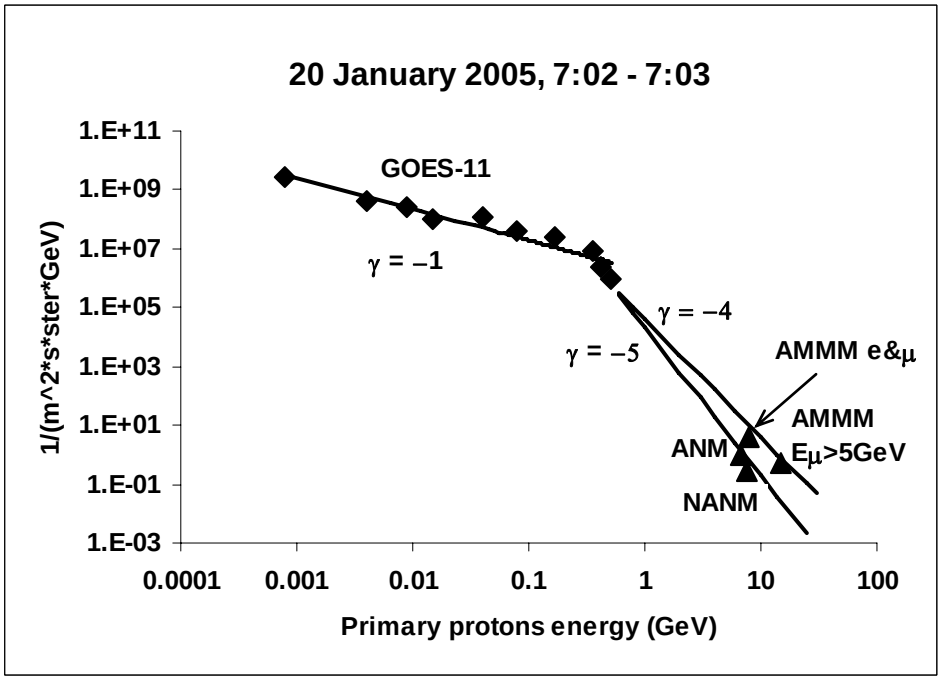


**Figure 6 Differential energy spectra of the SCR protons 20 January 2005**

Neutrons detected by the ASEC Neutron Monitors (ANM and NANM) and low energy charged particles have "parent" primary protons with energies slightly greater than cutoff rigidity threshold (see Figure 4). The most probable proton energy corresponding to the measured 5 GeV muon flux, as we can see from the same Figure 4 is in the region 20-25 GeV. Note that the reconstructed differential spectra of AMMM is between the lines corresponding to index of $\gamma$ = -4 and -5. It is

consistent with most spectra estimates reported at the 29th ICRC at Puna, India (Miysaka et al., 2005, Vashenuyok et.al., 2005). The uncertainty in the spectral index reflects the methodical difficulties of estimation of differential spectrum at such high energies.

The estimated energy spectra index of $\gamma$ = -4 - -5 at highest energies is a very good indicator of upcoming abundant SCR protons and ions with energies 50 - 100 MeV, extremely dangerous for the astronauts and high over-polar flights, as well as for satellite electronics.

Another way to estimate the index of power law exploits the different attenuation of the secondary fluxes depending on altitude or the particular specie of detected secondary particles. Estimation of the energy spectra index using data from NM located at same latitude, but different altitudes was suggested by (Lockwood et all, 2002). Recently same methodology was used for the determinations of the radiation dozes received on-board of airplanes during solar particle events (Lantos, 2006). We use this technique for estimation of the spectral index of the 20 January GLE from the data of the Aragats and Nor Amberd NM (Zazyan & Chilingarian, 2005).

Proceeding from detected fluxes at Aragats, we check if using the ratio of the enhancements of the flux of different secondaries (for example neutrons and low energy charged particles) it is possible to estimate the power law index. As one can see from Figure 7, indeed the ratio of the neutral-to-charge flux is more sensitive to the power index compared with neutron flux ratio measured at different altitudes.

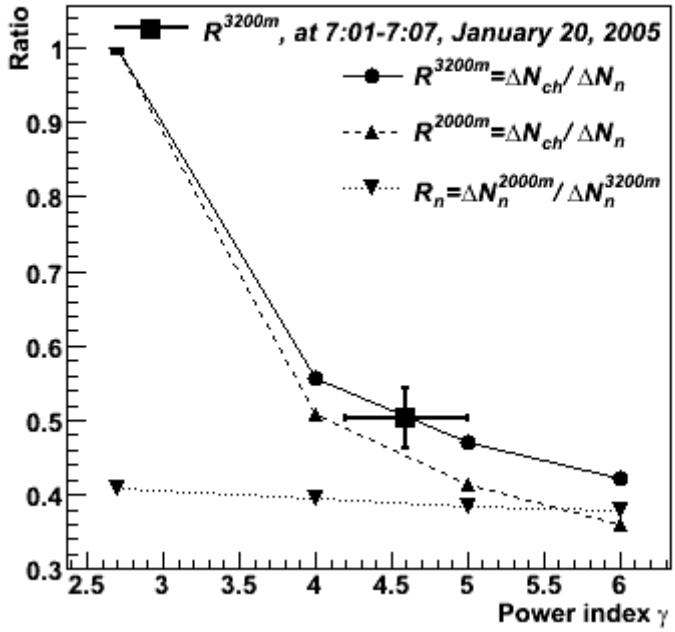


**Figure 7 Estimation of the energy Spectra index by comparing different secondary fluxes measured at same the location**

The estimate of the spectral index obtained by the proposed parameter $R^{3200}$, as one can see in Figure 6, coincides within statistical error bars, with the most probable value of the index obtained by the direct method (see Figure 6). However, to achieve reasonable statistical accuracy we integrate fluxes of neutrons and low energy charged particles over 7 minutes starting from 7:00. In Figure 4 we see very fast changing pattern of secondary fluxes, therefore, the estimate based on the $R^{3200}$ parameter is too smeared and can only be used for detectors with large surfaces and/or for very strong fluxes of solar particles.

### 2.4 On the possibility to forecast severe radiation storms by surface particle detectors

Large flux of relativistic particles accelerated in violent solar flares or/and by shock wave expanding in corona unleash Solar Energetic Particle event (SEP), sometimes causing Ground level enhancement (GLE), registered by networks of particle detectors at earth surface

In (Chilingarian et al, 2003, see also ACE news, 2005) based on the subsample of GLE events occurred during 23 $^{rd}$ solar activity cycle (1996 – 2008) and unambiguously detected by the monitors of the Aragats Space Environmental Center (ASEC, Chilingarian et al., 2005) we claimed that relativistic solar ions with GeV energies arrive well before MeV energy ions, thus providing possibility of alerting on upcoming radiation storm. In Table 1 (updated from Gevorgyan et al., 2005), we present the characteristics of these events along with times and statistical significances of peaks detected by ASEC neutron monitors (for 5-minite time series). For comparison in the last column we present the actual time of the S2 alert issued by the Space Environmental Center (SEC) of National Oceanic and Atmospheric Administration (NOAA), based on the enhanced 10 MeV proton flux ($I_p$ (E > 10Mev) > 100/cm$^2$ * sec*ster), registered by the facilities onboard of GOES satellite. The most important problem of detection of solar modulation effect at middle/low latitudes is proving that observed peak in time series is signal and not background fluctuation only. Assuming Gaussian nature of the count rate fluctuations we can calculate the chance probability to obtain randomly definite enhancement of the count rate. Usually not the chance probability, but the standard Gaussian distribution z-score ($\sigma$) is used as a measure of statistical significance. For all 3 events the significance of the peaks detected by surface particle detectors is $\geq 3.5\sigma$, thus the probability that the peak is due to random fluctuation only is rather small, we can expect one such enhancements in 5-minute time series in 3 months.

The chance probability to register random enhancement exceeding $3.5\sigma$ simultaneously by several ASEC monitors is vanishing small. However, we cannot exclude that in some cases magnetospheric or/and atmospheric disturbances influence the count rate of surface particle detectors.

**Table 2 GLE of 23rd cycle detected by the ASEC particle monitors**

| GLE number and date | X-Ray Flare | ASEC Monitor | GLE onset | First Peak time | σ | Second Peak time | σ | Time of S2 Alert by SEC/NOAA |
|---|---|---|---|---|---|---|---|---|
| GLE 60 | X14.4 | ANM | 13:55 | 14:00 | 3.8 | 14:30 | 5.3 | 14:25 |
| 4/15/2001 | | NANM | 13:55 | 14:00 | 3.5 | 14:30 | 4.1 | |
| GLE 65 | X17 | ANM | 11:25 | 11:45 | 4.6 | 12:10 | 4 | 12:40 |
| 10/28/2003 | | NANM | 11:30 | 11:35 | 3.5 | 12:05 | 3.6 | |
| GLE 69 | X7 | ANM | 6:55 | 7:10 | 5.6 | | | 7:01 |
| 1/20/2005 | | NANM | 6:55 | 7:00 | 4.5 | | | |

With the exception of the event on 20 January, when due to very good magnetic connection of the flare site with earth, all relativistic particles seem to come simultaneously, the enhancements of GeV SCR detected by the Neutron Monitors can alert on upcoming severe radiation storm (see also Figures 8 and 9). The alerts from middle and low latitude monitors are even more important compared to high latitude networks, because of lower probability of false alarms. If an enhancement occurs at monitors with large cutoff rigidity it indicates that spectral knee occurs at large enough energy and flux of the MeV ions will be very high. Of course, not all radiation storms will contain particles with GeV energies, but ones having such energies are of utmost hazard and should be reported as soon as possible to satellite operators. ASEC monitors can provide just such alerts. To detect very weak fluxes of highest energy solar ions in 2007 we enlarge the surface of 5 GeV muon detector at Aragats up to 100 m2, to achieve the relative accuracy of signal detection of 0.07% (for 5 minute time series).

On 2003 October 28 one of the biggest solar flares of the 23rd cycle occurs (X17.2 according to the NOAA scale, X-ray flux maximum at 11:10). It was a remarkable event not only because of its strength, but for many associated physical phenomena. Extended GLE event was registered by world-wide networks of Neutron Monitors (Panasyuk et al. 2004); some of monitors (Bieber et al., 2005) and satellite detectors (K. Watanabe et al., 2006) detect solar neutrons. The record cosmic ray depletion (Forbush decrease) was detected by the middle-latitude particle detectors (Chilingarian et al., 2005). The radiation storm (S4, according to the NOAA scale) was fourth largest in history since NOAA began keeping records in 1976. Due to this storm many satellites experience extensive surface charging, problems with orientation, uplink/downlink and tracking. Instruments on SOHO space station were shut down for safety reasons. Astronauts at Space station hide themselves in Russian module Zvezda, having best shielding against space radiation. Sever over-polar flights were rescheduled. The Geomagnetic Storm (GMS) triggered by the interplanetary coronal mass ejection reached earth 19 hours after flare. GMS also interfere with satellite communications; power grids in the northern United States and Canada are feeling the effects of the extreme geomagnetic storm and are experiencing power surges, voltage control problems and protective system problems. Event influence on the Earth's Atmosphere, the Ionospheric and Magnetospheric responses (see details in Gopalswamy et al., 2005) make this event unique in terms of the free energy available at the Sun and the geospace and heliospheric consequences. Therefore, it is of special interest compare the forecasts issued by Space Environment Center in Boulder, Colorado with possible alerts from the ASEC particle detectors. Of course, ASEC provides only post-event analysis, because in 2003 there was not operational Space Weather service established at ASEC.

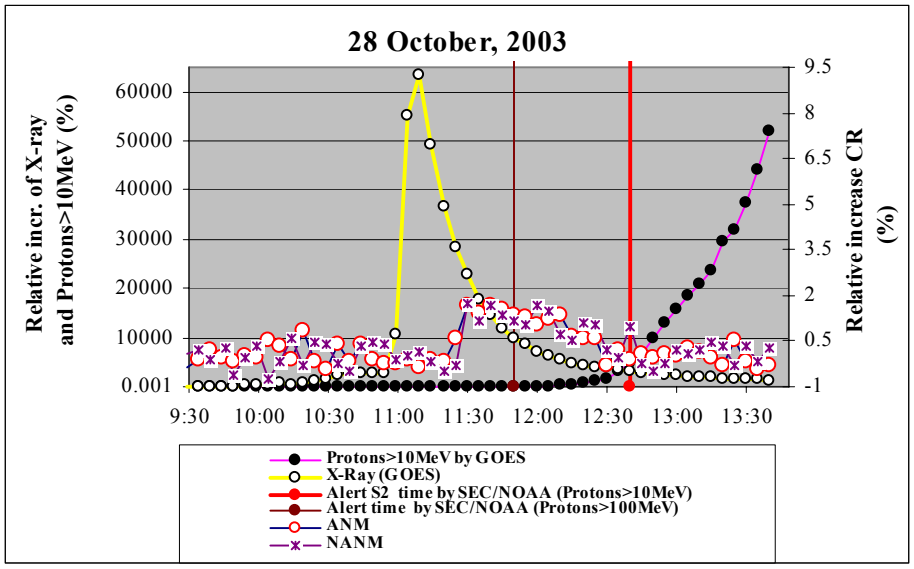


**Figure 8 Radiation from 28 October 2003 X14.4 flare. X-ray count rate is multiply by 2 (flux maximum at 11:10). SEC/NOAA alerts enhancement of 100 MeV protons at 11:50 and S2 alert for 10 MeV protons at12:40. Enhancement of the Aragats Neutron Monitor (ANM) and Nor Amberd Neutron Monitor (NANM) reaches ~1.7% and reaches maximum at ~11:30.**

In Figure 8 we can see that abrupt enhancement of the ASEC monitors count rates started at least 20 minutes earlier than 100 MeV protons alert and more than 1 hour earlier than S2 alert, both issued by SEC. The significance of ASEC alerts explained in the Figure 3. In Figure 9 we can see that at 11:20 correlations between particle fluxes on 2 research stations of ASEC as well as "delayed" correlations of both fluxes with X-ray flux are reaching peaked at 0.7-0.8.

Correlation information along with information on the GLE makes the false alarm probability extremely small. Information only on the GLE isn't enough due to not very big enhancement at middle-low latitudes (usually 1.5-2%) and rather large fluctuations of count rates. The relative accuracy of neutron monitor 5-minute count rate is at ASEC 0.3-0.4%, therefore, significance of 1.5-2% enhancement corresponds to 3.5 - 5σ, and related false alarm probability to $10^{-4}$ – $10^{-5}$, i.e.

occurs randomly several times in year by chance. The "delayed" correlations are calculated by the "memorization" of the X-ray flux enhancement (available on-line from SEC) and continuous (moving) calculations of the correlations with surface particle detector data.

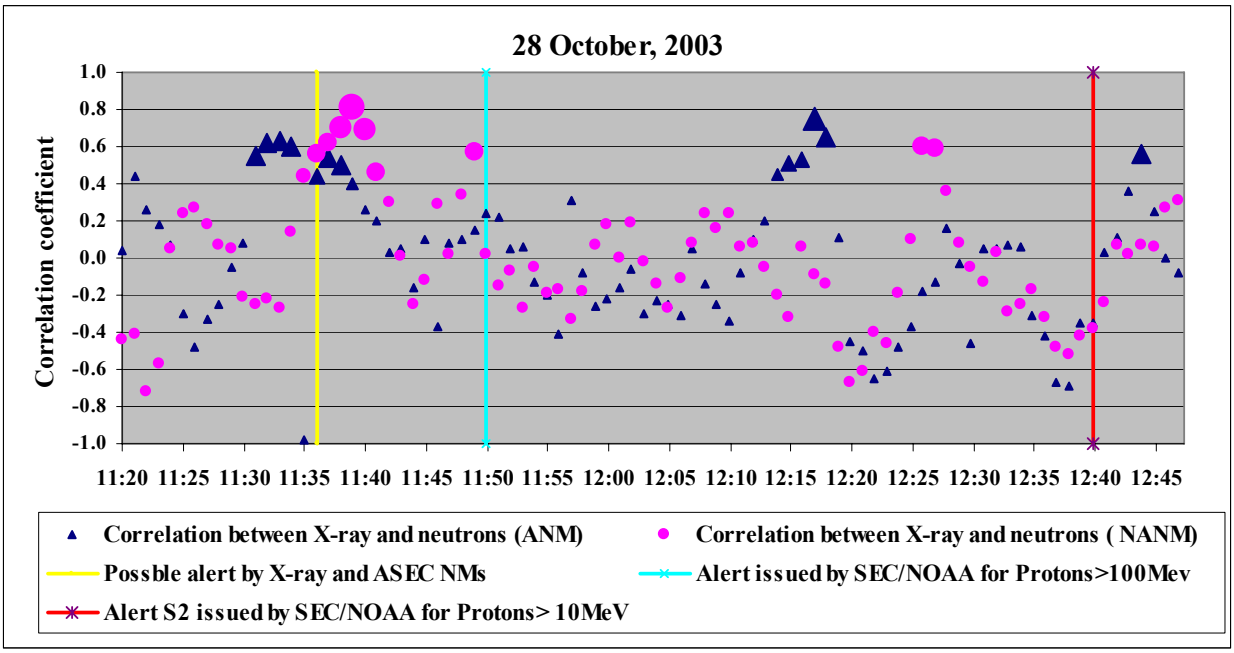


**Figure 9 Pattern of correlations between neutron fluxes measured by surface particle detectors and measured by GOES satellite X-ray flux. Correlations are calculated with 1-minute count rates, by memorizing the X-ray 10 minute peak and moving 10 minute intervals of surface particle detector count rates. The triangles, circles and diamonds are denoted the correlation coefficient between changing fluxes of particle detectors and X-rays.**

In Figures 8 and 9 we can see that X-ray flare maximum was at 11:10 and dangerous flux of abundant 10-MeV protons reach Earth more than1 hour later. 100 MeV protons alert was issued by SEC/NOAA 40 minutes after flare and surface monitors at ASEC can alert on GLE 20 minutes earlier and 1 hour in advance of SEC S2 alert. The correlation analysis of multiple ASEC monitors make ASEC alert reliable and confident. Correlation of X-ray peak and Neutron monitors peaks reach values 0.6-0.8 at 10:35, 25 minutes after X-ray maximum. In Figure 10 we can see that correlation of X-ray peak and rising charged component of secondary cosmic rays (mostly electrons and muons, measured by scintillators) reach values 0.6-0.8 even earlier at 10:26, 15 minutes after X-ray maximum. Time difference between neutron peak and charged secondary particle peak can be explained by difference in primary energy of protons giving rise to both types of secondaries; the most probable energy of "parent" protons is bigger for secondary charged particles comparing with neutrons (the time history of proton detection apparent in Figure 8 supported hypothesis that arrival time is inversely proportional to the proton energy). Correlations between X-ray radiation and particle fluxes unambiguously prove genetic relation between flare and surface particles and can be used for construction of an alert on most violent radiation storms. Continuous monitoring of the abrupt enhancement of monitors count rate and "moving" correlations calculation after severe solar flare will surely point on upcoming severe radiation storm. False alarm probability of such alerts will be negligible, efficiency for most violent storm – high.

Detected radiation from 28 October 2003 flare demonstrates power of combining information from space born spectrometers and surface particle detectors for constructing reliable and timely Space Weather forecasting services. Another example of the time history of radiation connected with violent solar flare is posted in Figures 11 and 12.

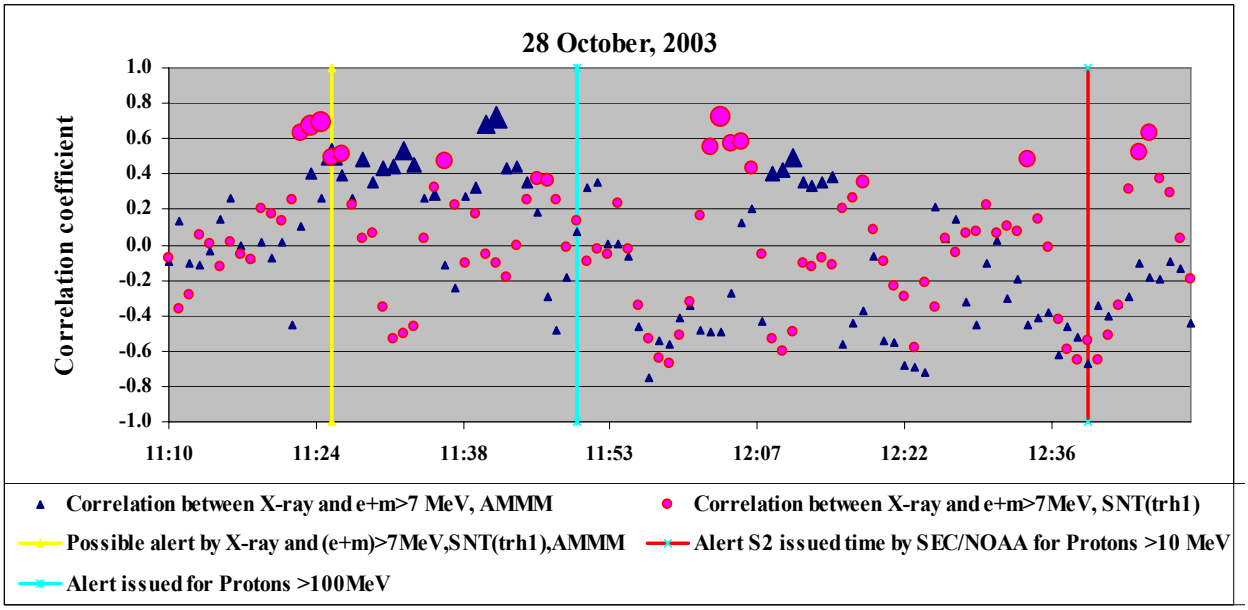


**Figure 10 Pattern of correlations between rising charged species of secondary cosmic rays and measured by GOES satellite X-ray flux at 28 October 2003. Correlations are calculated with 1-minute count rates, by memorizing the X-ray 10 minute peak and moving 10 minute intervals of surface particle detector count rates. The triangles, circles and diamonds are denoted the correlation coefficient between changing fluxes of particle detectors and X-rays.**

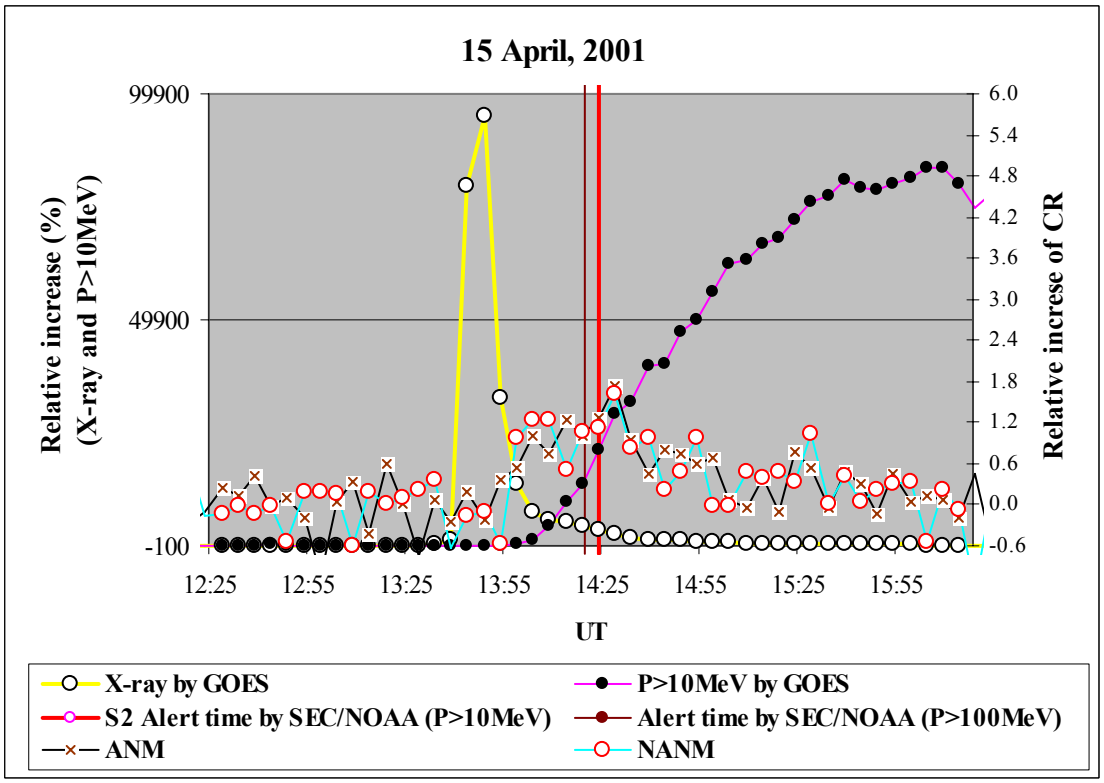


**Figure 11. Radiation from 15 April 2005 X17.2 flare. SEC/NOAA alerts enhancement of 100 MeV protons at 14:21 and S2 alert for 10 MeV protons at 14:25. Enhancement of the Aragats Neutron Monitor (ANM) and Nor Amberd Neutron Monitor (NANM) reaches ~1.4% and reaches maximum at ~14:00.**

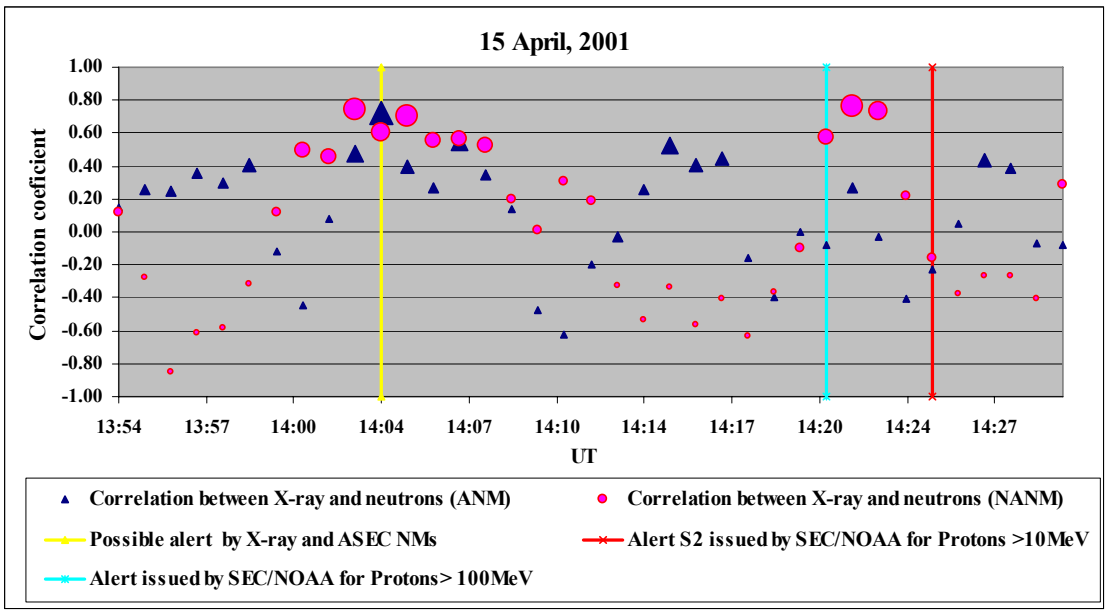


**Figure 12 Pattern of correlations between neutron fluxes measured by surface particle detectors and measured by GOES satellite X-ray flux at 15 April 2001. Correlation between X-ray and Neutrons peaks reach values 0.6-0.8 at 14:04, 20 minutes after X-ray maximum.**

In Figures 11 and 12 we can see that X-ray flare maximum was at 13:50 and dangerous flux of abundant 10-MeV protons reach Earth at 14:25, 35 minutes later. 100 MeV protons alert was issued by SEC/NOAA 31 minutes after flare and surface monitors at ASEC can alert on GLE ~20 minutes earlier.

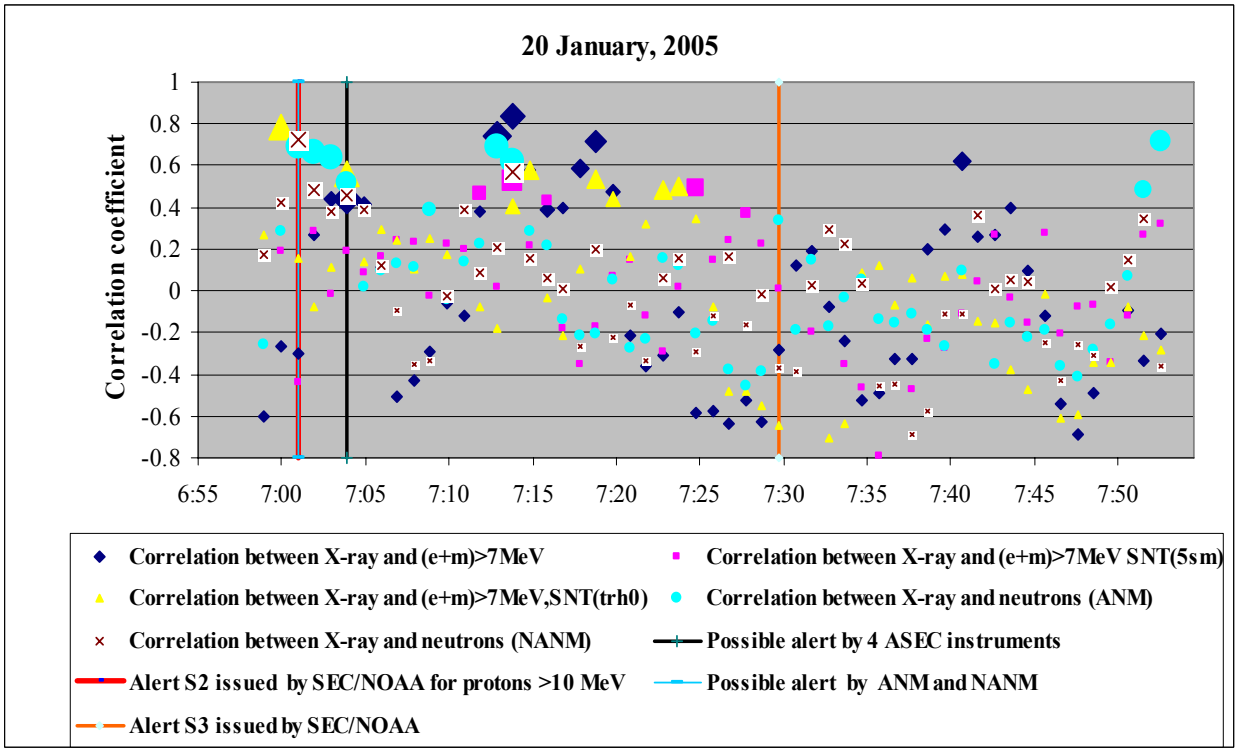


**Figure 13 Pattern of correlations between neutron fluxes measured by surface particle detectors and measured by GOES satellite X-ray flux at 15 20 January 2005. Correlation between X-ray and ASEC monitors reach values 0.6-0.8 at 7:01, 20 minutes after X-ray maximum.**

The reliable alert service for warning on upcoming SEP event can be established as follows. As soon as strong flare (X-class according to the NOAA scale) is reported by the GOES satellites (available on-line from SEC/NOAA) the 2 alert programs started:

1. The first one is examining the enhancement of count rates in all channels of neutron and muon monitor routinely calculated by the Aragats Data Acquisition System (ADAS); Enhancements and corresponding statistical significances are calculated each minute by twelve 5-second count rates. Examining of the inter-channel correlation matrix, also calculated by ADAS, will help to prove that enhancement is not failure of one of channels, but consistent enhancement.
2. The time history of the X-ray flux (from start till maximum, usually ten 1-minute numbers) is memorized and a "delayed correlation routine start to calculate correlation of X-ray peak with also 10 counts of ASEC monitors. Counts are shifted and map of moving correlations is constructed.
3. Dependent on the values of peak statistical significance and value of the correlation between X-ray flux enhancements and enhancements of neutral and charged fluxes, measured by surface particle detectors different warnings and alerts are issued.

Described scheme of alert service will be highly reliable, because it uses different particle fluxes measured at 3 altitudes (1000, 2000, 3200 m. A.S.L.) and X-ray flux measured by satellite facilities.

### 2.5 On the possibility to forecast severe geomagnetic storms by ASEC monitors

A new NOAA data-processing code, providing on-line measurement of the IMF direction and magnitude is used for real-time prediction of the severity of upcoming GMS. Measurements of the southward component of IMF upstream of Earth in L1 libration point (~1,5 mln. km. from the Earth) by the magnetometers onboard of Advanced Composition Explorer (ACE) gives 30-50 minutes advance before sudden commitment of GMS (ACE news 86, 2004). This time span is too short for the mitigation actions surface and space industries need to perform. For early prediction relationship should be established with directly observed CME features, as CME size and speed, available now from the Large Angle and Spectrometric Coronagraph (LASCO) on board the Solar and Heliospheric Observatory (SOHO) mission. Unfortunately, many statistical studies (see for example Kane, 2005 and references in it) prove that prediction methodology relaying on the estimated CME speed values, gives grossly erroneous predictions of the Dst or disturbance storm time index, a measure of geomagnetic activity used to assess the severity of magnetic storms. Presently, is no way to access more relevant features as southward component of magnetic field "frozen" in the embedded interplanetary structure (ICME), or, the so called "helicity" of magnetized cloud – the characteristic of the rotation of the magnetic field vector within ICME (see for details Georgieva et al, 2005).

Therefore, we have to examine GeV particle intensities nearby the Earth (i.e. their proxies – fluxes of the secondary particles, created by primary ones in interactions with atoms of terrestrial atmosphere). Isotropic and rather stable in our Galaxy flux of GeV GCR is interacting with magnetic structures of ICME on its way to Earth and in some sense "screen" the ICME.

The networks of particle detectors located at Earth surface are measuring the "pattern" of this screening, encompassing the modulation effects of ICME. Because of huge sizes of ICME (0.2 – 0.4 AU) and relativistic velocities of GeV particles the modulation effects started very early and particle detector evidence can provide timely (10 -20 hours) warnings on upcoming severe GMS.

Of course, GCR-IMSE interaction is highly nonlinear and we need to solve complicated multivariate unfolding problem with many unknown parameters to estimate Dst from pattern of changing particle fluxes. However, for some severe GMSs event post-analyses was very promising.

To illustrate the possibility of the early forecast based on particle detector data, we present here precursors of the strongest GMS from 20 November 2003. During recovering phase of the Fd on 20 November 2003, the most intense GMS ever detected was registered, DST reached value of -422.

Several fast CMEs were unleashed at 18 November 2003 from active regions 501 and 508; the characteristics of these CMEs are posted in the Table 3.

**Table 3 Parameters of the fast CMEs unleashed at 18 November 2003 from ASR 501 and 508**

| Date | Time UT | Heliocoorditas | Angular depth ($^0$) | CME velocity км/sec | Kinetic Energy erg |
|---|---|---|---|---|---|
| 18-10-2003 | 11:30 | S16E08 | 360 | 2459 | $1.3 \cdot 10^{33}$ |
| **18-11-2003** | **8:06** | **N01E19** | **>104** | **1223** | **$1.3 \cdot 10^{32}$** |
| **18-11-2003** | **8:50** | **N02E18** | **360** | **1660** | **$3.3 \cdot 10^{32}$** |
| 18-11-2003 | 9:50 | S13E89 | >197 | 1824 | $3.6 \cdot 10^{32}$ |

In Table 3 we can see that the first CME (out of two CMEs coming from the center of the solar disc, denoted by bold symbols) was started at 8:06 with initial speed of 1223 km/sec; second CME launched after 44 minutes with initial speed of 1660 km/sec. Both CMEs have approximately the same heliocoordinates; the other 2 CMEs were from the eastern limb and could not interact with the central CMEs.

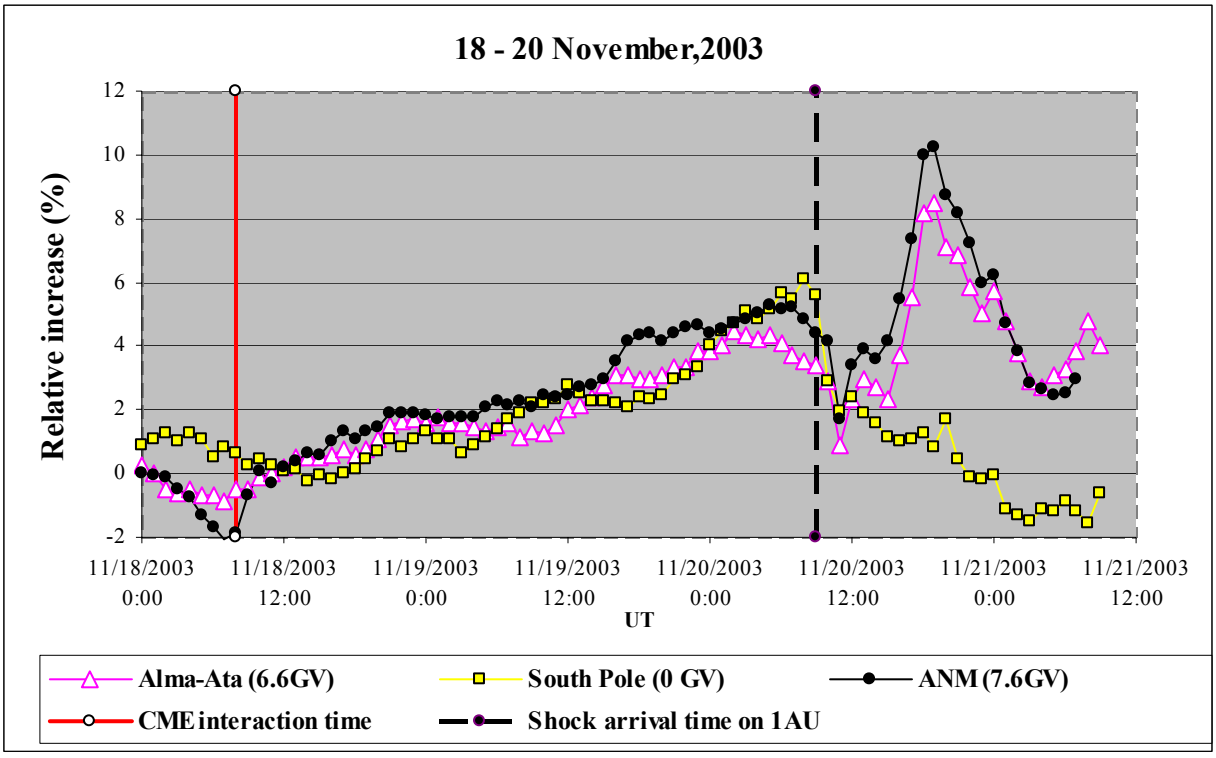


**Figure 14 Time history of count rate enhancements of high and middle latitude Neutron Monitors.**

The faster CME overtakes the first one 5.5 hours after start of the flare at a distance of ~ 48 $R_{sun}$ (0.22 AU) from the Sun. In (Gopalsvami et al., 2002) was shown that vast majority of the SEP events are correlated with interacted CMEs (83% for major SEPs, and 84% for minor SEPs). The analysis was based on the *GOES* proton and SOHO LASCO instrument data; 43 major ($I \geq 10$ pfu) and 39 minor (1 pfu $\leq I < 10$ pfu) SEP events from 1996 – 2001). *The conclusion was* that a major fraction of the SEP events occur at times of CME interaction and that the interaction rather than the solar flare strength, CME size or speed of the preceding CMEs seems to be important for the SEP production.

Starting from the time of the CME interaction, as can be seen from Figure 14 the precursors are detected at middle and high altitude. Therefore, we can assume that CME interaction forms a

"magnet-bottle" type structure "sending" (by reflecting particles from the approaching shock) additional flux of GeV particles in the Earth's direction.

Gradual increasing of NM count rates at Aragats and Alma-Ati neutron monitors, as we can see in Figure 14 already started on 19 November 2003 ~ 35 hours before the sudden commencement of the Geomagnetic storm, and several hours earlier comparing with high latitude South Pole monitor. World-wide network of Neutron Monitors as we can see from Figure 15, where the starts of the count rate enhancements are posted, strongly responds on the approaching ICME. Of course, *a-posteriori* determined start of enhancement cannot be used as precursor, but the steady multi-hour enhancement of the particle detector count rate can be used for construction of the early-warning system.

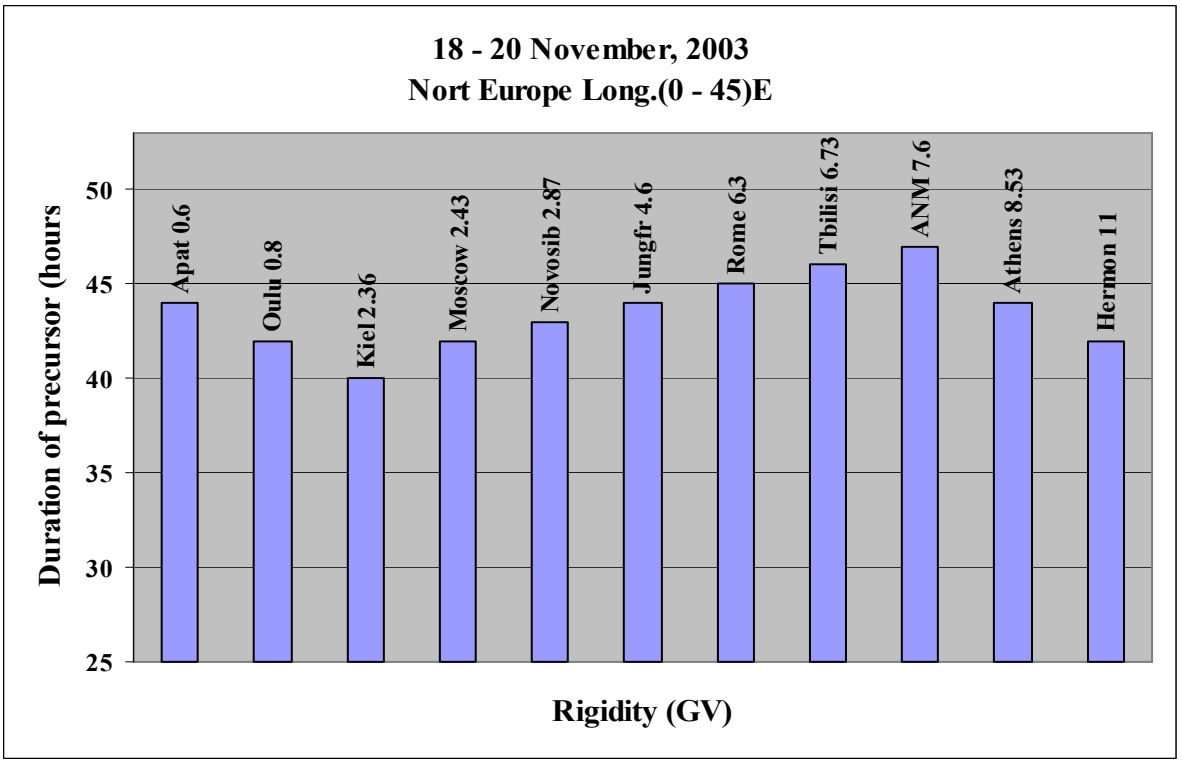


**Figure 15 Response of the European -Asian Neutron Monitors on the approaching to Earth magnetized structure. The numbers above columns are cutoff rigidities.**

In the poster below we illustrate possible explanation of this "rigidity" effect.

Background (isotropic galactic cosmic rays) GeV particles hitting the embedded magnetized structure (ICME) frontally or from the sides are "focused" and enhance usually rather stable flux of GeV particles in vicinity of earth. In turn these particles (mostly protons) initiate additional secondary cosmic rays in terrestrial atmosphere giving rise to particle detectors measuring neutrons, gammas, muons and electrons. This "focusing" effect is energy selective. From Figure 15 we can see that precursor effect is most effective for the energies 7-9 GeV. Highest energies are much influenced by the ICME and lower energies seem cannot keep the direction due to the scattering and bending in the interplanetary magnetic field (IMF). In Figure 16 we see that GOES MeV channels do not demonstrate any precursor feature; only after shock arrival there is noticeable enhancement of MeV particle flux.

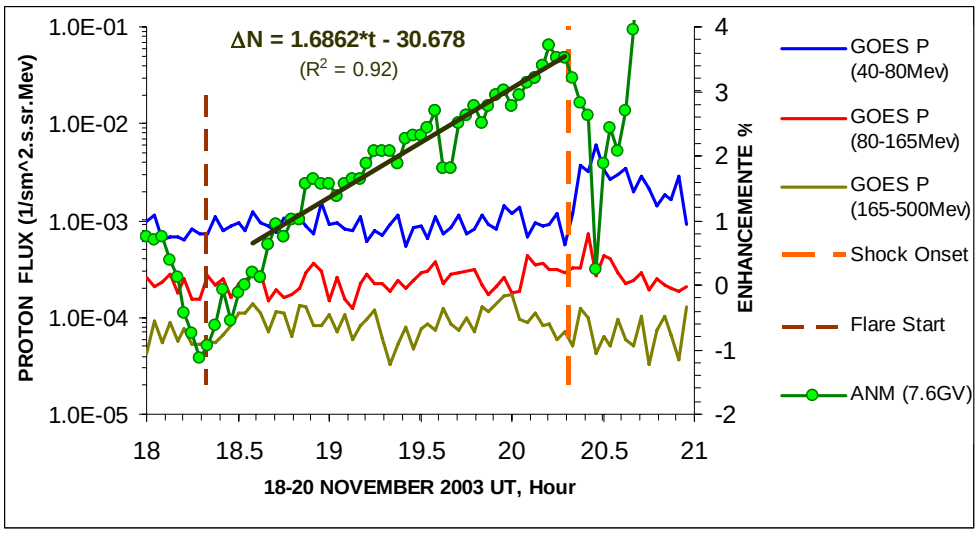


**Figure 16 Time history of count rate enhancements ANM and GOES MeV proton detector channels.**

Completely different pattern for lower energy particles (100-800 KeV) we can see in Figure 17.

Enhancement of KeV particle flux detected by the ACE SEPICA instrument started several hours after CME interaction. These particles are locally accelerated by ICME and usually are named as an Energetic Storm Particles (ESP) due to its strong association with geomagnetic storms. The gradually increasing intensity precursors observed upstream of ICME can be used to predict the passage of an ICME (ACE news 68, 2003). During an ESP event, < 1 MeV ion intensities can increase by orders of magnitude, as we can see in Figure. Because of the radiation hazards to astronauts and space-embedded technology posed by energetic particles, there is considerable interest in forecasting large IP shock-driven particle events.

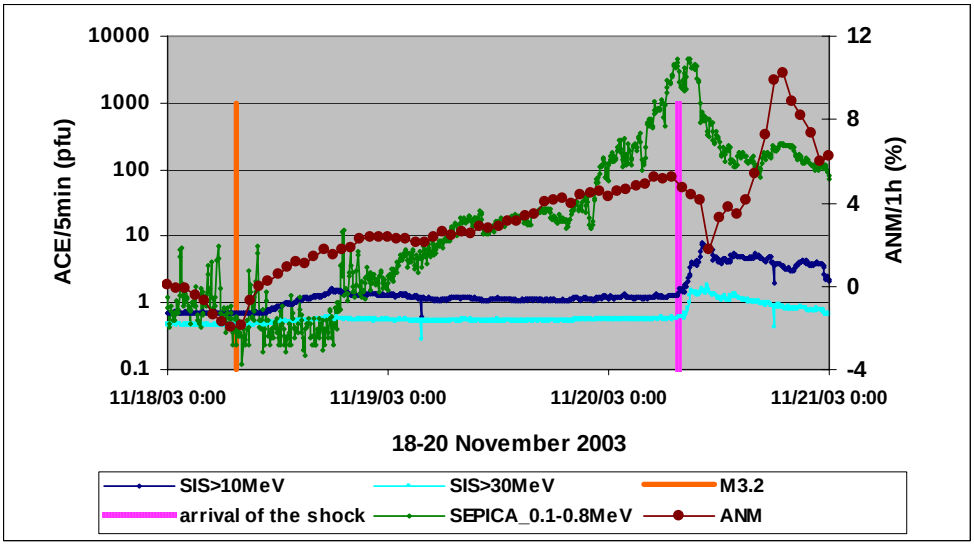


**Figure 17 ICME modulation effects in KeV; MeV; and GeV particle fluxes**

If we proceed to lower energies, the pattern again changes: Velocity of the ions of the Solar Wind is systematically decreasing in anti-correlation with GeV particles count rate enhancement.

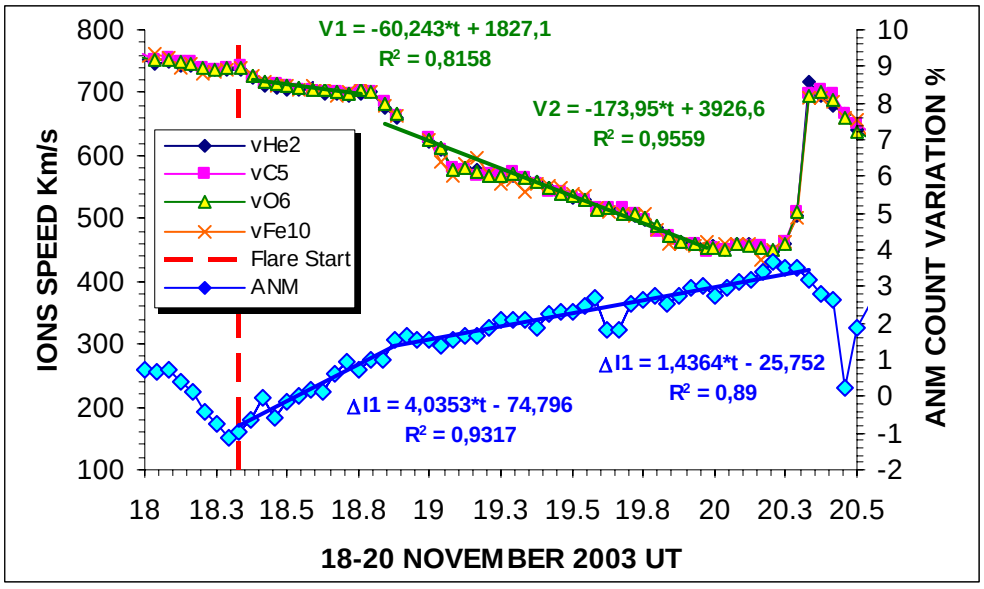


**Figure 18 ICME modulation effects on the Solar Wind speed and GeV particles flux**

It is important to note that only radial (pointed to Earth direction) of velocity component is diminished, leaving rest 2 unchanged. The same anti-correlation pattern was detected in electron velocities detected by WIND satellite facilities. In Figure 19 we can see that electron flux diminished ~15 hours after solar wind ions.

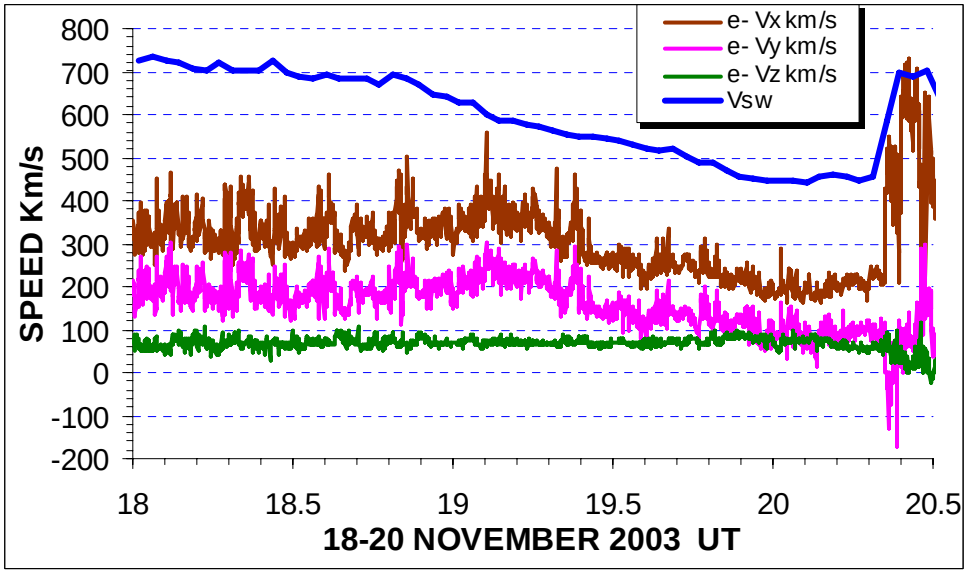


**Figure 19 ICME modulation effect on Solar Wind and electron velocities**

From the Figures 14- 19 we conclude that particle detector data provides valuable insight into the presence of ICMEs in the solar wind, and should be routinely incorporated into efforts to identify and study ICME modulation effects and Space Weather forecasting issues. .

Of course, accurate computational models of ICMEs and their associated modulation effects are essential for understanding the acceleration and transport of energetic particles. A critical gap in our present understanding concerns how ICME forms in interactions of several CMEs and evolve in the corona and solar wind. Ultimately, we would like to be able to simulate the formation and evolution of ICMEs by modeling the eruption of a CME, propagation through a realistic ambient solar corona, interactions with previously emitted CMS, interactions and modulations effects ICME poses on the Galactic Cosmic Rays on its way to 1AU . Such calculations represent a considerable challenge, till now little theoretical effort has been expended to model ICME transport in a

systematic and detailed manner. In (Gang Li et al., 2003) using a Monte-Carlo approach the shock propagation and particle acceleration at the shock as well as the subsequent particle transport were studied under the usual assumption of particle scattering near the shock front by magnetic irregularities of Alfve´n waves. The exact energetic distribution of particles escaping from ICME fronts was determined locally by the shock compression ratio and the local injection and maximum momentum. Once energetic particles escape from the shock front, their subsequent motion is along the ambient magnetic field, described by the usual Parker spiral; particles simply gyrate along the B field and experience only occasional pitch angle scattering by fluctuations in the magnetic field. From the simulations, some general features have emerged that characterize particle acceleration and transport at ICME, although due to many simplified assumptions in simulations and neglecting processes of the CME interaction and forming of ICME we cannot expect realistic description of particle fluxes covering KeV – GeV energy range.

Here we adopt a more pragmatic statistical approach to infer efficiency and false alarm probability of possible alerts on the severe Geomagnetic Storms. We made post-analyses of ICME events to calculate efficiency of alerts on severe geomagnetic storms (Kp≥8). From NOAA archive at:http://www.sec.noaa.gov/ftpdir/ the ICME events and corresponding Kp index were selected. Appropriate particle fluxes were selected from ACE and GO satellites and from ASEC monitors. In Table 4 is posted statistics of 83 ICME events from 2001 -2005 years which unleashed Geomagnetic storms with planetary index Kp $\geq$ 2. In the second and third columns the numbers of ICMEs accompanied with precursor feature and missed are posted. In third and forth columns the total number of ICMEs with unleashed GSM with definite Kp index and appropriate frequency of alert hits are posted. The alert implemented to these ISMEs was as following: at least 3 hours prior to ICME arrival the count rate of ASEC monitor is enhanced by 1%. 3 hours leading time is much more than a half-of-hour leading time provided by the magnetometers and other facilities onboard of ACE and SOHO satellites located at L1 Libration point 1,5 million km from Earth.

**Table 4 Statistics of GMS precursors based on ASEC particle detector data**

| Kp | Pr.: yes | Pr.: no | total | Npr./Ntotal |
|---|---|---|---|---|
| ≤3 | 3 | 17 | 20 | 0.15 |
| 4 | 2 | 17 | 19 | 0.105263 |
| 5 | 2 | 12 | 14 | 0.142857 |
| 6 | 0 | 11 | 11 | 0 |
| 7 | 2 | 6 | 8 | 0.25 |
| 8 | 5 | 0 | 5 | 1 |
| 9 | 5 | 1 | 6 | 0.833333 |

From the Table we can calculate that the efficiency of warning on the very severe geomagnetic storm (Kp ≥8) is very high ~0.91, unfortunately the corresponding false alarm probability is also rather high ~0.45.

One of the major advantages of multi-particle detectors is probing of the different populations of the primary cosmic rays. Cosmic Rays of different energies are modulated in different ways giving possibility to study ICME and understand its geoeffectiveness. Multivariate analysis of the particle data can lead path to reliable and timely forecasting of the dangerous consequences of solar storms.

It is worth to note that earliest precursor was detected in the flux of GeV particles detected by middle latitude particle detectors. Particle detectors of the Aragats Space Environmental center (ASEC) are measuring fluxes of neutrons and gammas, of low energy charged component and high energy muons. This diversity of information obtained from hybrid detectors network located mostly at low and middle latitudes will give possibility to estimate the energy spectra of the highest energy SCR. New establishing SEVAN particle detector network (Chilingarian et al., 2007) network will be sensitive to very weak fluxes of SCR above 10 GeV, coming very fast and bringing valuable information on upcoming geomagnetic storms.

The reliable alert service for warning on upcoming GMS can be established as follows. As soon as Halo CME is reported by the SOHO/LASCO or SOHO Extreme ultraviolet Imaging Telescope (available on-line from SEC/NOAA) the 2 alert programs started:

1. The first one is examining the enhancement of count rates in all channels of neutron and muon monitor routinely calculated by the Aragats Data Acquisition System (ADAS); the linear regression of cont rate enhancement on the time is constructed started from CME launch, or started from CMEs interaction. At each moment the correlation coefficient and linear regression parameters are available on-line.
2. The second program is reading MeV and KeV particle fluxes as well as Solar Wind velocity from appropriate channels of GOES and ACE satellites. The correlation coefficients and parameters of linear regression are calculated and made on-line accessible same as in point 1.
3. Dependent on the values of duration of the enhancement, correlation coefficients, percents of enhancements, parameters of linear regressions and other available information different warnings and alerts are issued.

Described scheme of alert service will be highly reliable, because it uses different particle fluxes measured at 3 altitudes (1000, 2000, 3200 m. A.S.L.) and lower energy particle fluxes and Solar Wind speed measured by satellite facilities.

## 2.6 Disabled space-born instruments during severe conditions of the Space Weather

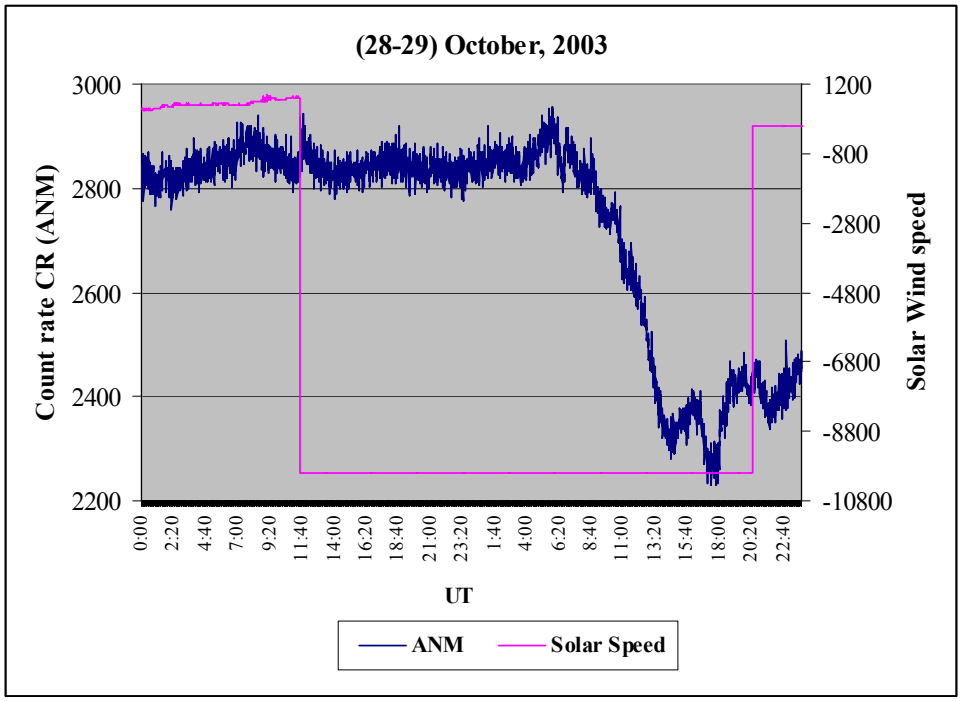


**Figure 20 Failure of the ACESWEPAM solar wind detector on board of the ACE space station during extreme solar event of 28 October 2003. In contrast the Aragats Neutron monitor is registering the ground level enhancement at 28 October and largest detected Intensity decrease (~20%) at 29 October.**

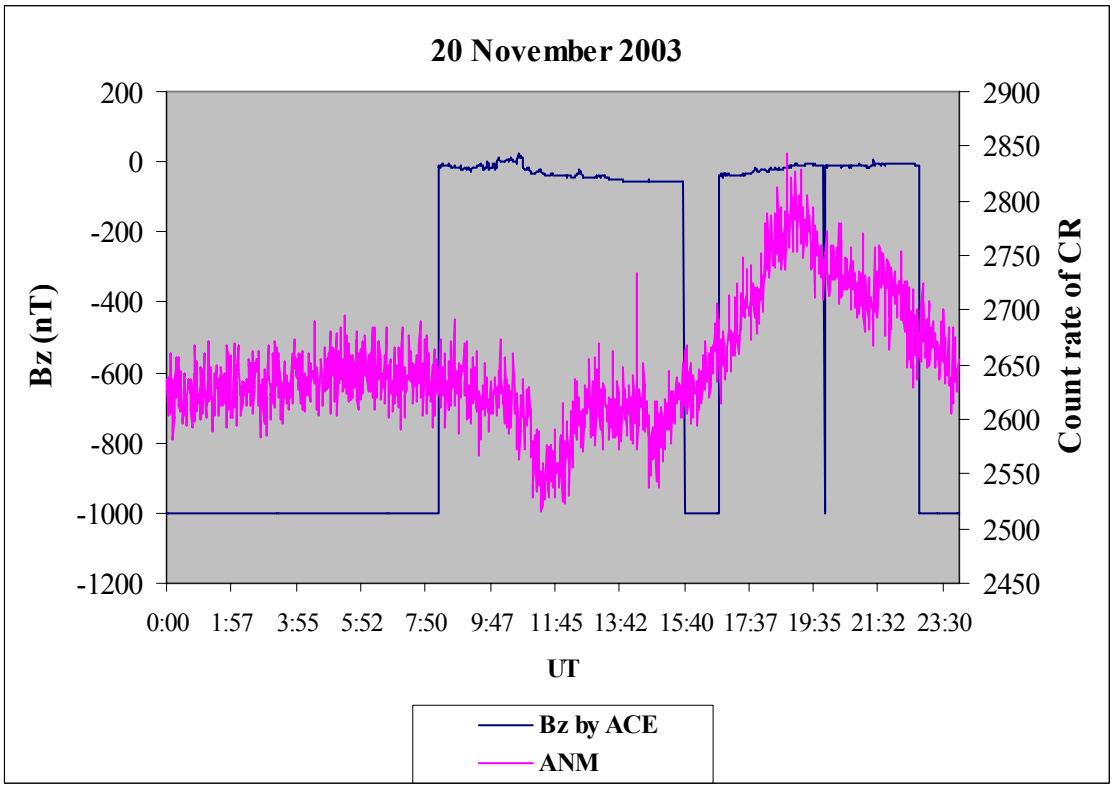


**Figure 21 Failure of the Magnetometer on board of the ACE space station during extreme geomagnetic storm of 20 November 2003 (The measurement of the $B_z$ component of the interplanetary magnetic field is disabled as well as of other parameters of the ICME) . In contrast the Aragats Neutron monitor is registering the huge increase of count rate due to effective decreasing of the geomagnetic cutoff energy at Aragats latitude.**

### 2.7 What is the place of Surface Particle detectors in future SW forecasting services?

Recently several groups publish results on possibility of forecasting of severe space storms by particle detectors located on the Earth surface. Among them are ASEC group (Gevorgyan et al., 2005), high-latitude neutron monitors network "Spaceship Earth" (Kuwabara et al, 2006), coordinated by the Bartol Research Center, Solar Neutron Telescopes network coordinated by the Nagoya University (Tsuchiya et al., 2001), Muon network coordinated by the group from Shinshu University (Munakata et al., 2000) and Athens Neutron Monitor Data Processing Center (Mavromichalaki, et al, 2005, 2006).

Unfortunately, till now forecasting provided by surface particle detectors are of *a-posteriori* character. Estimates of service expected efficiency and false alarm probability are empirical, based on historical data and post-event analysis. Expected for the GMS forecasting false alarm probability is rather high, for the radiation storm (SEP events) forecasting the efficiency is rather low. Therefore, better understanding of solar accelerators and forecast of the upcoming Solar Energetic Particle (SEP) events and GMS is crucial for establishing the SW forecasting service. The incorporation of the data from space-born facilities on the particle fluxes and flare/CME characteristics is also of biggest importance. In Figure 22 we present the chart of the SW alert service integrated space and surface data.

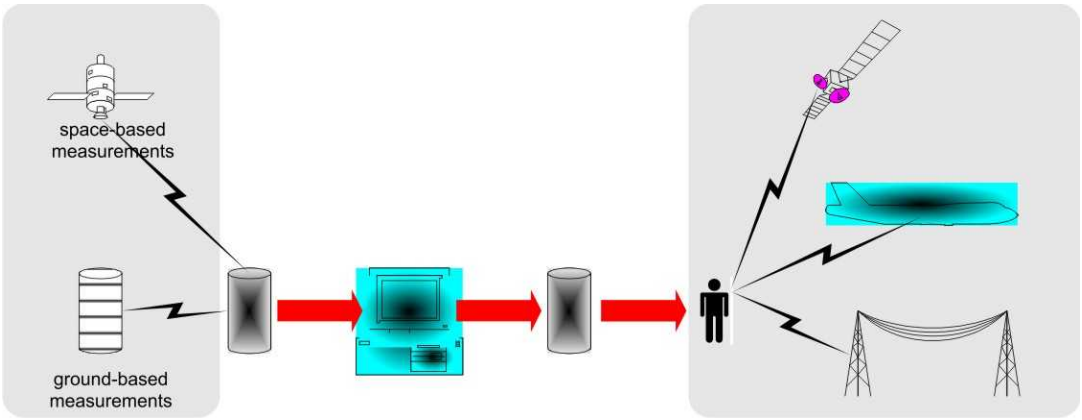


**Figure 22 Chart of the Planetary Space Weather Forecasting Service**

For the reliable forecast of the geomagnetic storms by surface particle detectors, we need fundamental research of the moving ICME on its journey from the Sun to Earth. An understanding of the fundamental physical processes of particle acceleration on the sun and by the coronal and interplanetary (IP) shocks is also crucial to establishing reliable alert service.

New missions like STEREO and Solar Sentinels will provide valuable information on particle acceleration, propagated ICME and its modulation effects including changing particle fluxes. The Database of ASEC monitors detection of modulation effects registered during 23$^{rd}$ solar cycle also will serve to better understanding of the causal relations between ICME "geoeffectivenes" and CR variations, see Attachment 2.

To establish reliable and timely forecasting service at ASEC we need to measure, simulate and compare:

- time series of neutrons, the low energy charged component (mostly electrons and muons) and the high energy muons;
- the correlations between changing fluxes of various secondary particles; and
- direction of the detected solar cosmic rays.

The SEVAN particle detector network can provide required information. SEVAN monitors detect charged and neutral components of the secondary cosmic rays with different energy thresholds and various angles of incidence. Therefore, using variety of particle detectors (fast and multispecies and directional) we can estimate, the so called, "spectral knees", the most important feature controlling the overall dose astronauts and crew and passengers of over-polar flights can collect. If the spectral knee is located at 1 MeV there is no danger, but if at 50 MeV, it is a serious radiation dose risk for astronauts and passengers of over-polar flights.

# 3. Space Environment Viewing and Analysis Network (SEVAN)

Ground based particle detectors measure time series of secondary particles born in cascades originated in the atmosphere by primary ions and solar neutrons. The networks of particle detectors can predict the upcoming geomagnetic and radiation storms hours before the Interplanetary Coronal M ass Ejection (ICME) arrival at the ACE and SOHO spacecrafts. The less than hour hour lead time (the time span of ICME travel from spacecrafts to magnetosphere) provided the particle detectors located at ACE and SOHO at libration point 1,5 million kilometers far from the Earth is short to take effective mitigation actions and protect satellites and surface industries from the harm of major geomagnetic storms.

To establish a reliable and timely forecasting service, we need to measure, model and compare:

- time series of neutrons and high energy muons;
- the correlations between changing fluxes of secondary particles; and
- the direction of the detected secondary cosmic rays.

Using our experience (see Chilingarian, et al., 2005; Gevorgyan, et al., 2005; Chilingarian et al., 2003a; Chilingarian, et al., 2003b, Chilingarian et al., 2007, Chilingarian and Reymers, 2007, Bostanjyan et al., 2007) with data analysis of multivariate time-series from ASEC monitors, we designed and fabricated a new-type of particle detector to meet the above goals, named SEVAN ( Space Environment Viewing and Analysis Network)

In order to keep the instruments inexpensive, the options are kept flexible by using modular designs. The price of a fully autonomous basic detector, with facility to send data to the internet will not exceed $20,000 US. For this reason the network of countries involved in space research can be significantly expanded, which will facilitate their part in International Heliophysical Year - 2007 (IHY – 2007).

At any time one can add additional similar units to achieve improved functionality: for example, add several new observational directions and enhance accuracy of particle fluxes measurements. As a world-wide network of neutron monitors (NM, Moraal et. al., 2000), the new monitors will measure neutron fluxes and, additionally, charged particle fluxes with different energy thresholds, thus allowing to investigate the additional populations of primary ions. These units plan to be deployed at universities and research centers of developing countries to perform survey and monitoring of the most dangerous space storms and involve new generations of students and scientists in space research.

The network is planned to be installed at middle and low latitudes. It will be compatible with the currently operating high-latitude neutron monitors network “Spaceship Earth” (Kuwabara et al, 2006), coordinated by the Bartol Research Center, with Solar Neutron Telescopes network coordinated by the Nagoya University (Tsuchiya et al., 2001), with the Muon network coordinated by the group from Shinshu University (Munakata et al., 2000) and with Athens Neutron Monitor Data Processing Center (Mavromichalaki et al, 2005, 2006).

The potential recipients of particle detectors in this new initiative are Croatia, Slovakia, Costa Rica, Bulgaria, Indonesia, and India (see Figure 22 and Table 5). When fully deployed the SEVAN network will provide the reliable monitoring of Sun by as minimum one detector 22 hours and by 2 detectors 18 hours of a day. We assume that particle fluxes measured by the new network at medium to low latitudes, combined with information from satellites and particle detector networks at high latitudes will provide experimental evidence on the most energetic processes in solar system and will constitute important element of the global space weather monitoring and forecasting service. In the paper we present results of the intensive simulation studies revealing the characteristics of the SEVAN network basic measuring module. We illustrate possibilities of the hybrid particle detectors to measure neutral and charged fluxes of secondary CR, estimate efficiency and purity of detection; corresponding median energies of the primary proton flux, ability to distinguish between neutron and proton initiated GLEs and some other important properties of hybrid particle detectors.


**Figure 23 Possible locations of Space Environment Viewing and Analysis Network (SEVAN)**

**Table 5 Geophysical characteristics of possible SEVAN sites.**

| Station | | Latitude | Longitude | Altitude [m] | $R_c$ (GV) |
|---|---|---|---|---|---|
| **Germany** | (Greifswald) | 54.5N | 13.23E | 6 | 2.34 |
| **Slovakia** | (Lomnicky Stit) | 49.2N | 20.22E | 2634 | 3.88 |
| **Croatia** | (Zagreb) | 45.82N | 15.97E | 120 | 4.89 |
| **Bulgaria** | (Musala) | 42.1N | 23.35E | 2430 | 6.19 |
| **Armenia** | (Aragats1) | 40.25N | 44.15E | 3200 | 7.1 |
| **Armenia** | (Aragats2) | 40.25N | 44.15E | 2000 | 7.1 |
| **Israel** | (Hermon) | 33.18N | 35.47E | 2025 | 10.39 |
| **Costa Rica** | (San Jose) | 10.0N | 84.0W | 1.2 | 10.99 |
| **China** | (Tibet) | 30.11N | 90.53E | 4300 | 13.86 |
| **India** | (Delhi) | 28.61N | 77.23E | 239 | 14.14 |
| **Indonesia** | (Jakarta) | 6.11S | 106.45E | 8 | 16.03 |

### 3.1 Construction of SEVAN particle detectors

The basic detecting unit of the SEVAN network (see Figure 22) is assembled from standard slabs of 50x50x5cm$^3$ plastic scintillators. Between 2 identical assemblies of 100 x 100 x 5 cm$^3$ scintillators (four standard slabs) are located two 100 x 100 x 5 cm$^3$ lead absorbers and thick 50 x 50 x 25 cm$^3$ scintillator assembly (5 standard slabs). A scintillator light capture cone and Photo Multiplier Tube (PMT) are located on the top, bottom and the intermediate layers of detector. The detailed detector charts with all sizes are available from http://crdlx5.yerphi.am/.

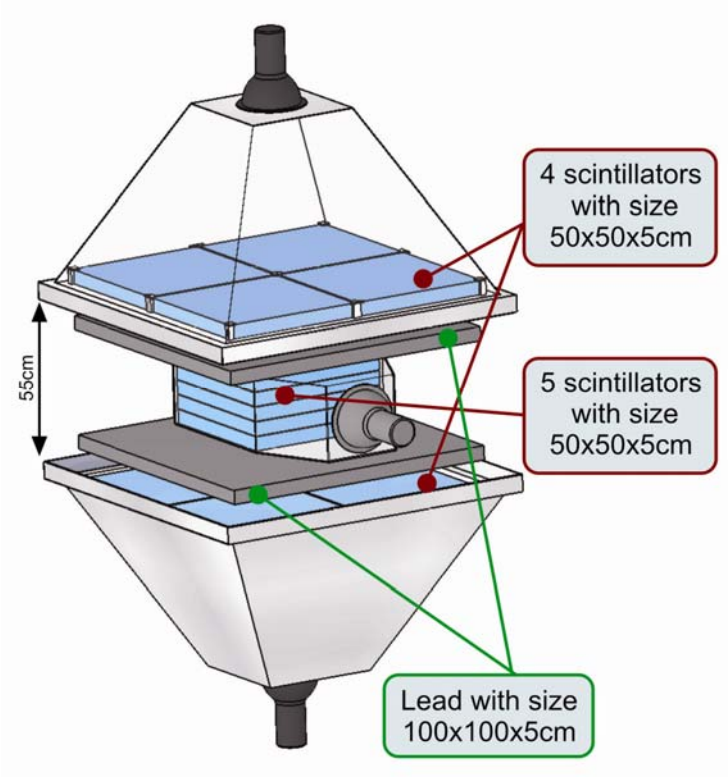


**Figure 24 Basic detecting unit of the SEVAN network**

Incoming neutral particles undergo nuclear reactions in the thick 25 cm plastic scintillator and produce protons and other charged particles. In the upper 5 cm thick scintillator charged particles are registered very effectively; however for the nuclear interactions of neutral particles there is not enough substance. When a neutral particle traverses the top thin (5cm) scintillator, usually no signal is produced. The absence of the signal in the upper scintillators, coinciding with the signal in the middle scintillator, points to neutral particle detection. The coincidence of signals from the top and bottom scintillators indicates traversal of high energy muons. Lead absorbers improve efficiency of the neutral flux detection and filtered low energy charged particles. If we denote by "1" the signal from scintillator and by "0" the absence of signal, the following combinations of the 3-layered detector output are possible:

111 – traversal of high energy muon;

011 and 010 – traversal of the neutral particle;

100 – traversal of low energy charged particle stopped in the scintillator or in the first lead absorber.

110 – traversal of higher energy charged particle stopped in the second lead absorber.

001 – registration of the inclined charged particles.

Microcontroller based Data Acquisition (DAQ) electronics and Advanced Data Analysis System (ADAS) provide registration and storage of all logical combinations of the detector signals for further off-line analysis and for on-line alerts issuing. The slow control system as ADAS subsystem allows providing the remote control of the PMT high voltage and important parameters of the DAQ electronics.

### 3.2 SEVAN DAQ Electronics

Data Acquisition electronics (see Figure 23) implementing registration of the charged and neutral fluxes of secondary cosmic rays consists of 8-Channel Discriminator/Counter Unit (8DCU) and 3 High Voltage supplies with presetting and automatic control, which are located in the corresponding PMT cases.

8DCU parts are:

- The 8-channel Programmable Threshold Comparator and Counter board (8CNT)
- Universal RS232/RS485 interface/power supply module - IFCC,
- Power transformer - 220V50Hz to 2x8V 0.5A + 2x15V 1.25A

The main features used in 8DCU are:

- 8 programmable threshold analog input,
- Threshold programming range 4mV-1000mV with 4mV step,
- Powered by AC 50-60Hz 220V, 30W
- Maximal counting frequency – 60kHz,
- LEDs to indicate the input pulses in each of 8channels, module power and programmable trigger condition,
- 8 input BNC connectors,

8CNT board is used as a standalone 8-channel counter (scalar) with programmable threshold. For the thresholds programming and the output data readout it can communicate to the host PC (local network) through the IFCC module by any of RS-232 or RS-485 interface ports.

The module counter and interface logic is based on the Atmel AVR Atmega88 8-bit microcontroller.

DAQ software consists of the host PC program and the microcontroller program (firmware). The firmware for the DAQ and control is written in C language and stored in the microcontroller reprogrammable flash memory. Below is presented the functionality, implemented for the SEVAN detector setup. In this case the microcontroller operates both for the thresholds presetting and control and as a main DAQ controller, with listed below functions:

1. Counting of signals in each of 8 channels,
2. Counting of all types of coincidences of signals in channels 1-3.

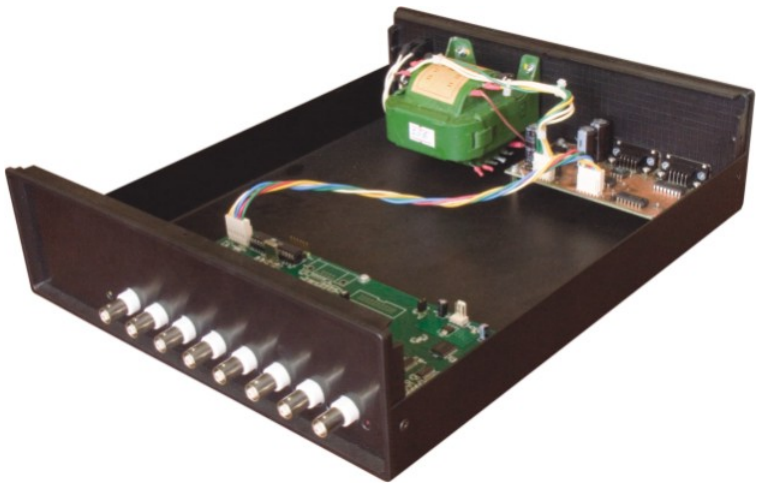

**Figure 21 8 channel DAQ electronics for SEVAN detector**

The counters contents are sent out via RS232 or/and RS485 interfaces each second in format:

Cnt1 Cnt2 Cnt3 Cnt4 Cnt5 Cnt6 Cnt7 Cnt8
Co12 Co13 Co23 Co123
<blank line>

where CntX – is the count of pulses in channel X in 1 second, CoXY(Z) – is the count of coincidences in channels X, Y. For example, Co12 is a number of coincidences in channels 1 and 2, without signals in channel 3.

The gate for the coincidences registration is in range 0.6us - 1us. If signals in two channels come with delay more than 1us, they are not considered as coincident.

The dead time of counters is 10us.

The data collection time is set by the microcontroller firmware, so any other value can be chosen.

The IFCC interface module has three connections: to the microcontroller, to the RS232 connector (DSUB9F) and RS485 connector (DSUB9M). The signals propagate from each of the mentioned connections to both of others. For example:

1. Microcontroller sends a byte to the TXD line. This byte is propagated both through RS232 TXD line and RS485 interface lines with corresponding voltage levels and polarities.
2. Byte is received in the RS485 line. It appears also on the microcontroller RXD line and the RS232 TXD line.
3. Byte received in the RS232 RXD line is transmitted to the microcontroller RXD line and RS485 interface lines.

In this way the IFCC module can operate coupled with a microcontroller.

The power for the PMT High Voltage supplies (15V unregulated, 1.2Amax) is supplied from the 8DCU through the RS485 interface connector.

## 3.3 Advanced Data Acquisition System for SEVAN (ADAS for SEVAN = ADASS)

### 3.3.1. Unified Readout and Control Server (URCS)

The ADAS (Chilingaryan, 2006) was developed having in mind the distributed nature of particle detector networks consisting of units hardly accessible world-wide. Therefore, the system is designed for the autonomous operation, error recovery and remote management capabilities. To simplify cooperation of research groups and open a way for data integration with other particle detection networks the inter component communication is released on top of high level standards. The new extensible XML based data format is used for the data storage and exchange.

ADASS is constructed from uniform autonomous components providing standard web service based control interfaces, named URCS (Unified Readout and Control Server). The URCS server make available readout of experimental data from SEVAN particle detectors provides detector control, preliminary analysis and distribution of the data to other system components. The URCS server is not dependent on any external information and can operate without connection to the rest of the data acquisition network for a long time.

To prevent information loss the collected data is stored in local data storage and distributed to clients by special automated WEB services. This service provide structured access to the collected data and, therefore, facilitates cooperation with remote system components giving a chance to correlate the obtained data with the data collected by other SEVAN detectors world-wide.

URCS server provides a set of control interfaces for both detector electronics and URCS software. On the basis of these control interfaces the WEB frontend provides the operator with a full set of remote management capabilities.

In addition to the URCS servers the ADASS incorporates alarm services, data storage subsystems running on file local servers. The alarm service is used to issue e-mail notifications about severe conditions of Space Weather or/and electronic failures. The data storage servers are periodically inquiring the data from all URCS servers and storing it in a database on reliable servers in each of the SEVAN sites. Further, the stored data is analyzed by off-line software and made available for the physical analysis by means of DVIN (Data Visualization Interactive Network, Yeghikyan and Chilingarian, 2005) interface. The Figure 24 presents the overall system design, realized at Aragats Space Environmental Center (Chilingarian et al., 2005).

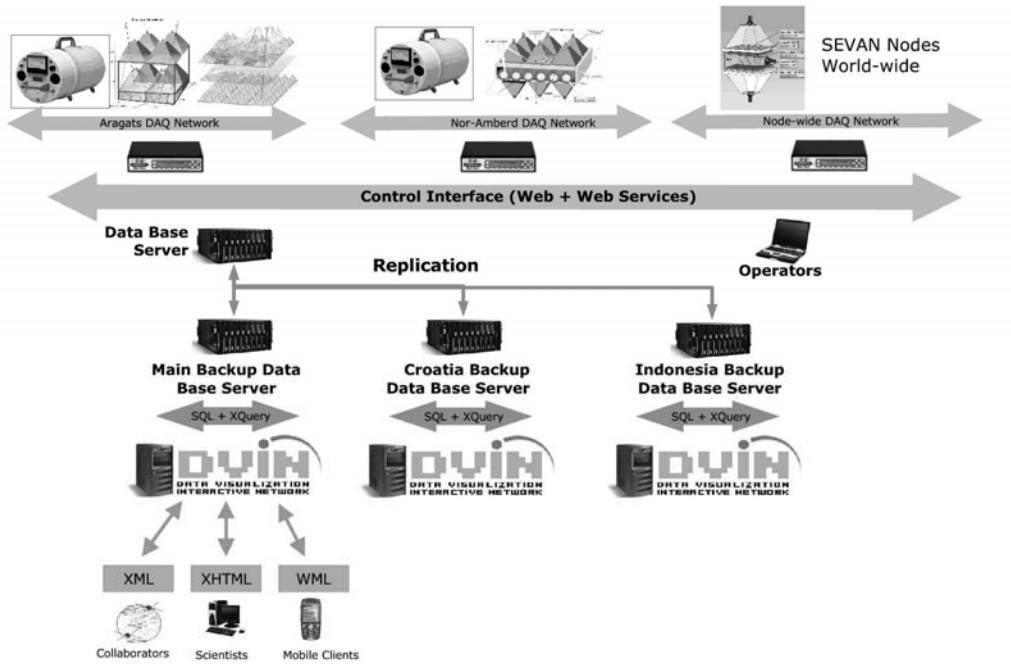


**Figure 22 Layout of the new ASEC data acquisition system. Several detector arrays are operating at Nor-Amberd and Aragats research stations. The detectors are controlled by URCS which are installed on each station. The data dissemination and detector control is performed by web services. The DVIN is used to distribute the data to end users.**

### 3.3.2. Embedded Software

The readout electronics of SEVAN particle monitor is described in the previous section. The embedded software is implemented using double buffer client-server architecture.

At first the devices are initialized in a dummy mode waiting for the control from the host system.

In order to reduce the amount of data transferred between embedded and host systems the first stage of data processing is performed on the embedded system. The embedded software counts the number of events registered on each of the detector channels as well as coincidences between all 3 SEVAN channels.

Embedded software expects what the host system is periodically issuing requests in order to retrieve the data. The double buffer architecture is used to relax timing demands. While the current data is prepared in the first buffer, the data of previous operation is available from the second one upon a driver request. After the data in the first buffer is ready, the buffers are switched. The data consistency is assured using CRC16 checksums carried along with data.

Besides the data retrieval the host system may control various parameters of the underlying electronics.

As a part of startup procedure the host system passes desired configuration (channel thresholds, time spans, etc...) to the embedded system, establishes time synchronization and issues initialization command. On each of iterations the time synchronization between host and embedded systems is checked. In the case of minor synchronization errors a time correction procedure is performed. If the error exceeds defined thresholds the embedded system is reinitialized and time synchronization is re-obtained.

### 3.3.3. Frontend Computers

In order to improve the system stability we plan to use the Minibox M300 (VIA C7 800MHZ, 1 GB RAM computers based on VIA Eden platform (URL: http://www.mini-box.com/ ). The computers are equipped with Gentoo Linux based operating system which is used in conjunction

with the 2.6 family Linux kernel optimized for the real-time applications. The major advantage of the platform is the complete absence of any moving mechanical parts. The system has passive (fan-less) cooling. Instead of a hard drive, the CF (Compact Flash) memory card is used. A small

LCD keypad embedded into the computers is used to represent current system status, notify operators about critical failures and provides a way for basic system management.

The particle monitors are connected to the frontend computers by means of the USB and Ethernet interfaces.

### 3.3.4. Unified Readout and Control Server

The URCS (Unified Readout and Control Server) server is a completely autonomous component of the data acquisition network. It is operating on the frontend computers and used for detector control and data readout. It is not dependent on any external information and can operate without connection to the rest of the data acquisition network for a long period of time. To prevent the information loss the collected data is stored on the local Compact Flash card and served to the clients upon requests. The amount of time the data remains stored on the server depends on the detector data bandwidth and may be controlled by the operator.

The URCS server is complex software consisting of multiple interacting components. In the first place it is a URCS daemon - a readout software which take care of communication with underlying electronics. The communication is performed by means of dedicated drivers while most of the software is the same for all supported detectors. The daemon reads the data from underlying detectors makes preliminary analysis if necessary and stores it in the files on the local file system. Furthermore, it hides detector access details from other URCS components providing a uniform way for the detector monitoring and control. The detailed architecture of the URCS daemon is provided in the next section.

### 3.3.5. URCS Control Interface

The communication with remote components is carried out by means of web services running on a Apache web server. These web services hide the details of the URCS daemon providing a very simple interface for both the data dissemination and control capabilities to the external world. The data access is well structured. Each underlying particle monitor has its own address space and may provide to end client one or more independent data sets. The data channels in all data sets are described by metadata properties. These properties may include information on SEVAN sites (names of destination, geographical co-ordinates, altitudes, cut-off rigidities, etc). The set of properties describing all data sets belonging to a certain SEVAN site are collected in the site description and are available to the clients upon a request as well.

The client applications are able to request the latest data from the desired data set or the data for certain historical periods.

### 3.3.6. URCS Operator Frontend

The operator web frontend is a URCS component providing a uniform way for the remote control of URCS servers and underlying electronics. By means of the interface the operator is able to perform a full range of monitoring and control operations. It is possible to view various aspects of the current URCS operation, modify actual configurations, start and stop readout daemons or access the URCS log files for the desired period.

The operator is able to browse the data stored on the remote URCS servers. The current data is presented in a fully annotated fashion using associated detector descriptions. The historical data is available in XML, HTML and/or CSV (Comma-Separated Values) forms. The continuous data quality monitoring is feasible by the provided AJAX (Asynchronous JavaScript and XML) interface which is depicting various aspects of the most recent data by means of SVG (Scalar Vector Graphics) charts. Additionally, metadata properties specify special conditions demanding the operator intervention. If such condition is met the interface will signal an alarm to the operator.

The web frontend is used as well to control the URCS configuration, including configurations of the underlying electronic devices. All system configurations are expressed in XML terms and, therefore, the uniform XForms (XML Forms) based interface is used to control all detectors and URCS itself. For each detector only the XForms representation providing mapping between UI (User Interface) elements and XML nodes in configuration is specified. The XForms engine processes user interactions and submits the altered XML configuration to the URCS server.

The

URCS server processes global configuration options and passes the individual information for the URCS drivers. To provide XForms functionality in XForms incapable browsers extra application (”FormFaces”) is used.

### 3.3.7. URCS Installation and Upgrade

The usage of CF (Compact Flash) cards drastically simplifies the software installation and upgrade. The installation can be performed on any computer equipped with CF card reader facility. The installation software asks several questions on the URCS configuration (Name, IP address, Type of Hardware etc.), then, install all required system files, URCS software and configuration files on a provided CF disk.

To upgrade URCS software on the running system it is only needed to replace current CF card with a newer one. This operation is very simple and can be performed by the technical staff.

### 3.3.8. Detector Network

The URCS daemon communicates with the data acquisition electronics using a Ethernet interfaceby means of UDP or TCP protocols. The Ethernet segment connecting to the detectors is isolated from the outer world in order to avoid unauthorized access and data corruption. Only a frontend computer running the URCS server is connected to this segment. In order to obtain the network address the connected devices are issuing a discovery request by means of the DHCP (Dynamic Host Configuration Protocol). The frontend computer accepts the request and assigns an IP address from the dedicated pool.

Usually, all operating detectors are listed along with their IP addresses in the URCS configuration file. However, it is possible to specify the IP range and default configuration in order to enable the device auto detection. In this case the URCS server will probe all IP’s in the range using discovery command. The identified detectors will be initialized using specified default configuration.

### 3.3.9. Configuration

The operation of a device is controlled by means of an XML configuration. The configuration is initialized from the supported URCS configuration file and mapped into the server memory using a DOM (Document Object Model) representation. The operators are able to adjust configuration using provided web interface.

The configuration structure is completely device specific. The DOM in-memory is passed to the device driver. It is up to the driver to process configuration and extract required information.

The device configuration consists of several parts. One part is controlling the driver operation.

It includes connection properties (type, address, timeouts), a list of writers to use for the data storage, properties of the data preprocessing algorithms and etc. Another part controls the detector hardware operation and is passed by the driver to the detector’s embedded software.

The configuration structure is described by the XML Schema Description. Both the current configuration and this schema description are used to generate XForms entries providing control interfaces.

### 3.3.10. Error Handling

The URCS server allows auto-recovery from system failures. In the case of a hardware failure the problem is logged and the controlling driver performs the hardware re-initialization. Most of

possible software problems are handled internally. If a non-recoverable error is encountered the daemon leave a emergency message in the log. In the last case it would be automatically restarted by a special system daemon which is monitoring status of all URCS components and restarting them in the case of a detected problem.

### 3.3.11. Data Format

To simplify cooperation of SEVAN research groups, to enable data processing automation and to open a way for integration of all SEVAN sites new extensible XML based data format is developed for the data storage and exchange.

The ADASS data is consisting of two components:

- Collected data along with several properties characterizing the data, including the data timestamp, data quality, etc.
- SEVAN site description providing detailed information on the detector location and orientation.

The detector description consists of three main components: Global Detector Description, Detector Geometry and Logical Data Layout. The Global Detector Description provides standard metadata describing the whole detector. It contains detector name, country, institution, group, principal investigators contact information, geographical location, etc.

The Detector Geometry describes the detector component parts as well as their positions and dimensions.

The multiple Data Layout sections indicate the physical meaning and acceptable value ranges of the data values. The first two components are preliminary filled during the detector setup and the data layout is automatically generated by the URCS software. Still additional properties may be specified manually on the setup stage.

The data collected by each of the detectors are divided into one or more independent data sets. Each data set is represented as a sequence of data vectors associated with the acquisition time (time series) and one or more Data Layout records in the detector description. The multiple layout records are considered to handle cases when the data set structure is changing during the detector operation. In a way similar to one used by the old data acquisition system at Aragats the data is represented by “space” delimited ASCII strings. These ASCII strings are enclosed in the

XML structure providing basic information about the enclosed data and referencing appropriate

Data Layout sections of the detector description with the information on the values meaning.

Example:

```
<Data installation="installationid" layout="layoutid">
<Time>2006-02-25T16:50:00.0000000+04:00</Time>
<Duration>PT30.0000000S</Duration>
<Quality>100.00</Quality>
<Value> 12013 3954 5217 0 956 394 828 1488</Value>
</Data>
```

This example illustrates the representation of a single data element by the ADASS format.

The installation and layout attributes are referencing the appropriate layout in the detector description. The Time and Duration elements are indicating the end and duration of the data integration time slice (both the timestamp and duration are represented following the encoding rules defined by the ISO-8601 specification). Special conditions encountered during the data acquisition are described using Quality element. Usually, this element indicates hardware failures resulting in partly or completely inaccurate data. The Value element holds a data vector in the space delimited ASCII representation.

The data storage subsystem at file servers downloads the data from the URCS server and stores it in the MySQL database. For each data set a separate table is created and for each attribute and element (installation, layout, Time, Duration, Quality) an individual column is used. All values will be represented by individual columns as well. Such mapping allows easy and fast access to the data, while the original XML form could be easily recovered. The description is not transported

together with the collected data but available upon request from the URCS servers. However, the collected data and detector description can be reconciled in a single document for data exchange with collaborating groups.

Using the described approach the legacy application can easily extract ASCII strings from the data set and use them in the old fashion. The new applications are considering the XML description in order to extract the appropriate data subset from the data set.

### 3.4 Calculation of the efficiencies, energy thresholds and count rates of SEVAN particle detectors

To quantify statements about the detection of different types of particles by the SEVAN modules, we need to perform detailed simulation of the detector response. We use simulated cascades of the charged and neutral secondary particles obtained with the CORSIKA (version 6.204) Monte Carlo code (Heck, et al., 1998). The threshold energies for the primary particles assumed as input for CORSIKA correspond to the vertical cutoff rigidity of the detector locations (see Table 2). All secondary particles were tracked until their energy drops below the predetermined value (50 MeV for hadrons, 10 MeV for muons and 6 MeV for electrons and photons) or reached all the way to the ground level. The spectra of primary protons and helium nuclei (99% of the flux at energies up to 100 GeV) are selected to follow the proton and helium spectra reported by CAPRICE98 balloon-borne experiment (Boezio, et al., 2003).

Among different species of secondary particles, generated in nuclear-electromagnetic cascades in the atmosphere, muons, electrons, $\gamma$ – s, neutrons, protons, pions and kaons were followed with CORSIKA and stored. These particles were used as input for the GEANT3 package (GEANT, 1993), implemented for detector response simulation. Also, we take into account the light absorption in the scintillator.

The efficiency of the charged particle detection by all 3 layers of SEVAN detector is about 95%; the neutron detection efficiency in the middle "thick" scintillator reaches 30% at 200 MeV, the efficiency of γ-quanta detection reaches 60% at the same energies. Responses of all SEVAN detecting layers to the "background" Galactic cosmic rays are presented in Figures 24-26. The figures show that different layers are sensitive to different particles. While the upper layer is "selecting" mostly electrons and muons, the middle layer is more sensitive to neutrals and the lower layer to the high energy muons. Also, it is apparent from the figures that the best location for SEVAN detector is at high altitudes, although its location at the sea level also would provide valuable information on neutral and charged fluxes. The lead absorbers filter low energy electrons and gammas. Figure 28 shows that the lower layer is sensitive to the high energy muon flux with the threshold energy ~250 MeV.

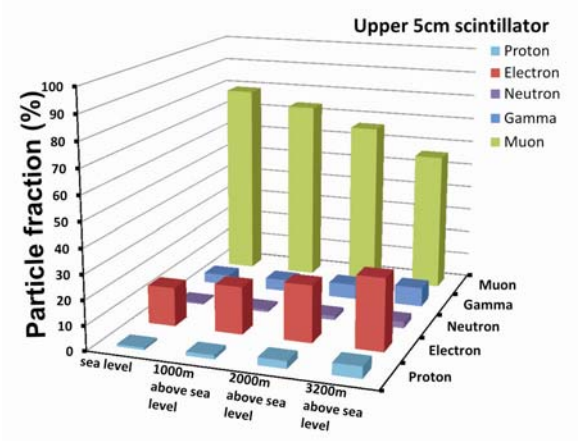


**Figure 27 Fractions of elementary particles detected by the upper layer of SEVAN detector**

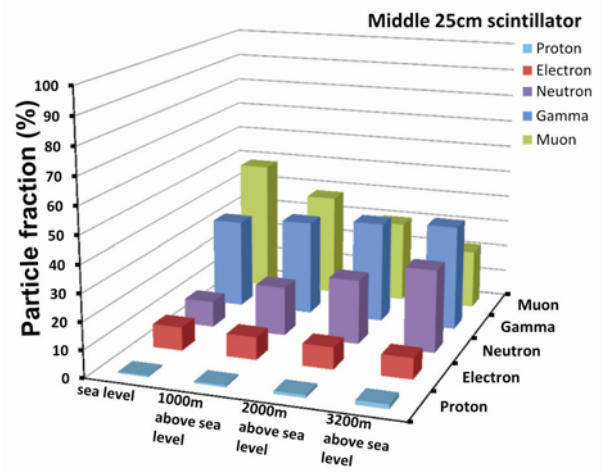


**Figure 28 Fractions of elementary particles detected by the middle layer of SEVAN detector**

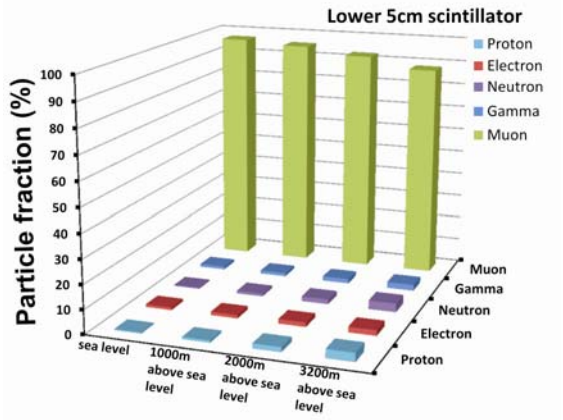


**Figure 29 Fractions of elementary particles detected by the lower layer of SEVAN detector**

The middle scintillator of the SEVAN detector intended to select neutrons is also sensitive to γ-quanta. Figure 25 shows that the fraction of the γ-quanta in particles detected by the middle thick SEVAN scintillator is higher than the fraction of neutrons for all latitudes. This contamination of the gammas can significantly deteriorate the ability of SEVAN detector to indicate the enhancement of the count rate caused by the additional flux of solar neutrons. The upper 5 cm. detector, of course, cannot exclude the neutral gammas, as it is excluded charged muons and electrons. For the distinguishing of the gammas we propose using the sandwich system of two 1 cm scintillators with an additional 1 cm layer of lead in between instead of the 5 cm scintillator, see Figure 27. The 1 cm scintillator under the 1 cm of lead will effectively detect γ-quanta by electron-positron pairs generated in lead. In turn probability of the nuclear interaction of neutrons in 1 cm of lead is much less and neutrons will escape from detection in the beneath 1 cm lead. Thus, the scintillator above 1 cm lead will reject muons and electrons and scintillator below the 1 cm lead will distinguish and reject gammas (see details in Reymers, 2007).

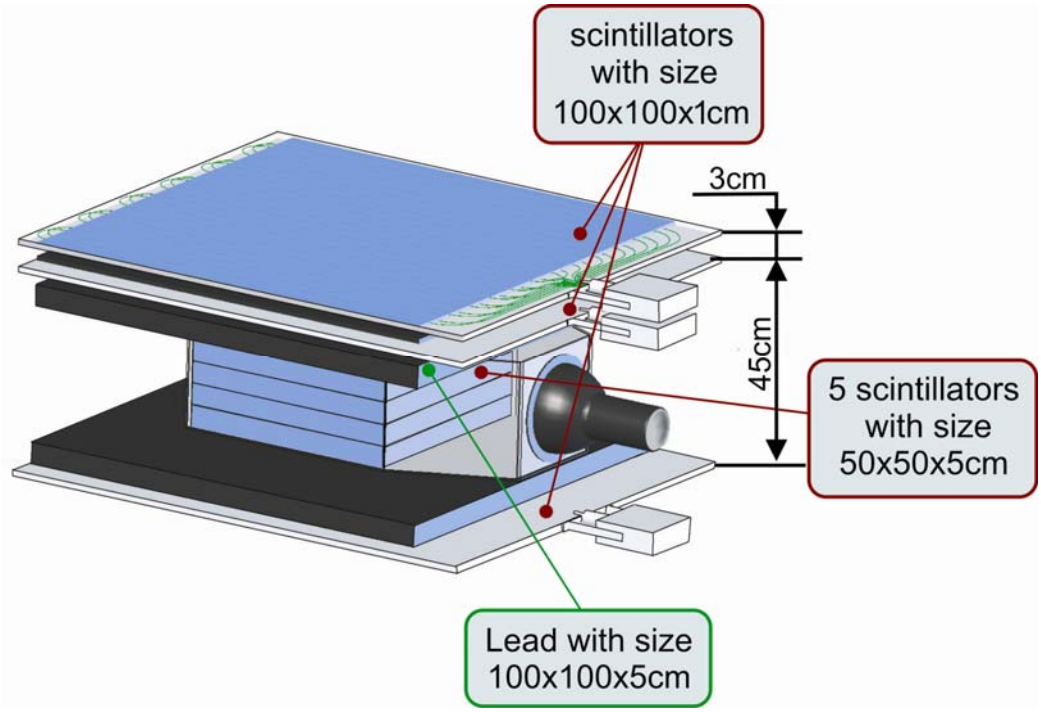


**Figure 30 4 layered basic unit of the SEVAN.**

If we again denote by "1" the signal from scintillator and by "0" the absence of signal, the following combinations of the 4-layered detector are of special interest:

1000 – low energy charged particle stopped in 1 cm of lead;

1100 – low energy charged particle stopped in 5 cm of lead;

0100 – low energy neutral particle mostly (γ-quanta) giving cascade in 1 cm of lead absorbed in 5 cm of lead

0110 - high energy neutral particle (γ-quanta or neutron) giving cascades both in 1 cm of lead and in 5 cm of lead

1110 – charged particle (muon) traversing 6 cm of lead;

1111 – traversal of high energy muon;

0010 – neutral particle (mostly neutron);

0011 – neutral particle (mostly neutron) generating large cascade in thick scintillator.

Table 6 compares the purity of neutron detection by both detector setups. Using the improved detector we not only suppress twice contamination of gamma quanta, but also improve the efficiency of neutron detection. "Resolving" the neutral flux to the neutron and gamma fractions will help to investigate complicated neutron GLE events like the event on November 28$^{th}$, 1998. From (Muraki, 2005) it is apparent that the knowledge of both gamma and neutron fluxes highly improved the understanding of the event origin.

**Table 6 Percent of different secondary particles detected by 25 cm thick scintillator in 2 versions of the SEVAN (Aragats station at 3200 above sea level).**

| | Electrons | Muons | Gamma | Neutrons | Protons |
|---|---|---|---|---|---|
| Veto 5cm Scintillator | 6.8 | 16.4 | 40.2 | 35.6 | 1 |
| Veto 1cm Scin.+ 1cm Lead + 1cm Scin. | 7.4 | 22.3 | 23.7 | 45.3 | 1.3 |

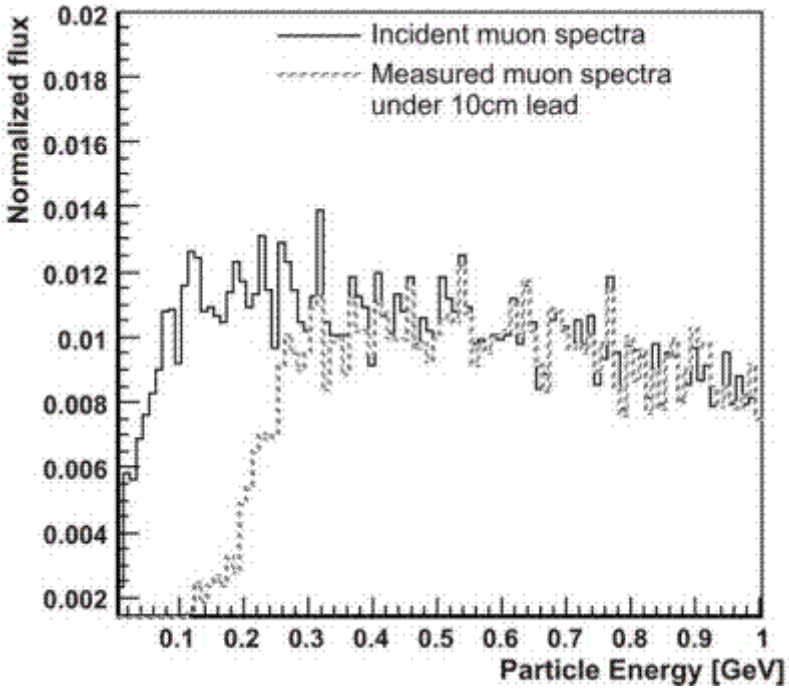


**Figure 31 The energy spectra of muons registered in upper and bottom 5 cm thick scintillators. The energy threshold of upper scintillator is ~7 MeV, bottom – ~250 MeV**

### 3.5 Calculation of the response of SEVAN particle detectors to Galactic and Solar Cosmic Rays (GCR and SCR).

Fluxes of secondary particles measured by the SEVAN detector are sensitive to different populations of the primary particles incident on the terrestrial atmosphere. Each type of the detected secondary particle (neutron, low energy electrons and muons, high energy muons) is produced by the primary solar and galactic ions having rather broad energy distributions. Nonetheless, the most probable energies corresponding to different secondary particles are shifted relative to each other. In Table 7 are presented the most probable energies (medians of the energy distribution of the parent protons) of primary protons producing in the terrestrial atmosphere different elementary particles. From the Table we can see that secondary muons and electrons are produced by the protons with higher primary energies comparing with secondary neutrons and protons.

**Table 7 The most probable energies of the Galactic protons corresponding to the different types of secondary particles at 3200m above the sea level.**

| Secondary particle type at 3200m | Most probable energy of GCR (GeV) |
|---|---|
| **Neutron** | 8.5 |
| **Proton** | 8.5 |
| **Gamma** | 10.5 |
| **Electron** | 11.5 |
| **Muon** | 12.5 |

Table 8**Error! Reference source not found.** demonstrates most probable energies of primary protons "selected" by the layers of the SEVAN detector. The difference of 8.5 and 14.5 GeV of the most probable energy of the primaries is significant if we take into consideration that differential energy spectra of GCRs is rapidly attenuated according to the power law with index of ~-2.7

**Table 8 Modes of the GCR Energy spectra corresponding to different species of secondary particles registered by SEVAN detector at 3200m above the sea level.**

| Layers of detector Located at 3200m | Most probable energy of GCR (GeV) |
|---|---|
| **Upper Layer** | 11.5 |
| **Middle 25cm layer** | 8.5 |
| **Down Layer** | 14.5 |

In Figure 29 we present the energy spectra of the primary protons of SCRs selected conditionally on SEVAN detector layer where signal was registered. The initial energy spectra were simulated according power function $E^{\gamma}$ with spectral index $\gamma = -4$.

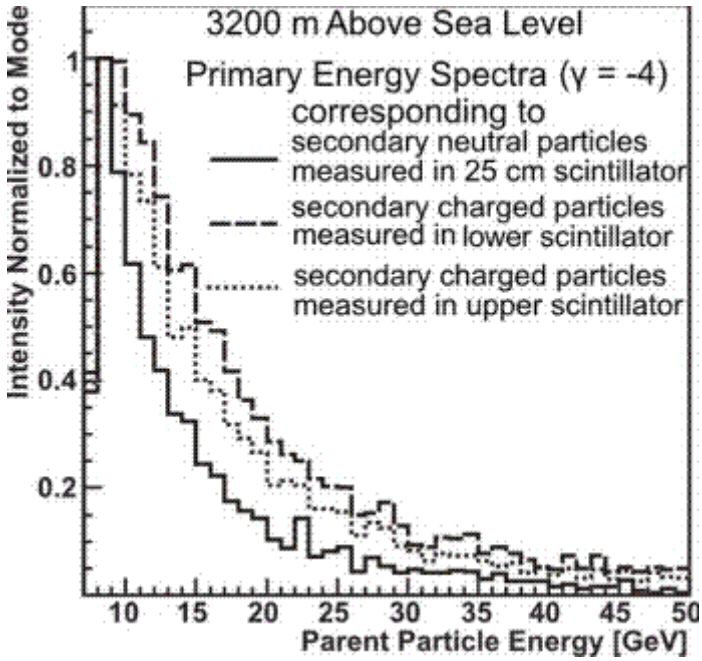


**Figure 32 Primary ("parent") SCR (power index equals to -4) protons spectra initiated counts in different layers of the SEVAN detector.**

The large energy spectra index of the SCRs at highest energies ($\gamma \geq -5$, hard spectra; usually SCR spectra is very steep at GeV energies: $\gamma \leq -7$) is a very good indicator of upcoming abundant SCR protons and ions with energies >50 MeV, extremely dangerous for the astronauts and high transpolar flights, as well as for satellite electronics.

Therefore, it is very important to estimate the index of power law. In (Lockwood, et al., 2002) was proposed to estimate the energy spectra index using the data of NM located as the same latitude but at different altitudes. The same methodology has been recently used for the determination of the radiation dozes received on-board airplanes during solar particle events (Lantos, 2005) and for estimating the spectral index of the 20 January 2005 GLE (for details of this outstanding event, see for example Plainaki, et al., 2007) using the data of the Aragats and Nor Amberd NM (Zazyan and Chilingaryan, 2005).

To simulate the proposed method of determination of the spectral index we need to know spectra of solar neutrons and protons above the atmosphere intense enough to generate significant enhancement at location of the ASEC monitors. The test neutron spectrum at the top of the terrestrial atmosphere was adopted from (Watanabe, et al., 2006):

$$I_n(E) = 176E^{-3.6}\left(\mathrm{m}^2 \cdot \mathrm{ster} \cdot \mathrm{sec} \cdot \mathrm{GeV}\right)^{-1}, E \in (0.1\text{–}2GeV) \qquad (1)$$

The spectra of secondary particles from the neutron traversal in the terrestrial atmosphere were obtained by the PLANETOCOSMICS code (http://cosray.unibe.ch/~laurent/planetocosmics/). The

majority of the secondary particles at 3200 m. are neutrons and gammas. The obtained spectra of secondary particles coincide well with the ones reported in (Shibata, 1994). The simulated test secondary fluxes were used as the input of GEANT3 code to simulate the detector's response.

The test solar proton spectra from 7 GeV (above the cutoff rigidity of Aragats station) to 30 GeV were adopted from (Zazyan and Chilingaryan, 2005) as follows:

$$I_p(E) = 4.1\times10^5 E^{-5}\left(\mathrm{m}^2\cdot\mathrm{ster}\cdot\mathrm{sec}\cdot\mathrm{GeV}\right)^{-1},\ (E \in 7.1-30GeV). \qquad (2)$$

The spectra of secondary particles were obtained in the same way as for the primary neutron flux. Proceeding from simulated enhancements initiated by the "proton" and "neutron" GLEs, it is possible to estimate the power law index of the SCR using the ratio of the enhancements of the neutron flux and low energy charged particles. We made simulations of the primary proton flux changing the power law index from -4 to -6. Figure 30 shows that the ratio of the neutral-to-charge flux is indeed sensitive to the power index abruptly decreasing with the decrease of the power index.

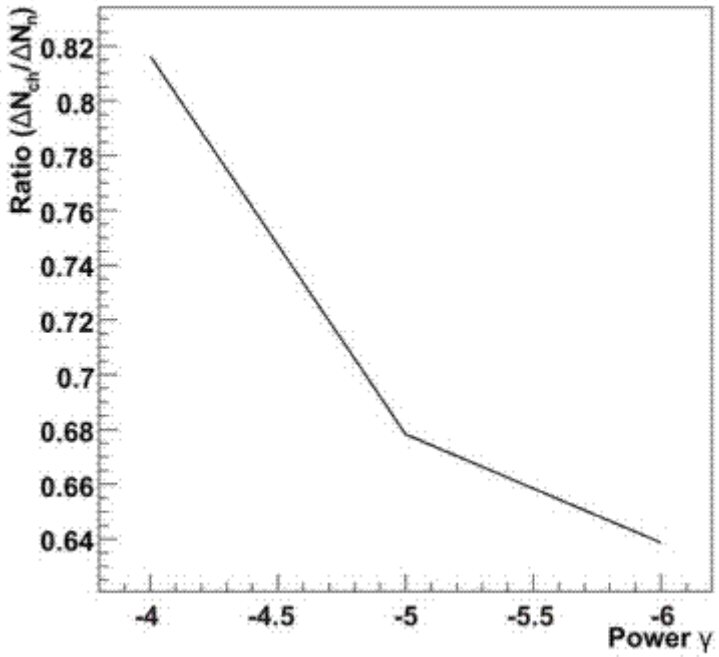


**Figure 33 The ratio of the enhancements of the flux of neutrons and low energy charged particles dependent on the power index of SCR**

The comparison of the count rate enhancement in SEVAN layers allows distinguishing very rare events of significant solar neutrons flux incident on terrestrial atmosphere. Table 9 shows that for neutron primaries there is a significant enhancement in the thick layer and much less enhancement in thin layer. For proton primaries the situation is visa-verse: the significant enhancement is in the thin layer, and thick layer did not demonstrate unambiguous additional flux.

**Table 9 Simulated enhancements (in standard deviations) of the "5-munute" count rates corresponding to fluxes of primary neutrons (1) and primary protons (2)**

| Detector layer | Solar Protons | Solar Neutrons |
|---|---|---|
| Upper 5 cm scintillator | 4.8σ | 2.6σ |
| Middle 25 cm scintillator | 1.7σ | 6.4σ |

### 3.6 Comparison of modeled and measured SEVAN count rates

At Nor – Amberd research station of ASEC starts tests operation of the SEVAN detector prototype with slightly reduced sizes: area of upper and lower 5-cm this scintillators are 0.65 $m^2$, instead of 1 $m^2$, and thickness of middle detector is 20 cm, instead of 25. The simulation of the detector response was made with this changed SEVAN geometric parameters in the same way as described in (Chilingarian and Reimers, 2007). The comparison of simulated and measured count rates are presented in the Table10.

**Table 10 Experimental and simulated one-minute count rates in the different layers of the SEVAN basic unit and different coincidences between 3 layers of the SEVAN (Thresholds to the registered energy releases equal to the 6.5 MeV); Altitude 2000 m.**

| | | Experimental count rate | simulated count rate |
|---|---|---|---|
| Upper Detector | | 12221 | 12581 |
| Middle Detector | | 3938 | 4526 |
| Lower Detector | | 5243 | 8017 |
| Coincidence | [110] | 952 | 752 |
| | [101] | 408 | 1567 |
| | [011] | 816 | 497 |
| | [111] | 1459 | 2561 |
| | [100] | 9402 | 7699 |
| | [010] | 710 | 715 |
| | [001] | 2561 | 3391 |
| | [011]+[010] | 1526 | 1212 |

10-30% enhancement of simulated upon measured count rates can be explained by uncertainties in the energy releases thresholds and in attenuation of the particle fluxes in the building where detector is located (first floor of 3-floored building). Nonetheless, the coincidence is satisfactory and we can draw several conclusions on the expected SEVAN operation. Different combination of the signals and absence of signals in 3 layers of SEVAN detector give possibility to select events enriched by low energy charged secondary particles, neutral particles and high energy muons (Chilingarian and Reimers, 2007). Following combinations are of upmost interest:

- The combination 100 (signal only in upper scintillator) represents flux of low energy charged particles (mostly electrons and muons) filtered by 5 cm of lead below upper scintillator;
- The sum of combinations 010 and 011 represents the neutral component of secondary CR flux, detected by nuclear interaction in "thick" scintillator with generation of charged particles;
- Combination 111 represents traversal of high energy muon with minimal energy 200 MeV;
- There exist also "exotic" channels, for example, – "trapping" of muon in lead and creation of a mesoatom – combination 110, but obviously signal of this effect is hidden by more frequent cases of filtering muon by the lower lead filter or by traversing of high energy electron throw first lead filter or nuclear interaction of neutral particle in upper scintillator with consequent birth of charged particles cascade reaching middle scintillator. For revealing of mesoatom cases we need more precise calculation of detector response

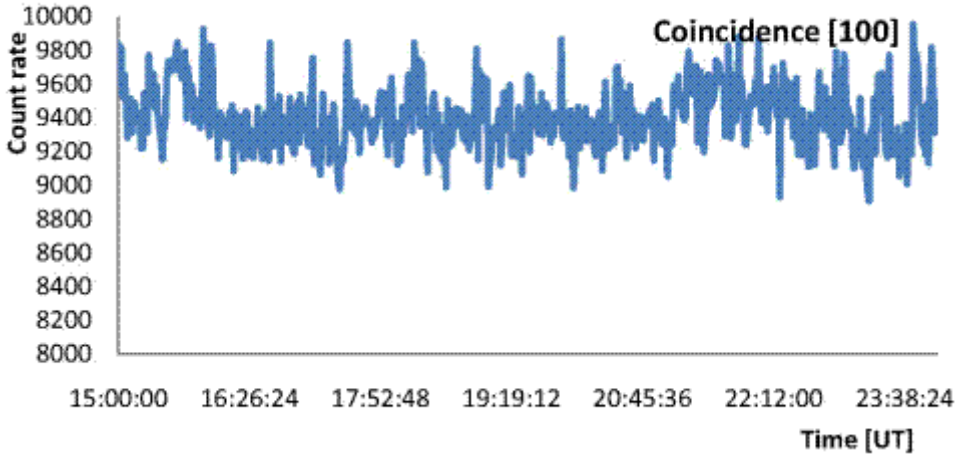


**Figure 34 Time series of low energy charged particles (mostly electrons and muons) detected by SEVAN module.**

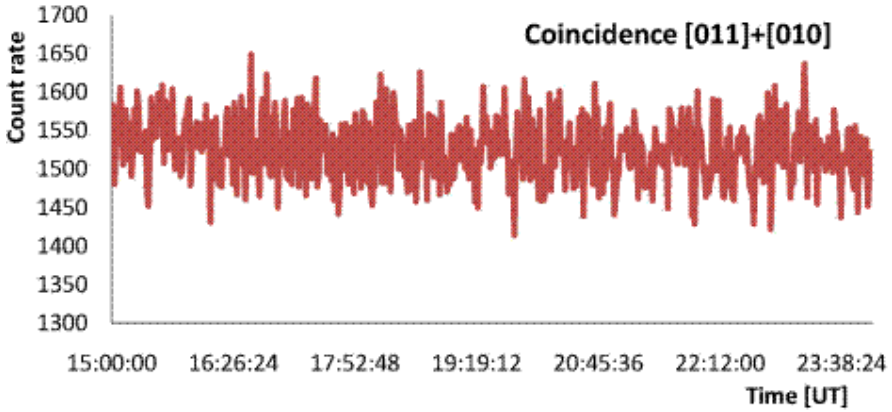


**Figure 35 Time series of neutral particles (mostly neutrons and gammas) detected by SEVAN module.**

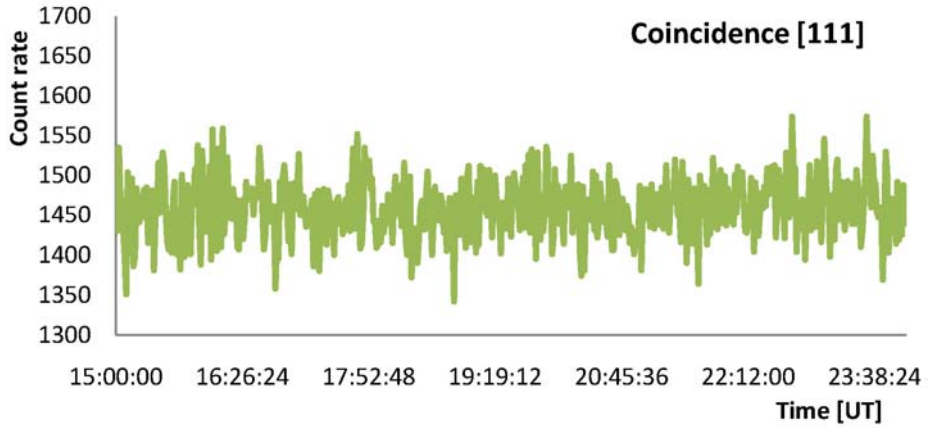


**Figure 36 Time series of high energy muons (E > 200 MeV) detected by SEVAN module.**

In the Figures 35-37 we present 1-minute time series of the different secondary particles born in atmosphere in interactions of the primary protons and ions of galactic cosmic rays. The purity of selected events and efficiency of registration were investigated in details in (Chilingarian and Reimers, 2007). As we can see in Table 11 SEVAN module is detected low energy charged component, neutral component and high energy muons with rather high accuracy.

**Table 11 One Minute Count rates of the secondary fluxes detected by SEVAN module.**

| Type of Secondary particle | Average | Standard deviation | Relative Error [%] |
|---|---|---|---|
| High energy muon | 1459 | 37 | 2.57 |
| Low energy charged particles | 9402 | 186 | 1.97 |
| Neutral particles | 1526 | 40 | 2.65 |

With SEVAN nodule it will be possible to detect modulation effects solar activity pose on galactic cosmic rays and magnetosphere, i.e. Forbush decreases and post-forbush increases of count rate due to coupling of “frozen” magnetic field of Interplanetary Coronal Mass Ejection (ICME). Also it will be possible to detect changes in count rates during travel of ICME from sun lasting 17-50 hours. Multivariate count rates can be used for forecasting of the severity of upcoming Geomagnetic storm. For detection of highest energy solar cosmic rays additional SEVAN modules should be installed, to improve signal-to-noise ratio. For reliable detection of Ground Level Enhancement (GLE) also additional SEVAN modules will be needed for, because at middle and low altitudes usually GLE do not exceed 2%. However for the extreme events like 1956, 1989 when count ray increase 50% even at middle latitudes GLE will be timely and reliably detected with one SEVAN module only.

# 4. Perspectives to create Planetary Space Weather forecasting service

Reliable forecasts of the major geomagnetic and radiation storms are of great importance because of associated Space Weather conditions leading to failures of space and earth surface based technologies as well as posing radiation hazard on crew and passengers of satellites and aircraft.

Measured solar and interplanetary parameters did not allow for reliable warning on severity of upcoming radiation and geomagnetic (GMS) storms (Kane, 2005). Measurements of the Solar Wind parameters performed at space station located at L1 libration point provide too short time span for mitigation actions. Another piece of valuable information on major storms is provided by networks of particle detectors located at Earth surface.

Networks of particle detectors on Earth surface will provide timely information and will be an important element of the creating planetary Space Weather warning services. Huge advantage of ground based particle detectors is its consistency, 24 hours coverage, multi-year operation. In contrast the planned life of the satellites and spacecraft is a few years only (STEREO – 2 years), they are affected by the same solar blast that they should alert, and space-born facilities instead of sending warning are usually set in the stand-by mode.

Multi-particle detectors proposed in the present paper will probe different populations of primary cosmic rays. The basic detector of the SEVAN network is designed to measure fluxes of neutrons and gammas, of low energy charged component and high energy muons. The rich information obtained from SEVAN network located mostly at low and middle latitudes will allow estimating the energy spectra of the highest energy SCR. SEVAN network will be sensitive to very weak fluxes of SCR above 10 GeV, a very poorly explored highest energy region. To understand the sensitivity of the new type of particle detectors to highest energy solar ions we investigate the response of SEVAN basic units to galactic and solar protons. The hard spectra of solar ions at highest energies ($\gamma \sim -4$ - -5 at rigidities $\geq 10$ GV) indicate the upcoming very intense solar ion flux with rigidities > 50 MV, very dangerous for satellite electronics and astronauts. The SEVAN network detectors will also allow distinguishing very rare and very important GLEs initiated by primary neutrons.

Summarizing, the hybrid particle detectors, measuring neutral and charged fluxes provide following advantages upon existing detector networks measuring single species of secondary CR:

- Enlarge statistical accuracy of measurements;
- Probe different populations of primary CR from 7 GV up to 20-30 GV;
- Reconstruct SCR spectra and determine position of the spectral “knees”;
- Classify GLEs in “neutron” or “proton” initiated events;
- Estimate and analyze correlation matrices between different fluxes;

SEVAN project was accepted by the United Nations Office for Outer Space Affairs and the International Heliophysical Year (IHY) in the small instrument program is envisioned as a partnership between instrument providers, and instrument hosts in developing countries as one of United Nations Basic Space Science (UNBSS) activity.

MOU’s with SEVAN network countries were signed, preparation of row materials and electronics for detector commission were done. In 2008 first SEVAN modules plan to be installed in Croatia, Bulgaria and India. In 2009 new modules will be installed in Slovakia, Costa Rica and Indonesia and network will be ready for research and Space Weather forecasting. Meanwhile several SEVAN detectors are under testing at research high-mountain stations on slopes of mountain Aragats in Armenia.

Future Space Weather forecast service need complicated system of measurements performed by space born facilities located as much as possible near to the sun, though it is extremely difficult technical problem. The proxies of near-sun facilities are the Space stations located at libration Lagrange point (1.5 mln km from Erath ant at geostationary orbit (40,000 km from Earth surface). Due to the small volumes of space-born particle detectors highest energy particles escape from the

detection of the satellite spectrometers. Therefore, large surface particle detectors can provide valuable information for the Space Weather forecast.

Detecting changing fluxes of high energy GCR (ICME modulation effects) we can prepare and certificate SW information products to be used for the forecasts by the NOAA SEC.

Also the multivariate nonparametric methods from ANI package can be very helpful in developing the models for forecasting severe consequences of Space Weather.

It should be noted that translation of research to operations (services) is not trivial and needs thoughtful scientist input: failure could have significant operational consequences. Therefore CRD needs 3 years (we submit for funding new ASTC project A1554 "Space Weather Research and Forecasting by Networks of Particle Detectors measuring neutral and charged fluxes") to prepare certificated Space Weather products:

- 1 minute time series of fluxes of different species of secondary cosmic rays with different energy thresholds and directions of incidence;
- Inter-channel and inter-detector correlation matrices; energy releases histograms; correlations with lower energy particle fluxes measured by space born facilities
- GLE warnings and alerts;
- Estimate of the SCR energy spectra;
- Estimate of the total fluency of SEP;
- Estimate of the expected strength of the upcoming GMS (in units of $K_p$ and Dst);
- Estimate of start time of the GMS.

We will use the ASEC monitors Database from 23rd solar activity cycle (1997-2007) for validation and verification of our models, as well as for minimizing false alarms.

Therefore, CRD can come with our products in line with new NASA satellites plan for launch for the SW research. NASA/NOAA plans to use 24th solar activity cycle (2008-2018) for developing and tuning high-accuracy SW forecasting services (comparable with accuracy of the meteorology). CRD's products will provide complimentary information and will be an important element of planetary SW services.

Huge advantage of ASEC is its consistency, 24 hours coverage, multi-year operation. In contrast the planned life of the satellites and space station is a few years only (STEREO – 2 years), they are affected by the same solar blast that they should alert, and space-born facilities instead of sending warning are put in the stand-by mode, see Attachment 6.

Not the least is the rather inexpensive operation of ASEC: annual budget of ASEC is ~200 times less than cost of one satellite.

The business scheme should be investigated and tuned according to activity of the "major national players" in the field: NASA, NOAA, JAXA, ESA. CRD established working relations with these organizations. Director of SEC operations Joseph Kunches is collaborator of the CRD projects.

The alerts available now fall far short of the requirements formulated in the Space Weather National programs. Therefore there is room for smaller and much less expensive institutions like CRD to participate in the field with very carefully determined strategy.

**References**


- O.Adriani, M., Van der Akker, et al (2002), The L3 +C detector, as unique tool-set to study cosmic rays, NIM A 488, 209-255.
- ACE News #87 – Feb 23, 2005: Space weather aspects of the January 20, 2005 solar energetic particle event, http://www.srl.caltech.edu/ACE/ACENews/ACENews87.html.

- ACE News #86 – Nov 14, 2004 Real-time Solar Wind Data from ACE make Accurate Forecasts of Magnetic Storms a Reality, http://www.srl.caltech.edu/ACE/ACENews/ACENews86.html.
- M.J. Aschwanden, (2005) AGU Monograph of AGU Chapman Conference "Solar Energetic Plasmas and Particles", Turku, Finland, 2-6 August 2004, (eds.N. Gopalswamy et al.).
- A.V.Belov, E.A.Eroshenko et al. (2006), in Proc. Int. Conf. SEE-2005, Nor Amberd, Armenia, p. 172.
- Belov, A.V., Bieber, J.W., Eroshenko, E.A., et al,(2003) Adv. Space Res., 31, No 4, 919-924.
- Bieber, J. W., Clem, J., Evenson, P., Pyle, R., Ruffolo, D., & Sariz, A. 2005, Geophys. Res. Lett., 32, L03S02.
- Boezio, M., Bonvicini, V., Schiavon, P., et al.: The cosmic-ray proton and helium spectra measured with the CAPRICE98 balloon experiment, Astroparticle Physics 19, 583-604, 2003.
- Bostanjyan, N.Kh., Chilingarian, A.A., Eganov, V.S., et. al.,: On the production of highest energy solar protons at 20 January 2005, Advances in Space Research 39, 1456–1459, 2007.
- K.S. Carslaw, R.G.Harrison, J.Kirkby, (2002), Cosmic Rays, Clouds, and Climate, Science, 289, 1732-1737
- Chilingarian et al, 1999 Proc. 24th Int. Cosmic Ray Conf. (Salt Lake City), 1, 240.
- Chilingarian, A., Avakyan, K., Babayan, V., et al.: Aragats Space – Environmental Center: status and SEP forecasting possibilities, J. Phys. G: Nucl. Part. Phys., Vol. 29, 939 – 952, 2003a.
- Chilingarian, A., Babayan, V., Bostanjyan, N., et al.: Monitoring and forecasting of the geomagnetic and radiation storms during the 23rd solar cycle: Aragats Regional Space Weather Center, Advances in Space Research, Vol. 31, 861-865, 2003b.
- Chilingarian, A., Arakelyan, K. Avakyan, K., et al.: Correlated measurements of secondary cosmic ray fluxes by the Aragats Space – Environmental Center monitors, Nucl. Instrum. Methods Phys. Res., Sect. A, 483-496, 2005.
- Chilingarian, G. Gharagyozyan, G.Hovsepyan, G.Karapetyan, (2006) Astroparticle physics, 25, pp. 269-276
- Chilingarian A., Melkumyan L., Hovsepyan G., et al.: The Response Function of the Aragats Solar Neutron Telescope, Nucl. Instr. and Meth. A 574, 255-263, 2007.
- Chilingarian, A., Reymers, A.,: Investigations of the response of hybrid particle detectors for the Space Environmental Viewing and Analysis Network (SEVAN), Ann. Geophys., 25, 1–9, 2007.
- A.Chilingarian et al, Study of Extensive Air Showers and Primary Energy Spectra by MAKET-ANI Detector on Mountain Aragats, Astroparticle Physics 28 (2007a) 58-71
- Chilingarian, A.A., Reymers, A.E., Particle detectors in solar physics and space weather research,Astropart. Phys., Astropart. Phys., 27, 465-472, 2007b.
- S.Chilingarian (2006), PhD thesis "High Speed Data Exchange Protocol for Modern Distributed Data Acquisition Systems and Its Implementation for Solar Monitor Networks", Institute for Informatics and Automation Problems of National Academy of Science of the Republic of Armenia
- M.Dziomba (2005), REU/NSF Program, Physics Department, University of Notre Dame, http://physics.nd.edu/Pdf/2005%20REU%20Papers/Dziomba.pdf
- *Dvornikov, V.M., Sdobnov, V.E., Sergeev, A.V.(1988),* Anomal'nye variacii kosmicheskih luchej v zhestkostnom diapazone 2–5 GV i ih svyaz' s geomagnitnymi vozmuscheniyami. Rep. AN USSR. Ser. Phys. 52, 12. pp. 2435–2437. (in Russian)

- Gang Li and G. P. Zank, W. K. M. Rice (2003), Energetic particle acceleration and transport at coronal mass ejection–driven shocks, JGR 108, 1082.
- K. Georgieva, B. Kirovet al., (2005), Impact of magnetic clouds on the middle atmosphere and geomagnetic disturbances, J.Atmos.Sol.Terr.Phys., 67, 163-176.
- N.Gevorgyan for the ASEC team, (2005) Test Alert Service Against Very Large SEP Events, Advances in Space Research (ASR), Vol. 36, issue 12, 2351-2356.
- GEANT - Detector Description and Simulation Tool, CERN Program Library Long Writeup W5013, CERN, 1993.
- R. E. Gold, S. M. Krimigis, et al., (1998), Space Sci. Rev., 86, 541.
- N. Gopalswamy, G. Barbieri, et al. (2005), Introduction to the special section: Violent Sun-Earth connection events of October–November 2003, Geophys. Res. Lett., 32, L03S01
- Heck, D., Knapp, J., Capdevielle, J.N., et al.: CORSICA: A Mote Carlo code to simulate Extensive Air Showers, Forschungszentrum Karlsryhe, FZKA Report 6019, 1998.
- R.P.Kane, How good is the relationship of soilar and interplanetary plazma parameters woth geomagnetic storms? (2005), JGR, 110, A02213.
- S.N. Karpov, Z.M. Karpova, Yu.V. Balabin and E.V. Vashenyuk (2005), in Proc. 29th ICRC, Pune, India, vol. 1, 193.
- KoskinenH.E.J., Huttunen K.M.J., Space Weather:From Solar Eruptions to Magnetospheric Storms, in Solar Eruptions and Energetic Particles, Geophysical Monograths Series 165, 375-385.
- Kudela, K. and Storini, M.: Possible tools for space weather issues from cosmic ray continuous records, Advances in Space Research, Volume 37, Issue 8, 1443-1449, 2006.
- Kuwabara, T., Bieber, J. W., Clem, J., Evenson, P. and Pyle, R.: Development of a ground level enhancement alarm system based upon neutron monitors, SPACE WEATHER, VOL. 4, S10001, doi:10.1029/2006SW000223, 2006.
- Lantos, P.: Radiation dozes potentially received on-board airplane during recent solar particle events, Radiation Protection Dosimetry, 118, 363-374, 2005.
- K. Leerungnavarat , D. Ruffolo, J. W. Bieber (2003), The Astrophysical Journal, 593, 587–596.
- J.Lilensten, J.Bornarel (2006) Space Weather, Environment and Societies, Springer ferlag.
- Lockwood, J.A., Debrunner, H., Flukiger, E.O., and Ryan, J.M.: Solar proton rigidity spectra from 1 to 10 GV of selected flare event since 1960, Solar Physics, 208 (1), 113-140, 2002.
- Mavromichalaki, H., Souvatzoglou, G., Sarlanis, C., et al.: The new Athens center on data processing from the neutron monitor network in real time, Annales Geophysicae, 23, 3103–3110, 2005.
- Mavromichalaki, H., Souvatzoglou, G., Sarlanis, C., et al.: Space weather prediction by cosmic rays, Advances in Space Research, Volume 37, Issue 6, 1141-114, 2006.
- Miroshnichenko L.I., Solar Cosmic Rays, Kluwer Academic Publishers, 2001.
- H. Miyasaka, E. Takahashi et al., (2005), Proc. of 29th ICRC, Pune, India, 1, 241-244.
- H. Miyasaka, E. Takahashi, et al., Proc. of of 29th ICRC, Pune, India vol. 1, 245.
- Moraal, H., Belov, A., Clem, J.M.: Design and co-Ordination of Multi-Station International Neutron Monitor Networks, Space Science Reviews 93, 285-303, 2000.
- Mulligan T., and Russell C.T. (2001), Multispacecraft modeling of the flux rope structure of in terplanetary coronal mass ejections, J.Geophys. Res.,106, 10581-10596.
- Munakata, K., Bieber, J.W., Yasue, S., et al.: Precursors of geomagnetic storms observed by the muon detector network, J. Geophys. Res. 105, 27457-27468, 2000.
- Muraki, Y.: Highest Energy Solar Neutrons Detected in the Solar Flare on November 28th 1998, 2rd International Symposium SEE-2005, Nor-Amberd, Armenia, 229-232, 2005.

- National Oceanic and Atmospheric Administration, National Weather Service, Silver Spring, Maryland
- NASA science, 20.03.08, http://science.nasa.gov/headlines/y2008/20mar_spring.htm
- Panasyuk, M. I., et al. 2004, Cosmic Res., 42, 489
- Plainaki, C. , Belov A., et al., (2007) Modeling ground level enhancements: Event of 20 January 2005, J. Geophys. res., 112, A04102.
- J. Poirier and C. D'Andrea, (2002), J. Geophys. Res., Space Physics, 107(A11), 1376-1384.
- Reymers, A., PhD Thesis: Determination of ground-based detectors response to Solar, Galactic and extragalactic Cosmic Rays, Yerevan Physics Institute after A. Alikhanyan, 2007.
- Shibata, S.: Propagation of the solar neutron through the atmosphere of the Earth, Journal of Geophysical Research, Vol. 99, NO. A4, 6651–6666, 1994.
- Tsuchiya, H., Muraki, Y., Masuda, K., et al.: Detection efficiency of a new type of solar neutron detector calibrated by an accelerator neutron beam, Nucl. Instrum. Methods Phys. Res., Sect. A 463, 183 – 193, 2001.
- Watanabe, K., Gros, M., Stoker, P.H., et al.: Solar neutron events of 2003 October–November, Astrophysical Journal, 636, 1135–1144, 2006.
- Zazyan, M.Z., Chilingaryan, A.A.: On the possibility to deduce proton energy spectrum of the 20 January 2005 GLE using Aragats and Nor-Amberd neutron monitors data, 2rd International Symposium SEE-2005, Nor-Amberd, Armenia, 200-202, 2005.
- M.A.Shea, D.F.Smart (2000), Space Science Reviews 93: 229-262.
- Valtonen E. (2007), Geoeffective Coronal Mass Ejections and Energetic Particles, in Solar Eruptions and Energetic Particles, Geophysical Monograths Series 165, 335-344.
- E.V. Vashenyuk, Yu.V.Balabin et. al., (2005a), 29th ICRC, Pune, India, 1,209-212.
- E.V. Vashenyuk, Yu.V. Balabin , B.B. Gvozdevsky, S.N. Karpov (2005b), Proc. XXVIII Annual Seminar “Physics of Auroral Phenomena”, Apatity,Russia, pp. 149-152.
- F.R. Zhu, Y.Q. Tang et. al., (2005), 29th ICRC, Pune, India, 1, 185-188.
- Yeghikyan, A.R, Chilingarian A.A.: Data visualization interactive network for Aragats Space Environmental Center, 2rd International Symposium SEE-2005, Nor-Amberd,

# 5. Attachment 1: List of published papers and reports with abstracts

1. **A. Chilingarian and A. Reymers, Investigations of the response of hybrid particle detectors for the Space Environmental Viewing and Analysis Network (SEVAN), Ann. Geophys., 25, 1–9, 2007**

**Abstract**

A network of particle detectors located at middle to low latitudes SEVAN (Space Environmental Viewing and Analysis Network) is being created in the framework of the International Heliophysical Year (IHY-2007). It aims to improve fundamental research of the particle acceleration in vicinity of sun and - space environment conditions. The new type of particle detectors will simultaneously measure changing fluxes of most species of secondary cosmic rays, thus turning into a powerful integrated device used for exploration of solar modulation effects. Ground-based detectors measure time series of secondary particles born in cascades originated in the atmosphere by nuclear interactions of protons and nuclei accelerated in the galaxy. During violent solar explosions sometimes additional secondary particles are added to this "background" flux. The studies of changing time series of secondary particles shed light on the high-energy particle acceleration mechanisms. The time series of intensities of high energy particles can also provide highly cost-effective information on the key characteristics of interplanetary disturbances. The recent results of the detection of the solar extreme events (2003 -2005) by the monitors of Aragats Space-Environmental Center (ASEC) illustrate wide possibilities provided by new particle detectors measuring neutron, electron and muon fluxes with inherent correlations. We present results of the intensive simulation studies revealing the characteristics of the SEVAN networks basic measuring module. We illustrate possibilities of the hybrid particle detector to measure neutral and charged fluxes of secondary CR, estimate efficiency and purity of detection; corresponding median energies of the primary proton flux, ability to distinguish between neutron and proton initiated GLEs and some other important properties of hybrid particle detectors.

2. **A.A. Chilingarian, A.E. Reymers, Particle detectors in Solar Physics and Space Weather research, Astroparticle Physics (2007), Astropart. Phys., 27, 465-472**

**Abstract**

The use of large area particle detectors, which can only be accommodated on the Earth's surface, is vital for measuring the low fluxes of high energy particles accelerated in the vicinity of the Sun. The mystery of particle acceleration in the Universe can not be explored without the understanding of solar particle accelerators. The energy spectra of highest energy solar particles, as measured by the surface detectors, will shed light on these universal processes of high-energy particle acceleration at numerous galactic and extragalactic sites. Detected at earth, energetic particles also can provide extremely cost-effective information on the key characteristics of the interplanetary disturbances. Because cosmic rays are fast this information travels rapidly and can be useful for space weather forecasting. Taking into account that only very few of a great number of Solar Flares (SF) and Coronal Mass Ejections (CME) produce intensive ion fluxes, the so called Solar Energetic Particle (SEP) events, it is not only critical to alert clients about the arrival of the most severe radiation storms, but also to minimize the number of false alarms against events which are not severe enough to cause damage. Using examples of extreme solar events from the 23-rd Solar Cycle, we present experimental results and analysis of the sensitivity of the secondary cosmic ray flux, registered at middle latitudes to the various parameters of the solar particle "beams" incident on the earth's atmosphere. We also present similar sensitivity studies for the magnetized solar plasma of CMEs approaching Earth.

3. **A.Chilingarian et al, Study of Extensive Air Showers and Primary Energy Spectra by MAKET-ANI Detector on Mountain Aragats, Astroparticle Physics 28 (2007) 58-71**

**Abstract**

Small and middle size surface detectors measuring extensive air showers (EAS) initiated by primary cosmic rays (PCR) incident on terrestrial atmosphere have been in operation for the last 50 years. Their main goal is to explore the ‘‘knee’’ in all particle spectrum to solve the problem of cosmic ray (CR) origin and acceleration. The recent achievements of atmospheric Cherenkov telescopes and X-ray space laboratories, establishing the supernova remnants (SNRs) as a source of hadronic cosmic rays, pose stringent conditions on the quality of EAS evidence. After establishing the existence of the ‘‘knee’’ itself, the most pronounced result from EAS studies is the rigidity dependent shift of the knee position to the highest energies. This feature was first observed by separation of the primary flux in different mass groups in MAKET-ANI, EAS-TOP and KASCADE experiments. The MAKET-ANI detector is placed on Mt. Aragats (Armenia) at 3200 m above the sea level (40_250N, 44_150E). More than 1.3 · 106 showers with size greater than 105 particles were registered in 1997–2004. The detector effectively collected the cores of EAS, initiated by primaries with energies of 1014–1017 eV. After proving that the quality of the EAS size and shape reconstruction was reasonably high, we present the lateral distribution function (LDF) for distances from 10 to 120 m from EAS core and EAS size spectra in 5 zenith angle intervals. We use CORSIKA simulations to present the energy spectra. The results from the MAKET-ANI experiment on the energy spectra of the ‘‘light’’(p + He) and ‘‘heavy’’(O + Si + Fe) nuclear groups are compared to the spectra obtained by balloon experiments and to other available spectra.

4. **A. Chilingarian, L. Melkumyan, G. Hovsepyan, A. Reymers, The response function of the Aragats Solar Neutron Telescope, Nuclear Instruments and Methods in Physics Research A 574 (2007) 255-263**

**Abstract**

The Aragats Solar Neutron Telescope (ASNT) is in operation at the Mt. Aragats research center (3200m above sea level) in Armenia and constitutes part of the worldwide network, coordinated by Nagoya University. In this paper, we calculate the response function of the ASNT to the galactic and solar cosmic rays and determine the energy thresholds of the four ASNT channels. The capability of ASNT to distinguish the Ground Level Enhancements (GLEs) originated by solar neutrons is proposed and tested on the largest GLEs of the 23rd solar cycle.

5. **Bostanjyan, N.K. et al., On the production of highest energy solar protons at 20 January 2005, J. Adv. Space Res. 39 (2007) 1456–1459**

**Abstract**

On January 20, 2005, 7:02–7:05 UT the Aragats Multidirectional Muon Monitor (AMMM) located at 3200 m a.s.l. registered 9 enhancement of the high energy secondary muon flux (threshold _5 GeV). The enhancement, lasting for 3 min, has statistical significance 10 of _4r and is related to the X7.1 flare seen by the GOES, and very fast (>2500 km/s) CME seen by SOHO, and the Ground Level 11 Enhancements (GLE) #69 detected by the world-wide network of neutron monitors and muon detectors. The energetic and temporal 12 characteristics of the muon signal from the AMMM are compared with the characteristics of other monitors located at the Aragats 13 Space-Environmental Center (ASEC) and with other neutron and muon detectors. Since secondary muons with energies >5 GeV are 14 corresponding to solar proton primaries with energies 20–30

GeV we conclude that in the episode of the particle acceleration at 7:02– 15 7:05 UT 20 January 2005 solar protons were accelerated up to energies in excess of 20 GeV.

6. **Y. Muraki et al., Detection of Solar Neutrons and Protons by Ground Level Detectors, Proceedings of the 20th European Cosmic Ray Symposium in Lisbon, Portugal**

**Abstract**

In association with the large solar flare of April 15th 2001, the Chacaltaya neutron monitor observed an 8 σ enhancement of the counting rate. Since the enhancement was observed from 14 minute before the GLE, we think that solar neutrons made this enhancement. At the same time the detectors located at Gornergrat and Mt. Aragats observed enhancements.

The high-energy protons that arrived on the Earth faster than the main stream of particles, the well-known GLE component, must induce those enhancements.

7. **A Konopelko, A Chilingarian and A Reimers, Study on cosmic ray background rejection with a 30 m stand-alone IACT using non-parametric multivariate methods in a sub-100 GeV energy range, J. Phys. G: Nucl. Part. Phys. 32 (2006) 2279.2291**

**Abstract**

During the last decade ground-based very high-energy $\gamma$ -ray astronomy achieved a remarkable advancement in the development of the observational technique for the registration and study of $\gamma$ -ray emission above 100 GeV. It is widely believed that the next step in its future development will be the construction of telescopes of substantially larger size than the currently used 10 m class telescopes. This can drastically improve the sensitivity of the ground-based detectors for $\gamma$ -rays of energy from 10 to 100 GeV. Based on Monte Carlo simulations of the response of a single stand-alone 30 m imaging atmospheric Cherenkov telescope (IACT), the maximal rejection power against background cosmic ray showers for low-energy $\gamma$ -rayswas investigated in great detail. An advanced Bayesian multivariate analysis has been applied to the simulated Cherenkov light images of the $\gamma$ -ray- and proton-induced air showers. The results obtained here quantitatively testify that the separation between the signal and background images degrades substantially at low energies, and consequently the maximum overall quality factor can only be about 3.1 for $\gamma$ -rays in the 10–30 GeV energy range. Various selection criteria as well as optimal combinations of the standard image parameters utilized for effective image separation have also been evaluated

8. **A. Chilingarian, G. Gharagyozyan, G.Hovsepyan, G.Karapetyan, Statistical Methods for Signal Estimation of Point Sources of Cosmic Rays, Astroparticle physics 25, pp 269-276**

**Abstract**

The estimation of the significance of the peaks in one- and two-dimensional distributions is one of the most important problems in high-energy physics and astrophysics. The physical inference from low-statistics experiments usually is biased and many discoveries lack further confirmation. One of the typical mistakes in physical inference is the use of non-adequate statistical models. We analyze the significance of the experimental evidence in the on-going efforts of detecting the point source of cosmic rays. We found that simple statistical models (Gaussian or Poisson) did not adequately describe the experimental situation of point source searches. To avoid drawbacks related to usage of the incorrect statistical model, we introduce new extremum statistical models

appropriate for the point source searches. The analysis is conducted in the framework of two models utilizing extremum statistics: first – using the fixed grid of celestial coordinates, and second – using the tuned grid (introducing more degrees of freedom in the search). The test distributions for the significance estimation are obtained both from simulation models and from the analytical model of extremum statistics. We show that the second model gives adequate physical inference, while the first model can lead to the positively biased conclusions of the point source significance.

9. **A.Chilingarian for the ASEC team, (2005) Correlated Measurements of Secondary Cosmic Ray Fluxes by the Aragats Space-Environmental Center Monitors, NIM-A, 543, 483-496.**

**Abstract**

The Aragats Space-Environmental Center provides monitoring of different species of secondary cosmic rays at two altitudes and with different energy thresholds. 1-minute data is available on-line from http://crdlx5.yerphi.am/DVIN/index2.php. We present description of the main monitors along with data acquisition electronics. Also we demonstrate the sensitivity of the different species of secondary cosmic ray flux to geophysical conditions, taking as examples the extremely violent events of October – November 2003. We introduce correlation analysis of the different components of registered time-series as a new tool for the classification of the geoeffective (events on earth affected by solar activity) events and for the forecasting of the severity of the upcoming geomagnetic storm.

10. **N.Gevorgyan for the ASEC team, (2005) Test Alert Service Against Very Large SEP Events, Advances in Space Research (ASR), Vol. 36, issue 12, pp 2351-2356**

**Abstract**

The Aragats Solar Environment Center provides real time monitoring of different components of secondary cosmic ray fluxes.We plan to use this information to establish an early warning alert system against extreme, very large solar particle events with hard spectra, dangerous for satellite electronics and for the crew of the Space Station. Neutron monitors operating at altitude 2000 and 3200 m are continuously gathering data to detect possible abrupt variations of the particle count rates. Additional high precision detectors measuring muon and electron fluxes, along with directional information are under construction on Mt. Aragats. Registered ground level enhancements, in neutron and muon fluxes along with correlations between different species of secondary cosmic rays are analyzed to reveal possible correlations with expected times of arrival of dangerous solar energetic particles.

11. **S.Blokhin, S.Gazaryan et al., (2005) The Lateral Distribution function of the EAS electrons as measured by the MAKET-ANI detector, Proceedings of the Russian Academy of Science, Physics series, 69, 535-355.**

**Abstract**

Функция пространственного распределения (ФПР) электронов при $N_e \geq 10^5$ измерена на установке, расположенной на высоте 3200 м от уровня моря на высокогорной станции Арагац (Армения). Плотности ливневых частиц определены до расстояний ≤120 м от оси ливня. Экспериментально наблюдаемые плотности описываются функцией Нишимуры – Каматы – Грейзена. Наблюдаемые ФПР сравниваются с результатом моделирования по CORSIKA 562(QGSJET, NKG).

12. **V.Eganov, V.Ivanov et al., Experimental Investigation of EAS Electron-Photon and Muon Component on Mount Aragats in the Spectrum Knee Region according to Particle Number, Proceedings of the Russian Academy of Science, Physics series, vol. 69, issue 3, pp. 334-336**

**Abstract**

Приведены результаты анализа электронно-фотонной и мюонной компонент широких атмосферных ливней, полученных на установке "Гамма" (г. Арагац, 3250 м над уровнем моря). Найдены критерии выделения ливней, генерированных частицами с разным атомным номером. Расчеты выполнены по схеме, которая приводит к росту среднего атомного номера частиц с ростом их энергии. Показано, что для объяснения некоторых характеристик широких атмосферных ливней космических лучей такого утяжеления недостаточно и необходимо предположение об изменении характера сильного взаимодействия элементарных частиц при энергии 3–5 ПэВ.

13. **A. Chilingarian, Babayan, N. Bostanjyan, G. Karapetyan (2005) Correlated Measurements of the Secondary Cosmic ray Fluxes by the Neutron Monitors and Muon Telescopes, International Journal of Modern Physics A, NIM-A, 543, 483-496**

**Abstract**

Radiation and Geomagnetic storms, which are elements of Space Weather, are part of the major obstacles for Space Operations. Reliable forecasting of the arrival of these dangerous elements is of vital importance for the orbiting flights and electric power distribution in near polar regions. In addition to the fleet of space-born instruments, worldwide networks of particle detectors spread along different latitudes and longitudes, provide valuable information on the intensity and anisotropy of the variable cosmic ray fluxes.

Aragats Space-Environmental Center provides monitoring of the different species of secondary cosmic rays at two altitudes and with different energy thresholds. 1-minute data is available on-line from URL <http://crdlx1.yerphi.am/DVIN>. We demonstrated the sensitivity of the different species of secondary cosmic ray flux to geophysical conditions, taking as examples extremely violent events of end of October – November 2003. Also we introduce the correlation analysis of the different components of registered time-series as a new tool for the classification of the geoeffective events.

14. **A. Chilingarian, Babayan V. , V. Eganov, N. Bostanjyan, G. Karapetyan (2005) The mutual treatment of 28 – 29.10.2003 events by the ASEC surface monitors and space-born spectrometers on board of ACE and GOES satellites, Proceedings of the Russian Academy of Science, Physics series 69, 815-817.**

**Abstract**

Проведен анализ октябрьских событий 2003 г. Сопоставлены временные профили солнечной вспышки (СВ) 28.10.2003 г., зарегистрированной приборами Арагацкого центра солнечно-земных связей (ASEC) и протонными детекторами спутника GOES-11, и показана возможность предсказывать солнечную радиационную опасность за 45 мин до наступления критического повышения интенсивности солнечных ионов на околоземной орбите. Приведены параметры форбуш-понижения (ФП), зарегистрированного приборами ASEC 29.10.2003 г. и показана возможность предсказания магнитных бурь.

15. **A. Chilingarian, G.Hovsepyan, G.Gharagyozyan, G.Karapetyan, (2005) On the Statistical Methods of the Signal Significance Estimation in the Detection of the Signal from the Point Sources of Cosmic Rays, International Journal of Modern Physics A, Vol. 20, No.29., 6765-6769**

**Abstract**

The estimation of the significance of the peaks in 1 and 2-dimensional distributions is one of the most important problems in high-energy physics and astrophysics. The physical inference from lowstatistics experiments usually is biased and many discoveries lack further confirmation. We analyze the significance of the experimental evidence in the on-going efforts of detecting the point source of Cosmic Rays. The analysis is carried out in the framework of two models utilizing the extremum statistics: first – using the fixed grid of celestial coordinates, and second – using the tuned grid (introducing more degrees of freedom in the search). The test distributions for the significance estimation are obtained both from simulation models and from the analytical treatment of the problem.

16. **E.O. Flueckiger, R. Butikofer, A. Chilingarian, G. Hovsepyan, Y. H. Tan, (2005) Solar Neutron Events that Have Been Found in Solar Cycle 23, International Journal of Modern Physics A, Vol. 20, No.29., 6646-6650**

**Abstract**

In this paper, we report solar neutron events detected in the solar cycle 23, especially three interesting events detected on November 23rd and 28th 1998 in Tibet and October 28th 2003 in Tsumeb.

# 6. Attachment 2: List of presentations at conferences and meetings with abstracts

1. **A.A. Chilingarian, Detection of the high energy solar protons by the particle detectors of Aragats Space-Environmental Center at 20 January 2005; Estimation of the significance of the peaks in the time –series. 2007 Fall Meeting of American Geophysical Union, San-Francisco, December 10-14.**

**Abstract**

On January 20, 2005, 7:02-7:05 UT the Aragats Multidirectional Muon Monitor (AMMM) located at 3200 m a.s.l. registered enhancement of the high energy secondary muon flux (threshold ~5 GeV). The enhancement, lasting for three minutes, has statistical significance of ~4σ and is related to the X7.1 flare seen by the GOES, and very fast (>2500 km/s) CME seen by SOHO, and the Ground Level Enhancements (GLE) #69 detected by the world-wide network of neutron monitors and muon detectors. The energetic and temporal characteristics of the muon signal from the AMMM are compared with the characteristics of other monitors located at the Aragats Space-Environmental Center (ASEC) and with other neutron and muon detectors. Since secondary muons with energies > 5 GeV are corresponding to solar proton primaries with energies 20-30 GeV we conclude that in the episode of the particle acceleration at 7:02 – 7:05 UT 20 January 2005 solar protons were accelerated up to energies in excess of 20 GeV.

To prove that detected peaks in the time-series are not only background flux (Galactic Cosmic Rays) fluctuations, but signal candidate (Solar Cosmic Rays), we perform additional investigations of the detectors count rates at 20 January. When calculated the chance probability we have to take into account the experimental procedures we use to reveal the signal. We made 3-minute time series from the 1 minute ones. The re-binning of time series is ordinary operation used by the all groups running the particle solar monitors. However, it has to be taken into account in calculating of the chance probability. Different attempts to obtain "best signal" considering different re-binning cannot be treated by standard Gaussian distribution, but can be considered by implementing Chapman statistics. To check this assumption and demonstrate the influence of the re-binning procedure we perform simulations with simple model of time series.

Our numerical modeling confirm that when testing different data binning the probability of obtaining "fake" signal during a given time period increases proportional to number of tests and should be corrected with tuning of parameters of Chapman statistics. Simple Gaussian statistics gives positively biased estimates of chance probability.

2. **A.Chilingarian Scientific networks for measuring geophysical parameters – fundamental research and international collaborations International conference "Making Science Global: Reconsidering the Social and Intellectual Implications of the International Polar and Geophysical Years.", Smithsonian, Washington October 31- November 1.**

**Abstract**

In 21-st century Space research became not only risky and costly pioneering exploration, but main source of fundamental information on basic knowledge about Universe and basis of extremely profitable space-based technologies. The networks of distributed measurements were very instrumental in this transition.

First network was created my Alexander fon Humboldt, Friedrich Gauss and Wilhelm Weber in 1828-1841. The world-wide network of magnetic measurements in Greenwich, Dublin, Toronto, St.

Helena, Cape of Good Hope Tasmania, in India and Singapore, 10 stations in Russia and one in Beijing started the first world-wide survey to understand terrestrial magnetism and solar-terrestrial connections.

The networks of particle detectors started monitoring of changing fluxes of cosmic rays in connection with the International Geophysical Year (IGY) of 1957-58.

A network of middle to low latitude particle detectors called SEVAN (Space Environmental Viewing and Analysis Network) is planned in the framework of the International Heliophysical Year (IHY), to improve fundamental research of the space weather conditions and provide possibilities to perform short and long-term forecasts of the dangerous consequences of the space storms. The network will detect changing fluxes of the most of species secondary cosmic rays at different altitudes, latitudes and altitudes those constituting powerful integrated device in exploring solar modulation effects.

Based on our experience with data analysis of multivariate time-series from particle detectors located at Aragats Space-Environmental Center in Armenia we designed and fabricated several new-types of particle detectors measuring charged and neutral component of secondary cosmic rays. In order to keep the instruments inexpensive the options are kept flexible by using modular designs. The price of a fully autonomous single unit, with facility to send data to the internet will not exceed $20,000 US, so that the network of nations involved in space research can be significantly expanded to enable them to participate in IHY. At any time one can cascade these single units to achieve additional functionality. *Like the world network of neutron monitors, created during IGY the new monitors will measure the neutron fluxes and in addition they will measure charged particle fluxes with different energy thresholds, thus allowing the investigation of additional populations of primary ions.* These units plan to be deployed at universities and research centers of the developing countries to perform survey and monitoring of most dangerous space storms and to introduce the space research to new generations of students and researchers.

3. **A. Chilingarian, Hybrid particle-detector networks located at Middle-Low latitudes for Solar Physics and Space Weather research, Invited talk presented at the international symposium "Solar Extreme Events 2007" , September 24 -27, 2007 Athens, Greece**

**Abstract**

A network of middle to low latitude particle detectors called SEVAN (Space Environmental Viewing and Analysis Network) is planned in the framework of the International Heliophysical Year (IHY), to improve fundamental research of the solar accelerators and space weather conditions. The network will detect changing fluxes of the most of species secondary cosmic rays at different altitudes, latitudes and altitudes those constituting powerful integrated device in exploring solar modulation effects.

Surface detectors measure time series of secondary particles born in cascades originated in the atmosphere by nuclear interactions of protons and nuclei accelerated in galaxy. During violent solar explosions sometimes additional secondary particles are added to this "background" flux. Studies of changing time series of secondary particles shed light on the high-energy particle acceleration mechanisms by flares and Coronal Mass Ejection driven shocks.

Time series of intensities of high energy particles can also provide highly cost-effective information on the key characteristics of the interplanetary disturbances.

Recent results on of the detection of the extreme solar events (2003, 2005) by the monitors of the Aragats Space-Environmental Center (ASEC) illustrate wide possibilities opening with introduction of new particle detectors measuring neutron, electron and muon fluxes with inherent correlations.

4. **S.Chilingarian, A.Chilingarian, V.Danielyan, Advanced Date Analyses System (ADAS) for the Space Environmental Viewing and Analysis Network (SEVAN), presented at the international symposium "Solar Extreme Events 2007" , September 24 to September 27, 2007 Athens, Greece**

**Abstract**

The Advanced Data Analyses System (ADAS) is designed as a distributed network of the uniform components connected by means of Web Service interfaces. The units connected by ADAS are particle detectors equipped with modern electronics monitoring changing fluxes of the Cosmic Rays. For the timely and reliable forecasting of the severe conditions of the Space Weather we need uninterruptable operation of the whole network and on-line treatment of the data from remote detectors.

The main component of the ADAS is Unified Readout and Control Server (URCS) controlling the underlying electronics by means of the detector specific drivers and makes a preliminary analysis of the on-line data. Then, the data is made available for other system components by means of the Web Service interfaces. The interface provides remote structured access to the current and archived data and facilitates cooperation with remote system components giving a chance to correlate the data collected by detectors of the SEVAN network worldwide. Additionally the URCS server provides a set of control interfaces to control multiple detector electronics and URCS software behavior.

In addition to certain amount of URCS servers the distributed data acquisition system consists of the operator web frontends and data storage subsystem. The web frontend provides operators with a possibility to monitor current data and adjust electronic states and URCS configuration. The data storage servers are periodically inquiring the data from all detectors of the SEVAN network and storing it in the MySQL database.

ADAS is in operation starting from November 2006 at Aragats Space Environmental Center (ASEC), in Armenia. The reliability of the multi-client service was proved by continuous monitoring of neutral and charged components of incident cosmic ray flux with 7 particle monitors located at 2000 and 3200 meters above sea level on the distance of 40 and 60 km. from the main data server.

5. **A.Chilingarian, G.Hovsepyan, K.Arakelyan, A.Avetisyan, S.Chilingarian, V.Danielyan, K.Avakyan, A.Reymers, S.Tserunyan, Characteristics of the Space Environmental Viewing and Analysis Network (SEVAN), presented at the international symposium "Solar Extreme Events 2007" , September 24 to September 27, 2007 Athens, Greece**

**Abstract**

One of the major advantages of multi-particle detectors is probing of the different populations of the primary cosmic rays, initiated particle cascades in terrestrial atmosphere. With basic detector of SEVAN network we are measuring fluxes of neutrons and gammas, of low energy charged component and high energy muons. This diversity of information obtained from SEVAN network located mostly at low and middle latitudes will give possibility to estimate the energy spectra of the highest energy SCR. SEVAN network will be sensitive to very weak fluxes of SCR above 10 GeV, very poorly explored highest energy region.

To understand sensitivity of new type of particle detectors to highest energy solar ions we investigate the response of SEVAN basic units to galactic and solar protons. Methods of estimation of the index of power spectra of solar cosmic rays incident on the terrestrial atmosphere and – for the distinguishing of the ground level enhancements initiated by solar neutrons also are proposed.

6. **A.Chilingarian, G.Hovsepyan, K.Arakelyan, A.Avetisyan, S.Chilingarian, V.Danielyan, K.Avakyan, A.Reymers, S.Tserunyan, On the Possibility to modernize existent network of Neutron Monitors, presented at the international symposium "Solar Extreme Events 2007" , September 24 to September 27, 2007 Athens, Greece**

**Abstract**

Despite decades of tradition, Neutron Monitors (NM) remain the state-of-the-art instrumentation for measuring spectral variations in the energy range from about 500 MeV to 20 GeV of the primary cosmic ray component (above the Earth's atmosphere). The worldwide network presently consists of about ~50 standardized IGY and NM64 neutron monitors.

We propose an update of this network by introducing new detectors and new electronics to be added to existing detectors, significantly enlarging its performance for solar physics and Space Weather research.

We propose to locate scintillation detectors above and below (if construction of NM allows) the standard sections of NM. New scintillator detectors of size 1 x 1 x 0.01 $m^3$ produced by the Institute of High Energy Physics, Protvino, Russia are compact and provide uniformity light collection. Measuring both neutral and charged flux of the secondary cosmic rays will allow to:

- Significantly enlarge the count rate of detector; note that flux of low energy charged particles is ~10 times higher than neutron flux;
- Explore more energetic population of the primary cosmic rays, giving possibility to estimate spectra of the solar cosmic rays;
- Distinguish Ground level Enhancements originated by solar neutrons;
- Estimate the incident direction of the additional flux of solar cosmic rays.

New Data Acquisition (DAQ) electronics will provide also possibility to count total number of the evaporated neutrons originated in lead by hadrons entering NM. Number of neutrons is good proxy of the incident hadron energy.

7. **K.Arakelyan, A.Avetisyan, A.Chilingarian, G.Hovsepyan, S.Chilingarian, V.Danielyan, K.Avakyan, A.Reymers, S.Tserunyan, Electronics for the Space Environmental Viewing and Analysis Network (SEVAN), presented at the international symposium "Solar Extreme Events 2007" , September 24 to September 27, 2007 Athens, Greece**

**Abstract**

A network of middle to low latitude particle detectors called SEVAN (Space Environmental Viewing and Analysis Network) is planned in the framework of the International Heliophysical Year (IHY), to improve fundamental research of the solar accelerators and space weather conditions.

The functionality of the Data Acquisition (DAQ) unit for the SEVAN is very flexible and strongly depends on the software. It has 8 analog inputs, receiving the pulses from the scintillator detectors buffer amplifiers. The pulse amplitudes are converted to a standard TTL/CMOS pulses sequences, about 23 for the order of magnitude. These pulses then are counted by the CPLD module and send to the microcontroller, which can collect the data and perform preprocessing, according to the experiment requirements, i.e. a total count of events for the each channel, coincidences, anticoincidence, etc. For the program selectable condition, the unit generates a pulse in the TRIGGER output. All analog data is stored and for the each channel the amplitude spectrum is connected. The spectrum output for the chosen channel can be observed using any standard digital oscilloscope, connected to the SPECTRUM output on the front panel.

Besides the main DAQ function, the unit also acts as the master for the detector control Local Area Network (LAN) which is used for programming and monitoring high voltage values and programming the ADC thresholds.

The threshold of the each channel is program selectable in the range about 2 - 500 mV in 2mV steps. The host Mini-PC is connected to the CRD intranet by the Ethernet interface. All experimental data is thus available on the net. Additionally it is possible remote reprogramming of the C32USB module microcontroller, according to the desired physical experiment.

8. **A.Chilingarian, Neutron Monitors operated at Aragats Space –Environmental Center (ASEC), presented at the international symposium "Solar Extreme Events 2007" , September 24 to September 27, 2007 Athens, Greece**

**Abstract**

The Aragats Space Environmental Center (ASEC) provides monitoring of different species of secondary cosmic rays and consists of two high altitude research stations on Mt. Aragats in Armenia. Geographic coordinates: 40°30'N, 44°10'E, cutoff rigidity: ~7.1 GV. Among various particle detectors In 1996 we restarted our first detector - the Nor Amberd Neutron Monitor 18NM64 typeNeutron Monitors (NM) are operating at Nor Amberd research station (2000m above sea level) and at the Aragats research station (3200m above sea level).

Recently modernized electronics of both monitors allows simultaneously registration of 3 time series according to 3 prefixed dead times. New installed "slow control" system allows control and automatic tuning of high voltage for each proportional camber of NM.

Advanced Data Analysis system provides data storage on file servers, data transfer to computer center and various possibilities of control and visualization.

Very interesting features of ASEC NMs consist in possibility of measuring simultaneously neutral and charged fluxes of cosmic rays. System of scintillator detectors build around NM allows estimation of the arrival direction of the primary cosmic rays.

Research on Galactic and Solar Cosmic Rays at the Aragats Cosmic Ray Observatory Correlated information on neutral and charged fluxes is very useful for alerting on dangerous conditions of the Space Weather and for fundamental research in Solar Physics.

9. **A.Yegikyan, A.Chilingarian, Data Visualization Interactive Network (DNIN), presented at the international symposium "Solar Extreme Events 2007", September 24 to September 27, 2007 Athens, Greece**

**Abstract**

Data Visualization Interactive Network 3-rd version was developed to give the following services:

- Gathering and storing data in database.
- Online presentation of data.
- Online processing of data.
- Data exchange between users of DVIN.
- Managing online collaborations between users.

The system is highly interactive and exceptional information is easily accessible online. Data can be monitored and analyzed for desired time spans in a fast and reliable manner by the remote users world-wide. Data from particle detectors from space and earth surface is automatically downloaded and stored in DVIN for joint analysis with ASEC monitors. DVIN provides wide possibilities for sharing data and sending warnings and alerts to scientists and world-wide, which have fundamental and practical interest in knowing the space weather conditions. DVIN gives

opportunity to remote groups to share the process of analyzing, exchange data analysis methods, prepare joint publications and maintain networks of particle detectors. DVIN gives users set of online features for physical interface from the time series of changing secondary particle fluxes.

To overcome difficulties due to slow Internet connection at DVIN host site it is planned to establish several mirrors for DVIN in Russia, Europe and USA. During last 2 years several new particle detectors are commissioned in Aragats Space Environmental Center. Also new possibilities will added to existent detectors. Each minute are registered not only count rates, but also histograms of energy releases in thick and thin plastic scintillators, variances of measuring channels and correlation matrices. All this information is incorporated in new edition of DVIN package and is assessable for the DVIN users.

### 10. A.Chilingarian, Research on Galactic and Solar Cosmic Rays at the Aragats Cosmic Ray Observatory, report to scientific council of High energy Astrophysics division of Lebedev Institute, October 2, 2007, Moscow

**Abstract**

Recently several groups report on the development of the alarm system based on the surface particle detector data. Among them are high-latitude neutron monitors network "Spaceship Earth", coordinated by the group from Bartol Research Center; Muon network coordinated by the group from Shinshu University and Athens Neutron Monitor Data Processing Center.

Surface monitors located at the Aragats Space Environmental Center (ASEC) at 2000 and 3200 m altitudes (40˚25′N, 44˚15′E; Vertical cut-off rigidity in 2007: 7.1 GV) detect charged and neutral components of the secondary cosmic rays with different energy thresholds and various angles of incidence. ASEC monitors reliably detect the highest energy CR due to unique geographical location and large underground high energy muon detector.

Forecasting of the Solar Energetic Proton (SEP) events by surface particle detectors is based on the detection of the Ground Level Enhancements (GLE). Unfortunately not all SEPs contain particles energetic enough to produce GLE, therefore, the efficiency of the warnings will not be very high. Nonetheless, we can expect that the major events, (like 1859, 1956, 1972, 1989) for sure will generate GLEs and surface detectors can provide forewarnings on upcoming abundant SEP particles. With the exception of the event on 20 January, when due to very good magnetic connection of the flare site with earth, all relativistic particles seem to come simultaneously, the enhancements of GeV solar particles detected by the Neutron Monitors can alert on upcoming severe radiation storm. The alerts from middle and low latitude monitors are even more important compared to high latitude networks, because of lower probability of false alarms. If an enhancement occurs at monitors with large cutoff rigidity it indicates that spectral knee occurs at large enough energy. Enhancements in the ASEC detectors count rates indicate higher solar ion energies, and, consequently hard spectra of the GLE in progress.

The triggers of the Geomagnetic Storms are huge magnetized clouds (Coronal mass ejections – CMEs), emitted by sun and traveling in the Interplanetary Space (IP). This gigantic plasma clouds with "frozen" magnetic field (Interplanetary CMEs, - ICMEs) disturb the Interplanetary Magnetic Field and "modulate "the ambient flux of the Galactic Cosmic rays (GCR). Because only highest energy cosmic rays can generate particle cascades reaching at the Earth surface, the information on the disturbances of the IP magnetic carried by these energetic particles may prove useful for the forecasting of the severity of geomagnetic storm unleashed by ICME at the arrival at magnetosphere. On the way to Earth (15 – 70 hours) the magnetic cloud and shock modulate the GCR flux, changing its intensity and making it anisotropic. The strength of these modulation effects correlate with geomagnetic indices of the geomagnetic storm. Networks of the particle detectors located on Earth surface detect these modulation effects and can predict the upcoming

geomagnetic storms hours before the ICME arrival at the magnetometers on ACE and SOHO space stations.

**11. Ashot Chilingarian, Gagik Hovsepyan, Studies of the Energy Spectra of incident cosmic radiation by the networks of particle detectors, JENAM 2007: Armenian Astronomical Society Joint European and National Astronomy Meeting, Yerevan, Armenia, August 20-25, 2007**

**Abstract**

There are numerous indications that particle acceleration took place in supernovae remnants, by pulsars, super-massive black holes, in the galaxy clusters and by stars. As a universal mechanism operated on different scales the stochastic and shock acceleration is pointed. It is very important to use our nearest star – the sun, as laboratory in studying particle acceleration phenomena. The surface particle detectors, along with space-born spectrometers are capable of detecting solar particles in the energy range from KeVs till several Tens of GeV. The large surface arrays are detecting particle in energy range from ~100 TeV till EeV. This richness' of information on particle fluxes on different scales can be used in studying physical processes responsible for particle acceleration in Universe.

Surface detectors measuring Extensive Air Showers (EAS) initiated by Primary Cosmic Rays (PCR) incident on terrestrial atmosphere have been in operation since the last 50 years with main goal to explore the major enigma of Cosmic Ray (CR) origin and acceleration. Recent achievements of the Atmospheric Cherenkov Telescopes and X-ray space laboratories, establishing the supernova remnants (SNRs) as source of hadronic cosmic rays pose stringent conditions on the quality of the EAS evidence. After establishing the existence of the "knee" in all particle spectrum the most pronounced result from EAS studies is the rigidity dependent shift of the knee position to the highest energies. This feature first observed by the exploiting the separation of the primary beam in different groups of mass in MAKET-ANI, EAS-TOP and KASCADE experiments also pointed to the SNR blast shocks as CR source. The MAKET ANI detector is placed on mountain Aragats (Armenia) on 3200m above sea level ( $40.5^0$N, $44.2^0$E ). More than $1.3\cdot10^6$ showers with size greater than $10^5$ particles were registered in 1997-2004. The detector has effectively collected the cores of EAS, initiated by primaries with energies of $5\cdot10^{14}$ – $10^{17}$eV. Results from the MAKET-ANI experiment on the energy spectra of the "light"(p+He) and "heavy" (O+Si+Fe) nuclear groups are compared with spectra obtained by balloon experiments, as well as with other available EAS spectra.

**12. A. Chilingarian, G. Hovsepyan, V.Ivanov, E.Mamadjanyan A.Daryan, K. Arakelyan, V. Danielyan, K. Avakyan, A. Reymers, S. Tserunyan, Research of the Galactic Cosmic Rays from "knee" till "cutoff" ($10^{16}$-$10^{19}$) eV at Aragats Cosmic Ray Observatory, JENAM 2007: Armenian Astronomical Society Joint European and National Astronomy Meeting, Yerevan, Armenia, August 20-25, 2007**

**Abstract**

Measured intensities of the galactic cosmic rays are described rather satisfactory till energy ~$10^{17}$ eV by the acceleration of protons and nuclei in supernovae explosion blasts in presence of strong magnetic fields. At ~$10^{15}$eV this mechanism faded producing the first "proton" knee; at ~$10^{15}$eV, the iron nuclei also cannot gain additional energy crossing SNR generated blast and leave the SNR rim region with energies ~$10^{17}$eV.

The energy domain $10^{17}$eV~$10^{18}$eV is an enigmatic region where may be mysterious extragalactic CRs, presumably produced in Active Galactic Nuclei is mixing with fading galactic

iron flux. There are different scenarios of mixing of both components and absolutely not enough experimental evidence for comparisons. KASCADE, MAKET-ANI and HighRes data seem to suggest a "bump" after $10^{17}$ eV, although error bars are too large for the physical inference. AKENO data suggested rather smooth transition. This important question of transition from galactic to extragalactic component can only be solved by measuring partial energy spectra, and not only all-particle energy spectra. The explanation of the spectra features (2nd knee, ankle and the GZK cutoff) are possible only after disentangling all-particle spectra into 2 or more components. Furthermore, the attenuation length of the particles due to the various energy loss mechanisms depends on the particle type and without determination of the primary particle type on the event-by-event basis even all-particle energy spectra will be biased. Of course, new type of particle detectors with enhanced flexibility to precisely and simultaneously measure changing fluxes of different secondary particles with different energy thresholds will be a key element of new Extensive Air Shower array.

We propose to build the new large EAS detector in Nor-Amberd – Antarut region on slopes of mt. Aragats at altitude ~ 2000 m. 2 networks of particle detectors will be formed around central part of ~ 20 $m^2$ hybrid particle detectors, measuring neutrons, electrons and muons of the shower. The third site will be formed by the particle detectors of MAKET-ANI and GAMMA EAS arrays at top of mt. Aragats. All 3 sites have total area ~0.35 $km^2$, and will detect primary particles with energies up to several units of $10^{17}$ eV. Huge events triggering 2 arrays from 3 will correspond to the primary energies above $10^{19}$ eV, EAS core collection area will be ~15 $km^2$ and 75 $km^2$ correspondingly for 2 and 5 km radii circles(~150 events with energy above $10^{19}$ eV are expected per year). As a second phase of project we consider incorporation of the Aragats research station EAS arrays into NewANI. MAKET-ANI and GAMMA detectors operated at altitude 3200 and within 10 km distance from NewANI. Adding additional detection site equipped with ~300 $m^2$ of scintillators can significantly enlarge the area of collecting EAS cores and enlarge maximal attainable energy of array up to $10^{20}$ eV if all 3 detecting sites register EAS electrons(of course only very few events above $10^{20}$ eV per year are expected). In the second phase of the project we plan to deploy additional scintillator modules in Burakan Astrophysical Observatory (BAO), in the Institute of radio-measurements in Orgoff, in village schools fallen within big detector area. Ultra-high energy cosmic rays detected by the NewANI detector will be correlated with optical data obtained by NOMOT mini observatory now under construction in Nor Amberd and with data from world largest Cherenkov Atmospheric Telescope MAGIC operated on Canarian Islands.

**13. A. Chilingarian, Nor-Amberd Optical mini-observatory for detection of energetic Transient events (NOMOT), JENAM 2007: Armenian Astronomical Society Joint European and National Astronomy Meeting, Yerevan, Armenia, August 20-25, 2007**

**Abstract**

NOMOT is located on the slope of Mount-Aragats in Armenia at Aragats Space Environmental Center (ASEC) belong to Cosmic Ray Division (CRD) of Alikanyan Physics Institute, geographical coordinates (40˚25′N, 44˚15′E); altitude 2000m. NOMOT observations planned to be connected with a search of optical transients due to gamma ray bursts (GRB). After photometric verification of the GRB NOMOT telescopes will follow the afterglow down to 22th magnitude. A large fraction of optical afterglows decays as ~ 1/t, and ~$1/t^2$ after spectra brake (turnover) (http://grad40.as.utexas.edu/~quimby/tu2006/. Operation of NOMOT planned to be correlated with measurements of the Atmospheric Cherenkov Telescope (ACT) MAGIC, located at Canarians. MAGIC is equipped with Active Mirror System (AMS) allowing tuning the detectors huge 17 m. diameter dish in very few minutes for looking at new celestial coordinates.

This made MAGIC very sensitive device for detecting energetic transient phenomena like gamma-ray bursts (GRB). NOMOT, receiving the same alert from satellites will be able to detected afterglow of the same objects in optical diapason, thus providing multivariate observations of GRBs, Supernovae explosions and other energetic phenomena in the Universe.

**14. A. Chilingarian, T.Dudok, Detection of weak ground level enhancements, Management Committee Meeting and Scientific Event COST Action 724, "Developing the basis for monitoring, modeling and predicting Space Weather", Sofia (Bulgaria), May 21-25, 2007**

**Abstract**

Whereas strong ground level enhancements (GLE) are easy to detect with neutron monitors, the statistical evidence for weak events (that still correspond to strong fluences in space) is much more problematic. These weak events must be discriminated against various effects such as background noise, transients caused by Forbush effects, terrestrial rotation, etc. One of the way of enhacing the detection of weak events consists in analysing several simultaneous neutron measurements, making use of the fact that the imprint of different physical mechanisms is latitude- and detector-dependent. These imprints are defined by statistical means. Using a few events, we show how weak GLEs can be better detected that way.

**15. A.Chilingarian (invited talk) Research of highest energy Solar Cosmic Rays, IHY 2007: 1st Coordinated Investigation Programme meeting, Bad Honnef, Germany, May 18 - 19, 2007**

**Abstract**

Available experimental data on the GLEs confirm proton acceleration up to ~20 GeV, acceleration to higher energies is not reliably proved. Middle and high-latitude neutron monitors can not be used for the reconstruction of the primary energy spectra well above 5 GeV due to very weak fluxes and rather small sizes of the detectors

The *Aragats Multidirectional Muon Monitor* (AMMM) is located at 40.5°N, 44.17°E (cutoff rigidity 7.6 GV)on the altitude 3200 m. a.s.l. (cutoff rigidity 7.6 GV) and consists of 100 m.sq. of plastic scintillators. Relative accuracy of measuring 1-minute time-series is ~0.17%, which enables registration of the very small enhancements of count rate, initiated by the SCR of highest energies. At 20 January 2005 AMMM detects an excess of count rate, correspondent to the Solar protons with energies above 20 GeV.

Along with operation of the AMMM we plan to develop new type world-wide network of particle detectors, measuring neutral and charged fluxes simultaneously and to be installed at middle and low latitudes. New particle detectors will perform monitoring of various species of secondary cosmic rays with different energy thresholds.

The modernization of the AMMM at Aragats mountain will be performed to significantly enhance the reliability of the detector. We plan to design and install new Data Acquisition system, for fast access and control of detector parameters, additional hardware and software facilities for achieving data and sending data on-line to Internet.

A network of middle to low latitude particle detectors called SEVAN (Space Environmental Viewing and Analysis Network) is proposed to improve fundamental research of the space weather conditions and provide possibilities to perform short and long-term forecasts of the dangerous consequences of the space storms. The network will detect changing fluxes of the most species of secondary cosmic rays at different altitudes and latitudes, thus constituting powerful integrated device in exploring solar modulation effects. The network is planned to be installed at middle and

low latitudes and will be compatible with the currently operating high latitude particle detector network *Spaceship Earth*, coordinated by the group from Bartol Research Institute of University of Delaware in USA with Solar Neutron Telescopes network coordinated by the Nagoya University and with the Muon network coordinated by the group from Shinshu University in Japan.

We plan to develop new statistical methods for the analysis of multivariate time series from multiple channels of the ASEC monitors to make physical inference on the maximal energy of the solar protons and on estimates of the spectral knees reliable. The statistical procedures as Neural Networks with stochastic algorithms of net training, Bayesian decision rules with nonparametric estimation of the multivariate probability density function, Independent component analysis will be tuned for multiple time series treatment.

Particle fluxes measured at the medium to low latitudes with the SEVAN network, combined with information from space-born facilities, including new proposed Solar Sentinels fleet will provide experimental evidence on the most energetic processes in solar system and will constitute important plan of the creating global space weather monitoring and forecasting service.

16. **A.Chilingarian, Particle detectors networks for fundamental research, alert services and for promoting international collaborations, INTAS # 06-1000017-8777 Project Kickoff Meeting, February 27- March 3,2007, Tbilisi-Nor Amberd-Aragats-Yerevan**

**Abstract**

In 21-st century Space research became not only risky and costly pioneering exploration, but main source of fundamental information on basic knowledge about Universe and basis of extremely profitable space-based technologies. INTAS 8777 project is focused on the investigation of the characteristics of violent Solar Energetic Particle events by a proposed Eurasian network of cosmic ray detectors at Armenia, Germany, Israel, and Switzerland. Making use of advanced and sophisticated data analysis an improved Space Weather warning system shall be established from which society will benefit. We shall create a special web portal which will show the project background and obtained results including additional information of interest to the scientific community and to society. Other social and economic impacts include: the active participations of younger scientists and post graduate students in this project; the collaboration between the teams that lead to a transfer of knowledge used by each side.

17. **A. Chilingarian, Cosmic Rays in Space Weather Research, Third European Space Weather Week, Brussels, Belgium, November13-17, 2006**

**Abstract**

Particle fluxes in the vicinity of Earth are one of the global Geophysical parameters and one of major drivers of the Space Weather. Solar flares and coronal mass ejections trigger intense particle acceleration processes in solar corona. These particles are reaching terrestrial atmosphere and adding to the background flux of ambient population of isotropic galactic cosmic rays enhance total flux of secondary particles registered by the particle detectors on earth surface. Interplanetary coronal mass ejections on their way to earth also modulate the intensity of the galactic cosmic rays, thus introducing additional changes in the secondary fluxes detected by surface particle detectors.

Information on changing fluxes of secondary cosmic rays, as well as observations in soft x-ray, hard x-ray and h-alpha emission can be used to characterize and forecast Space Weather conditions. Surface monitors located at Aragats Space Environmental Center (ASEC) on Mt. Aragats in Armenia at 2000 and 3200 m altitude detect charged and neutral components of secondary cosmic rays with different energy thresholds and various angles of incidence. This richness of information

gives hope that after proper simulation of the physical phenomena we will be able to estimate the shock size and magnetic field strength "frozen" in the Interplanetary Coronal Mass Ejecta, and, consequently predict the expected hazard of upcoming geomagnetic storms hours before shock arrival and detection by the magnetometers on ACE and SOHO.

Based on our experience with correlation analysis of multivariate time-series from ASEC monitors, we have designed and commissioned several types of particle detectors. In order to keep the instruments inexpensive, the options are kept flexible by using modular design. With these relatively portable and inexpensive detectors, the network of nations involved in space research can be significantly expanded and be enabled to participate in International Heliophysical Year.

**18. A.Chilingarian, Nor-Amberd Declaration, Global E-Content Summit: Empowering Creators and Educators, Yerevan, Armenia, October 5-7, 2006**

**Abstract**

Today, advances of science allow effective gathering of large amounts of critical data. Examples of scientific projects amassing large amounts of data on the state and current conditions of Earth and Sun are abound. Scientific networks monitor environment for natural and man-made hazards, such as the atomic bomb testing monitoring, or solar activity monitoring. These existing networks already have enormous possibilities to warn against such hazards as impending earthquakes or solar storms. Humanity has developed also infrastructure for quick and efficient information delivery. What is missing is the global system that will timely deliver to end users information obtained by scientists, informing people and governments about hazards, and allowing them take steps to avoid or minimize their risks. The humanity needs to make this step urgently.

**19. A.Chilingarian, CRD Activity Review, Global E-Content Summit: Empowering Creators and Educators, Yerevan, Armenia, October 5-7, 2006**

**Abstract**

The Geographic advantages, the historic intellectual capacity handed down from generation to generation, the innovation of new and powerful methodology, state of the art electronics development, the powerful servers and networking equipment used for on-line data acquisition, transfer, analysis and display make CRD uniquely vital for the world-effort to understand our universe and specially Space Weather. The experimental physics, electronics, and computer laboratories are equipped with modern facilities to design and assemble state of the art components, including sophisticated miniaturized Control and Data Acquisition (DAQ) electronic boards. The lecture halls and laboratories serve as a center of space education for Yerevan State University (YSU) and Yerevan State Engineering University students and international conferences. CRD develops and implements Undergraduate, Master and PhD programs for students of the Physics Department of universities.

**20. A. Chilingarian (invited talk), Solar Flares and CME as modulated agents of the Cosmic Ray flux incident on terrestrial atmosphere. What can we deduce from particle detector data?, 8th Hvar Astrophysical Colloquium, Dynamical Processes in the Solar Atmosphere, September 24-29, 2006, Hvar, Croatia**

**Abstract**

Particle fluxes in the vicinity of Earth are one of the global Geophysical parameters and are influenced by the most energetic processes in the solar atmosphere. Solar flares and coronal mass

trigger intense particle acceleration processes in solar corona. These particles are reaching terrestrial atmosphere and change the intensity of background flux of ambient population of isotropic galactic cosmic rays. Interplanetary coronal mass ejections on their way to earth also modulate the intensity of the galactic cosmic rays detected by surface particle detectors.

Information on changing fluxes of secondary cosmic rays, as well as observations in soft x-ray, hard x-ray and h-alpha emission can be used to characterize processes in solar atmosphere.

Time series of intensities of the charged and neutral particles can provide also highly cost-effective information on the key characteristics of the interplanetary disturbances. Surface monitors located at Aragats Space Environmental Center (ASEC) on Mt. Aragats in Armenia at 2000 and 3200 m altitude detect charged and neutral components of secondary cosmic rays with different energy thresholds and various angles of incidence. This richness of information gives hope that after proper simulation of the physical phenomena we will be able to estimate the shock size and magnetic field strength "frozen" in the Interplanetary Coronal Mass Ejecta, and, consequently predict the expected hazard of upcoming geomagnetic storms hours before shock arrival and detection by the magnetometers on ACE and SOHO. Based on our experience with correlation analysis of multivariate time-series from ASEC monitors, we have designed and commissioned several types of particle detectors. In order to keep the instruments inexpensive, the options are kept flexible by using modular design. With these relatively portable and inexpensive detectors, the network of nations involved in space research can be significantly expanded and be enabled to participate in International Heliophysical Year.

**21. A. Eghikyan, A. Chilingarian, Data Visualisation Interactive Network for the Aragats Space-environmental Center, 36th COSPAR Scientific Assembly, Beijing, China, July 16-23, 2006**

**Abstract**

The ASEC facilities provide real time monitoring of cosmic particle fluxes with a number of particle detectors located at high-altitude research stations at mt. Aragats, Armenia. Data from ASEC monitors is widely used in research of the solar physics and Space Weather. DVIN is strategically important as a scientific application to help develop space science and to foster global collaboration in solar physics and in forecasting potential hazards of solar storms. The system is highly interactive and exceptional information is easily accessible online. Data can be monitored and analyzed for desired time spans in a fast and reliable manner by the remote users world-wide. DVIN provides wide possibilities for sharing data and sending warnings and alerts to scientists and world-wide, which have fundamental and practical interest in knowing the space weather conditions. DVIN gives opportunity to remote groups to share the process of analyzing, exchange data analysis methods and schemes, prepare joint publications and maintain networks of particle detectors.

**22. K. Arakelyan et al.,New Detector for Space Weather research on mt. Aragats, 36th COSPAR Scientific Assembly, Beijing, China, July 16-23, 2006**

**Abstract**

The Nor-Amberd Muon Multidirectional Monitor (NAMMM) consists of two layers of plastic scintillators above and below one of the two sections of the Neutron Monitor NM-64. The lead filter of the NM absorbs electrons and low energy muons. The threshold energy of the detected muons is estimated to be 350 MeV. Therefore detector simultaneously measures particles of 3 types: low energy charged component, neutrons and high energy muons. The data acquisition system of the NAMMM can register all coincidences of detector signals from the upper and lower

layers, thus, enabling measurements of the arrival of the muons from different directions. In the report we will demonstrate the sensitivity of the different species of secondary cosmic ray flux to geophysical conditions, taking as examples the extremely violent events of 2003 and 2005.We introduce correlation analysis of the different components of registered time-series as a new tool for the classification of the geoeffective (events on earth affected by solar activity) events and for the forecasting of the severity of the upcoming geomagnetic storm.

**23. A. Chilingarian et al., A new type Particle Detector Network for Solar Physics and Space Weather Research, 36th COSPAR Scientific Assembly, Beijing, China, July 16-23, 2006**

**Abstract**

A network of middle to low latitude particle detectors called SEVAN (Space Environmental Viewing and Analysis Network) is planned in the framework of the International Heliophysical Year (IHY), to improve fundamental research of the solar accelerators and space weather conditions. The network will detect changing fluxes of the most of species secondary cosmic rays at different altitudes, latitudes and altitudes those constituting powerful integrated device in exploring solar modulation effects. Surface detectors measure time series of secondary particles born in cascades originated in the atmosphere by primary ions. Studies of these particles shed light on the high-energy particle acceleration mechanisms by flares and Coronal Mass Ejection driven shocks. Time series of intensities of high energy particles can also provide highly costeffective information on the key characteristics of the interplanetary disturbances.

Recent results on of the detection of the extreme solar events (2003, 2005) by the monitors of the Aragats Space-Environmental Center (ASEC) will illustrate wide possibilities opening with introduction of new particle detectors measuring neutron, electron and muon fluxes with inherent correlations.

**24. A. Chilingarian et al.,Characteristics of Proton Acceleration at the Sun on January 20, 2005, observed by the surface particle detectors, 36th COSPAR Scientific Assembly, Beijing, China, July 16-23, 2006**

**Abstract**

On January 20, 2005, 7:02-7:05 UT the Aragats Multidirectional Muon Monitor (AMMM) located at 3200 m a.s.l. registered enhancement of the high energy secondary muon flux (threshold _5 GeV). The enhancement, lasting three minutes, has statistical significance of _4_ (for the three-minute time series) and is related to the X7.1 flare seen by the GOES satellite and the Ground Level Enhancement detected by the world-wide network of neutron monitors and by muon detectors. The energetic and temporal characteristics of the muon signal from the AMMM are compared with the same characteristics of other solar monitors located at the Aragats Space-Environmental Center (ASEC). Various ASEC detectors select different energetic populations of the Solar Cosmic Rays (SCR). Therefore, from the multivariate time-series we conclude that in the episode of the particle acceleration at 6:55 – 7:05 UT 20 January 2005: (a) protons were accelerated at the Sun up to energies of 20GeV in excess; (b) the relativistic protons with energies <10 GeV were ejected in the interplanetary space earlier than the highest energy protons (>20 GeV); (c) protons accelerated in the episode (maximum at 7:12 -7:15 UT), have lower energy compared with first acceleration episode.

25. **A. Eghikyan, A. Chilingarian, Data Visualisation Interactive Network for the Aragats Space-environmental Center, 13th Young Scientists Conference on Astronomy and Space Physics, Kiev, Ukraine, April 25-29, 2006**

**Abstract**

The ASEC facilities provide real time monitoring of cosmic particle fluxes with a number of particle detectors located at high-altitude research stations at mt. Aragats, Armenia. Data from ASEC monitors is widely used in research of the solar physics and Space Weather. DVIN is strategically important as a scientific application to help develop space science and to foster global collaboration in solar physics and in forecasting potential hazards of solar storms. The system is highly interactive and exceptional information is easily accessible online. Data can be monitored and analyzed for desired time spans in a fast and reliable manner by the remote users world-wide. DVIN provides wide possibilities for sharing data and sending warnings and alerts to scientists and world-wide, which have fundamental and practical interest in knowing
the space weather conditions. DVIN gives opportunity to remote groups to share the process of analyzing, exchange data analysis methods and schemes, prepare joint publications and maintain networks of particle detectors.

26. **K. Arakelyan et al.,New Detector for Space Weather research on mt. Aragats, 13th Young Scientists Conference on Astronomy and Space Physics, Kiev, Ukraine, April 25-29, 2006**

**Abstract**

The Nor-Amberd Muon Multidirectional Monitor (NAMMM) consists of two layers of plastic scintillators above and below one of the two sections of the Neutron Monitor NM-64. The lead filter of the NM absorbs electrons and low energy muons. The threshold energy of the detected muons is estimated to be 350 MeV. Therefore detector simultaneously measures particles of 3 types: low energy charged component, neutrons and high energy muons. The data acquisition system of the NAMMM can register all coincidences of detector signals from the upper and lower layers, thus, enabling measurements of the arrival of the muons from different directions. In the report we will demonstrate the sensitivity of the different species of secondary cosmic ray flux to geophysical conditions, taking as examples the extremely violent events of 2003 and 2005.We introduce correlation analysis of the different components of registered time-series as a new tool for the classification of the geoeffective (events on earth affected by solar activity) events and for the forecasting of the severity of the upcoming geomagnetic storm.

27. **A.Chilingarian, Particle detectors networks for the Fundamental Physics, Space Weather and Education, The First International Symposium on Space Education, Moscow, Russia, June 26-30, 2006**

**Abstract**

Involvement of students in the experimental studies is of crucial importance. It is necessary to select a topic interesting from scientific point of view and simple enough to allow students understand and participate in all stages of experiment from measurements via data analysis to physical inference. Also the results of experiment should be apparent and allow on-line analysis and interpretation. Very important is to connect the physical inference not only with progress of the fundamental science, but also with applied problems, and, if possible, with real life problems.

In my report I will try to prove that networks of particle detector designed and commissioned in Cosmic Ray Division of Alikhanyan Physics Institute fulfilled these requirements. Detailed

information on our experience with students of Physical Department of Yerevan State University is contained in 3 posters: New Particle Detector for Space Weather Research; Simple Detectors for Educational Studies; Data Visualization Interactive Network.

**28. Karen Arakelyan, Ashot Chilingarian, New Detector for Space Weather Research at Mt. Aragats, The First International Symposium on Space Education, Moscow, Russia, June 26-30, 2006**

**Abstract**

The Nor-Amberd Muon Multidirectional Monitor (NAMMM) consists of two layers of plastic scintillators above and below one of the two sections of the Neutron Monitor NM-64. The lead filter of the NM absorbs electrons and low energy muons. The threshold energy of the detected muons is estimated to be 350 MeV. Therefore detector simultaneously measures particles of 3 types: low energy charged component, neutrons and high energy muons. The data acquisition system of the NAMMM can register all coincidences of detector signals from the upper and lower layers, thus, enabling measurements of the arrival of the muons from different directions. In the report we will demonstrate the sensitivity of the different species of secondary cosmic ray flux to geophysical conditions, taking as examples the extremely violent events of 2003 and 2005.We introduce correlation analysis of the different components of registered time-series as a new tool for the classification of the geoeffective (events on earth affected by solar activity) events and for the forecasting of the severity of the upcoming geomagnetic storm.

**29. A. Chilingarian, A middle-to-low magnitude particle detector network for Space Weather research, Annual Meeting of the Balkans, Black Sea and Caspian Sea Regional Network on Space Weather Studies, March 30 - April 1, 2006 / Manavgat - Antalya, TURKEY**

**Abstract**

Time series of intensities of high energy particles can provide highly cost-effective information on the key characteristics of the interplanetary disturbances. Surface monitors located at Aragats Space Environmental Center (ASEC) on Mt. Aragats in Armenia at 2000 and 3200 m altitude detect charged and neutral components of secondary cosmic rays with different energy thresholds and various angles of incidence. This richness of information gives hope that after proper simulation of the physical phenomena we will be able to estimate the shock size and magnetic field "frozen" in the ICME, and, consequently predict the expected hazard of upcoming geomagnetic storms hours before its arrival and detection by the magnetometers on ACE and SOHO.

Particle fluxes in the vicinity of Earth are one of the global Environmental parameters and major elements of Space Weather.

Because of the highly indirect nature of surface measurements, we need sophisticated procedures of error estimates on the predictions. To identify the major sources of error we need to compare measured and simulated characteristics of secondary fluxes. To accomplish this we need to measure, simulate and compare:

- time series of neutrons, low energy charged component (mostly electrons and muons) and high energy muons);
- the correlation between changing fluxes of various secondary particles;
- directional information.

Based on our experience with correlation analysis of multivariate time-series from ASEC monitors, we have designed and fabricated several new-types of particle detectors. In order to keep the instruments inexpensive, the options are kept flexible by using modular design. With these

relatively portable and inexpensive detectors, the network of nations involved in space research can be significantly expanded and be enabled to participate in International Heliophysical Year.

**30. A.Chilingarian, IHY Activity in Armenia, The First IHY European General Assembly, January, 10-13th 2006, Paris (France)**

**Abstract**

Particle fluxes in the vicinity of Earth are one of the global Geophysical parameters and major elements of Space Weather. Time series of intensities of high energy particles can provide highly cost-effective information on the key characteristics of the interplanetary disturbances. Surface monitors located at Aragats Space Environmental Center (ASEC) on Mt. Aragats in Armenia at 2000 and 3200 m altitude detect charged and neutral components of secondary cosmic rays with different energy thresholds and various angles of incidence. This richness of information gives hope that after proper simulation of the physical phenomena we will be able to estimate the shock size and magnetic field strength "frozen" in the Interplanetary Coronal Mass Ejecta, and, consequently predict the expected hazard of upcoming geomagnetic storms hours before shock arrival and detection by the magnetometers on ACE and SOHO.

Based on our experience with correlation analysis of multivariate time-series from ASEC monitors, we have designed and commissioned several types of particle detectors. In order to keep the instruments inexpensive, the options are kept flexible by using modular design. With these relatively portable and inexpensive detectors, the network of nations involved in space research can be significantly expanded and be enabled to participate in International Heliophysical Year. We propose the deployment of such detectors in neighboring countries, expanding to the Middle East and Europe, and eventually in the rest of the world.

**31. A. Chilingarian, Space Weather Research for Developing Countries, UN/ESA/NASA Workshop on International Heliophysical Year (IHY 2007), Abu-Dhabi and Al-Ain, United Arab Emirates, November 19-25, 2005**

**Abstract**

Space Weather Research, and for that matter space research, need not be confined to the most affluent and most developed countries only. In many instances of space research, our entire planet can be considered as a space probe, thus development of space research programs in various geographic locations, locations not necessarily populated with economically affluent countries is very important. Along with these research opportunities for the developing countries and for the benefit of the world at large, the development of a very effective and efficient Information Technology network is necessary world wide – again both in economically affluent and developing countries. With today's global economy and interdependence of countries on each other, the quality of life for all societies is directly dependent on effective use of Information Technology for the whole of society.

**32. A. Chilingarian, Modular Particle Monitor for Neutral and Charged CR fluxes, UN/ESA/NASA Workshop on International Heliophysical Year (IHY 2007), Abu-Dhabi and Al-Ain, United Arab Emirates, November 19-25, 2005**

**Abstract**

There are 2 aspects of Information Technology trends in science: first connected with tools to provide all possibilities to researcher in making new knowledge and the second – to share crucial

scientific information with society. And if the first problem is easy to solve (new powerful search machines, user friendly interfaces, security), the most of scientific information necessary for the decision making is hidden in scientific reports and special journals, not assessable to the decision makers. A good example of the sharing scientific information wirh society is the DVIN 1 platform, developed in CRD – the winner of world-wide competition of information products belonging to category electronic science at the First Information Summit in Geneva, December 2003.

The development of DVIN with enlarged functions of analysis and visualization was presented by A. Yghikyan. Unfortunately, very few crucial pieces of scientific data are easy to find in Internet, and not all essential information is delivered to user in time. The tragic example of December 2004 Tsunami, gives an example of very poor state of distribution of information on upcoming catastrophes.

Another example of dependence of human technologies on natural catastrophes is the Space Weather. About 1500 satellites are working in space. The cost of building these satellites was $160 billion, launching them into orbit $30 billion. To USA alone the space-born technologies return $225 billion in profits every year and have rapidly become one of largest segments to USA Gross National Product.Space-based systems providing critical infrastructure that support the quality of life on Earth. Because of humanity's increasing dependence on space-based systems, spacecraft that can survive and operate through all space environment conditions are required. It is not possible to achieve cost-effective, "all weather" space systems without accurate knowledge of the Space Weather. Space Storms lead to loss of data, degradation of capability, service outages, and, in extreme cases, the loss of satellite.

### 33. A. Chilingarian (invited talk), Aragats Space Environmental Center (ASEC): Space Weather Observatory in Armenia, Solar Extreme Events 2005:Fundamental Science and Applied Aspects, Nor-Amberd, Armenia, 26-30 September, 2005

**Abstract**

The Aragats Space-Environmental Center (ASEC) provides monitoring of different species of secondary cosmic rays and consists of two high altitude research stations on Mt. Aragats in Armenia. Geographic coordinates: 40°30'N, 44°10'E, cutoff rigidity: ~7.6 GV. The two 18NM-64 neutron monitors, are operated at Nor-Amberd (2000m elevation), and at Aragats, (3200m elevation) research stations; the monitors are equipped with interface cards, providing time integration of counts from 1 sec up to 1 minute. The Solar Neutron Telescope (SNT), is in operation at the Aragats research station. The main detecting volume consists of four 1 m2 surface, 60 cm thick scintillation blocks overviewed by photomultipliers. The Nor-Amberd Muon Multidirectional Monitor (NAMMM )consists of two layers of plastic scintillators above and below two of the three sections of the Nor Amberd NM. The lead (Pb) filter of the NM absorbs electrons and low energy muons. The NAMMM consists of 6 up and 6 down scintillators, each having the area of 0.81 $m^2$. The distance between layers is ~ 1 m. The data acquisition system of the NAMMM can register all coincidences of detector signals from the upper and lower layers, thus enabling monitoring of the directional information.

### 34. A.A. Chilingarian, Particle Detectors in Solar Physics and Space Weather Research Solar Extreme Events 2005:Fundamental Science and Applied Aspects, Nor-Amberd, Armenia, 26-30 September, 2005

**Abstract**

The use of large area particle detectors which can only be accommodated at Earth surface is vital for measuring the low fluxes of high energy particles accelerated in the vicinity of the Sun.

The enigma of particle acceleration in the Universe can not be explored without understanding of solar particle accelerators. The energy spectra of highest energy solar particles, as measured by the surface detectors will shed light on these universal processes of high-energy particles acceleration at numerous galactic and extragalactic sites. Detected at earth, energetic particles also can provide highly cost-effective information on the key characteristics of the interplanetary disturbances. Because cosmic rays are fast and have large scattering mean free paths in the solar wind, this information travels rapidly and can be useful for space weather forecasting. Taking into account that only very few of a great number of Solar Flares (SF) and Coronal Mass

Ejections (CME) produce intensive ion fluxes (so called – Solar Energetic Particle events – SEP), it is not only critical to alert clients about the arrival of the most severe radiation storms, but also to minimize the number of false alarms against events which are not severe enough to cause damage. Because the flux of high-energy ions is weak and because the most violent particle events are usually highly anisotropic, the network of the large area particle detectors, located at low latitudes and high mountain altitudes is necessary for their reliable detection. The information about primary ion type and energy is mostly smeared during its successive interactions with atmospheric nuclei, therefore, only coherent measurements of all secondary fluxes (neutrons, muons, and electrons), along with their correlations, can help to make unambiguous forecasts and estimations of the energy spectra of upcoming dangerous flux.

Particle detectors of Aragats Space Environmental Center (ASEC) in Armenia perform monitoring of various species of secondary cosmic rays with different energy thresholds at altitudes 2000 and 3200 m. a.s.l. We present results on sensitivity of secondary cosmic ray flux to parameters of the incident “beams” of solar particles and – to approaching clouds of the magnetized solar plasma of CME, taking as examples the solar extreme event of 20 January 2005.

**35. N. Kh. Bostanjyan, A.A. Chilingarian, V.S. Eganov, G.G. Karapetyan, On the Highest Energies of Proton Acceleration at the Sun on January, 20 2005, Solar Extreme Events 2005:Fundamental Science and Applied Aspects, Nor-Amberd, Armenia, 26-30 September, 2005**

**Abstract**

On January 20, 2005, 7:02-7:05 UT the Aragats Multidirectional Muon Monitor (AMMM) located at 3200 m a.s.l. registered enhancement of the high energy secondary muon flux (threshold ~5 GeV). The enhancement,lasting three minutes, has statistical significance of ~4σ (for the three-minute time series) and is related to the X7.1 flare seen by the GOES satellite and the Ground Level Enhancement detected by the world-wide network of neutron monitors and by muon detectors. The energetic and temporal characteristics of the muon signal from the AMMM are compared with the same characteristics of other monitors located at the Aragats Space-Environmental Center (ASEC). Various ASEC detectors select different energetic populations of the Solar Cosmic Rays (SCR). Therefore, from the multivariate time-series we conclude that in the episode of the particle acceleration at 7:00 – 7:05 UT 20 January 2005: (a) protons were accelerated up to energies of 20GeV in excess; (b) the relativistic protons with energies <10 GeV were ejected in the interplanetary space earlier than the highest energy protons (>20 GeV); (c) protons accelerated in the episode (maximum at 7:12 -7:15 UT), have lower energy compared with first acceleration episode.

**36. H.S. Martirosyan, Event of January 20, 2005: Ion, Proton and Electron Injection Times, Solar Extreme Events 2005:Fundamental Science and Applied Aspects, Nor-Amberd, Armenia, 26-30 September, 2005**

**Abstract**

Knowledge of CR injection time is very important in terms of location detection and acceleration mechanism of these particles (flare or interplanetary shock wave). During some large events (e.g. 15-04-01, 26-12-01, 20-01-05) the first CR protons (electrons) with energies from 0,1MeV to ~1GeV (~1KeV to 0,5MeV) at the distance of 1 au are simultaneously registered within 5 minutes-long intervals. In contrast to protons and electrons the first ions in these events were registered with relative delay. We can assume that the first ions of this type of all energies were injected simultaneously and propagated without collisions. This assumption allows assessing ion injection times for the event of 15-04-01[1] with great precision by using linear regression method. This article provides assessment of He, C, O, Mg, Fe ion injection times for the event of 20-01-05, during which the largest GLE in the 23rd cycle of solar activity was registered.

Simultaneous registration does not allow applying this technique with protons and electrons. In this paper we used another method of assessing proton and electron injection times. Neutron monitors data were also used.

**37. V.Kh. Babayan, A.A. Chilingarian, Response of the Aragats Space Environmental Center Particle Detectors on the Geoeffective Solar events, Solar Extreme Events 2005:Fundamental Science and Applied Aspects, Nor-Amberd, Armenia, 26-30 September, 2005**

**Abstract**

Starting from autumn 2002 Aragats Space Environmental Center (ASEC) detectors perform monitoring of different species of secondary cosmic rays at two altitudes and with different energy thresholds. We present results on sensitivity of secondary cosmic ray flux to Space Weather conditions, taking as examples the solar extreme events of 2003-2005. We compare the response of charged and neutral components of secondary cosmic rays on

Forbush decreases (Fd) and geomagnetic storms (GMS) .We introduce multivariate correlation analysis of the different components of registered time-series as a tool for the classification of the geoeffective events, i.e., Fd and reductions of the geomagnetic cutoff rigidity.

**38. M.Z. Zazyan, A.A. Chilingarian, On the Possibility to Deduce Solar Proton Energy Spectrum of the 20 January 2005 GLE using Aragats and Nor-Amber Neutron Monitors Data, Solar Extreme Events 2005:Fundamental Science and Applied Aspects, Nor-Amberd, Armenia, 26-30 September, 2005**

**Abstract**

Modeling of Aragats and Nor-Amberd neutron monitors responses to solar proton flux was performed for different possible spectral indexes. By comparing the relative response of two neutron monitors with observations the spectral index of the power-law proton energy spectrum for the Ground Level Enhancement on January 20, 2005 at the time of maximum increase (7:15 UT) was found to be ~5 - 6. The simulation of the primary protons transport through the Earth atmosphere was performed using the well-known software package CORSIKA. The test proton spectra for the simulation were derived using the low energy proton fluence spectrum from instruments on ACE and SAMPEX spacecraft, and the intensity of >100 MeV protons measured by GOES11 spacecraft.

**39. M.Z. Zazyan, A.A. Chilingarian, Modelling of the Aragats Space Environmental Center Monitors Response to Galactic and Solar Cosmic Rays, Solar Extreme Events 2005:Fundamental Science and Applied Aspects, Nor-Amberd, Armenia, 26-30 September, 2005**

**Abstract**

Detectors of Aragats Space Environmental Center (ASEC) are monitoring different species of secondary cosmic rays at 2 altitudes according to various energy thresholds. Using CORSIKA code we have calculated the response of ASEC monitors to galactic cosmic rays and to different transient events, such as Ground Level Enhancements (GLEs) and geomagnetic storms, influencing cutoff rigidity. The response of ASEC monitors, simulated for historic events of 23-rd solar cycle, is compared with corresponding measurements.

**40. A.A. Chilingarian, L.G. Melkumyan, A.E. Reimers, Calculation of the Threshold Energies for Aragats Solar Neutron Telescope, Solar Extreme Events 2005:Fundamental Science and Applied Aspects, Nor-Amberd, Armenia, 26-30 September, 2005**

**Abstract**

The Aragats Solar Neutron Telescope (SNT) is in operation at the Mt. Aragats research center (3200 m. above sea level) in Armenia and constitutes part of the world-wide network, coordinated by Nagoya University. In this paper we calculate the response function of the SNT to the galactic cosmic rays and determine the energy thresholds of the four SNT channels. Results of Monte–Carlo simulation and experimental calibration are compared. The capability of SNT to select different energetic populations of the primary particles is demonstrated taking as example very severe geomagnetic storm at 20 November 2003.

**41. G.G. Karapetyan, A.A. Chilingarian, Multidetector Correlation Study of Solar Transient Events, Solar Extreme Events 2005:Fundamental Science and Applied Aspects, Nor-Amberd, Armenia, 26-30 September, 2005**

**Abstract**

Ground Level Enhancements (GLE), measured by the low latitudes particle detectors are not as well pronounced as measured by detectors located at high latitudes due to their larger geomagnetic cutoff rigidity. Proceeding from the measurements of several particle detectors located at the Aragats Space Environmental Center (ASEC), we develop a methodology, which combines the data from 3 monitors to reveal solar transient events. Method utilizes correlation information from 3 detectors measuring neutrons on different latitudes and low energy charged particles. The product of 3 correlation coefficients (CC) between the time series of Aragats Neutron Monitor, Nor-Amberd Neutron Monitor and Solar Neutron Telescope gets large values when all three time series are changed similarly, otherwise the product fluctuates around zero. Thus, being a composite characteristic of three different monitors the product presents more pronounced indication of solar transient events – GLE, Forbush decreases (Fd) and geomagnetic storms (GMS). Statistical distribution of the null hypotheses (H0 - no signal hypothesis), obtained by Monte-Carlo simulations, proves very low chance probability of “false alarm”.

**42. G.G. Karapetyan, A.A. Chilingarian, N.Kh. Bostanjyan, Channel-to-Channel Analysis of Aragats Muon Monitor Detection of >5GeV Muons in 20 January 2005 Ground Level Enhancement, Solar Extreme Events 2005:Fundamental Science and Applied Aspects, Nor-Amberd, Armenia, 26-30 September, 2005**

**Abstract**

During the famous solar flare of 20 January 2005, the 3-min time series of the Aragats Multidirectional Muon Monitor (AMMM) demonstrated maximum muon count in excess of ~ 4σ at 7:02 UT. The probability that this excess is caused by random fluctuation is ~ 4.3×10–5. We applied Binomial statistical analysis of excesses in each of 42 independent detector channels. We estimated the probability that in n channels the count surpass the given level L, and then by changing L obtained minimal value of this probability. For example: using 3-min data we find that at 7:01signal fluctuation greater than 0.9σ is observed in 21 out of 42 channels, which leads to the probability about 3.1×10–6, an order of magnitude less than the Gaussian chance probability. Thus the applied approach of analyzing the counts from each channel separately leads to lower value of probability of signal to be random.

**43. A.R. Eghikyan, A.A. Chilingarian, Data Visualisation Interactive Network for the Aragats Space - Environmental Center, Solar Extreme Events 2005:Fundamental Science and Applied Aspects, Nor-Amberd, Armenia, 26-30 September, 2005**

**Abstract**

The ASEC (Aragats Space Environmental Center) facilities provide real time monitoring of cosmic particle fluxes with a number of particle detectors located at high-altitude research stations at mt. Aragats, Armenia. For the issuing of warnings and alerts on sudden changing of the near-earth radiation environments and for the detailed collaborative analysis of the most important solar modulation events we developed distributed data analysis interface with automatic data storage and processing. For the physical inference based on the changing particle fluxes the DVIN (Data Visualization Interactive Network) software is use). Data from ASEC monitors is accessible on-line from http://crdlx5.yerphi.am/DVIN3 and currently is widely used in research of the solar physics and Space Weather. In the paper we illustrate the how DVIN should be operated taking as example famous Halloween events (28October -2 November 2003).

**44. A Chilingarian et al, Multivariate correlation analysis of transient solar events by the facilities of Aragats Space Environmental Center (ASEC), 29th International Cosmic Ray Conference (ICRC 2005), 03-10 August, Pune, India**

**Abstract**

Starting from autumn 2002 ASEC detectors perform monitoring of different species of secondary cosmic rays at two altitudes and with different energy thresholds. We present results on sensitivity of secondary cosmic ray flux to geophysical conditions, taking as examples the solar extreme events of 2003-2005. We introduce multivariate correlation analysis of the different components of registered time-series as a tool for the classification of the geoeffective events, i.e. Ground Level Enhancements (GLE), Forbush decreases (Fd) and effective reductions of the geomagnetic cutoff rigidity.

**45. H Martirosyan et al, Correlation of the estimated arrival time of the relativistic solar ions at 1 AU and start of ground level enhancement (GLE) 29th International Cosmic Ray Conference (ICRC 2005), 03-10 August, Pune, India**

**Abstract**

We are investigated possible correlations between the calculated arrival times of the first relativistic ions at Earth and GLE start times registered by surface monitors. The analysis is based on the arrival times and energies of the first solar ions, registered by the Solar Isotope Spectrometer (SIS) on board of the ACE satellite, and protons, registered by GOES satellites.

We consider both cases when the interplanetary propagation of the first high energy ions is essentially scatter-free and the diffusion of high energy ions during propagation in the interplanetary magnetic field. We extrapolate the time-velocity and time-rigidity relationships to calculate the expected arrival times of the relativistic ions that are energetic enough to enter the atmosphere at the Aragats geographical location and produce secondary fluxes that reach the monitors.

**46. A.Chilingarian et al., Space Weather Observatory at Aragats mountain in Armenia, 29th International Cosmic Ray Conference (ICRC 2005), 03-10 August, Pune, India**

**Abstract**

The Aragats Space-Environmental Center (ASEC) provides monitoring of different species of secondary cosmic rays and consists of two high altitude research stations on Mt. Aragats in Armenia. Geographic coordinates: 40°30'N, 44°10'E, cutoff rigidity: ~7.6 GV. The two 18NM-64 neutron monitors, are operated at Nor-Amberd (2000m elevation), and at Aragats, (3200m elevation) research stations; the monitors are equipped with interface cards, providing time integration of counts from 1 sec up to 1 minute. The Solar Neutron Telescope (SNT), is in operation at the Aragats research station. The main detecting volume consists of four 1 m2 surface, 60 cm thick scintillation blocks overviewed by photomultipliers. The Nor-Amberd Muon Multidirectional Monitor (NAMMM )consists of two layers of plastic scintillators above and below two of the three sections of the Nor Amberd NM. The lead (Pb) filter of the NM absorbs electrons and low energy muons. The NAMMM consists of 6 up and 6 down scintillators, each having the area of 0.81 m2. The distance between layers is ~ 1 m. The data acquisition system of the NAMMM can register all coincidences of detector signals from the upper and lower layers, thus enabling monitoring of the directional information.

**47. K Arakelyan et al., Nor-Amberd multidirectional muon monitor: new detector for the world-wide network29th International Cosmic Ray Conference (ICRC 2005), 03-10 August, Pune, India**

**Abstract**

For early forecasting of possible dangerous impacts of the interplanetary shocks headed toward Earth, the network of the surface cosmic ray detectors are used, measuring the modulation effects of the solar plasma cloud approaching. To measure precisely the directional anisotropy of the cosmic ray intensity enhanced by the modulation effects, the muon detector network should have a wide directional coverage. Nor Amberd multidirectional muon monitor (NAMMM) located on the slope of mountain Aragats in Armenia at 40°30'N, 44°10'E, altitude 2000 m, provides on-line data in 15 asymptotic directions, significantly improving the directional coverage of the pre-existing network and the capability of advance warning on the onset of space weather effects at Earth.

Detector is equipped with a modern electronics, allowing various software triggers; microcontroller based electronic units (HV power supply and counting modules) together with optional environmental sensors. The wireless Internet and satellite modems ensure the real-time data transmission rates sufficient for the forecasting within 3 minutes after signal detection.

**48. G Hovsepyan et al., The Size Spectra of Extensive Air Showers in the "Knee" region Measured by Maket- ANI detector 29th International Cosmic Ray Conference (ICRC 2005), 03-10 August, Pune, India**

**Abstract**

The MAKET-ANI detector is operating at altitude 3200 m. at slope of mt. Aragats in Armenia. More than million showers with size greater than 105 were registered by the MAKET-ANI detector in 1999-2004. Detector has effectively collected the cores of EAS, initiated by primaries with energies of 5·1014-3·1017 eV. After calculating the detector response function and accounting on the registration efficiency we present the EAS size spectra in 5 azimuth angle intervals. Taking into account reach statistics and high quality of data, it can serve for the estimation of the attenuation lengths and phenomenological characteristics of the strong interaction of primary cosmic rays with atmosphere.

**49. G Hovsepyan et al., The Lateral Distribution Function of Extensive Air Showers Measured by Maket-ANI detector29th International Cosmic Ray Conference (ICRC 2005), 03-10 August, Pune, India**

**Abstract**

The MAKET-ANI detector is operating at altitude 3200 m., at slope of mt. Aragats in Armenia. More than million showers with size, greater than 105 were registered, by the MAKET-ANI detector in 1999-2004. Detector has effectively collected the cores of EAS, initiated by primaries with energies of 5·1014 - 3·1017eV. After proving that the quality of the reconstruction of the Extensive Air Showers (EAS) size and shape are reasonably good we present the LDF functions for the distances up to 120 m. from EAS core. The obtained LDF functions are compared with CORSIKA562 (QGSJET, NKG) [1,2] simulations. Proceeding from thedependences of shower age on shower size we discuss the mass composition models supported by experimental evidence.

**50. A.Chilingarian (invited talk), Regional Network for the Space Weather research Regional Planning Meeting for the Balkan and Black Sea Region, Sozopol, Bulgaria, 6-8 June, 2005**

**Abstract**

Space-based systems provide critical infrastructure that support the quality of life on Earth. Because of humanity's increasing dependence on space-based systems, spacecraft that can survive and operate through all space environment conditions are required. It is not possible to achieve cost-effective, "all weather" space systems without accurate knowledge of the Space Weather. Space Storms lead to loss of data, degradation of capability, service outages, and, in extreme cases, the loss of satellite.

Aragats Space Environmental Center monitors:

- Measure as much as possible secondary CR fluxes with different energy thresholds;
- Monitor not only changing count rates, but also correlations between changing CR fluxes;
- Measure directional information;

- Use same detectors for both SW and high energy CR studies;
- Perform simulation of the time-series registered by the ASEC monitors;
- Correlate surface and space-born detectors data assessable from the Internert;
- Be part of world-wide networks;
- Provide forecasting and alerts on severe conditions of the Space Weather;
- Design and fabricate particle monitors detecting various species of cosmic rays.

***Balkan and Black Sea region countries should also find their ways to participate in this crucially important endeavor, because:***

- Most of technical progress in 21 century will come from Space Operations;
- New Space vision has Space Weather research and forecasting as a vital element for Space Operations;
- Information from networks of surface based detectors measuring secondary cosmic rays are compatible to data from space-born particle detectors and can be used for the reliable and timely SW forecasting;
- Developing countries should be a part of such networks to participate in the exploration of the Solar System and Universe;
- Necessary equipment is rather cheap and can be installed in scientific and educational institutions, schools, to make Space Research and Physics interesting and important for new generations.

The Space Weather detectors of new generation now under construction in CRD can serve as a good basis for the implementation of the regional scientific and forecasting network including Armenia, Georgia, Azerbaidjan, Iran, Turkey, Emirates, Dubaj and other countries. Installation and networking expenses will not exceed $50,000 and will permit the developing countries produce data vitally necessary for the space operations, those making links to the science and technology of 21st century.

### 51. A. Chilingarian, Space Weather and Solar Physics: basic science influencing everyday life SENCER Workshop in Armenia, May 26, 2005

**Abstract**

Space-based systems providing critical infrastructure that support thequality of life on Earth. Because of humanity's increasing dependence on space-based systems, spacecraft that can survive and operate through all space environment conditions are required.

- An example of dependence of human technologies on natural catastrophes is the Space Weather. About 1000 satellites are working in space. The cost of building these satellites was $160 billion, launching them into orbit $30 billion. The telecommunications industry relies on them to generate $250 billion in profits each year. To USA alone the space-born technologies return $225 billion in profits every year and have rapidly become one of largest segments to USA Gross National Product. Space Storms lead to loss of data, degradation of capability, service outages, and, in extreme cases, the loss of satellite.
- It is not possible to achieve cost-effective, "all weather" space systems without accurate knowledge of the Space Weather. Space Storms lead to loss of data, degradation of capability, service outages, and, in extreme cases, the loss of satellite.

- Very few crucial pieces of scientific data are easy to find, and not all essential information is delivered to user in time. The tragic example of December 2004 Tsunami, gives an example of very poor state of distribution of information on upcoming catastrophes. We are developing early warning system on severe Space Storms –our project ***"Data Visualization***

***Interactive Network for the AragatsSpace-environmental Center"–****DVIN for ASEC*, was announced as the world's best project in the category of e-science at the first World Summit on the Information Society (WSIS) 2003 in Geneva, December 9-13.

**52. A. Chilingarian, Space Weather Research for Developing Countries, 3rd Iranian Conference on Machine Vision, Image Processing & Applications (MVIP2005)**

**Abstract**

The space-born technologies have rapidly become one of largest segments of the world industry,providing critical infrastructure that support the quality of life on Earth. Because of humanity'sincreasing dependence on space-based systems, spacecraft that can survive and operate through all space environment conditions are required. It is not possible to achieve cost-effective, "all weather" space systems without accurate knowledge of the Space Weather. Space Storms lead to loss of data, degradation of capability, service outages, and, in extreme cases, the loss of satellite.

**53. A. Chilingarian, CRD Business Proposition: Armenian Neural Network Center; Commercialization of R&D Results in Armenia, April 18-20, Tsaghkadzor, Armenia**

**Abstract**

This is a business proposition to create the Armenian Neural Network Center (ANNC). Proceeding from the problem the customer needs to investigate, we will work with them to help them gather relevant data, then we will provide the solution in the form of "trained" network software, specific to the problem. The trained network for solving the problem can be easily tested and certified and easily implemented as a decision-making tool at the customer's site. As new data becomes available, the network can be "re-trained" and sent as an upgrade to the user in a very short time. Taking into account the positive feedback from current users of our packages in the scientific community, we feel we can apply our expertise in Neural Network solutions to industrial, medical, defense, management, and other users. Problems dealing with stochastic processes in complex nonlinear systems require robust algorithms for effective analysis of large amounts of nonparametric stochastic data. With our experience in writing successful algorithms and successfully implementing them in software, we can offer our expertise to various categories of customers. The solution will be available in user-friendly, ready-to-use format to the customer.An example of implementing our methods for a practical, and important problem solution is the patent ***"Multivariate random search method with multiple starts and early stop for identification of differentially expressed genes based on microarray data"***, described in a provisional application filed in the United States Patent and Trademark Office on March 1, 2002, and accorded Application No. 60/361,068.In 2004 patent was authorized in US, Canada and Europe under N 03713675/1-24-02-US0305730. Another our Internet information product – ***"Data Visualization Interactive Network for the Aragats Space-environmental Center" –*** *DVIN for ASEC*, was officially announced as the world's best project in the category of e-science at the first World Summit on the Information Society (WSIS) 2003 in Geneva, December 9-13.

# 7. Attachment 3: New electronics of the prototype detectors for Space Weather monitoring world-wide network

At the start of the ISTC project in April 2004 in CRD was organized electronics group for design and fabrication of modern electronic devices for read out and storage of physical information (for so called, Data Acquisition – DAQ) from the new particle detectors, developing in the framework of the project. The standard requirements for the DAQ system consist in reliable and consistent registration of the all electronic signals from particle detectors. During multiyear measurements the parameters of DAQ system should be continuously monitored to keep them stable. Electronics should not introduce loss of particle detection efficiency due to "dead times" and miscounts. Additional complexity of DAQ design was introduced by following requirements:

1. Counting not only the number of registered particle in the definite time span, i.e., time series, but also the amplitude of the Photomultiplier (PM) signals. This amplitude is proportional to the amount of light reaching PM cathode. This light in turn is proportional to the energy release of particle in body of scintillator (you have to take into account also light attenuation, see Chilingarian, Reimers, 2007a). For the charged particles energy release (when properly calibrated) is proportional to the number of particles hitting the detector. And energy release is also good proxy of neutral particle energy when neutral particle generates nuclear cascades in the thick scintillator. Therefore, the time series of the histograms of the energy releases in plastic scintillators provide additional information (as we can see from the chapter 3) on the type of solar particles incident the terrestrial atmosphere. Information on the number of particles hitting array of plastic scintillators, along with relative timing can be used also for the reconstruction of the energy and angles of incidence of the very high energy Galactic Cosmic Rays (GCR).

2. Particle identification by registering of all logical combination of the signal occurrence in the multilayered particle detector systems; particle detectors of operating world-wide networks monitoring solar activity have very limited possibility of particle identification and energy estimation. New electronics combined with multilayered detectors interlayer by the lead filters enables much wider options for the identification of the particles, various solar activity events and different physical phenomena. It became possible:

    - to identify charged and neutral particles hitting detector;
    - to identify primary solar particle hitting terrestrial atmosphere;
    - to estimate direction of the incident muons, which is good proxy of the incidence of the primary particle on the terrestrial atmosphere;
    - to investigate very rare events of muon capture by lead nuclei;
    - to measure burst spectra of cosmic rays;
    - to measure spectra of horizontal muons, and many others…

3. Correlating information from different particle detectors; Secondary cosmic rays are products of interactions of the primary high energy particle with terrestrial atmosphere, therefore fluxes of charged and neutral particles are correlated. Registration of the correlated time series, gives possibility not only detect peaks, deeps and other features connected with solar modulation effects, but also correlation matrices containing new interesting information on the nature of primary solar cosmic rays. Correlation matrices also are very useful for the continuous monitoring of trustworthiness of the detector channels

and estimation of important parameters of detector, as, for eample, multiplication of neutrons in the sections of neutron monitor.

Functionally, the new electronics of Aragats Solar Neutron Telescope (ASNT, see Fig. 1) and Nor Amberd Multidirectional Muon Monitor (NAMMM, see Fig. 2) consists of two parts: Data Acquisition (DAQ) and Detector Control System (DCS).

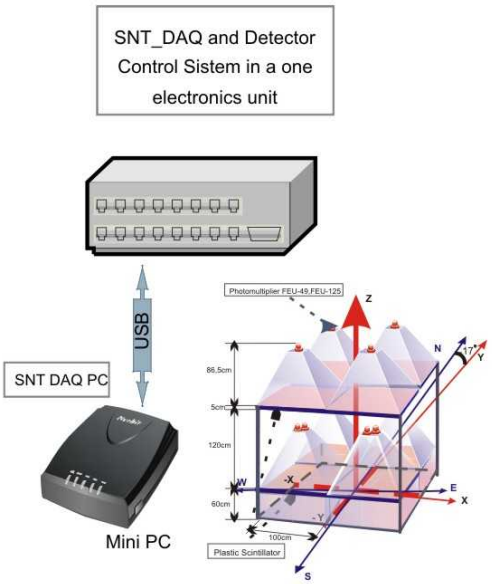


**Figure 1 Scheme of DAQ electronics of ASNT**

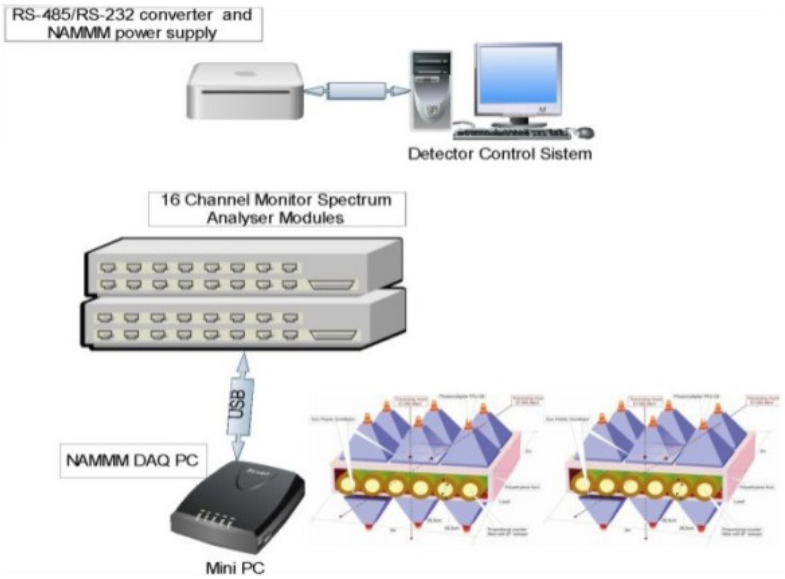


**Figure 2 Scheme of DAQ electronics of NAMMM**

The DAQ chain comprises Photomultiplier (PMT) FEU49, Buffer Preamplifier, Coaxial Cable, Logarithmic Analog-to-Digital Converter (LogADC), 32-bit ARM Microcontroller board, USB/COM interfaces and the Host PC. For the ASNT, all DAQ electronics, except of preamplifier is integrated into one 8-channel input unit, for the NAMMM in two 16-channel units, see Fig**. 3.**


**Figure 3 16-channel electronics Unit of NAMMM**

The DAQ of both detectors are similar, except for the channel numbers, while the DCS is slightly different. The ASNT is a single setup, that is why, one electronics unit is used for its both subsystems. The NAMMM is only a part of a large experimental setup, consisting of two identical NAMMM detectors and 3 neutron monitors sections. That is why, for the NAMMM, the DCS for all mentioned detectors are integrated into a separate (from DAQ) DCS net as shown in **Fig. 4**.

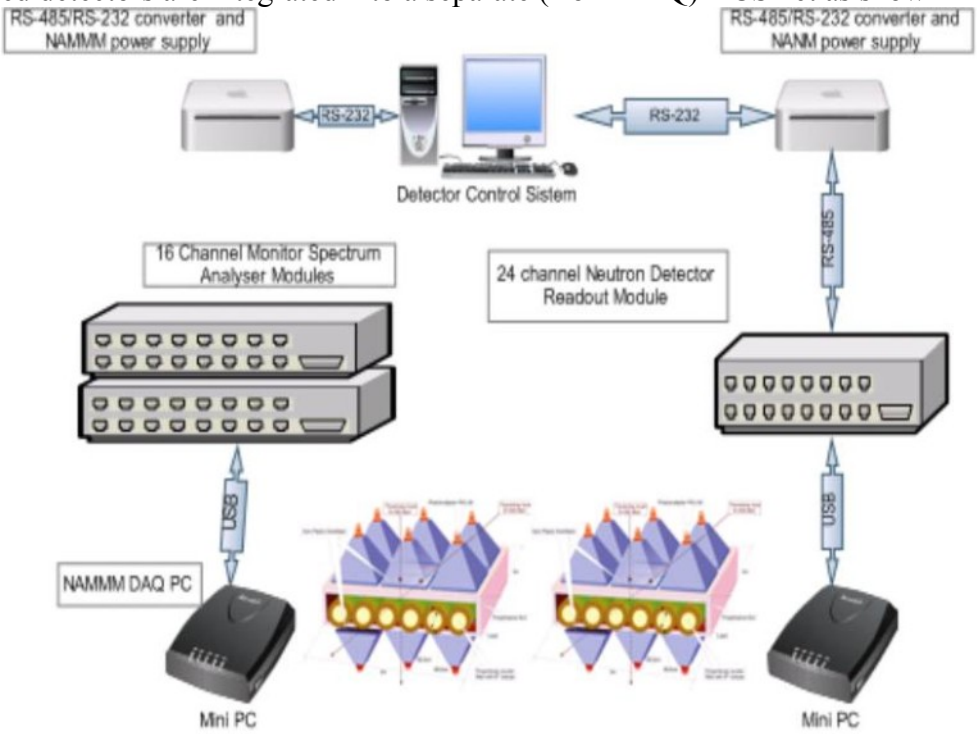


**Figure 4 DAQ and DCS networks in Nor Amberd**

The DCS of ASNT consists of: Programmable Local High Voltage Power Supply for PMT, RS-485 Local Net, Microcontroller and PC. The same Microcontroller is shared by DAQ and DCS. The DCS of the Nor Amberd setup includes all Programmable Local High Voltage Power Supplies for Muon scintillator detectors PMTs and Neuton Monitor proportional chambers as well as discriminators thresholds of the Neutron Detector Readout Module (see description of the 24 Channel Neutron Detector Readout Module below).

As far as the frontend hardware is concerned, both DCS and DAQ subsystems are tightly integrated. The PMT, Preamplifier and HV Supply are places inside the metal screen case on the top of the scintillation detector. There are two connectors on the case: standard BNC for the main signal connecting cable and round multiple connector for RS-485 interface and unregulated +15V for powering the Preamplifier and HV Source.

The interface/power connections of the ASNT detector are divided into two daisy/chain lines, one line for the upper four detectors and the second one for the lower four. All electrical connections from the detectors come to the ASNT Electronics Unit; see **Fig. 5**, containing both DAQ and DCS circuits.

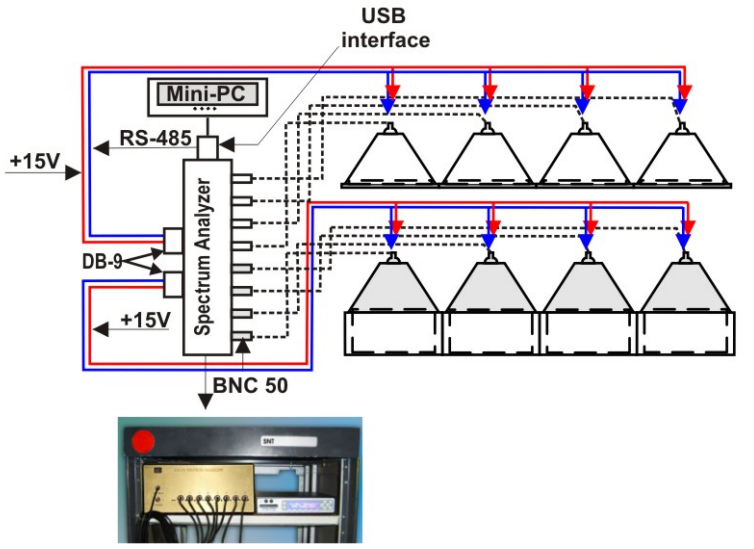


**Figure 5 ASNT setup with electronics unit**

The interface/power connections of the NAMMM detectors are divided into four daisy/chain lines, two to upper groups of 6 detectors and the two for lower groups.

Fig. 6 shows the charts of the metal case of the PMT tube with the PMT and electronics boards inside. There are three connectors placed on the case, A and C for the system interconnections and B for the high voltage manual measurement.

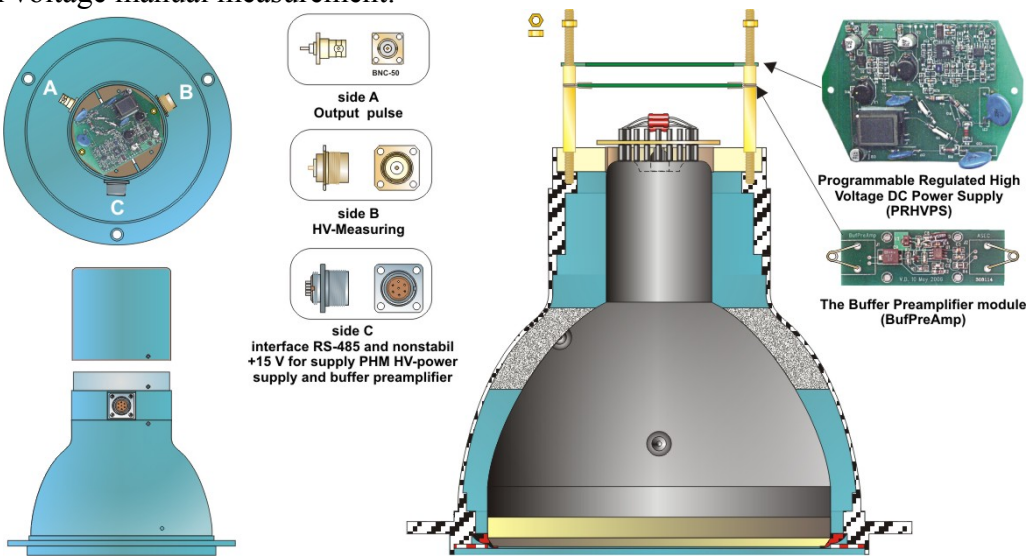


**Figure 3 PM installation guide with housing, connectors and electronics**

The High Voltage Power Supply (Fig.7) is based on a current fed push-pull topology DC/DC converter, working in a sinusoidal mode, to reduce the Electromagnetic Interferences (IMI) influence on the weak PMT output signal. To reduce the HV pulsations to sub-millivolt level, a two stage RC filter is used.

The HV Converter is powered by the switching regulator, controlled by the 8-bit ATMEL microcontroller chip. The microcontroller is integrated into the whole DCS by the RS-485 interface. The microcontroller receives the value of the HV setting from the RS-485 line and sends the measured value of HV to the line by request. The necessary HV value, sent by command from DCS is stored in the microcontroller permanent memory, so at microcontroller restarts, caused by power spikes, watchdog reset, etc., the HV value is restored without additional setting.

The Fig. 7 presents as well the Buffer Preamplifier schematics. It is powered from the same +15V unregulated line as the HV Power Supply through the local linear voltage regulator. The preamplifier is based on the wideband repeater chip LMH6559. Its purpose is to match impedances of the PMT anode load resistor and the 50 Ohm coaxial line. Along with a wide frequency band of preamplifier, another requirement is high dynamic range of output pulses. The polarity of pulses is negative, therefore initial working point of the repeater is chosen close to the upper saturation limit of the chip output voltage.

The rest of electronics is placed inside the ASNT Electronics Unit. The output pulses from the preamplifier are feed through coaxial cables and BNC connectors to the Logarithmic ADCs inputs.

The principle of logarithmic ADC operation is based on the measurement of decay time of oscillation in the parallel RC tank. The oscillations are caused by current pulses in the parallel RLC tank with a well known Q-factor **[1].** We are aware of several realizations of this principle **[2] [3]**. In all these cases the Photomultiplier Tube (PMT) of the scintillation detector, which can be considered as an almost perfect current source, was used as the generator of current pulses. The entire electronics of the logarithmic ADC was mounted inside the PMT case and the output signal was the sequence of standard pulses with ~1 MHz frequency and the quantity proportional to the logarithm of the area (charge) of the measured current pulse.

The advantage of this approach is the simplicity and the high noise tolerance provided by the complete shielding of the low-signal circuit in the PMT case.

Building large experimental setups with a large number of different particle detectors requires universal data processing schemes. Our overall strategy for cosmic ray research is to detect simultaneously with one and the same particle detectors both solar modulation effects and high energy galactic cosmic rays. This implies precise timing measurements (3-5 nanoseconds) and requires installation of the fast preamplifiers.

LADCs cannot provide necessary time precision. Since number of incident particles can reach $10^4$ per 1 $m^2$ scintillator LADC can generate pulse sequences with duration 80-90 microseconds, respectively. It is possible to decrease the dead time value by increasing the tank resonance frequency. However, this frequency is limited by the 1.5 - 2 MHz value because if the duration of the input pulses exceeds the quarter of resonance frequency period, the proportionality of the number of output pulses to the logarithm of input signal is disrupted.

To guarantee greater flexibility of experimental setup construction, we used another scheme of electronic circuit, see Fig.7.

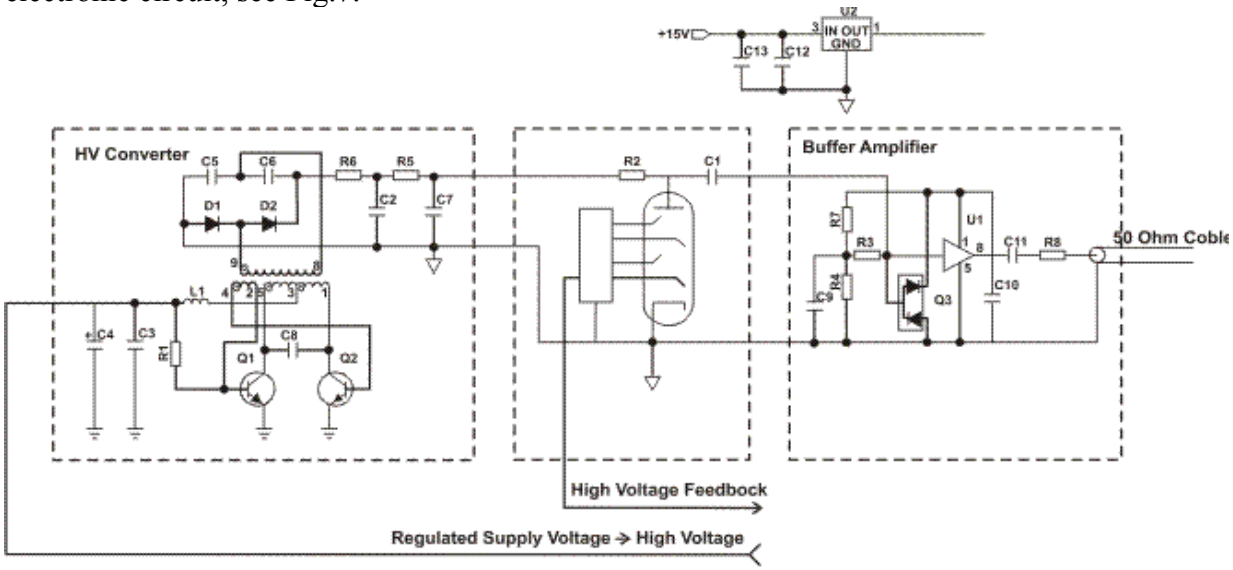


**Figure 7 the pm output readout scheme**

The voltage pulse from the PMT anode load resistor is amplified by the current by the buffer preamplifier with a +1 voltage gain. The amplifier with the output resistance of 50 Ohm sends the

pulse signal, completely repeating the shape of PMT anode current pulse, through the impedance matched 50 Ohm coaxial transmission line to the counting room for further processing. Thus, the whole information about the event registered by the detector enters the laboratory practically without any losses. It can be subjected to various forms of processing, depending on the requirements of a particular physical experiment. The same output signal can simultaneously enter different electronic devices. For example, to undergo processing with short dead time, it can enter the discriminator with a fixed threshold and for the amplitude analysis to Analog-to-Digital Converter (ADC). Different types of ADC can be used simultaneously: inexpensive logarithmic ADC (LADC) with low amplitude resolution, similar to that described in the present paper, and the complex universal multi-channel amplitude analyzer.

The simplified schematic diagram of logarithmic LADC front-end is presented in Fig.8.

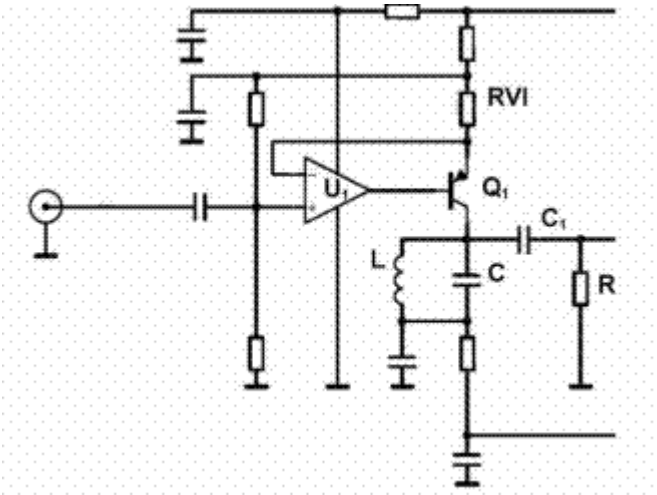


**Figure 8 LADC_Frontend**

The voltage-to-current converter is assembled on the elements U1, Q1, RVI, its conversion gain is

$$Gain_{vi} = \frac{1}{RVI} = 2\frac{mA}{V} \tag{0.1}$$

This value is selected so that for the standard shape of PMT pulse, the peak voltage of the first half-wave on the oscillating LRC tank would be equal to the amplitude of the input pulse. Since the maximum amplitude of the input pulse is set in the preamplifier to the level of approximately 7V, the same amplitude is obtained at the entrance of Operational Amplifier (OA) U2. The greater maximal voltage values cause the limitation of oscillations amplitudes due to the sharp increase of the U2 input current, whereas with the smaller values the dynamic range of converter decreases due to an increase in the portion of OA inherent noise, the Radio-Frequency Interferences (RFI) from the radio stations and other kinds of Electromagnetic Interferences (EMI).

As it was already mentioned, the oscillation amplitude on the RLC tank is proportional to the area of the pulse shape, if its duration is shorter, than one fourth of the tank resonance period, i.e.

$$V_0 = \frac{1}{C}\int I_{pulse}dt \tag{0.2}$$

The current pulses from the Q1 collector cause oscillations damping in the LCR tank. The fact that R is connected to the tank through the capacitor C1 (not directly) is not relevant for the work of the circuit, since the C1 value is considerably higher than the C tank capacity. Fig.9 presents the input pulse and the damping oscillations it causes. These oscillations are further amplified by the two-stage amplifier-limiter on OA U2 and U3 (Fig.10).

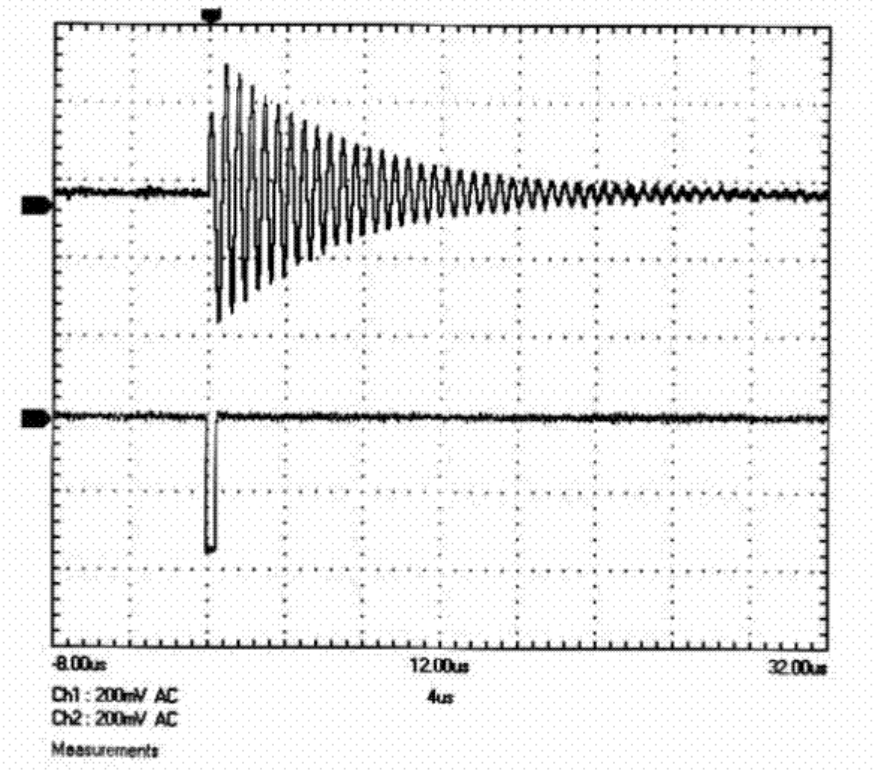


**Figure 9 an input signal (lower) and damping oscillations (upper)**

The amplifier-limiter consists of two identical non-inverting stages. The gain of each amplifier stage at 1.5 - 2 MHz operating frequency is equal to:

$$Gain_{amp} = 1 + \frac{R\_FB}{R_0} = 6.1 \qquad (0.3)$$

Respectively, the complete gain is equal to $Gain_{full} = Gain^2_{amp} = 37.21$

The output signal from the amplifier enters the comparator $U_4$ non-inverting input.

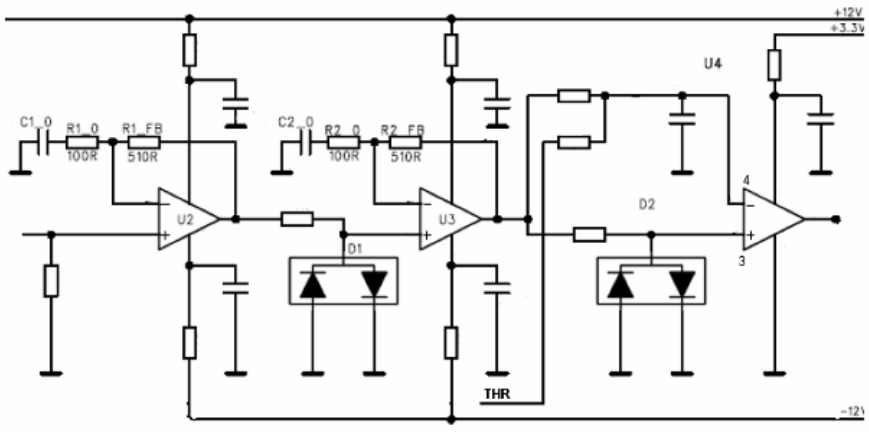


**Figure 10 amplifier-limiter**

At large signal values operational amplifiers go saturated, limiting the magnitude of the half-waves of damping oscillations. An even larger level of limitation is provided by the diode limiters $D_1, D_2$. Since the threshold of the comparator is significantly lower than the limitation level, when the amplitude of oscillation decreases to the value close to the threshold, the amplifier returns to the linear work. It is very important to ensure that the operating point - the constant

component of the input signal of comparator, returns to the initial level (which was before the excitation of the tank by the input pulse). In view of a certain asymmetry of levels of limitation, both of OA and of diodes, the capacitive coupling between the stages of the amplifier and the comparator can results in the displacement of operating point after large input signals, because of the recharge of coupling capacitors, which might require significant time for their discharge and operation point restoring. To avoid this, the DC connection is used between the stages of the amplifier and the comparator. At the same time, to decrease the influence of the temperature and time drift of input current of the $U_2$ and the bias voltages of $U_2$ and $U_3$, the DC gain of the amplifier is limited by means of capacitors C1_0 and C2_0 to the value of 1. Since even in this case the zero drift at the $U_3$ output can reach $20mV$ and more, the threshold of $U_4$ comparator is set relative not to ground, but to the DC output voltage of the amplifier $U_3$.

The shapes of signals in different points of amplifier are demonstrated in the oscillograms presented in Fig.11. The output signal of the amplifier can be divided into 2 zones. In the zone I the amplifier works in the limitation mode, while in the zone II it works in the linear mode. To ensure the correct work of LADC, it is necessary to provide a threshold of comparator significantly lower than the limitation level, i.e., so that the comparison of the amplitude of oscillations with the threshold value would occur in the zone II, which actually occurs in our case. The threshold of the comparator is determined by the voltage entering from the output of the Digital-to-Analog Converter (DAC), signal THR1, and can be remotely programmed.

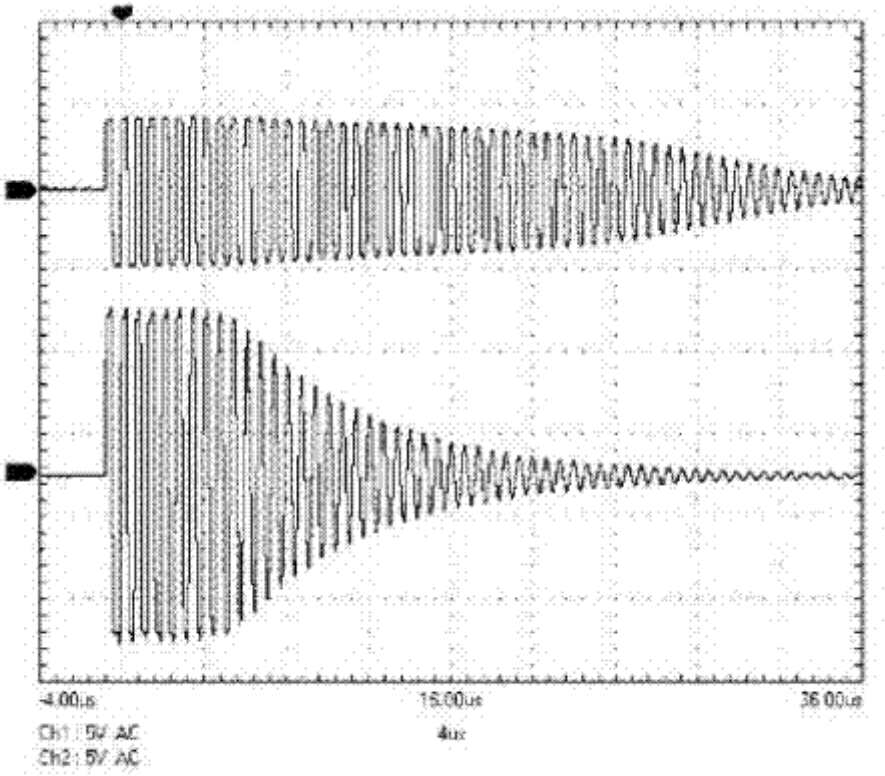


Fig.11 ВС chto takoe BC?

**Figure 11 output signal of the first stage of amplifier (lower) and inpur signal of comparator (upper)**

While the amplitude of the oscillations entering the comparator U4: 3 exceed the threshold value of VU4: 4, each oscillation causes the generation of an output pulse of standard amplitude 3.3V, Fig.12 CompOut. The comparator IC used has input hysteresis about 4mV, which ensures the pure form of the output signal.

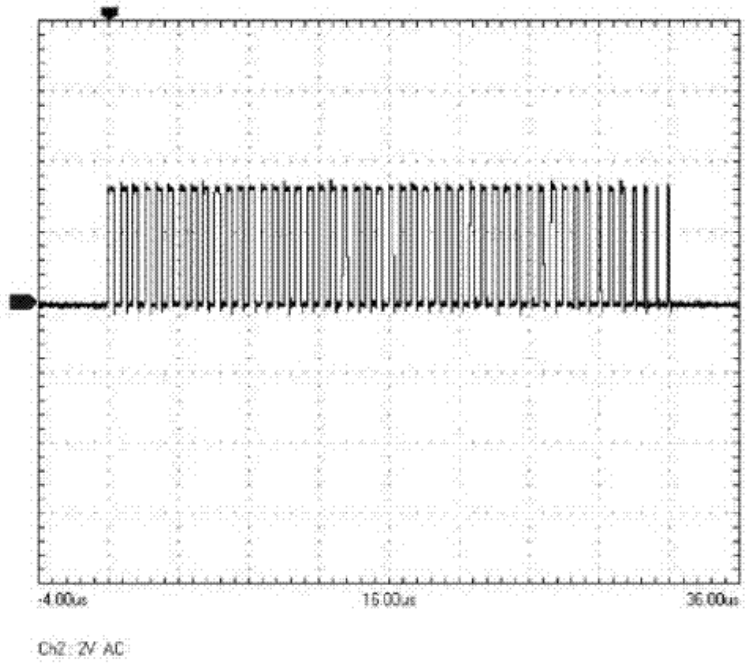


**Figure 12 comparator output signal**

After the excitation of oscillations, their amplitude falls according to the law:

$$V = V_0 e^{-\frac{wt}{2Q}} \tag{0.4}$$

where $V_0$ is the initial amplitude of voltage, w the resonance frequency, Q - the quality factor of the tank. It is possible to rewrite the formula as

$$V = V_0 \cdot e^{-\frac{\pi N}{Q}} \tag{0.5}$$

from which

$$N = \text{int}[\frac{Q}{\pi} \ln \frac{V_0}{V_{th}}], \text{ for } V_0 > V_{th} \tag{0.6}$$

where $V_{th}$ – is the threshold voltage of comparator.

The (1.6) shows, that for providing the necessary conversion coefficient, it is necessary to have the stable Q-factor and a possibility to choose its value. In the previous versions of LADC the home-made induction coils with screw core from soft iron for the introduction of the necessary quantity of losses were used as L. The regulation of Q-factor was produced by the rotation of screw, which simultaneously changed the resonance frequency of the oscillatory tank. However, we implemented a different approach to guarantee the ease of fabrication, high reliability and stability.

A highly reliable industrial inductor with the high Q-factor initial value is used as L. The desired resulting Q-factor is hard set by shunting LC tank with a stable and precise resistor R. Since the resistance of resistor depends on the temperature and other destabilizing factors much less than losses in iron core, this solution allows to choose the necessary Q-factor, simply by selecting the resistance of R, and high stability of its value.

In our case the Q-factor is selected so that the change of the amplitude to 10 times, produce a change in the number of pulses of output sequence equal to 23. Respectively, (1.6) is changed into:

$$N_1 = \text{int}[\frac{Q}{\pi}\ln\frac{V_0}{V_{th}}]$$

$$N_2 = \text{int}[\frac{Q}{\pi}\ln 10\cdot\frac{V_0}{V_{th}}]$$

where $N_2 = N_1 + 23$.

$$\frac{Q}{\pi} = \frac{23}{\ln 10} = 10$$

where $Q = 10\cdot\pi = 31.415$

Hence, the required value of the tank Q-factor is approximately 31.

As (2) demonstrates, the total conversion factor is affected by the PMT pulse shape and amplitude, which, in turn, depends on the efficiencies of the scintillator, photo-collection, photoelectric cathode, on the PMT feedings voltage and so on. In the described device the controlled parameters are the feeding voltage of FEU and the threshold of LADC comparator. These parameters are remotely preset and they can be re-set in the process of the experiment. However, tuning of these two parameters is insufficient to guarantee the complete identity of the channels and, ideally, additional adjustments are required (PMT anode load, resonant frequency, Q factor). Since the absolute calibration of the entire chain from scintillator to the output sequence is completely stored for calibration and stability monitoring purposes in the off-line mode, we decided not to use in the hardware design such additional adjastment components as potentiometers and trimming capacitors, which significantly worsened the reliability and maintenance.

Structurally, all 8 LADC are located on one printed-circuit board. To simplify the installation and decrease the cost, the channels are not separated from each other by external screens; the problem of the channel interaction is solved as follows. First, the inductors of the oscillatory tanks of adjacent channels are chosen in a mutually perpendicular fashion, which sharply decreases the magnetic coupling. Secondly, by alternating the capacitances of contour capacitors, the resonance frequencies of adjacent channels are relatively shifted according to each-other approximately by 10-15%. In case of maximum amplitude values of input pulses, low oscillations can be observed in the adjacent channels. However, because of the sufficiently high values of the Q-factor, the oscillations increase gradually and up to the moment of the end of time gates (see below) they do not reach the lowest threshold level**.** The comparator threshold is set by the output signal of programmable DAC. One eight-channel DAC IC is used for threshold setting of all eight channels of the LADC board.

The output pulses of the comparator are taken to the IC of Complex Programmable Logic Device (CPLD) of the XILINX CoolRunner-II type that is used for identifying the event, counting the pulses of LADC outputs and sending the counters data to the microcontroller module.

All signals from the detectors, received during the specific interval of time, named gate, are considered as belonging to the same physical event. The gate value is set by CPLD and indicated as a logical signal GATE. The identification of the event and the corresponding trigger of the gate are initiated by the pulse, received in any of the 8-channels. The information about detectors which pulses where received during the gate interval is read out and stored at the end of the gate. Information is stored in the CPLD as a bite mask, named EVENT, in which one bit corresponds to the one input channel. The 1 in this bit means, that the pulse from the detector entered this channel during the gate period. The gate duration is fixed with the binary code ($N_{Gate}$) hard soldered on the input pins GWIDTH0-GWIDTH3 of CPLD and is equal to

$$T_{Gate} = \frac{N_{Gate}+1}{12}\mu S \qquad (0.7)$$

In our case $N_{Gate}$ is selected as equal to 7 which corresponds to the gate duration of 0.666 microseconds (us). On the one hand, this value ensures time sufficiently large to register all pulses caused by one physical event, taking into account the spread of detector parameters, the lengths of coupling cables and so on. On the other, it reduces the probability of registering two different events as one to the negligibly low value.

In addition, the parasitic oscillations in the tanks, induced by the large amplitude pulses from the adjacent channels, mentioned above, do not manage to increase to the threshold values.

With the beginning of the time gate, the inputs of all eight counters in CPLD opened and counter start counting the pulses of the packets, entering from the LADC outputs. The signal DURATION, reporting to the microcontroller that the process of event registering goes on is also generated when the event starts. This signal is removed approximately in 1 microsecond after the longest pulse packet ends. After the signal ends, the inputs of all counters are closed and the microcontroller begins reading out the information accumulated in CPLD: EVENT bite and one bite of counter for each of eight channels.

After registering channel information, the microcontroller issues the RESET pulse on CPLD, indicating the end of event. Receiving this pulse, CPLD resets all counters and EVENT byte into the initial (zero) state. Thus, the system is ready to register the following event.

The total dead time of system consists of the count time of the longest pulse packet plus the information processing time of the microcontroller (see below) and is about 100us long for the worst case of the maximal input pulse amplitude. For signals, corresponding to the maximum of the so called “one-particle distribution” tuned for 5-th channel of spectrum, value of the dead time is about 20us.

The LADC module is designed in such a way that up to four LADC boards can be connected to one microcontroller, thus, forming the 32- channel DAC system. Fig.13 demonstrates such connection carried out with flat cables with 5 connectors on each. To simplify the construction, all connectors are fixed to the cable directly, without any over-twisting for the selection of the device number (practice standard for PC). Instead, each of four boards is identified by the address set on the board collected with the jumpers J10, J14.

The accepted scheme of jumper setting is as follows:
1 board (ASNT)– do not install,
2 boards (NAMMM) – do not install on the lower board, install both jumpers on the upper one,
4 boards- from bottom to top: 0,0; J10,0; 0, J14; J10, J14

The setting of the addresses serves both for the selection of internal information of CPLD (EVENT byte + 8 counters) and for determination of the thresholds. In case of erroneous setting of the cross connections DAC is not programmed and the threshold values are set as equal to zero, which is easily detected by the continuous counting (the LED burn) along all channels, no matter whether the cables are plugged or not.

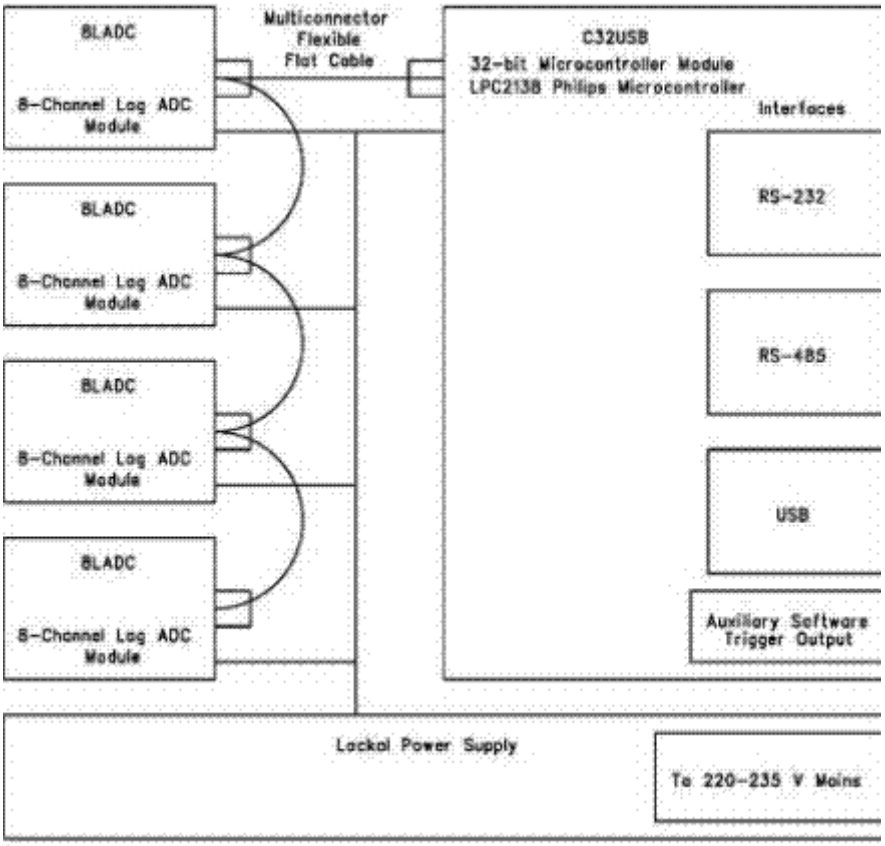


**Figure 13 assembling 4 ladc and microcontroller modules in one unit**

When cascading, it is important to satisfy the following condition: the impulse arrival on the entrance of any of the LADC boards is considered as an event, whereas completion of longest of the pulse packets of all boards is viewed as the end of an event. Therefore, the CPLD outputs for the signals GATE and DURATION are programmed as outputs with the open collector and the logical inputs connected to it. This allows combining these signals as a wired OR.

The readout of information from CPLD of the 8LADC boards into the module of microcontroller C32USB is provided by the parallel code on the 8- bit bus. Eight 8-bit pulse counters of LADC and 8- bit EVENT register, total 9 registers, are addresses inside CPLD. To address them, it is necessary to have the 4-bit address, presented by the microcontroller at the lines SEL0-SEL3. The addresses from 0 to 7 are used to select each of 8 counters, while any address in range 8-15 selects one and the same register - the register of event mask (EVENT).

The C32USB module is based on the NXP company LPC2138 microcontroller of the ARM. It is designed as a multifunctional embedded data processing device for the initial on-line processing of data of arbitrary nature. The flexibility of the module application is provided by the possibility to work with any one of interfaces included in the system. The following interfaces are realized:

1. RS-232 for the connection to PC COM port. The rate of exchange is up to 115200 Baud. This port can be used also for the microcontroller IC firmware reprogramming.
2. USB 1- for connection to PC with virtual COM port driver. The exchange is provided through the UART micro-controller interface. The rate of exchange is up to 115200 Baud. This port can be used also for the microcontroller IC firmware reprogramming.
3. USB 2- for the high-speed exchange of information between PC and the microcontroller. Uses the parallel exchange of information between the USB interface IC and the microcontroller. The program access from the PC is provided with the driver of virtual COM port with the speed of exchange up to 115200 Baud and with DLL driver, which, in theory, can ensure the rate of exchange approaching the maximum speed, full USB2 - 10 MBaud.

4. RS-485. It is used for connecting the microcontroller to the local detector control system DCS network.

As the electronic devices, assembled on the basis of C32USB module can be used for the detector setups placed in distant places with difficult maintenance, it is very important to have WEB interface not only for the installation of the detector parameters (thresholds, the voltage of PMT supply), but also for the reprogramming of microcontroller itself. This possibility is necessary for the software modernization at changing conditions of physical experiments, i.e. for changing of so called "software triggers", selecting data for different physical problems. Software triggers are altered by replacement of the consequences of coincidence and anti-coincidence, replacement of the conditions of the program-generated triggers and so on. Two of the realized interfaces make it possible to remote reprogramming the microcontroller by WEB interface.

The micro-controller software consists of system and problem-oriented parts. The system part includes initialization of I/O ports, watchdog and interval timers, interruption handlers and main input-output, local network managing, and other similar functions. The problem-oriented part includes pre-processing, storage and sending to the host PC data, collected from the detectors. In particular, the amplitude spectrum for each of the detectors is accumulated, coincidences and anti-coincidence are processed, the particle arrival directions statistics is accumulated, the program triggers are generated and so on. The software is written in the C language, using the free distributed GNUARM software. Some fragments of the code are written on the assembler to achieve the peak output.

### 7.1 24 Channel Neutron Monitor (NM) Readout Module

The main function of the 24 Channel Readout Module is receiving and count of the 18-channel Neutron Monitor signals. It also has 6 auxiliary universal counter channels.

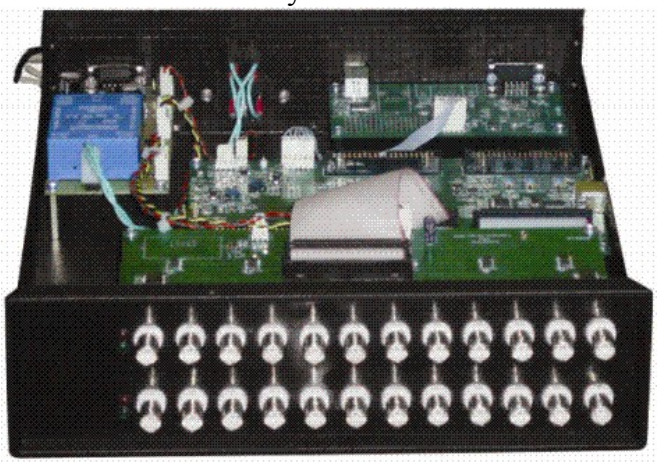

**Figure 14 functional diagram of the nm readout electronics**

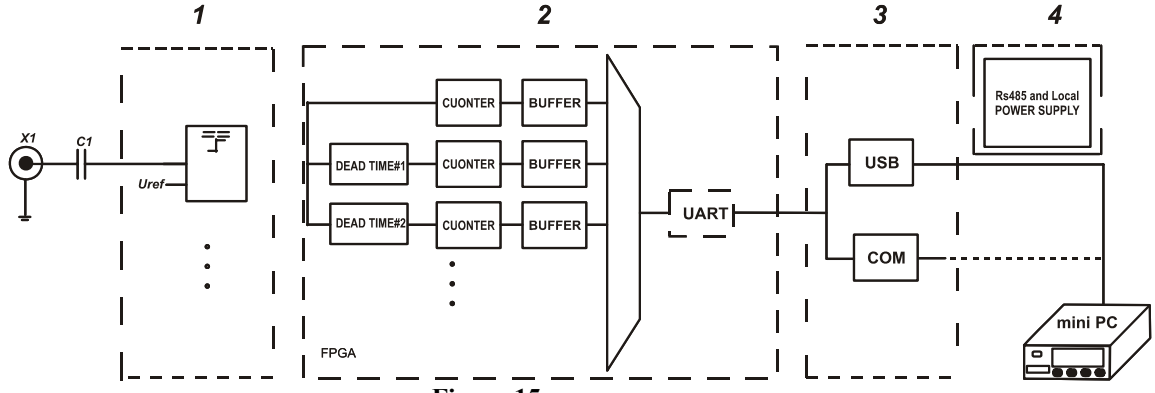


**Figure 15**

1. **Two Programmable Threshold 12-channell Discriminator/Counter boards.**
2. **Universal Multichannel Event Counter (UMEC) board.**
3. **Universal Microcontroller Interface module (MultiIFC) board.**
4. **RS-485 and Local Power supply module.**

Pulses from the detector preamplifier are discriminated and shaped in the unit 1. The discrimination threshold can be programmed in range 4mV-1000mV with 4mV step. Duration of the output TTL pulses is 400ns. The shaped pulse enters the input of Xilinx Spartan 3E FPGA (Field Programmable Gate) in the unit 2.

Inside module, the FPGA pulse is applied to three counters: to the first – directly, and to other two through programmable dead time circuits. The dead time values are preset to values of 250us (#2) and 1250us (#3). The last value coincides with one used for both Neutron Monitors at Aragats and Nor-Amberd during 23$^{rd}$ solar activity cycle (1996-2007).

Along with 18 programmable channels with 3 dead times (total 3x18 counters), the unit has 6 inputs for direct counting (without dead time circuits). The contents of all 60 (3*18 + 6) counters are downloaded each second in plane ASCII code to the PC through USB (or COM) interface. After downloading, all counters are instantly zeroed and start to count again.

Along with the main output connection, the unit has a RS-485 interface for connecting to the Detector Control Local Net of experimental setup for the on-line programming of the thresholds.

Each energetic hadron (mostly a neutron or proton) generates a number of evaporated neutrons in lead. Only small fraction of these neutrons (~5.7% for NM64) is registered by the counter. One of most important parameters of NM is the so called, multiplication coefficient" – the mean number of the termalized neutrons registered by the NM section as response to one incident high energy hadron. The first value of the dead time is very small and allows us to calculate all thermilized neutrons entering the same proportional counter. The last biggest value of the dead time counts only primary particles, because "decay" time of the termalized neutrons in NM section ~350 us. Therefore by dividing count rates correspondent to the shortest and biggest dead times we can estimate the multiplication coefficient in one proportional chamber. Due to tight connections of the lead filters of each of 8 chambers of a NM section there is probability that termilized neutrons will be registered also by neighboring counter. Therefore we should correct obtained multiplication coefficient to effect of the "correlated counts" in neighboring counters. Our measurements and simulation studies of NM cross-channel correlations give preliminary value of 1.45 for the multiplication coefficients of a section of Nor Amberd NM (2000 m. above sea level). Number of thermalized neutrons is good proxy of the incident hadron Energy.

Therefore, with the new first option of new DAQ electronics, we can detect variability of neutron multiplicity at level as detailed as 1-second. Second and Third options emulate standard NM64 operation with 2 options of dead time.

**Reference**

1. А. Н. Гадалов, И.И. Каганов, А.А. Силаев ПТЭ, 1973, 1, 39
2. В.И. Степанов ПТЭ, 1969, 3, 115
3. А.А. Силаев, О.А. Силантьев ПТЭ, 1981, 1, 100
4. А.В. Дарьян, С.А. Долганов, А.Р. Хачатрян Препринт ЕрФИ 1485(2)-97

# 8. Attachment 4: Description of the ASEC data, its formats and locations

## 8.1 Description of the ASEC data, its formats and locations

The Aragats Space-Environmental Center (ASEC) provides monitoring of different species of secondary cosmic rays at three altitudes. The ASEC, (Chilingarian, et al., 2003; Chilingarian, et al., 2005) consists of two high altitude stations on Mt. Aragats in Armenia and Yerevan headquarters of Cosmic Ray Division (CRD) of Yerevan Physics Institute (YerPhI). Geographic coordinates for Aragats station is 40°28'N, 44°10'E and for Nor-Amberd station is 40°22'N, 44°15'E, Yerevan - 40°11'N, 44°31'E, cutoff rigidity: ~7.1 GV, altitudes 3250m, 2000m and 1000 m correspondingly. At these 3 destinations different types of particle detectors are continuously measure the intensity of the secondary cosmic ray fluxes and send data to the Internet in real time. In this report we present short description of the ASEC detectors and data acquisition possibilities as well as obtained data structures and Internet links.

### 8.1.1. Aragats Solar Neutron Telescope (ASNT)

Aragats Solar Neutron Telescope (ASNT) located on the slope of the mountain Aragats in Armenia, 3250m above sea level. Geographical coordinates is 40°28'N, 44°10'E. ASNT is formed from 4 separate identical modules, as shown in Figure 4. Each module consists of standard slabs of 50x50x5 $cm^3$ plastic scintillators stacked vertically on a 100x100x10 $cm^3$ horizontal plastic scintillator slab. Scintillator slabs are fine polished to provide good optical contact of the assembly. The slab assembly (scintillator housing) is covered by white paper from the sides and bottom and firmly kept together with special belts. Total thickness of the assembly is 60 cm. Four detectors of 100x100x5 $cm^3$ size each located above the thick scintillator assembly as is seen in Figure 4, are used to indicate if charged particle traverse near vertically. This information is used for selecting neutral particles and "vetoing" charged particles. A scintillator light capture cones and Photo Multiplier Tubes (large cathode, FEU 49 type) are located on the top of scintillator housing in special iron shielding, where as well the Amplitude-to-digital convertor and other electronics is located.

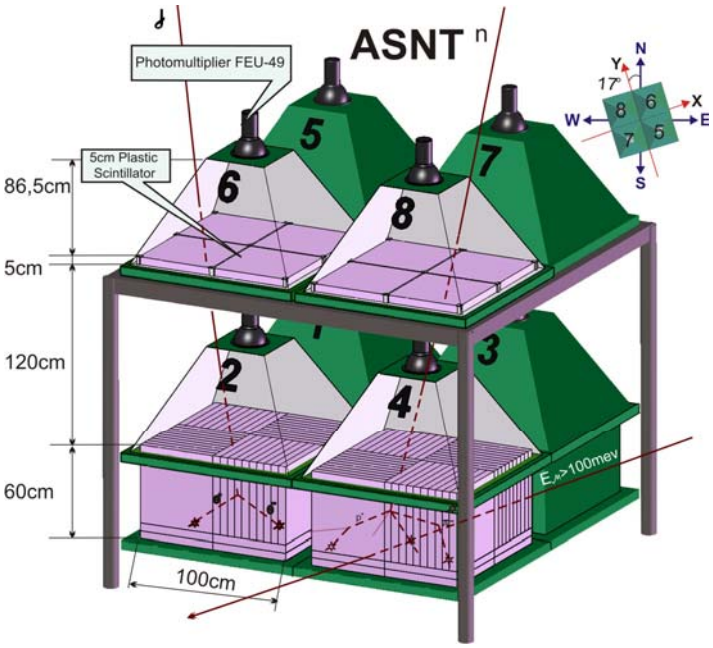


**Figure 4 The assembly of ASNT with enumeration of 8 measuring channels (scintillators) and chart indicating orientation of detector axes relative to direction to the North Pole.**

### 8.1.2. Structure of the information content from ASNT

Initial goal of the ASNT was to be a part of the worldwide network aimed to detect neutrons born in photosphere and reach Earth bringing direct information from its origin. The network is coordinated by the Solar-Terrestrial laboratory of the Nagoya University (Tsuchiya et al., 2001) and consists of seven same type detectors distributed at different longitudes to observe the sun 24 hours daily. In addition to the primary goal of detecting the direct neutron flux from the Sun, the SNT also has the possibility to detect charged fluxes (mostly muons and electrons) and roughly measure the direction of the incident muons. Also ASNT constitutes a central part of the new surface array to be in operation at Aragats in 2009 (see MAKET section below). The main ASNT trigger reads and stores the analog signals (PMT outputs) from all 8 channels if at least one channel reports signal. The frequency of triggers is ~4 KHz due to hit of charged and neutral particles. Big advantage of ASNT is additional, so called, software triggers, exploiting the information from Amplitude-Digital-Converters (ADC) on energy releases in scintillators.

This, additional information, not assessable yet from other particle detectors from world-wide networks, allows as we will see, solving additional physical problems. The software triggers are not fixed in electronics and it is possible to remote add or change them very flexible. The list of available information from modernized ASNT is as follows:

1. 1 minute count rates (easily can be changed to 10 seconds, or to another time span) of all 8 channels of ASNT (see Table 1, Figure 5);
2. Count rates from
3. different incident directions separately, 16 possible coincidences of 4 upper and 4 bottom scintillators are related to 9 different directions (see Table 2);
4. Count rates of the special coincidences (see details in Table 3, Figure 6);
5. Estimates of the variances of count rates of each ASNT channel, variances are calculated by 12 five-second count rates (see Table 4, Figure 7);
6. 8 x 8 correlation matrix of ASNT channels calculated by five-second count rates in 1 minute (see Table 5);
7. Count rates correspondent to old SNT 4 threshold on the energy release in thick scintillators (see Table 6);
8. The same as in previous point put only for particles that did not registered in upper layer (veto on charged particles to select samples enriched by neutrons) (see Table 6);
9. Histograms of energy releases in all 8 channels of ASNT (see Figure 8);
10. The same as in previous point with invoking veto option;
11. Time and values of energy releases in ASNT channels conditioned on existence of signals in all 8 scintillators, so called, EAS trigger (accuracy of time stamp is ~50 μsec), (Figure 9);
12. Energy releases in upper or bottom scintillators conditioned on absence of signal in correspondingly down and upper layers and on minimal energy release, i.e. horizontal muon trigger.

We use XML format of data, allowing metafiles with detailed information about detector location, and operation conditions. After transfer by wireless connections to CRD headquarters in Yerevan the data are archived and stored in MySQL data base. The main data analysis platform, Data Visualization Interactive Network (DVIN (Eghikyan and Chilingarian, 2005)) now is operated with data in XML format and allow us download data also in ASCII format.

All raw data in the XML format is available from HTTP server at CRD headquarters in Yerevan from the link.

http://crdlx5.yerphi.am/ASEC_Data/ADAS/asnt/snt

In the directory “DEFOULT” following information is stored:

1. snt (columns 1-8) - the count rates of all 8 ASNT channels: first 4 columns – from 60 cm scintillators, 5-8 columns – from 5 cm scintillator. The numbering of scintillators is explained in the Figure 4. The count rates are posted in the Table 1;
2. snt (columns 9-24) – the count rates corresponding to the 16 coincidences in upper and bottom ASNT layers, i.e. – corresponding to the traversal of the single charged particle (the probability that neutron will generate energy release in 5 cm scintillator is rather small). The order of the different directions in the file is following: [1-5] [1-6] [1-7] [1-8] [2-5] [2-6] [2-7] [2-8] [3-5] [3-6] [3-7] [3-8] [4-5] [4-6] [4-7] [4-8], where the first number corresponds to the lower layer and the second – to the upper (see Figure 4) Also on the same Figure you can see the orientation of ASNT axes according to direction to the North Pole, thus we can calculate the interval of the horizontal angles of incidence related to each coincidence.
3. snt (columns 25-31) – the count rates of the "special" coincidences different from listed above and forming the "full system" of possible configurations of the channel operation. Conditioned on the existing as minimum 1 signal in 8 ASNT channels there could be the following possibilities of number of counts in top and bottom layers (the first sign in the pair is corresponding to the bottom thick scintillator): many-many [m-m] (more than one count in 4 bottom and 4 top layers), many-zero [m-z] (more than 1 in bottom and nothing in 4 top), zero-many [z-m], zero-one [z-o], one-zero [o-z], many-one [m-o], one-many [o-m]. The fraction of the "special" coincidences relative to the "main" trigger is posted in the Table 3 the time-series of the s "special" triggers are posted in the Figure 6.
4. snt (columns 32) - the number of the "main" triggers – at least one signal in 8 channels in preselected time span (1 minute). If we consider all logical configurations of ASNT operation outcomes, this number will be equal to sum of the columns 9-31. As we mention already the number of triggers is ~ 4 KHz, dependent on the hardware settings: PMT high voltage and threshold of channel "firing".
5. snt (columns 33-40) - the variances of 8 channels, see Table 4 and Figure 7;
6. snt (columns 41-68) – the correlation matrix, see Table 5.

In the directories "spectrum" following information is stored:

1. spectrum1, … spectrum4 the histograms of the energy releases in thick 60 cm scintillator;
   In files with extension;
2. spectrum5, … spectrum8 the histograms of energy releases in 5 cm thin scintillators;
3. spectrum9,..., spectrum12 histograms of energy releases in 60 cm thick scintillators (with invoking veto option on the charged particles in the upper "anticoincidence" shielding);

By integrating the histograms spectrum1,..., spectrum4 and spectrum9,...,spectrum12 we calculate the count rates according to 4 predefined thresholds on the value of the energy release (PMT output), to continue time series in the same data format as old version of ASNT started from 1996 (http://crd.aragats.am/DVIN/). As a first (or zero- threshold) we use the sum of all channels of the histogram. To get number of particles with Threshold 1 we must calculate sum of the channels of the histogram from 16 to 127. For the Threshold 2 – sum of the 23-127 channels, Threshold 3 – 27-127 channels and Threshold 4 – 31-127 channels.

To calculate count rate of the particles with thresholds for the detector 1-4 (60cm) we need spectrums 1-4 files. To calculate count rate of the particles with veto for the detector 1-4 we need spectrums 9-12 files (see Table 6).

The CRD "ARSRV" local file server contain files with following information:

1. The detailed information on the many-many case: the time stamp and energy releases in all 8 ASNT cannels. This case is related to the Extensive Air Showers (EAS), when energy of primary particle is high enough to generate particle cascade with numerous secondary particles reaching earth surface. By selecting different subsamples of many-many case according to the number of detected secondary particles (energy releases) we can select

events with different primary energy, thus constructing the energy spectra of the primary particles. The calibration of the ASNT can be done with MAKET-ANI EAS array (Chilingarian, et al., 2004). In the Figure 9 the time series of the count rates correspondent to different energy releases are posted.

2. Another kind of events stored in the files with "events" extension is related to the horizontal muon traversal. The logical software trigger selects events when there are more than 2 signals in top or bottom layers only, i.e. selecting horizontally traversing particle, or group of particles. The additional condition of large energy release (the code >25) is rejecting coincidences of the vertical traversal of low energy particles. The acceptance of the system of bottom thick scintillators is rather large ~(+/- $8.5^0$), the acceptance of very narrow system of the top thin scintillators will select horizontal muons within ~(+/- $0.7^0$) of zenith angles.

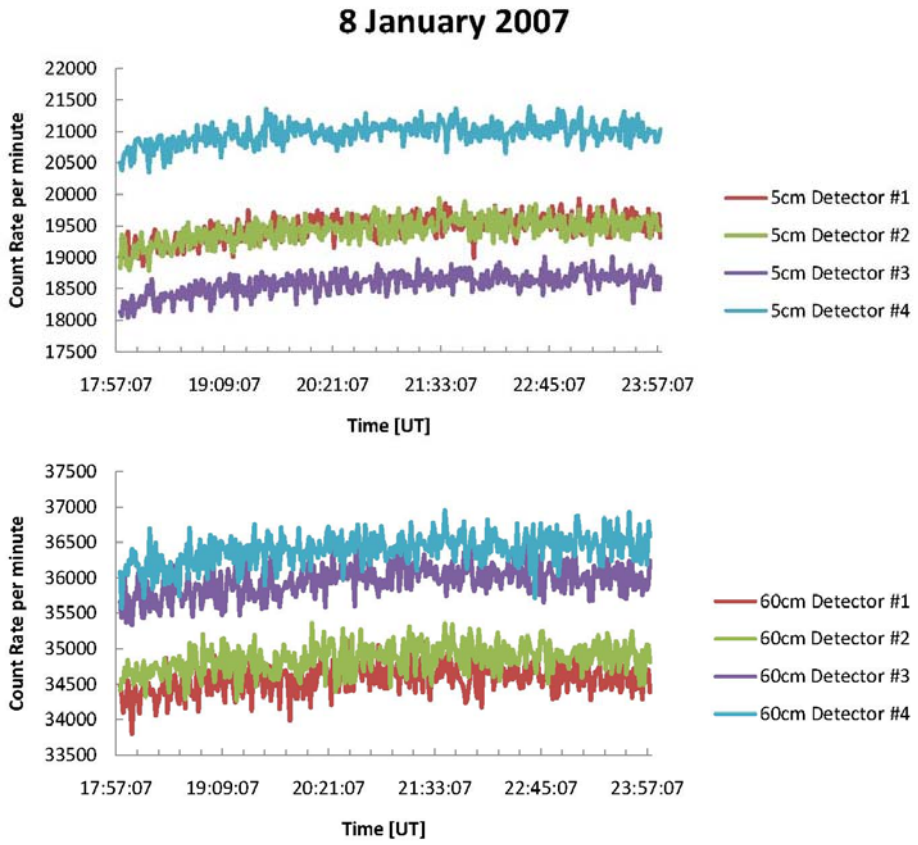


**Figure 5: Time series of count rates of 8 ASNT channels. The difference of mean values is due to peculiarities of PMT used.**

**Table 1: Count rates of the ASNT channels, variances and relative errors (07.02.2008).**

| Detector | Average | Standard deviation | Relative error [%] |
|---|---|---|---|
| 60cm Detector 1 | 34465 | 244 | 0.70 |
| 60cm Detector 2 | 33027 | 238 | 0.72 |
| 60cm Detector 3 | 34864 | 238 | 0.68 |
| 60cm Detector 4 | 35235 | 252 | 0.71 |
| **SUM 60 cm** | **141784** | | |
| 5cm Detector 5 | 22254 | 178 | 0.80 |
| 5cm Detector 6 | 19775 | 201 | 1.01 |
| 5cm Detector 7 | 22315 | 178 | 0.80 |
| 5cm Detector 8 | 20871 | 209 | 1.00 |
| **SUM 5 cm** | **78459** | | |

**Table 2: Mean count rates related to the different incident directions, variances, relative errors and fractions according the number of "main" triggers (181474/ minute). φ is true north-based azimuth angle, θ is zenith angle (07.02.2008).**

| Direction | | Average | Standard deviation | Relative error [%] | Fraction |
|---|---|---|---|---|---|
| Vertical Directions | [1-5] | 3965 | 70 | 1.77 | 1.66 |
| | [2-6] | 2899 | 76 | 2.66 | 1.67 |
| | [3-7] | 3754 | 68 | 1.83 | 1.39 |
| | [4-8] | 3128 | 79 | 2.54 | 1.86 |
| **$\varphi=163^0\pm31^0$ E $\theta=30^0\pm11^0$** | [1-6] | 1278 | 37 | 2.92 | 0.69 |
| | [3-8] | 1306 | 38 | 2.98 | 0.73 |
| **$\varphi=73^0\pm31^0$ E $\theta=30^0\pm11^0$** | [1-7] | 1544 | 40 | 2.64 | 0.67 |
| | [2-8] | 1346 | 40 | 3.01 | 0.80 |
| **$\varphi=343^0\pm31^0$ E $\theta=30^0\pm11^0$** | [2-5] | 1458 | 38 | 2.64 | 0.74 |
| | [4-7] | 1496 | 39 | 2.63 | 0.67 |
| **$\varphi=253^0\pm31^0$ E $\theta=30^0\pm11^0$** | [3-5] | 1454 | 38 | 2.67 | 0.68 |
| | [4-6] | 1267 | 38 | 3.00 | 0.72 |
| **$\varphi=118^0\pm20^0$ E $\theta=38^0\pm10^0$** | [1-8] | 691 | 27 | 4.00 | 0.39 |
| **$\varphi=28^0\pm20^0$ E $\theta=38^0\pm10^0$** | [2-7] | 672 | 26 | 3.86 | 0.33 |
| **$\varphi=208^0\pm20^0$ E $\theta=38^0\pm10^0$** | [3-6] | 591 | 25 | 4.27 | 0.33 |
| **$\varphi=298^0\pm20^0$ E $\theta=38^0\pm10^0$** | [4-5] | 730 | 27 | 3.83 | 0.37 |
| **SUM** | | **27579** | | | **13.70** |

**Table 3: Mean count rates of "special" cases; variances, relative errors and fractions according the number of "main" triggers (181474/ minute) (07.02.2008).**

| Coincidence | Average | Standard deviation | Relative error [%] | Fraction |
|---|---|---|---|---|
| Many – Many | 568 | 24 | 4.27 | 0.31 |
| Many – Zero | 5536 | 87 | 1.58 | 3.33 |
| Zero – Many | 759 | 28 | 3.78 | 0.33 |
| Zero – One | 51735 | 274 | 0.53 | 26.57 |
| One – Zero | 93191 | 345 | 0.37 | 54.55 |
| Many – One | 1551 | 47 | 3.05 | 0.90 |
| One – Many | 690 | 29 | 4.20 | 0.32 |
| **SUM** | **154030** | | | **86.30** |

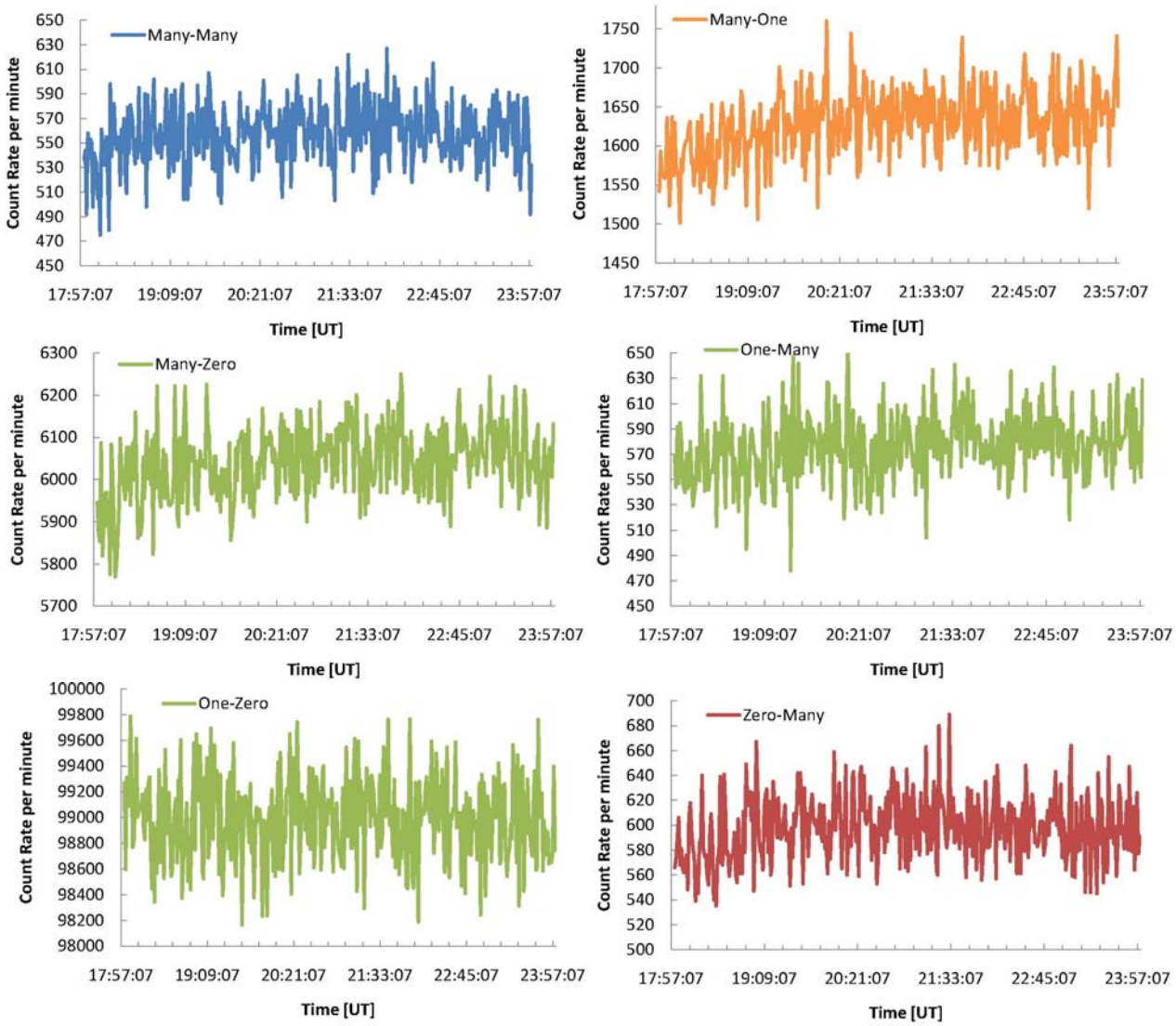


**Figure 6: Time series of the "special" cases, see description in the in the text and in the Table 2.**

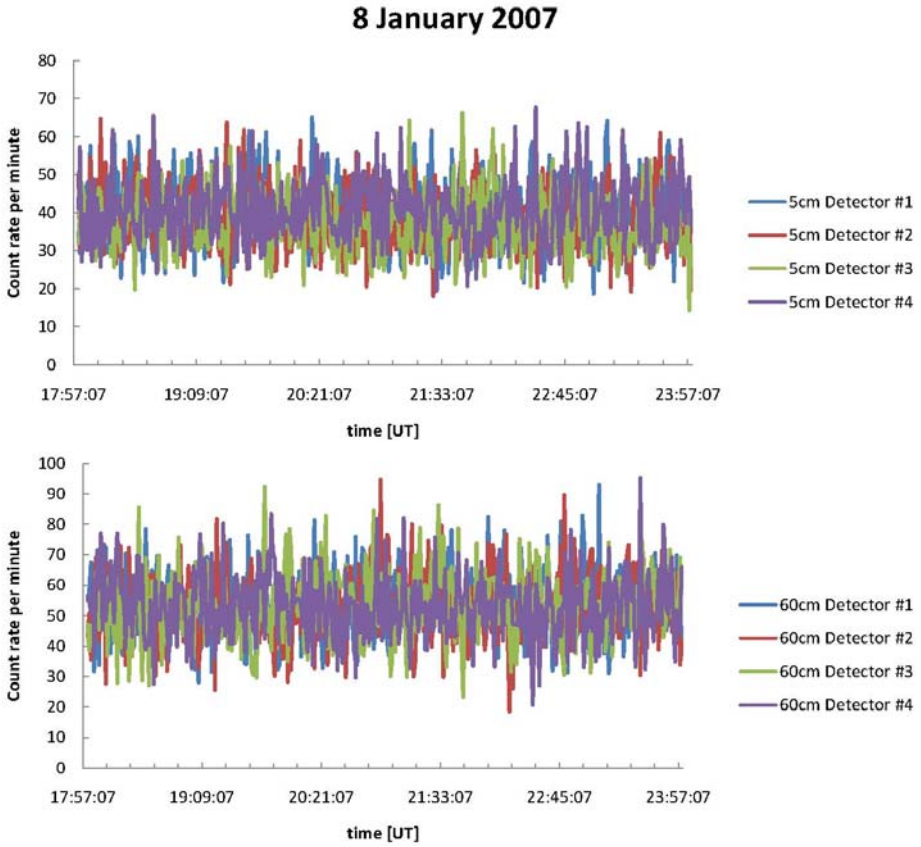


**Figure 7: Time series of the ASNT channel variances. Despite the mean values of ASNT channels slightly differ, the variances are very close to each-other, thus proving uniformity of ASNT channels.**

**Table 4: Mean value of the variance, its variance and relative error calculated by 5-sec count rates of 1 minute time span (total 12 5-dec count rates) (07.02.2008).**

| Detectors | Average | Standard deviation | Relative error [%] |
|---|---|---|---|
| 60cm Detector 1 | 52 | 11 | 21.36 |
| 60cm Detector 2 | 50 | 10 | 21.36 |
| 60cm Detector 3 | 51 | 11 | 21.71 |
| 60cm Detector 4 | 52 | 11 | 21.71 |
| 5cm Detector 1 | 42 | 9 | 21.30 |
| 5cm Detector 2 | 39 | 8 | 21.00 |
| 5cm Detector 3 | 42 | 9 | 21.36 |
| 5cm Detector 4 | 40 | 9 | 21.69 |

**Table 5: Mean value of the correlation matrix, calculated by 5-sec count rates of 1 minute time span and averaged over time span of 6 hours at 7 January 2008. Emphasized (red) values are related to ASNT channels stacked one above another, for which correlation should be non zero.**

| | Det 1 | Det 2 | Det 3 | Det 4 | Det 5 | Det 6 | Det 7 | Det 8 |
|---|---|---|---|---|---|---|---|---|
| Det 1 | 1 | | | | | | | |
| Det 2 | 0.041 | 1 | | | | | | |
| Det 3 | 0.042 | -0.003 | 1 | | | | | |
| Det 4 | -0.003 | 0.032 | 0.042 | 1 | | | | |
| Det 5 | 0.154 | 0.067 | 0.049 | 0.024 | 1 | | | |
| Det 6 | 0.066 | 0.118 | 0.006 | 0.053 | 0.015 | 1 | | |
| Det 7 | 0.053 | 0.027 | 0.135 | 0.049 | 0.022 | -0.007 | 1 | |
| Det 8 | 0.048 | 0.052 | 0.057 | 0.122 | 0.021 | 0.018 | 0.023 | 1 |

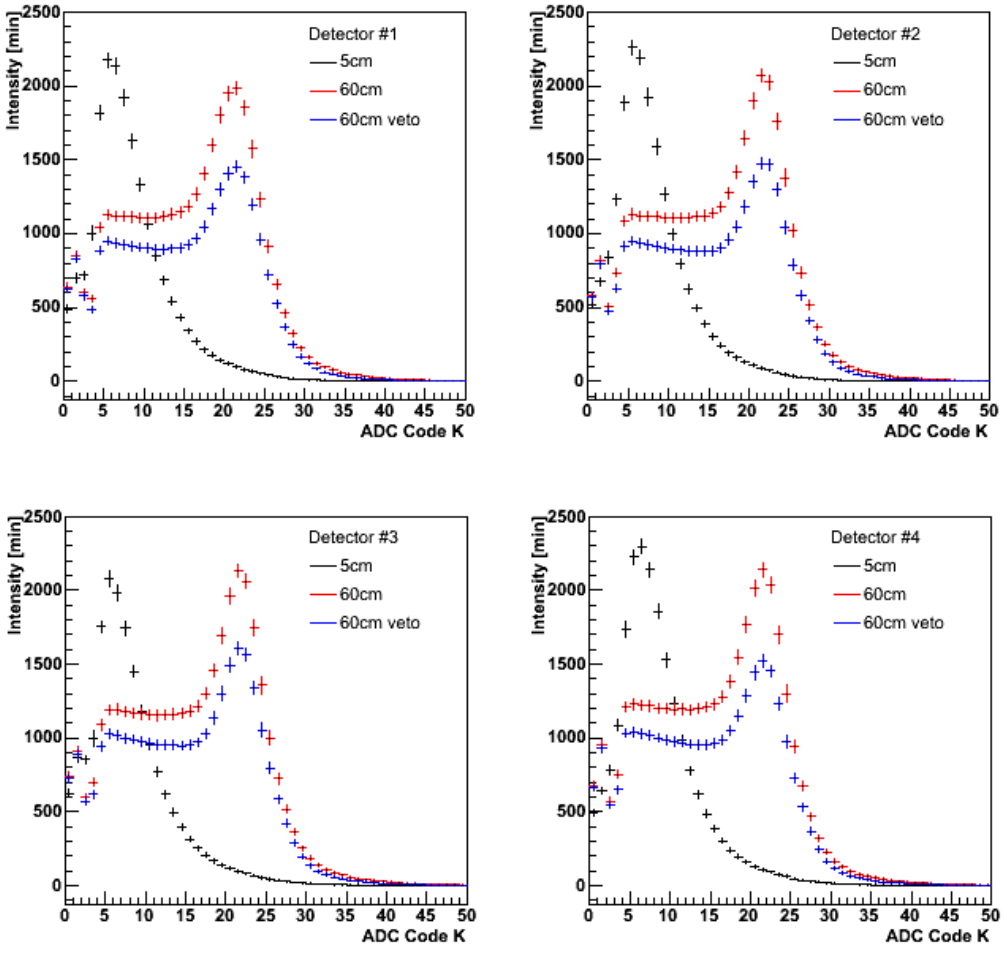


**Figure 8: Spectra of the energy releases in thick and thin scintillators. Veto option suppresses contamination of the charged particles by ~25%.**

**Table 6: Count rates correspondent to old SNT 4 threshold on the energy release in thick scintillators.**

| Threshold | Average | | Standard deviation | | Relative error [%] | |
|---|---|---|---|---|---|---|
| | | Veto | | Veto | | Veto |
| Threshold1 | 78586 | 58705 | 551.77 | 300.14 | 0.70 | 0.51 |
| Threshold2 | 34460 | 25737 | 895.00 | 587.74 | 2.60 | 2.28 |
| Threshold3 | 10550 | 7725 | 353.88 | 268.68 | 3.35 | 3.48 |
| Threshold4 | 4410 | 2866 | 139.61 | 99.23 | 3.17 | 3.46 |

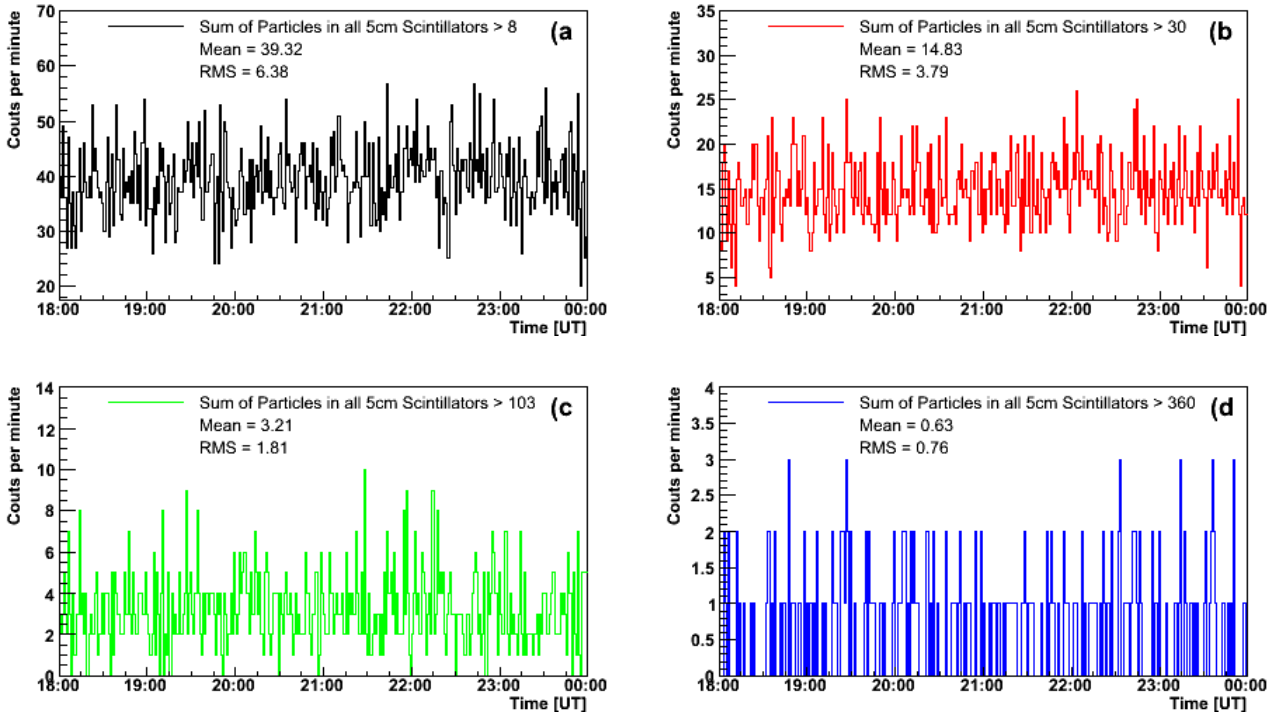


**Figure 9: The time series of the EAS initiated triggers (many-many case) conditioned on the value of the minimal number of incident particles (shown in the Figures) in 5 cm scintillator.**

### 8.2.1. Nor-Amberd Multidirectional Muon Monitor (NAMMM)

Nor-Amberd Multidirectional Muon Monitor (NAMMM) (Dorman 1975; Beglaryan, et al., 1989) located on the slope of the mountain Aragats in Armenia, at 2000m above sea level. Geographical coordinates is 40°22'N, 44°15'E. The NAMMM, shown in Figure 10 consists of two layers of plastic scintillators above and below two of the three sections of the Nor Amberd Neutron Monitor (NM). The lead (Pb) filter of the NM absorbs electrons and low energy muons. The threshold energy of the detected muons is estimated to be ~250 MeV. The NAMMM consists of 6 up and 6 down scintillators, each having the area of 0.8 $m^2$. The distance between layers is ~ 1 m., and the interval of zenith angles determined by the paired coincidences of upper and lower scintillators is not greater than 25º. The data acquisition system of the NAMMM, the same as ASNT, can register all coincidences of detector signals from the upper and lower layers, thus, enabling measurements of the arrival of the muons from different directions.

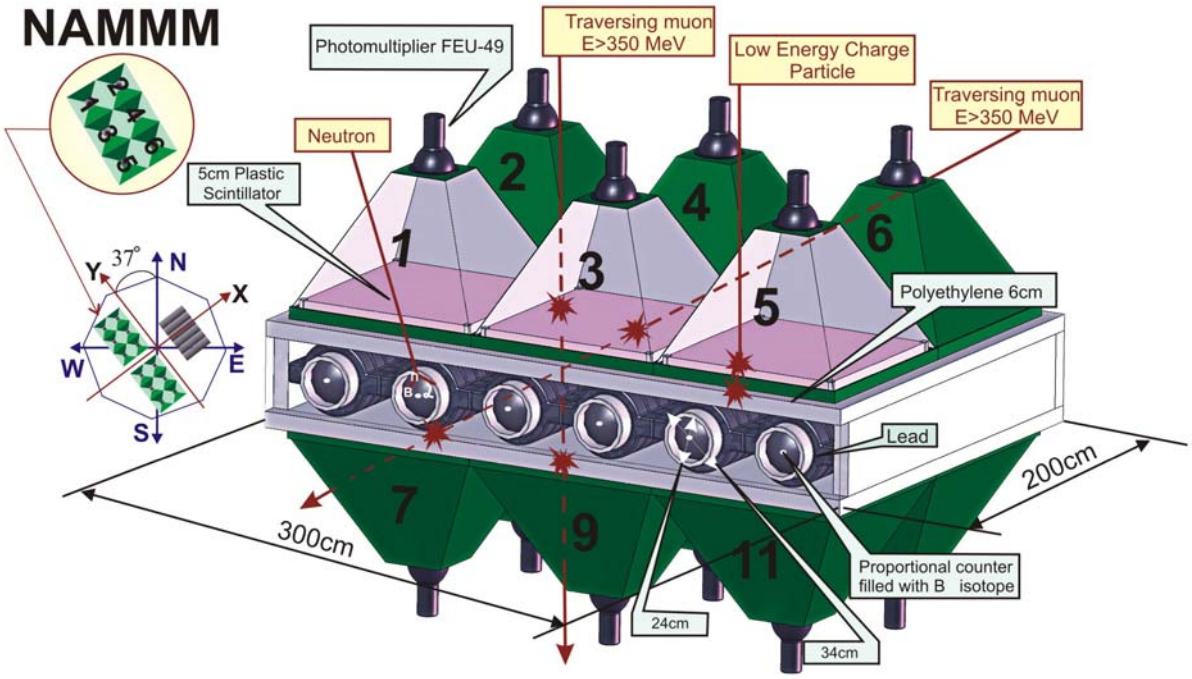


**Figure 10 Nor-Amberd Multidirectional Muon Monitor (NAMMM), section 1**

### 8.2.2. Structure of the information content from NAMMM

The list of available information from NAMMM is as follows:

- 1 minute count rates (easily can be changed to 10 seconds, or to another time span) of all 12 channels of NAMMM (see Table 7);
- Count rates of different incident directions separately, 36 possible coincidences of 6 upper and 6 bottom scintillators are related to 15 different directions (see Table 9);
- Count rates of the special coincidences (see details in Table 11);
- 1 minute estimates of the variances of count rates of each NAMMM channel, variances are calculated by 12 five-second count rates (see Table 12);
- 12 x 12 correlation matrix of NAMMM channels calculated by five-second count rates in 1 minute (see Table 13);

The raw data of the two sections of NAMMMs in the XML format available from CRD http server.

http://crdlx5.yerphi.am/ASEC_Data/ADAS/nammm/nammm1
http://crdlx5.yerphi.am/ASEC_Data/ADAS/nammm/nammm2

In the directory "DEFAULT" of both mentioned links the following information is stored correspondingly for the first and second sections of detector, namely NAMMM1 and NAMMM2:

- columns 1-12 - the count rates of all channels of NAMMM: first 6 columns – from upper layer scintillators, 7-12 columns – from lower layer scintillator. The numbering of scintillators is explained in the Figure 10. The count rates are posted in the Table 7;
- columns 13-48 – the count rates corresponding to the 36 coincidences in upper and lower NAMMM layers, i.e. – corresponding to the traversal of the single charged particle (mostly muons with energy > 250 MeV). The order of the different directions in the file is following: [1-7] [1-8] [1-9] [1-10] [1-11] [1-12] [2-7] [2-8] [2-9] [2-10] [2-11] [2-12] [3-7] [3-8] [3-9] [3-10] [3-11] [3-12] [4-7] [4-8] [4-9] [4-10] [4-11] [4-12] [5-7] [5-8] [5-9] [5-10] [5-11] [5-12] [6-7] [6-8] [6-9] [6-10] [6-11] [6-12], where the first number corresponds to the upper layer and the second – to the lower (see Figure 10) Also on the same Figure you

can see the orientation of NAMMM axes according to direction to the North Pole, thus we can calculate the interval of the horizontal angles of incidence related to each coincidence.

- columns 49-55 – the count rates of the "special" coincidences different from listed above and forming the "full system" of possible configurations of the channel operation. Conditioned on the existing as minimum 1 signal in 12 NAMMM channels there could be the following possibilities of number of counts in top and bottom layers (the first sign in the pair is corresponding to the upper scintillator): many-many (more than one count in 6 top and 6 bottom layers), many-zero (more than 1 in top and nothing in 6 bottom), zero-many, zero-one, one-zero, many-one, one-many. The fraction of the "special" coincidences relative to the "main" trigger is posted in the Table 11.
- columns 56 - the number of the "main" triggers – at least one signal in 12 channels in preselected time span (1 minute). If we consider all logical configurations of NAMM operation outcomes, this number will be equal to sum of the columns 13-55.
- columns 57-68 - the variances of 12 channels, see Table 12;
- columns 69-134 – the correlation matrix, see Table 13.

In the directories "spectrum" the 127-channel histograms of the energy releases are stored for each minute, in files with extensions:

- spectrum1 - spectrum6, the histograms of the energy releases in the upper scintillators are stored.
- spectrum7 - spectrum12, the histograms of the energy releases in the lower scintillators are stored;
- spectrum13 - spectrum18, histograms of energy releases, in upper detectors are stored with condition that in lower detectors there was now signal, i.e., the energy releases of electrons and low energy muons filtered in the lead absorber.

The information on the spectra of energy releases is essential for the continuous calibration of the all measuring channels. As one can see in Figure 11 the maximum of smoothed histograms are in the region 10-11 MeV, and this value should be monitored and kept constant during multiyear detector operation. In Figure 8 are presented 1-minute spectra summed over all four detectors and averaged over several hours. The blue curve is energy releases of the low energy muons and electrons (spectrum13-18) and the red curve is corresponding to high energy muons (subtracting from spectrum 1-6, spectrums 13-18). We can see than high energy muons in average can give much higher energy releases comparing with low energy muons and electrons. This additional information can be useful if Ground Level Enhancements (GLE) was originated by the primary particles having higher energy comparing with the GCR flux. Additionally to enhancement of the count rate we may notice some unusual features in the histograms of energy releases.

**Table 7 Count Rates of the NAMMM1 channels and variances (25-01-2008; 14:00-19:00).**

| Detectors | Average | Standard deviation | Relative Error (%) |
|---|---|---|---|
| Detector 1 | 14660 | 118 | 0.80 |
| Detector 2 | 14667 | 120 | 0.82 |
| Detector 3 | 15409 | 121 | 0.79 |
| Detector 4 | 16665 | 130 | 0.78 |
| Detector 5 | 17480 | 147 | 0.84 |
| Detector 6 | 16526 | 125 | 0.76 |
| **SUM of upper layer** | **89528** | | |
| Detector 7 | 9327 | 100 | 1.07 |
| Detector 8 | 10554 | 103 | 0.98 |
| Detector 9 | 9143 | 92 | 1.01 |
| Detector 10 | 8581 | 97 | 1.13 |
| Detector 11 | 9250 | 106 | 1.15 |
| Detector 12 | 10459 | 99 | 0.95 |
| **SUM of lower layer** | **54658** | | |

**Table 8 Count Rates of the NAMMM2 channels and variances (25-01-2008; 14:00-23:00).**

| Detectors | Average | Standard deviation | Relative Error (%) |
|---|---|---|---|
| Detector 1 | 14619 | 100.09 | 0.68 |
| Detector 2 | 15526 | 128.45 | 0.83 |
| Detector 3 | 15970 | 107.3 | 0.67 |
| Detector 4 | 15893 | 103.18 | 0.65 |
| Detector 5 | 15887 | 128.36 | 0.81 |
| Detector 6 | 14627 | 129.3 | 0.88 |
| **SUM of upper layer** | **92192** | | |
| Detector 7 | 9277 | 108.56 | 1.17 |
| Detector 8 | 8823 | 110.01 | 1.25 |
| Detector 9 | 9729 | 94.06 | 0.97 |
| Detector 10 | 10225 | 132.03 | 1.29 |
| Detector 11 | 9090 | 88.63 | 0.98 |
| Detector 12 | 9621 | 112.76 | 1.17 |
| **SUM of lower layer** | **55642** | | |

**Table 9 Mean count rates related to the different incident directions detected by the NAMMM1; variances, relative errors and fractions according the number of the "main" triggers (113109/ minute). Angle φ calculated relative XY axes (see Figure 10); φ is true north-based azimuth angle, θ is zenith angle.**

| Directions | | Average | Standard deviation | Relative Error (%) | SUM |
|---|---|---|---|---|---|
| **Vertical** | [1-7] | 2459 | 52 | 2.11 | 15509 |
| | [2-8] | 2621 | 53 | 2.02 | |
| | [3-9] | 2641 | 51 | 1.93 | |
| | [4-10] | 2313 | 49 | 2.12 | |
| | [5-11] | 2693 | 53 | 1.97 | |
| | [6-12] | 2782 | 49 | 1.76 | |
| **$\varphi=53^0\pm28^0$ E $\theta=37^0\pm13^0$** | [1-8] | 504 | 24 | 4.76 | 1538 |
| | [3-10] | 494 | 22 | 4.45 | |
| | [5-12] | 539 | 22 | 4.08 | |
| **$\varphi=233^0\pm28^0$ E $\theta=37^0\pm13^0$** | [2-7] | 955 | 29 | 3.04 | 3070 |
| | [4-9] | 1112 | 36 | 3.24 | |
| | [6-11] | 1003 | 32 | 3.19 | |
| **$\varphi=323^0\pm30^0$ E $\theta=37^0\pm13^0$** | [3-7] | 751 | 29 | 3.86 | 3092 |
| | [4-8] | 833 | 28 | 3.36 | |
| | [5-9] | 753 | 27 | 3.59 | |
| | [6-10] | 755 | 28 | 3.71 | |
| **$\varphi=143^0\pm30^0$ E $\theta=37^0\pm13^0$** | [1-9] | 689 | 27 | 3.92 | 2694 |
| | [2-10] | 583 | 25 | 4.29 | |
| | [3-11] | 724 | 26 | 3.59 | |
| | [4-12] | 699 | 26 | 3.72 | |
| **$\varphi=98^0\pm25^0$ E $\theta=49^0\pm11^0$** | [1-10] | 155 | 12 | 7.74 | 349 |
| | [3-12] | 194 | 14 | 7.22 | |
| **$\varphi=278^0\pm18^0$ E $\theta=49^0\pm10^0$** | [4-7] | 357 | 18 | 5.04 | 699 |
| | [6-9] | 341 | 19 | 5.57 | |
| **$\varphi=188^0\pm18^0$ E $\theta=49^0\pm10^0$** | [2-9] | 321 | 19 | 5.92 | 647 |
| | [4-11] | 326 | 18 | 5.52 | |
| **$\varphi=8^0\pm25^0$ E $\theta=49^0\pm11^0$** | [3-8] | 219 | 14 | 6.39 | 420 |
| | [5-10] | 201 | 14 | 6.97 | |
| **$\varphi=143^0\pm13^0$ E $\theta=61^0\pm6^0$** | [1-11] | 49 | 6 | 12.24 | 101 |
| | [2-12] | 52 | 7 | 13.46 | |
| **$\varphi=323^0\pm13^0$ E $\theta=61^0\pm6^0$** | [5-7] | 53 | 7 | 13.21 | 115 |
| | [6-8] | 61 | 7 | 11.48 | |
| **$\varphi=116^0\pm12^0$ E $\theta=64^0\pm6^0$** | [1-12] | 28 | 6 | 21.43 | 28 |
| **$\varphi=296^0\pm12^0$ E $\theta=64^0\pm6^0$** | [6-7] | 34 | 6 | 17.65 | 34 |
| **$\varphi=170^0\pm12^0$ E $\theta=64^0\pm6^0$** | [2-11] | 34 | 6 | 17.65 | 34 |
| **$\varphi=350^0\pm12^0$ E $\theta=64^0\pm6^0$** | [5-8] | 32 | 5 | 15.63 | 32 |
| | **SUM** | **28360** | | | |

**Table 10 Mean count rates related to the different incident directions detected by the NAMMM2; variances, relative errors and fractions according the number of the "main" triggers (113109/ minute). Angle φ calculated relative XY axes (see Figure 10); φ is true north-based azimuth angle, θ is zenith angle.**

| Directions | | Average | Standard deviation | Relative Error (%) | SUM |
|---|---|---|---|---|---|
| **Vertical** | [1-7] | 2318 | 48.44 | 2.09 | 15406 |
| | [2-8] | 2251 | 47.98 | 2.13 | |
| | [3-9] | 2779 | 54.52 | 1.96 | |
| | [4-10] | 2679 | 48.96 | 1.83 | |
| | [5-11] | 2667 | 48.96 | 1.84 | |
| | [6-12] | 2711 | 53.19 | 1.96 | |
| **$\varphi=53^0\pm28^0$ E $\theta=37^0\pm13^0$** | [1-8] | 481 | 21.44 | 4.46 | 1525 |
| | [3-10] | 517 | 22.8 | 4.41 | |
| | [5-12] | 527 | 22.37 | 4.24 | |
| **$\varphi=233^0\pm28^0$ E $\theta=37^0\pm13^0$** | [2-7] | 990 | 32.31 | 3.26 | 3261 |
| | [4-9] | 1130 | 32.92 | 2.91 | |
| | [6-11] | 1141 | 33.52 | 2.94 | |
| **$\varphi=323^0\pm30^0$ E $\theta=37^0\pm13^0$** | [3-7] | 665 | 26.15 | 3.93 | 2766 |
| | [4-8] | 667 | 26.26 | 3.94 | |
| | [5-9] | 711 | 26.63 | 3.75 | |
| | [6-10] | 724 | 26.34 | 3.64 | |
| **$\varphi=143^0\pm30^0$ E $\theta=37^0\pm13^0$** | [1-9] | 815 | 27.29 | 3.35 | 3229 |
| | [2-10] | 777 | 27.48 | 3.54 | |
| | [3-11] | 836 | 28.17 | 3.37 | |
| | [4-12] | 800 | 28.01 | 3.50 | |
| **$\varphi=98^0\pm25^0$ E $\theta=49^0\pm11^0$** | [1-10] | 192 | 13.83 | 7.20 | 400 |
| | [3-12] | 208 | 13.24 | 6.37 | |
| **$\varphi=278^0\pm18^0$ E $\theta=49^0\pm10^0$** | [4-7] | 321 | 17.88 | 5.57 | 660 |
| | [6-9] | 339 | 18.97 | 5.60 | |
| **$\varphi=188^0\pm18^0$ E $\theta=49^0\pm10^0$** | [2-9] | 385 | 20 | 5.19 | 778 |
| | [4-11] | 393 | 19.76 | 5.03 | |
| **$\varphi=8^0\pm25^0$ E $\theta=49^0\pm11^0$** | [3-8] | 183 | 13.51 | 7.38 | 364 |
| | [5-10] | 181 | 13.46 | 7.44 | |
| **$\varphi=143^0\pm13^0$ E $\theta=61^0\pm6^0$** | [1-11] | 56 | 7.53 | 13.45 | 114 |
| | [2-12] | 58 | 7.79 | 13.43 | |
| **$\varphi=323^0\pm13^0$ E $\theta=61^0\pm6^0$** | [5-7] | 47 | 7.36 | 15.66 | 95 |
| | [6-8] | 48 | 6.87 | 14.31 | |
| **$\varphi=116^0\pm12^0$ E $\theta=64^0\pm6^0$** | [1-12] | 28 | 5.27 | 18.82 | 28 |
| **$\varphi=296^0\pm12^0$ E $\theta=64^0\pm6^0$** | [6-7] | 32 | 5.92 | 18.50 | 32 |
| **$\varphi=170^0\pm12^0$ E $\theta=64^0\pm6^0$** | [2-11] | 39 | 6.34 | 16.26 | 39 |
| **$\varphi=350^0\pm12^0$ E $\theta=64^0\pm6^0$** | [5-8] | 26 | 5.29 | 20.35 | 26 |
| | **SUM** | **28722** | | | |

**Table 11 Mean count rates of "special" cases (NAMMM1) ; variances, relative errors and fractions according the number of "main" triggers (113109/ minute).**

| Coincidence | Average | Standard deviation | Relative Error [%] |
|---|---|---|---|
| Many – Many | 39 | 6.11 | 15.67 |
| Many – Zero | 1790 | 43.44 | 2.43 |
| Zero – Many | 322 | 17.55 | 5.45 |
| Zero – One | 27469 | 168.89 | 0.61 |
| One – Zero | 62117 | 248.32 | 0.40 |
| Many – One | 376 | 19.26 | 5.12 |
| One – Many | 170 | 12.64 | 7.44 |

**Table 12 Mean values of the count rates and variances, calculated by 5-sec count rates of 1 minute time span (total 12 5-dec count rates) (NAMMM1).**

| Detectors | Mean value of the count rate | Mean value of the variance | Relative error (variance/count rate) |
|---|---|---|---|
| Detector 1 | 1272 | 15.95 | 0.0125 |
| Detector 2 | 1191 | 15.34 | 0.0129 |
| Detector 3 | 1044 | 14.40 | 0.0138 |
| Detector 4 | 1287 | 16.02 | 0.0124 |
| Detector 5 | 1269 | 15.87 | 0.0125 |
| Detector 6 | 1284 | 15.94 | 0.0124 |
| Detector 7 | 811 | 12.69 | 0.0156 |
| Detector 8 | 923 | 13.53 | 0.0147 |
| Detector 9 | 690 | 11.63 | 0.0169 |
| Detector 10 | 735 | 12.03 | 0.0164 |
| Detector 11 | 749 | 14.81 | 0.0197 |
| Detector 12 | 780 | 12.43 | 0.0159 |

**Table 13 Mean value of the correlation matrix, calculated by 5-sec count rates of 1 minute time span and averaged over time span of 5 hours at 25 January 2008. Emphasized (red) values are related to NAMMM1 channels stacked one above another, for which correlation should be significant.**

| | Det 1 | Det 2 | Det 3 | Det 4 | Det 5 | Det 6 | Det 7 | Det 8 | Det 9 | Det 10 | Det 11 | Det 12 |
|---|---|---|---|---|---|---|---|---|---|---|---|---|
| **Det 1** | 1 | | | | | | | | | | | |
| **Det 2** | 0.014 | 1 | | | | | | | | | | |
| **Det 3** | 0.011 | 0.017 | 1 | | | | | | | | | |
| **Det 4** | 0.001 | 0.006 | -0.010 | 1 | | | | | | | | |
| **Det 5** | 0.018 | -0.027 | -0.009 | 0.013 | 1 | | | | | | | |
| **Det 6** | 0.001 | 0.038 | 0.010 | 0.015 | 0.023 | 1 | | | | | | |
| **Det 7** | **0.209** | 0.072 | 0.080 | 0.015 | -0.004 | 0.008 | 1 | | | | | |
| **Det 8** | 0.004 | **0.213** | 0.035 | 0.034 | 0.012 | 0.018 | -0.000 | 1 | | | | |
| **Det 9** | 0.056 | 0.044 | **0.216** | 0.085 | 0.063 | 0.009 | -0.000 | 0.005 | 1 | | | |
| **Det 10** | 0.015 | 0.045 | 0.013 | **0.166** | 0.006 | 0.066 | -0.030 | -0.004 | 0.005 | 1 | | |
| **Det 11** | -0.005 | 0.010 | 0.067 | 0.040 | **0.217** | 0.077 | -0.020 | 0.018 | 0.022 | -0.001 | 1 | |
| **Det 12** | 0.000 | 0.006 | 0.051 | 0.051 | 0.029 | **0.191** | 0.002 | 0.027 | 0.003 | 0.020 | 0.007 | 1 |

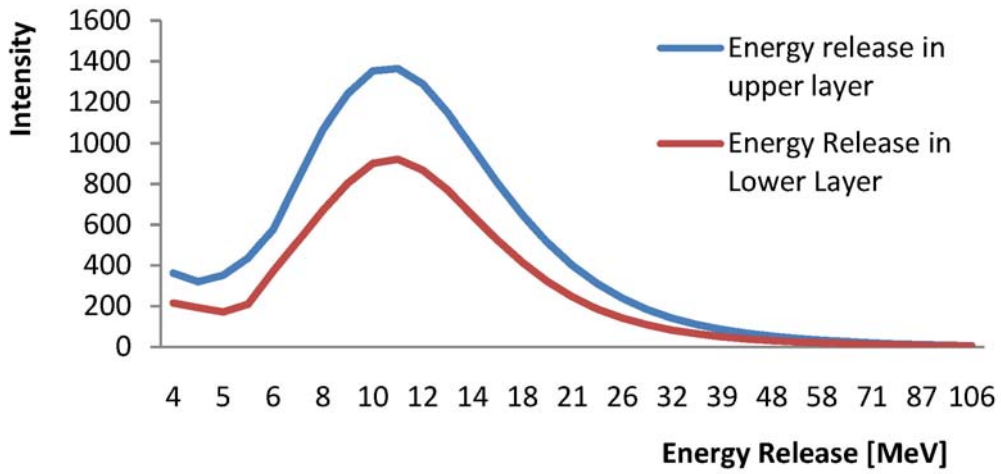


**Figure 11 Histogram of energy releases in NAMMM1 upper and lower scintillators (1 minute data).**

### 8.3.1. Nor-Amberd and Aragats Neutron Monitors (NANM & ArNM)

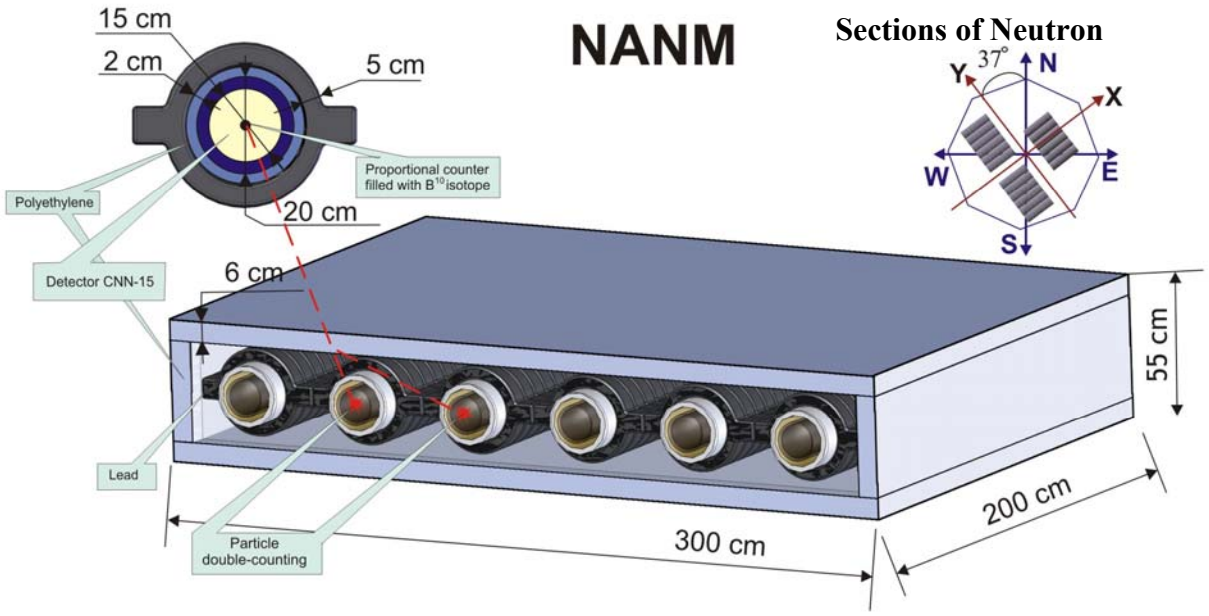


**Figure 12 Nor-Amberd Neutron Monitor (NANM)**

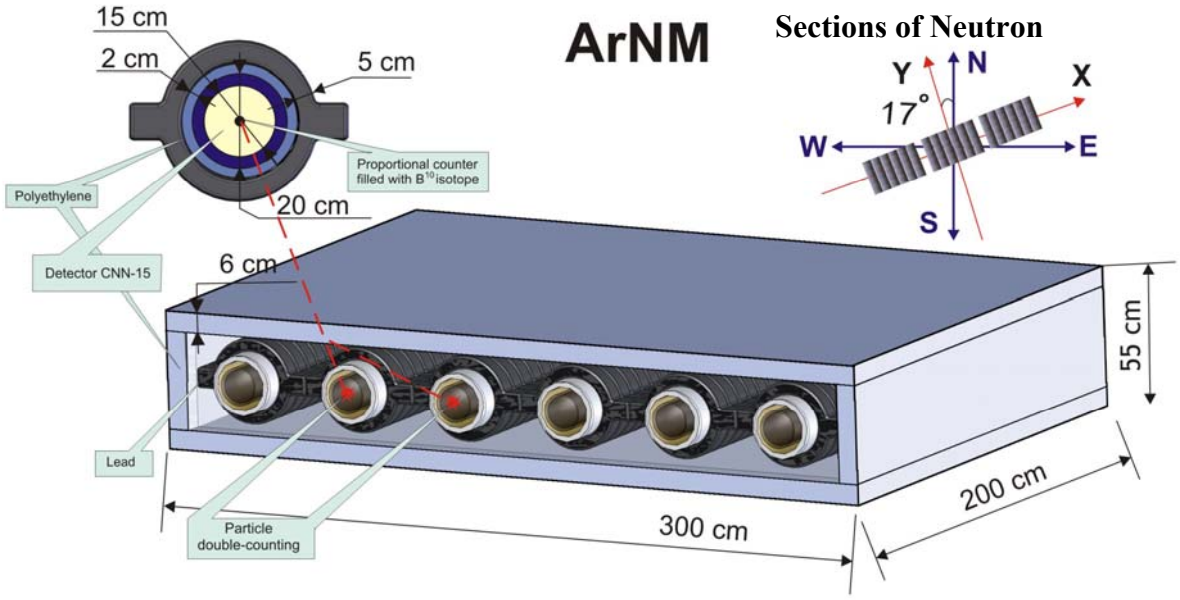


**Figure 13 Aragats Neutron Monitor (ArNM).**

Two 18NM-64 neutron monitors (see Figure 12, Figure 13) (Moraal, et al., 2000), are in operation at Nor-Amberd (40°22'N, 44°15'E, 2000m above sea level), and at Aragats, (40°28'N, 44°10'E, 3250m above sea level) research stations. They called the Nor Amberd Neutron Monitor (NANM), and the Aragats Neutron Monitor (ANM), respectively. The monitors are equipped with new electronics providing time integration of counts by three dead times. The first dead time equals to 400ns for collecting almost all thermalized neutrons entering the proportional chamber from the lead. The second dead time is equal to the 0.25ms and the third one equal 1.25ms (as most of NM

from world-wide network). Also 2 proportional chambers without lead coverage are added to NANM.

The raw data of the NANM and ArNM is available from CRD http server by these links:

http://crdlx5.yerphi.am/ASEC_Data/ADAS/nanm/nanm/DEFAULT/

http://crdlx5.yerphi.am/ASEC_Data/ADAS/arnm/arnm/DEFAULT/

In the data files of the NM following information is stored (Table 14 and Table 15):

1. columns 1+3i (i=0,…,17) - the count rates of all 18 channels of NM with dead time 400ns.
2. columns 2+3i (i=0,…,17) - the count rates of all 18 channels of NM with dead time 0.25ms.
3. columns 3+3i (i=0,…,17) - the count rates of all 18 channels of NM with dead time 1.25ms.
4. column 55 – the pressure coefficient.
5. columns 56 – 60 yet unused channels, additional neutron detectors to be attached soon.

**Table 14. Count rates of the 18 channels of the NANM (07.02.2008).**

| | **Number of Column** | Average Count Rate (0.4us) | Std. Dev. | SUM | **Number of Column** | Average Count Rate (250us) | Std. Dev. | SUM | **Number of Column** | Average Count Rate (1250us) | Std. Dev. | SUM |
|---|---|---|---|---|---|---|---|---|---|---|---|---|
| Detector 1 | **1** | 1530 | 57 | | **2** | 1312 | 39 | | **3** | 1172 | 33 | |
| Detector 2 | **4** | 1375 | 47 | | **5** | 1216 | 37 | | **6** | 1101 | 32 | |
| Detector 3 | **7** | 1608 | 52 | | **8** | 1405 | 40 | | **9** | 1262 | 35 | |
| Detector 4 | **10** | 1628 | 52 | | **11** | 1425 | 39 | | **12** | 1277 | 33 | |
| Detector 5 | **13** | 1580 | 53 | | **14** | 1379 | 41 | | **15** | 1243 | 35 | |
| Detector 6 | **16** | 1391 | 64 | | **17** | 1198 | 37 | | **18** | 1082 | 32 | |
| Detector 7 | **19** | 1676 | 54 | | **20** | 1455 | 41 | | **21** | 1310 | 34 | |
| Detector 8 | **22** | 1608 | 51 | | **23** | 1412 | 41 | | **24** | 1268 | 35 | |
| Detector 9 | **25** | 1539 | 50 | **27483** | **26** | 1345 | 38 | **23993** | **27** | 1215 | 32 | **21633** |
| Detector 10 | **28** | 1553 | 53 | | **29** | 1361 | 41 | | **30** | 1228 | 35 | |
| Detector 11 | **31** | 1592 | 54 | | **32** | 1370 | 41 | | **33** | 1232 | 35 | |
| Detector 12 | **34** | 1417 | 49 | | **35** | 1236 | 38 | | **36** | 1114 | 32 | |
| Detector 13 | **37** | 1471 | 51 | | **38** | 1260 | 39 | | **39** | 1133 | 33 | |
| Detector 14 | **40** | 1369 | 46 | | **41** | 1226 | 37 | | **42** | 1120 | 33 | |
| Detector 15 | **43** | 1561 | 53 | | **44** | 1362 | 41 | | **45** | 1234 | 35 | |
| Detector 16 | **46** | 1620 | 52 | | **47** | 1426 | 41 | | **48** | 1286 | 34 | |
| Detector 17 | **49** | 1581 | 51 | | **50** | 1395 | 40 | | **51** | 1260 | 35 | |
| Detector 18 | **52** | 1374 | 47 | | **53** | 1202 | 36 | | **54** | 1086 | 31 | |

**Table 15. Count rates of the 18 channels of the ArNM (07.02.2008).**

| | **Number of Column** | Average Count Rate (0.4us) | Std. Dev. | SUM | **Number of Column** | Average Count Rate (250us) | Std. Dev. | SUM | **Number of Column** | Average Count Rate (1250us) | Std. Dev. | SUM |
|---|---|---|---|---|---|---|---|---|---|---|---|---|
| Detector 1 | **1** | 2574 | 72 | | **2** | 2235 | 51 | | **3** | 1997 | 43 | |
| Detector 2 | **4** | 2521 | 64 | | **5** | 2249 | 52 | | **6** | 2031 | 44 | |
| Detector 3 | **7** | 2840 | 68 | | **8** | 2528 | 54 | | **9** | 2259 | 45 | |
| Detector 4 | **10** | 2800 | 68 | | **11** | 2495 | 54 | | **12** | 2235 | 46 | |
| Detector 5 | **13** | 2314 | 59 | | **14** | 2092 | 48 | | **15** | 1907 | 42 | |
| Detector 6 | **16** | 2335 | 59 | | **17** | 2074 | 47 | | **18** | 1866 | 40 | |
| Detector 7 | **19** | 2437 | 64 | | **20** | 2169 | 51 | | **21** | 1938 | 43 | |
| Detector 8 | **22** | 2648 | 63 | | **23** | 2368 | 50 | | **24** | 2131 | 43 | |
| Detector 9 | **25** | 2650 | 62 | **43261** | **26** | 2392 | 50 | **38769** | **27** | 2166 | 44 | **35055** |
| Detector 10 | **28** | 2731 | 63 | | **29** | 2469 | 51 | | **30** | 2239 | 44 | |
| Detector 11 | **31** | 2459 | 62 | | **32** | 2209 | 52 | | **33** | 2000 | 45 | |
| Detector 12 | **34** | 2315 | 62 | | **35** | 2055 | 49 | | **36** | 1852 | 42 | |
| Detector 13 | **37** | 2145 | 59 | | **38** | 1910 | 46 | | **39** | 1733 | 40 | |
| Detector 14 | **40** | 1877 | 51 | | **41** | 1723 | 44 | | **42** | 1589 | 39 | |
| Detector 15 | **43** | 2069 | 53 | | **44** | 1900 | 45 | | **45** | 1746 | 39 | |
| Detector 16 | **46** | 2043 | 54 | | **47** | 1861 | 45 | | **48** | 1709 | 39 | |
| Detector 17 | **49** | 2396 | 63 | | **50** | 2146 | 50 | | **51** | 1943 | 44 | |
| Detector 18 | **52** | 2097 | 58 | | **53** | 1886 | 48 | | **54** | 1705 | 41 | |

### 8.4.1. The basic detecting unit of the SEVAN network

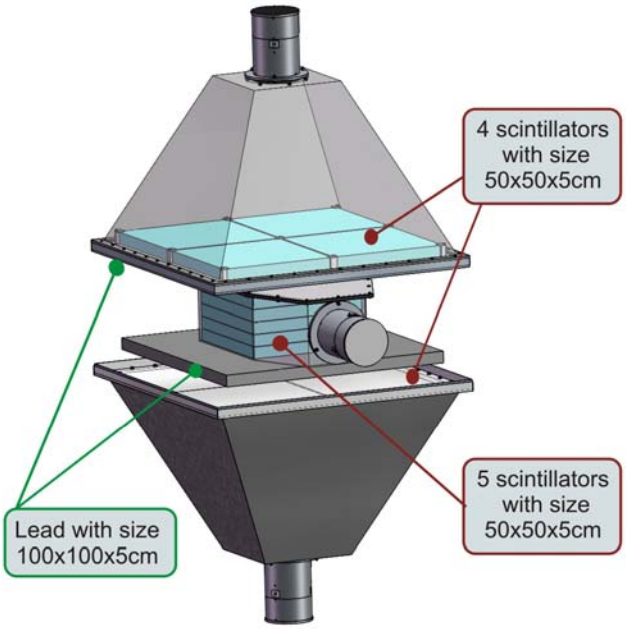


**Figure 14 The basic detecting unit of the SEVAN network**

The basic detecting unit of the SEVAN network (see Figure 14) is assembled from standard slabs of 50x50x5cm$^3$ plastic scintillators. Between 2 identical assemblies of 100 x 100 x 5 cm$^3$ scintillators (four standard slabs) are located two 100 x 100 x 5 cm$^3$ lead absorbers and thick 50 x 50 x 25 cm$^3$ scintillator assembly (5 standard slabs). A scintillator light capture cone and Photo Multiplier Tube (PMT) are located on the top, bottom and the intermediate layers of detector. The detailed detector charts with all sizes are available from http://crdlx5.yerphi.am/

Incoming neutral particles undergo nuclear reactions in the thick 25 cm plastic scintillator and produce protons and other charged particles. In the upper 5 cm thick scintillator charged particles are registered very effectively; however for the nuclear interactions of neutral particles there is not enough substance. When a neutral particle traverses the top thin (5cm) scintillator, usually no signal is produced. The absence of the signal in the upper scintillators, coinciding with the signal in the middle scintillator, points to neutral particle detection. The coincidence of signals from the top and bottom scintillators indicates traversal of high energy muons. Lead absorbers improve efficiency of the neutral flux detection and filtered low energy charged particles. SEVAN world-wide network will consist of modules located in Croatia, Bulgaria, India (to be installe din 2008), Slovakia, Costa-Rica and Indonesia (to be installed in 2009). We present data from SEVAN module operated at Nor Amberd research station, another module is under construction in Yerevan at altitude 1000 m in CRD headquarters.

### 8.4.2. Structure of the information content from SEVAN detector

The following information is providing by SEVAN detector:

1. Count rates from the all 3 layers (see Table 16).
2. Count rates of the all coincidences of upper, middle and lower detectors (see Table 16 and Table 17).
3. Correlation matrix between all detected signals (Table 18)

The data is stored in

http://crdlx5.yerphi.am/ASEC_Data/ADAS/sevan01/sevan1/

In the directory "DEFAULT" the following information is stored:

1. columns 1-3 - the count rates of all channels of the SEVAN. The count rates are posted in the Table 16;
2. column 4 unused (this channel we can use as input of the atmospheric pressure sensor).
3. columns 5-8 – the count rates of the coincidences of the all channels of the SEVAN. If we denote by the sign "1" signal from scintillator, and by sign "0" absence of signal, following combinations of the 3-layered detector output are stored: 110, 101, 011, 111 (see Table 16).

**Table 16 Count Rates of the SEVAN channels and variances.**

| | Average | Standard deviation | Relative Error [%] |
|---|---|---|---|
| Upper Detector | 9548 | 103 | 1.08 |
| Middle Detector | 4183 | 63 | 1.50 |
| Lower Detector | 5444 | 77 | 1.41 |
| Coincidence 110 | 1052 | 32 | 3.04 |
| Coincidence 101 | 512 | 23 | 4.44 |
| Coincidence 011 | 676 | 25 | 3.69 |
| Coincidence 111 | 1713 | 43 | 2.51 |

**Table 17 Additional coincidences corresponding to different type particles by the SEVAN detector**

| | Average | Standard deviation | Relative Error [%] |
|---|---|---|---|
| **Coincidence100** = Upper Detector – Coincidence110 – (low energy charged) Coincidence101 – Coincidence111 | 6271 | 82 | 1.31 |
| **Coincidence010** = Middle Detector – Coincidence110 – (neutral) Coincidence011 – Coincidence111 | 742 | 28 | 3.75 |
| **Coincidence001** = Lower Detector – Coincidence101 – (near horizontal) Coincidence011 – Coincidence111 | 2543 | 51 | 2.01 |

**Table 18 Correlation between coincidences of the SEVAN 3 layers .**

| Coincidence | [110] | [101] | [011] | [111] | [100] | [010] | [001] |
|---|---|---|---|---|---|---|---|
| [110] | 1 | | | | | | |
| [101] | 0.034 | 1 | | | | | |
| [011] | -0.018 | -0.020 | 1 | | | | |
| [111] | -0.081 | 0.052 | -0.055 | 1 | | | |
| [100] | 0.026 | 0.014 | -0.087 | 0.067 | 1 | | |
| [010] | 0.023 | 0.021 | -0.026 | 0.019 | 0.057 | 1 | |
| [001] | -0.022 | 0.102 | -0.009 | 0.031 | -0.072 | -0.043 | 1 |

### 8.5.1. MAKET-ANI Extensive Air Shower Detector.

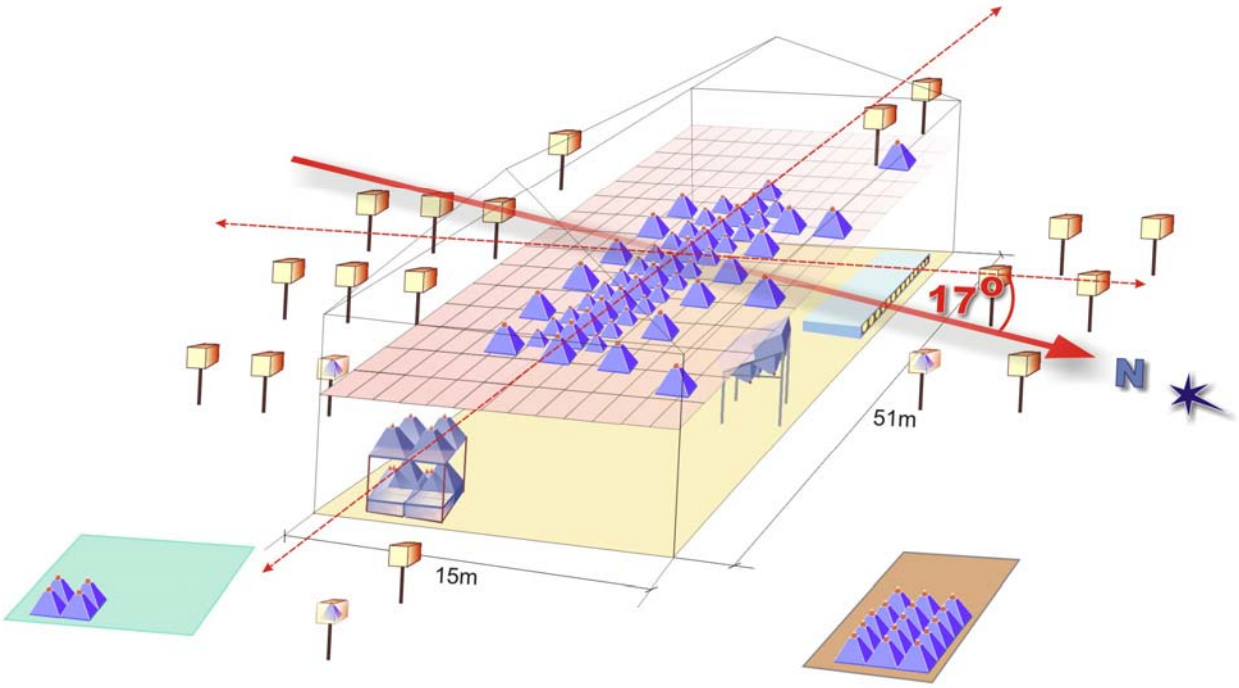


**Figure 15 MAKET-ANI Extensive Air Shower Detector.**

In the assembly of the ANI Cosmic Ray experiment (Danilova, et al., 1992), two detectors measuring the Extensive Air Showers (EAS) are operated on the Aragats research station. The main goal of the GAMMA (Garyaka, et al., 2002) and MAKET-ANI (Avakian, et al., 1986; Chilingarian, et al., 1999) detectors are to investigate the energy spectra of cosmic rays to understand the origin and accelerator mechanisms. Both detectors use the same particle density detection techniques to determine the number of electrons in the shower and infer the energy and type of the primary particle.

After obtaining and publishing final results of the MAKET-ANI (see Figure 15) experiment (Chilingarian, et al., 2007) the experiment was stopped for collecting high energy galactic cosmic rays. Some of the scintillators were used for rearranged smaller detector. Around the ASNT detector (consisted of four 60 cm thick scintillators and four 5 cm thick scintillators another 8 5 cm scintillators were arranged and attached to the 16 channel spectrum analyzer. We plan to test with this array new fast-timing technique to be used for new big array in Nor Amberd (Chilingarian, Hovsepyan, et al, 2007). Meanwhile new MAKET array provides following information:

1. 1 minute count rates of all 16 channels of the MAKET (see Table 19);
2. Count rate of the EAS triggering 8 and all 16 detectors;
3. Estimates of the variances of count rates of each MAKET channel, variances are calculated by 12 five-second count rates (see Table 21);
4. 16 x 16 correlation matrix of MAKET channels calculated by five-second count rates in 1 minute.

The data is stored in
http://crdlx5.yerphi.am/ASEC_Data/ADAS/maket/maket/
In the directory “DEFOULT” following information is stored:

1. Columns 1-16 - the count rates of all 16 MAKET channels: first 4 columns – from 60 cm scintillators, 5-16 columns – from 5 cm scintillator. The count rates are posted in the Table 19;

2. Columns 17-18 – the count rates corresponding to the EAS initiated triggers. 17th column corresponds to the coincidence of the first 8 channels (ASNT scintillators), 18th column corresponding to the coincidence in all 16 channels. The count rates are posted in the Table 20;
3. Columns 19-34 – the variances of 16 channels, see Table 21;
4. Columns 35-154 – the correlation matrix.

In the directories "spectrum" following information is stored:

1. spectrum1, … spectrum4 the histograms of the energy releases in thick 60 cm scintillator are stored. In files with extension;
2. spectrum5, … spectrum16 the histograms of energy releases in 5 cm thin scintillators are stored;

In the CRD local server available files with following information:

- In the files with "events" extension is related to the Extensive Air Showers (EAS). The logical software trigger selects events when signals are more than in 8 detectors.

**Table 19 Count Rates of the MAKET channels, variances and relative errors.**

| Detector | Average | Standard deviation | Relative error [%] |
|---|---|---|---|
| Detector 1 (60cm) | 37973 | 201 | 0.53 |
| Detector 2 (60cm) | 29869 | 185 | 0.62 |
| Detector 3 (60cm) | 33244 | 188 | 0.57 |
| Detector 4 (60cm) | 32074 | 164 | 0.51 |
| Detector 5 | 23732 | 152 | 0.64 |
| Detector 6 | 28100 | 167 | 0.59 |
| Detector 7 | 17125 | 146 | 0.85 |
| Detector 8 | 24845 | 174 | 0.70 |
| Detector 9 | 22956 | 144 | 0.63 |
| Detector 10 | 18313 | 140 | 0.76 |
| Detector 11 | 23722 | 159 | 0.67 |
| Detector 12 | 18901 | 148 | 0.78 |
| Detector 13 | 22589 | 152 | 0.67 |
| Detector 14 | 19492 | 134 | 0.69 |
| Detector 15 | 22964 | 152 | 0.66 |
| Detector 16 | 21154 | 144 | 0.68 |

**Table 20 Count Rates of the MAKET EAS initiated triggers, variances and relative errors.**

| Detector | Average | Standard deviation | Relative error [% |
|---|---|---|---|
| Coincidence in thirst 8 channels | 20 | 4 | 21.02 |
| Coincidence in all 16 channels | 5 | 2 | 41.95 |

**Table 21 Mean value of the variance, its variance and relative error calculated by 5-sec count rates of 1 minute time span (total 12 5-dec count rates).**

| Detector | Average | Standard deviation | Relative error [%] |
|---|---|---|---|
| Detector 1 (60cm) | 53 | 11 | 21.46 |
| Detector 2 (60cm) | 49 | 10 | 21.06 |
| Detector 3 (60cm) | 52 | 12 | 22.63 |
| Detector 4 (60cm) | 50 | 11 | 21.37 |
| Detector 5 | 44 | 10 | 21.87 |
| Detector 6 | 47 | 10 | 22.18 |
| Detector 7 | 37 | 8 | 20.79 |
| Detector 8 | 45 | 11 | 23.28 |
| Detector 9 | 43 | 9 | 20.85 |
| Detector 10 | 38 | 8 | 21.16 |
| Detector 11 | 43 | 9 | 20.96 |
| Detector 12 | 39 | 8 | 20.66 |
| Detector 13 | 42 | 9 | 20.62 |
| Detector 14 | 39 | 8 | 21.22 |
| Detector 15 | 43 | 9 | 21.68 |
| Detector 16 | 41 | 8 | 20.50 |

### 8.6.1. Aragats Multidirectional Muon Monitor (AMMM)

The Aragats Multidirectional Muon Monitor (AMMM) consists from 2 layers of the scintillation detectors. 29 scintillation detectors (each detector have $1m^2$ surface and 5cm thickness), located on top of the top of ANI concrete calorimeter and 100 the same type detectors 14 m below (under 4m concrete and 7m soil), as shown in Figure 13 and 14. Zenith angle between axes of AMMM and direction to South pole is ~-17º. Count rate in the upper detectors is ~28000 counts per minute and variance ~170. Count rate of each of 1 $m^2$ scintillators in the underground hall(high energy muons with energy threshold 5 GeV) is ~3000 counts per minute and variance ~55. The relative accuracy of 1-minute count rates of underground high energy muon detector is ~0.2%, of the low energy muons and electrons on surface ~ 0.12%.

The new electronics will be installed in the summer 2008. The present DAQ consists of scalers attached to on-line PC by COM port.

AMMM data is available from SKYNET local server. Data from first 59 channels of the NAMMM lower layer you can find by this link \\soul\ASEC_data\amet. The last 30 channels of the NAMMM lower layer you can find here \\soul\ASEC_data\arme in the files with extension .ame. The first 30 columns are corresponding to the lower layer AMMM, the second 29 columns corresponding to the upper layer AMMM.

In Figure 15 we present the daily variations of the high energy secondary muons averaged over 21 days.

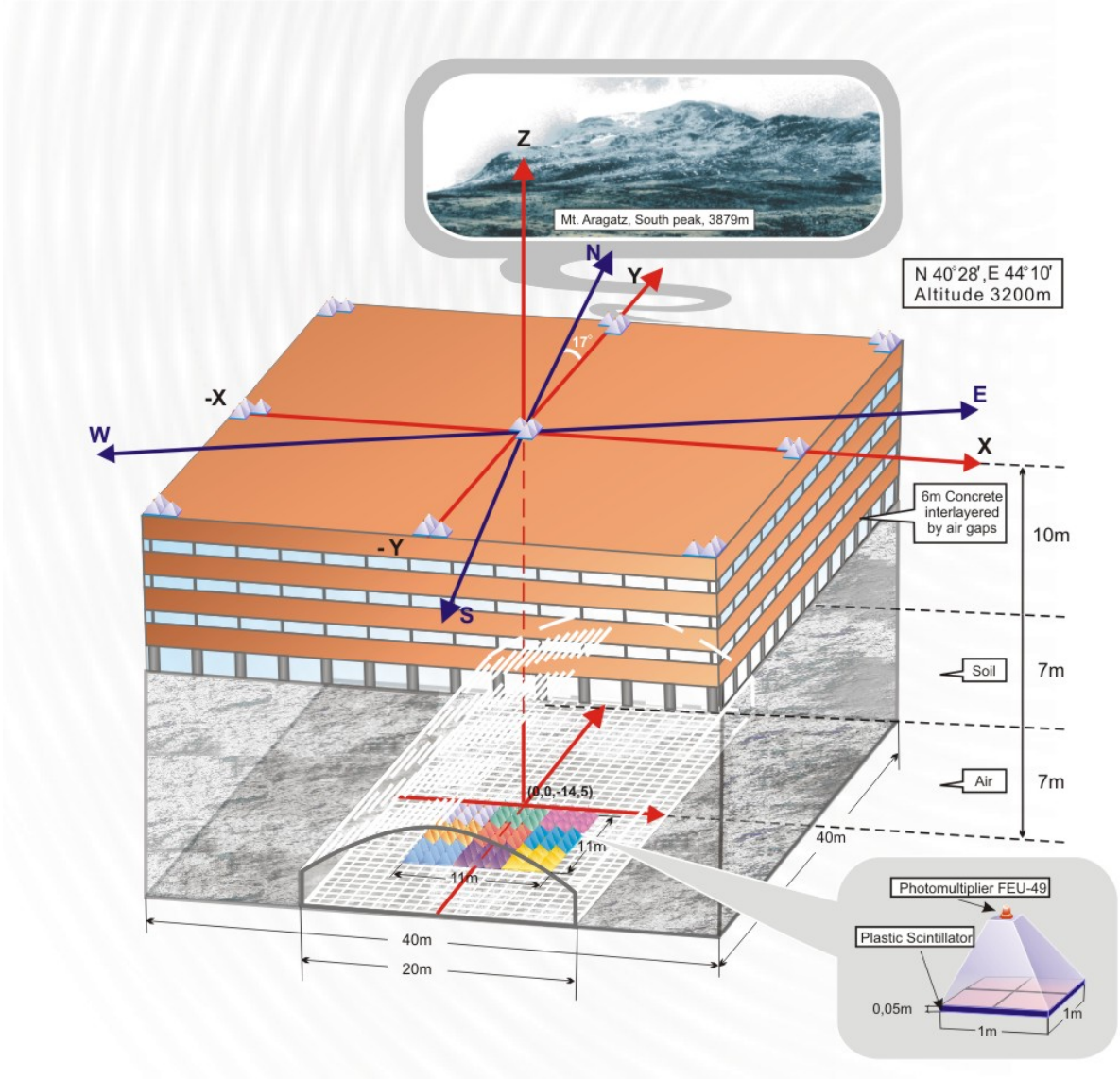


**Figure 16: Aragats Multidirectional Muon Monitor (AMMM).**

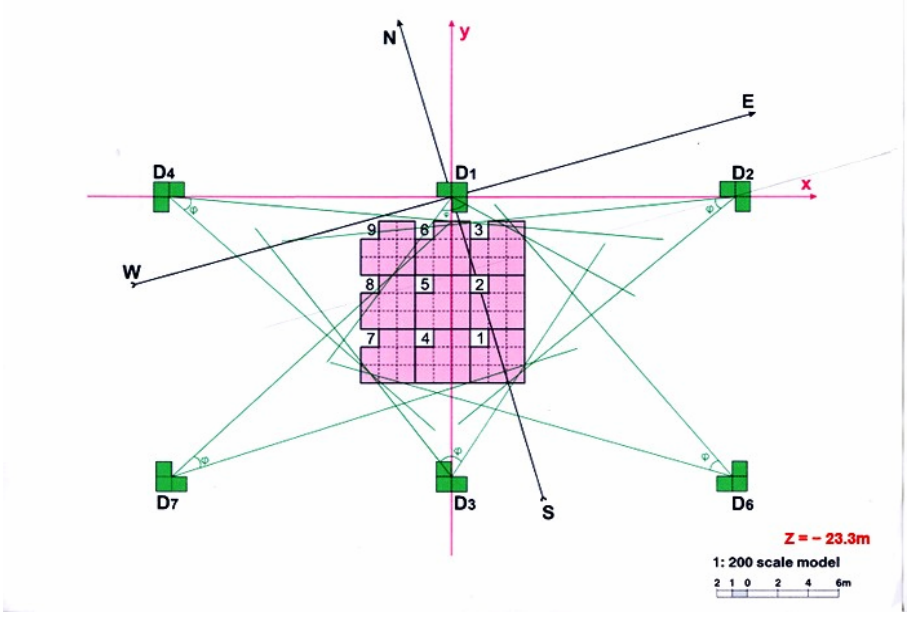


**Figure 17 Projection of the AMMM on the X-Y plane**

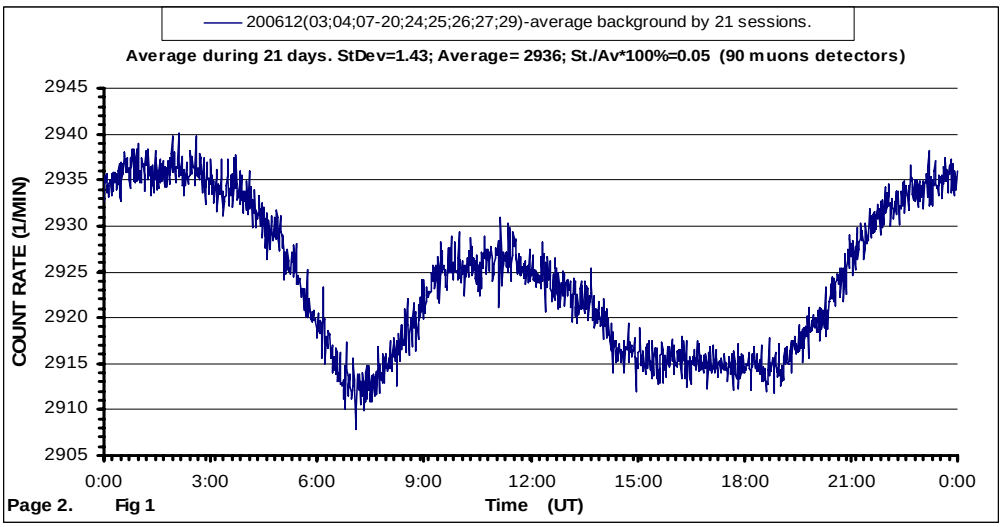


**Figure 18 The "daily wave" – the time variations of the count rate of high energy muons.**

In tables 22 and 23 we present averaged count rates as measured at 8 December 2007 and total number of muons measured by each detector per day. Total 248,292,843 muons were detected.

**Table 22 Average minute count rates and standard deviations of 5 GeV muons measured at 8 December 2007**

| Nº | Average | Standard deviation | Relative error [%] | Nº | Average | Standard deviation | Relative error [%] | Nº | Average | Standard deviation | Relative error [%] |
|---|---|---|---|---|---|---|---|---|---|---|---|
| **1** | 2914 | 43.1 | 1.48% | **31** | 2939 | 52.2 | 1.78% | **61** | 3003 | 54.4 | 1.88% |
| **2** | 3052 | 55.9 | 1.83% | **32** | 2875 | 55.7 | 1.94% | **62** | 2883 | 55.6 | 1.93% |
| **3** | 3027 | 56.7 | 1.87% | **33** | 2834 | 56.3 | 1.99% | **63** | 2687 | 54.9 | 2.04% |
| **4** | 2804 | 53.5 | 1.91% | **34** | 2749 | 55.0 | 2.00% | **64** | 2854 | 59.5 | 2.08% |
| **5** | 2997 | 56.9 | 1.90% | **35** | 2933 | 55.8 | 1.90% | **65** | 2931 | 56.2 | 1.92% |
| **6** | 3013 | 55.0 | 1.83% | **36** | 2704 | 53.6 | 1.98% | **66** | 2674 | 52.4 | 1.96% |
| **7** | 2957 | 54.5 | 1.84% | **37** | 2854 | 55.6 | 1.95% | **67** | 3049 | 63.5 | 2.08% |
| **8** | 2829 | 55.5 | 1.96% | **38** | 2834 | 54.8 | 1.93% | **68** | 2832 | 59.9 | 2.12% |
| **9** | 2896 | 53.6 | 1.85% | **39** | 2873 | 52.6 | 1.83% | **69** | 2988 | 52.8 | 1.77% |
| **10** | 2930 | 54.7 | 1.87% | **40** | 2768 | 55.1 | 1.99% | **70** | 2837 | 53.9 | 1.90% |
| **11** | 2945 | 55.3 | 1.88% | **41** | 2756 | 53.0 | 1.92% | **71** | 2732 | 55.1 | 2.02% |
| **12** | 2912 | 54.0 | 1.86% | **42** | 2683 | 53.6 | 2.00% | **72** | 2708 | 50.8 | 1.88% |
| **13** | 2800 | 53.6 | 1.91% | **43** | 2845 | 58.3 | 2.05% | **73** | 2827 | 51.0 | 1.80% |
| **14** | 2785 | 54.1 | 1.94% | **44** | 2773 | 53.4 | 1.93% | **74** | 2844 | 56.1 | 1.97% |
| **15** | 2972 | 55.5 | 1.87% | **45** | 2713 | 55.5 | 2.05% | **75** | 2608 | 52.8 | 2.03% |
| **16** | 2815 | 53.5 | 1.90% | **46** | 2771 | 55.2 | 1.99% | **76** | 3042 | 56.7 | 1.86% |
| **17** | 2874 | 55.0 | 1.91% | **47** | 3006 | 56.4 | 1.88% | **77** | 3112 | 58.5 | 1.88% |
| **18** | 2904 | 54.5 | 1.88% | **48** | 3105 | 56.4 | 1.82% | **78** | 3061 | 55.8 | 1.82% |
| **19** | 2917 | 56.2 | 1.93% | **49** | 3047 | 56.4 | 1.85% | **79** | 2824 | 56.9 | 2.01% |
| **20** | 2753 | 54.1 | 1.97% | **50** | 3087 | 58.5 | 1.90% | **80** | 2988 | 52.8 | 1.77% |
| **21** | 2858 | 54.2 | 1.90% | **51** | 2942 | 49.6 | 1.69% | **81** | 2950 | 56.8 | 1.93% |
| **22** | 2824 | 53.7 | 1.90% | **52** | 3053 | 56.9 | 1.86% | **82** | 3014 | 56.6 | 1.88% |
| **23** | 2704 | 53.6 | 1.98% | **53** | 2950 | 56.5 | 1.92% | **83** | 3214 | 57.2 | 1.78% |
| **24** | 2833 | 54.3 | 1.92% | **54** | 3148 | 58.8 | 1.87% | **84** | 3069 | 59.4 | 1.94% |
| **25** | 2765 | 53.8 | 1.94% | **55** | 2813 | 54.7 | 1.94% | **85** | 3063 | 57.7 | 1.88% |
| **26** | 2810 | 55.7 | 1.98% | **56** | 2871 | 55.4 | 1.93% | **86** | 3133 | 58.5 | 1.87% |
| **27** | 2686 | 50.7 | 1.89% | **57** | 2964 | 55.8 | 1.88% | **87** | 2934 | 58.1 | 1.98% |
| **28** | 2706 | 53.2 | 1.96% | **58** | 3070 | 55.3 | 1.80% | **88** | 3048 | 54.7 | 1.79% |
| **29** | 2799 | 54.6 | 1.95% | **59** | 2785 | 55.0 | 1.98% | **89** | 2847 | 52.3 | 1.84% |
| **30** | 2883 | 54.7 | 1.90% | **60** | 2717 | 54.4 | 2.00% | | | | |

**Table 23 One day count rates and standard deviations of 5 GeV muons measured at 8 December 2007**

| № | $\sum_{n=1}^{1440}$ | $\sigma_i = 1/\sqrt{\sum}$ | № | $\sum_{n=1}^{1440}$ | $\sigma_i = 1/\sqrt{\sum}$ | № | $\sum_{n=1}^{1440}$ | $\sigma_i = 1/\sqrt{\sum}$ |
|---|---|---|---|---|---|---|---|---|
| **1** | 4196468 | 0.0488% | **31** | 4232101 | 0.0486% | **61** | 4324100 | 0.0481% |
| **2** | 4395304 | 0.0477% | **32** | 4139766 | 0.0491% | **62** | 4150894 | 0.0491% |
| **3** | 4359005 | 0.0479% | **33** | 4080938 | 0.0495% | **63** | 3869546 | 0.0508% |
| **4** | 4037325 | 0.0498% | **34** | 3958483 | 0.0503% | **64** | 4109263 | 0.0493% |
| **5** | 4315526 | 0.0481% | **35** | 4222960 | 0.0487% | **65** | 4219990 | 0.0487% |
| **6** | 4338958 | 0.0480% | **36** | 3893592 | 0.0507% | **66** | 3851007 | 0.0510% |
| **7** | 4258254 | 0.0485% | **37** | 4110259 | 0.0493% | **67** | 4390325 | 0.0477% |
| **8** | 4073309 | 0.0495% | **38** | 4081318 | 0.0495% | **68** | 4077850 | 0.0495% |
| **9** | 4169796 | 0.0490% | **39** | 4137306 | 0.0492% | **69** | 4303104 | 0.0482% |
| **10** | 4218662 | 0.0487% | **40** | 3986352 | 0.0501% | **70** | 4085042 | 0.0495% |
| **11** | 4240291 | 0.0486% | **41** | 3968941 | 0.0502% | **71** | 3933727 | 0.0504% |
| **12** | 4192812 | 0.0488% | **42** | 3863947 | 0.0509% | **72** | 3900099 | 0.0506% |
| **13** | 4032229 | 0.0498% | **43** | 4096364 | 0.0494% | **73** | 4071561 | 0.0496% |
| **14** | 4010753 | 0.0499% | **44** | 3992580 | 0.0500% | **74** | 4095402 | 0.0494% |
| **15** | 4279079 | 0.0483% | **45** | 3907415 | 0.0506% | **75** | 3754887 | 0.0516% |
| **16** | 4053002 | 0.0497% | **46** | 3989798 | 0.0501% | **76** | 4381165 | 0.0478% |
| **17** | 4138683 | 0.0492% | **47** | 4328704 | 0.0481% | **77** | 4481856 | 0.0472% |
| **18** | 4181801 | 0.0489% | **48** | 4471243 | 0.0473% | **78** | 4408270 | 0.0476% |
| **19** | 4199887 | 0.0488% | **49** | 4387797 | 0.0477% | **79** | 4066982 | 0.0496% |
| **20** | 3963823 | 0.0502% | **50** | 4445565 | 0.0474% | **80** | 4303104 | 0.0482% |
| **21** | 4115385 | 0.0493% | **51** | 4236352 | 0.0486% | **81** | 4248538 | 0.0485% |
| **22** | 4067173 | 0.0496% | **52** | 4396528 | 0.0477% | **82** | 4340346 | 0.0480% |
| **23** | 3894107 | 0.0507% | **53** | 4247376 | 0.0485% | **83** | 4628072 | 0.0465% |
| **24** | 4079820 | 0.0495% | **54** | 4533420 | 0.0470% | **84** | 4420002 | 0.0476% |
| **25** | 3980961 | 0.0501% | **55** | 4050083 | 0.0497% | **85** | 4411247 | 0.0476% |
| **26** | 4046710 | 0.0497% | **56** | 4134758 | 0.0492% | **86** | 4511576 | 0.0471% |
| **27** | 3868109 | 0.0508% | **57** | 4268051 | 0.0484% | **87** | 4225168 | 0.0486% |
| **28** | 3897071 | 0.0507% | **58** | 4420483 | 0.0476% | **88** | 4389114 | 0.0477% |
| **29** | 4031055 | 0.0498% | **59** | 4010297 | 0.0499% | **89** | 4099514 | 0.0494% |
| **30** | 4152082 | 0.0491% | **60** | 3912626 | 0.0506% | | | |

In Table 24 we present analogical characteristics for 29 plastic scintillators located on the top of ANI calorimeter.

Along with 1-minute data from ASEC monitors available from MSQL data base, the summary of daily plots can be observed from http://crdlx5.yerphi.am/ADVANCED_DAILY_IMAGES/. Same plots are also available from mirror site http://aragats.am

CRD continuously enlarge operating particle detectors number. In 2008 we plan to install several SEVAN modules in Yerevan and Burakan village. A new type multilayered detector is under testing in Yerevan headquarters. 10 one cm thick plastic scintillators interlayer by 1 cm thick lead will measure muon and hadron energy by detecting electromagnetic and hadron showers. New electronics and new type of micro computers will be used to make Data Acquisition from particle detectors faster and multi-functional.

New user-friendly interface to ASEC monitor data, named DVIN-4, is under final tuning and will highly improve physical analysis possibilities.

**Table 24 Averaged 1 minute and dayly count rates of surface low energy charged flux measured at 8 December 2007**

| № | Average | Standard deviation | Relative error [%] |
|---|---|---|---|
| **1** | 29279 | 180 | 0.62% |
| **2** | 28238 | 249 | 0.88% |
| **3** | 28721 | 261 | 0.91% |
| **4** | 29703 | 223 | 0.75% |
| **5** | 29283 | 181 | 0.62% |
| **6** | 28333 | 256 | 0.90% |
| **7** | 29948 | 247 | 0.82% |
| **8** | 28859 | 301 | 1.04% |
| **9** | 29119 | 244 | 0.84% |
| **10** | 29076 | 178 | 0.61% |
| **11** | 28789 | 282 | 0.98% |
| **12** | 28460 | 166 | 0.58% |
| **13** | 29077 | 178 | 0.61% |
| **14** | 29895 | 229 | 0.77% |
| **15** | 28972 | 250 | 0.86% |
| **16** | 28734 | 245 | 0.85% |
| **17** | 29056 | 240 | 0.83% |
| **18** | 27832 | 248 | 0.89% |
| **19** | 29461 | 230 | 0.78% |
| **20** | 29767 | 236 | 0.79% |
| **21** | 28782 | 229 | 0.80% |
| **22** | 27445 | 247 | 0.90% |
| **23** | 29092 | 238 | 0.82% |
| **24** | 29076 | 177 | 0.61% |
| **25** | 28207 | 281 | 0.99% |
| **26** | 29053 | 224 | 0.77% |
| **27** | 28370 | 257 | 0.91% |
| **28** | 28111 | 175 | 0.62% |
| **29** | 28491 | 248 | 0.87% |

| № | $\sum_{n=1}^{1440}$ | $\sigma_i = 1/\sqrt{\sum}$ |
|---|---|---|
| **1** | 42161758 | 0.0154% |
| **2** | 40662397 | 0.0157% |
| **3** | 41357704 | 0.0155% |
| **4** | 42772070 | 0.0153% |
| **5** | 42167188 | 0.0154% |
| **6** | 40799310 | 0.0157% |
| **7** | 43124876 | 0.0152% |
| **8** | 41557256 | 0.0155% |
| **9** | 41931409 | 0.0154% |
| **10** | 41870013 | 0.0155% |
| **11** | 41455964 | 0.0155% |
| **12** | 40982046 | 0.0156% |
| **13** | 41871011 | 0.0155% |
| **14** | 43049245 | 0.0152% |
| **15** | 41719295 | 0.0155% |
| **16** | 41377597 | 0.0155% |
| **17** | 41840189 | 0.0155% |
| **18** | 40078730 | 0.0158% |
| **19** | 42423917 | 0.0154% |
| **20** | 42864930 | 0.0153% |
| **21** | 41446634 | 0.0155% |
| **22** | 39520922 | 0.0159% |
| **23** | 41891844 | 0.0155% |
| **24** | 41868918 | 0.0155% |
| **25** | 40618066 | 0.0157% |
| **26** | 41835649 | 0.0155% |
| **27** | 40853231 | 0.0156% |
| **28** | 40480268 | 0.0157% |
| **29** | 41026404 | 0.0156% |

**References**


- Avakian V.V., Bazarov E.B., et. al., (1986), VANT, ser. Tech. Phys. Exp., 5(31), p.1.
- Beglaryan A.S., Bujukyan S.P., et al., (1989) Scientific Publication of YerPhI, 1197 (74).
- Chilingarian A., Hovsepyan G., Gharagyozyan G., et al.: (1999) The EAS Size Spectrum measured at ANI Cosmic Ray Observatory in the region of Knee, 26th International Cosmic Ray Conference, Salt Lake City, vol 1, p. 240-243.
- Chilingarian, A., Avakyan, K., Babayan, V., et al.: (2003) Aragats Space-Environmental Center: status and SEP forecasting possibilities, J. Phys. G: Nucl. Part. Phys., Vol. 29, p. 939-952.
- Chilingarian A., Gharagyozyan G., Hovsepyan G., et al.: (2004) Light and heavy cosmic-ray mass group energy spectra as measured by the MAKET-ANI detector, Astrophysical Journal, 603, p. L29–L32.
- Chilingarian A., Arakelyan K., Avakyan K., et al.: (2005) Correlated measurements of secondary cosmic ray fluxes by the Aragats Space – Environmental Center monitors, Nucl. Instr. and Meth. A 543, p. 483-496.
- Eghikyan A., Chilingarian A., (2005) Data Visualization Interactive Network for the Aragats Space – Environmental Center, 2rd International Symposium SEE-2005, Nor-Amberd, Armenia, p. 245-251. (http://crdlx5.yerphi.am/DVIN/)
- Chilingarian A., Hovsepyan G., et al, (2007)Study of Extensive Air Showers and Primary Energy Spectra by MAKET-ANI Detector on Mountain Aragats, Astroparticle Physics **28**, 58-71
- Chilingarian A., Hovsepyan G., et al, Research on Galactic Cosmic Rays from the "knee" to the "cutoff" ($10^{16}$ -$10^{19}$) eV at the Aragats Cosmic Ray Observatory; *Measurements of the ultra -high energy Cosmic Rays by hybrid particle detectors located on the Earth surface, report on JENAM-2007 conference.*
- A.Chilingarian et al, (2007) Study of Extensive Air Showers and Primary Energy Spectra by MAKET-ANI Detector on Mountain Aragats, Astroparticle Physics 28, p. 58-71.
- Dorman L.I., (1975) Variations of the Galactic Cosmic Rays, Publishing house of the Moscow State University.
- Danilova T.V., Danilova E. A., Erlikin A. B., et al.: (1992) The ANI experiment: on the investigation of interactions from hadrons and nuclei in the energy range 103–105 TeV, Nucl. Instr. and Meth. A 323, p. 104-107.
- Garyaka A.P., Martirosov R.M., Procureur J., et al.: (2002) The cosmic ray energy spectrum around the knee measured with the GAMMA array at Mt. Aragats, J. Phys. G: Nucl. Part. Phys. 28, p. 2317-2328.
- Moraal H., Belov A., Clem J.M.: (2000) Design and co-Ordination of Multi-Station International Neutron Monitor Networks, Space Science Reviews 93, p. 285-303.
- Tsuchiya et al. (2001), NIM, **A 463**, 183 – 193.

# 9. Attachment 5: DVIN: Data Visualisation Interactive Network for the Aragats Space-environmental Center

Networks of particle detectors are continuously monitoring changing fluxes of particles reaching earth surface. Charged and neutral particles are born in cascade processes initiated by protons and nuclei incident on the terrestrial atmosphere. Fast majority of these primaries are from numerous galactic sites traveling tens of millions years in Galaxy and arriving to solar system as rather stable and isotropic population. Balloon and satellite spectrometers enumerate the Galactic Cosmic Ray (GCR) fluxes with rather high accuracy. Our nearest star, the sun, by disturbing interplanetary magnetic field and by accelerating protons and ions (producing so called Solar Cosmic Rays – SCR) is modulating the GCR flux, and as a result – the particle fluxes measured by surface detectors. Among numerous sun modulation effects Ground Level Enhancements (GLE) is one of the most essentials, both from point of view of fundamental physics processes and Space Weather effects.

The universal processes of particle acceleration in the Universe can be studied although on the much smaller scale, but much more detailed by measuring fluxes of protons and ions from solar accelerators. The satellite spectrometers due to tiny sizes can measure only huge fluxes of low energy particles; surface detectors are much larger and they use atmosphere for the particle multiplication. Therefore, rather small highest energy fluxes of solar particles can be studied by measured secondary particle flux on earth surface.

The problem of revealing signal (SCR) against overwhelming background (GCR) is one of the most complicated in high energy astrophysics. We implement several data analysis procedures in DVIN to solve this problem. Measuring highest energy particles it will be possible to determine the spectra of the major solar event in progress. Hard spectra at highest energies will manifest abundant SCR flux at low and medium energies and consequently radiation hazard to crew of space stations, to space-born and surface industries. There is not much time for issuing warnings and alerts (15-45 minutes), therefore physical inference have to be made very fast. Physical analysis should invoke also data from space spectrometers and particle detectors from world-wide networks.

It is why DVIN is strategically important as a scientific application to help develop space science and to foster global collaboration in solar physics and in space weather research. The system is highly interactive and exceptional information is easily accessible online. Data can be monitored and analyzed for desired time spans in a fast and reliable manner by the remote users world-wide.

Data from particle detectors from space and earth surface is automatically downloaded and stored in DVIN for joint analysis with ASEC monitors.

DVIN provides wide possibilities for sharing data and sending warnings and alerts to scientists world-wide, which have fundamental and practical interest in knowing the space weather conditions.

DVIN gives opportunity to remote groups to share the process of analyzing, exchange data analysis methods, prepare joint publications and maintain networks of particle detectors. DVIN gives users the set of online methods enabling physical interface from the time series of changing secondary particle fluxes.

### 9.1 DVIN Structure

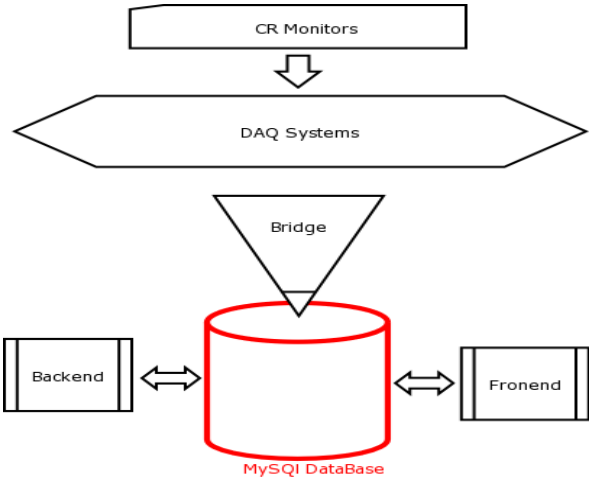


**Figure 1. DVIN structure**

The structure of the DVIN is presented in Figure 1.

DVIN is developed at the base of several software technologies:

- MySQL Database for data storage;
- PHP, DHTML as a front-end interface.

Backend is a set of software, which interconnects users with database. Software developed at the base of a number of programming languages like Python, Perl, C/C++.

Front-end software is developed at the base of PHP as a server side part and DHTML as a client side part. The splitting of Front-end to two parts allows optimization of Internet bandwidth to make the number of reloads of the site minimal.

Figure 2 presents a screenshot of the DVIN operation menu. In the “Operations” menu user performed and displayed following operations with different time-series obtained from particle detectors:

- Plot time series with rich styles;
- Make Distributions from time series;
- Calculate Correlation Matrix;
- Perform Periodic operations on time series;
- Add Time Series to analysis;
- SQL operations;
- Exchange of the Work Areas.

It is possible to display simultaneously up to 6 time series on one plot for the comparative purposes. The distributions of residuals of time series point on the peaks and check for the proper operation of the detector channels; periodic operations perform detailed analysis of the time series, revealing the peaks, estimating the statistical significance of peaks, inspecting the detector channels, etc… Add Time series is for importing data from database. SQL operation gives additional functionality for the experienced with SQL users and imports data from Internet. Work areas operation stores “work areas” - sets of processed time series for continuing analyses later and for sharing with collaborators of data and analysis methods.

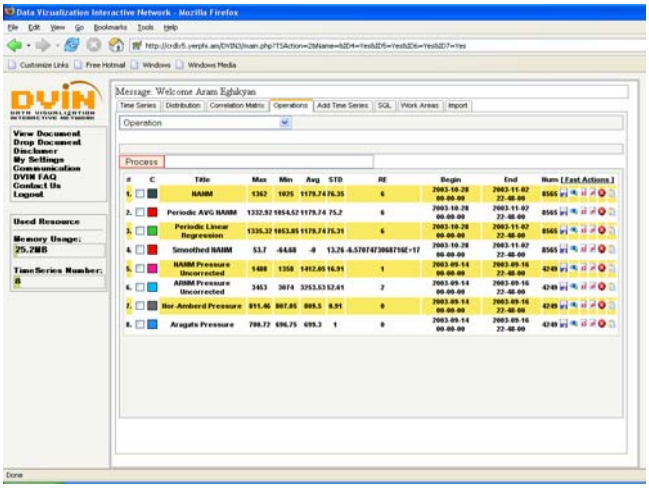

**Figure 2. Operations Menu**

In Figure 3 the toolbox of Operations menu is presented. Each string corresponds to definite time series initial, before or after performing desired operation.

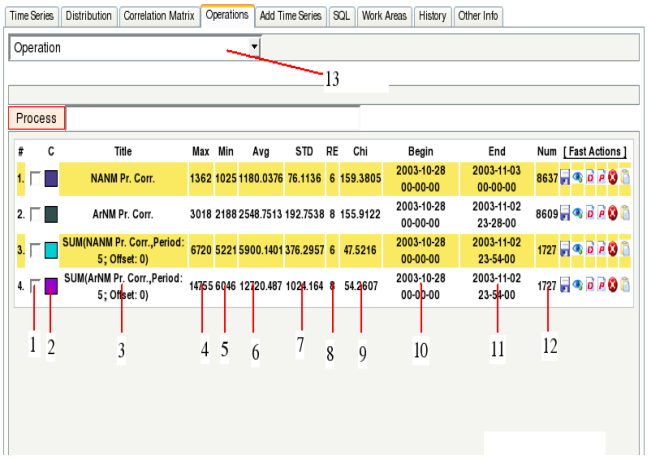


**Fig. 3 Toolbox of the "Operations" menu**

In the toolbox following options can be selected:

1. Check box for selecting Time Series
2. Color used for plots ( time series and diagrams)
3. Title of time Series
4. Maximum value of Time Series
5. Minimum value of Time Series
6. Average value of Time Series
7. Standard Deviation of Time Series
8. Relative Error of Time Series
9. Begin Time Stamp
10. End Time Stamp
11. Number of Elements in Time Series
12. Operations Drop Down menu

### 9.2 Fast Actions

Most important operations are displayed at the right of each Time Series string in the Drop Down menu, as shown in Figure 4.


**Fig. 4 "Fast Actions" panel**

Following operations menu are presented in Figure 4 from left to right:

1. Save Time Series to local system
2. View Time series (in ASCII format, for not too large time series)
3. Plot Distribution of Time Series
4. Plot Time Series
5. Delete time series
6. View Notes attached to this Time Series.

### 9.3 "Add Time Series" Section

"Add Time Series" section (Figure 5) is developed for easy data import from MySQL database into DVIN and contain following operations:

1. Select Time Range
2. Select preserved solar events
3. Select Monitor
4. Select Time Series of Monitor
5. History of selected Time Ranges

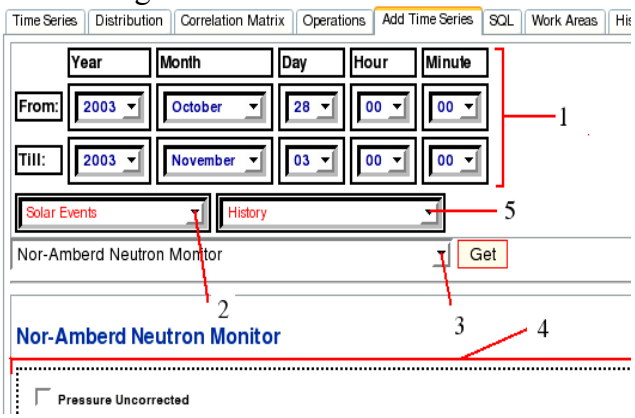


**Fig. 5. "Add Time Series" Section**

The "Check boxes" of Time Series give to users the ability to import any number of Time Series of selected monitor in one action. The Time Series of monitors are divided to subsections. For example Nor-Amberd Neutron Monitor data consisted of several groups: Pressure Corrected data, Pressure uncorrected and raw data (data from each detector separately).

### 9.4 "SQL" Section

"SQL" section's main purpose is to grant a direct access to MySQL database for importing data, see menu in Figure 6. It is more complicated than "Add Data" section, but gives to user flexible tool for importing data, enabling:

1. Easy SQL generation form
2. Advance SQL generation window
3. Name of imported Time Series

Users can make data processing during the import, for example, to import sum of several detectors, check the data for upper-down limits and replace ones with another set if necessary, or produce another filtering operation. To use this feature user must be familiar with SQL language.

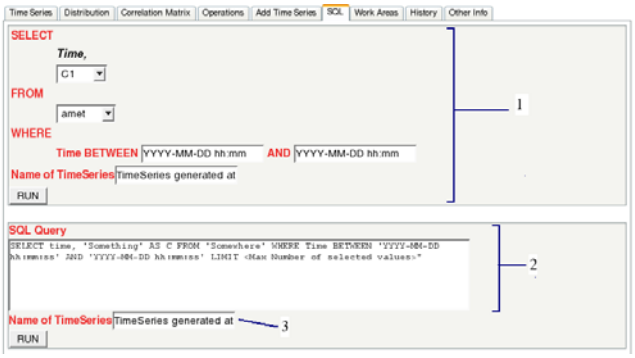


**Fig. 6. "SQL" Menu**

### 9.5 "Work Areas" Section

This section is implemented for managing user's work areas, see Figure 7. Three operations are available:

1. "Switch" is for switching current work area to the saved one. The old one will be lost if not saved
2. "Concatenate" produces the concatenation of two sets of Time Series from the current and saved.

"Remove" just removes the saved work area.

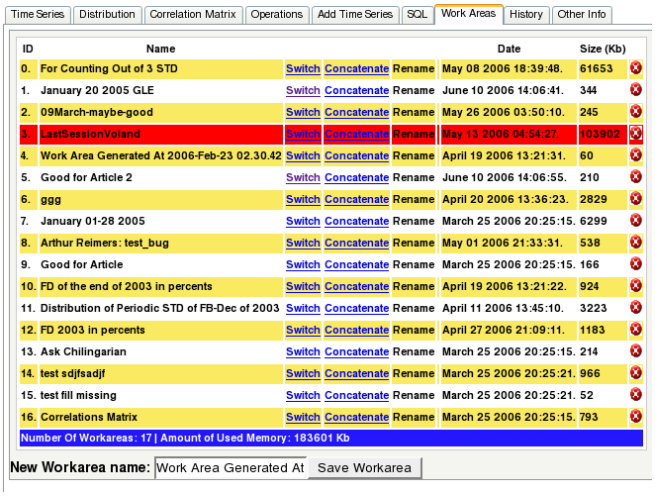


**Figure 7 "Work areas" menu**

### 9.6 Overview of the Main Operations

There are two main types of Operations so called moving and periodic operations.

The periodic and moving operations are calculated by 3 given values: the length of period, function type and offset. The difference between the moving and periodic operations is in defining of the next portion of time series. In periodic operations the next portions are selected with step given by the "Period" option and in the moving operations the step is always 1.

Periodic functions are as following:

- Average;
- Standard Deviation;
- Median;
- Linear Regression;
- Periodic rebinning (adding successive time series in larger time unit) of the initial time series

Periodic and moving operations provide very flexible and powerful tool for examining of time series. User controls the time period, offset of period (start point of rebinning operation) and interpolation mode (within chosen time period) of time series. Using these options user can rebin (add) successive monitor counts for examining long time periods and reveal non-trivial structures

in time series. For example, adding initial (parent) 1-minute time series in 3 minute by the "periodic sum operation" helps to discover the Ground Level Enhancement (GLE) detection on 20 January 2005 by the AMMM monitor, obscured by the large fluctuations of 1-minute time series. "Offset" option defines the particular grouping of initial time series. There is 3 possible ways to group 1 minute time series in 3 minute ones; each outlining slightly different structures. "Periodic Average Operation" and "Linear Regression Operation" are interpolating time series by the piecewise continuous functions (see Figure 8). All the periodic operations have "compatibility" option, leaving the number of elements in time series unchangeable. For example, if we interpolate 1 minute time series by hourly average, in each of 60 hourly minutes of transformed time series will be the same average value.

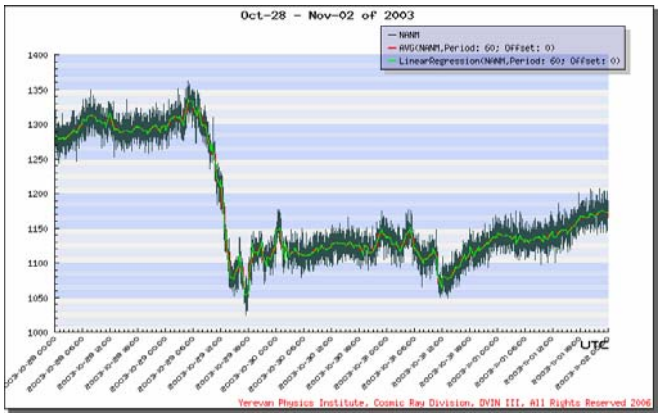


**Figure 8 Average (red) and Linear Regression (green) interpolation of the Nor Amberd neutron monitor time series.**

Then, by subtracting one time series from another user can obtain the residuals time series (see Figure 9). By dividing obtained residuals to the variance we obtain the, so called, normalized residuals obeying the standard Gaussian law (see Figure 11). By the time series of normalized residuals we can select the outliers for the further analysis. The histograms of the residuals (see Figure 11) can be compared with standard Gaussian probability density function by $\chi^2$ test. Large values of $\chi 2$ point on failures in detector channel operation. Therefore, the described operations modes of DVIN can be used for the check of detector channels.

After proving the "Gaussian" nature of the residuals positive outliers are examined as candidates for the Ground Level Enhancement (GLE) or "Geomagnetic storm" events. Large positive deviations (greater than $4\sigma$) pointed on the possible non-random character of the deviation from mean count rate, i.e. on the solar modulation effects.

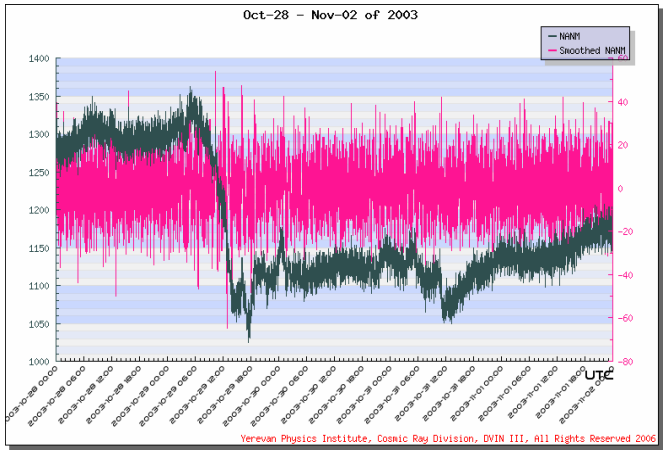


**Figure 9. The residuals time series (in red) of Nor Amberd NM time series (black).**

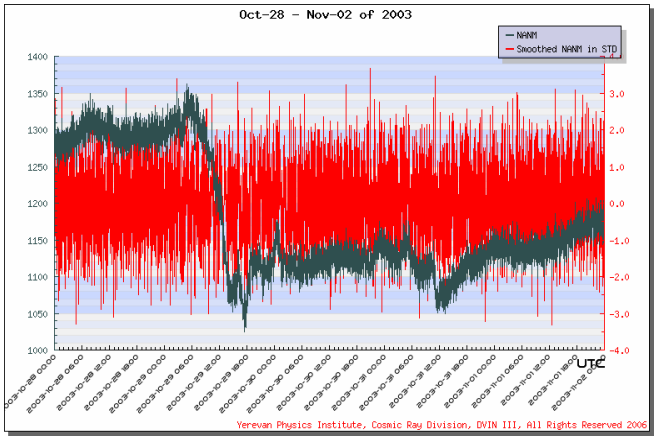


**Figure 10. Standard Deviation of residuals, of Nor-Amberd Neutron Monitor**

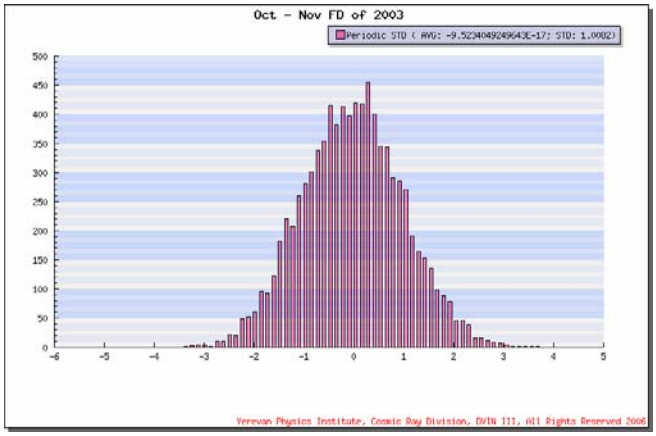


**Figure 11 Histogram of the normalized residuals of Nor-Amberd Neutron Monitor**

In the figure 12 are presented the same Forbush decrease (Fd) as in figure 8, but expressed in percents. To calculate the decrease in percents we get the average count rate at the not disturbed period at Oct 28 and using this value as a 100 percent recalculating the values into percents.

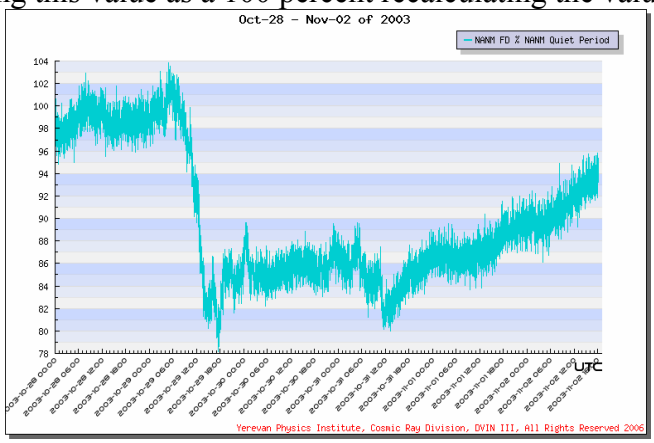


**Figure 12 Nor-Amberd Neutron Monitor, FD of Oct-Nov of 2003. FD: 22 Percent in comparison**

The transformation of the time series into percents of observed period relatively to the "quiet" period is widely used for getting quantitative description of the "deepness" of Forbush decrease.

Transformation of the Time Series into percents relatively to the other time series are made by following steps

1. Selection examined time periods;
2. Selection of reference time period;
3. Using the "%" operation in "Binary Mode" .

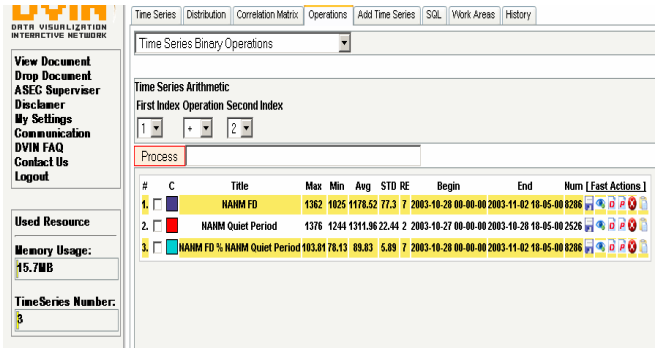


**Fig 13 The "Operations menu.**

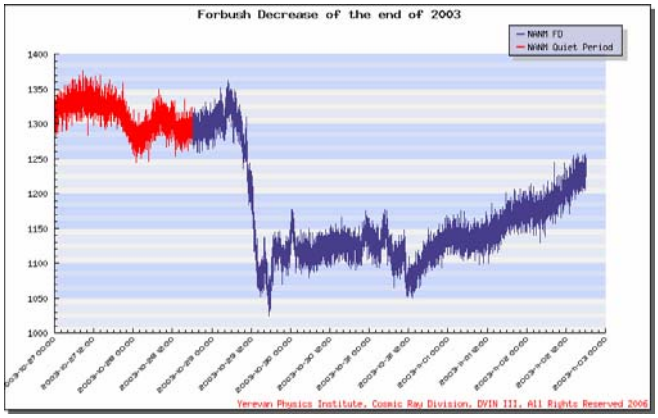


**Fig. 14 Red part is the normal period, Blue part is observed period. The transformation to percents are produced relatively the "Red" one.**

In the figure 14 are presented the non disturbed (in red) and Forbush Decrease (in blue) periods of October-November of 2003 which was translated to percents.

### 9.7 Analyzes of the candidate of GLE with AMMM detector

Variety of the ASEC monitors is "selecting" different populations of the primary energy spectra, because of different energy thresholds. Among ASEC monitors the Aragats Multidirectional Muon Monitor (AMMM) selects highest primary energies, because detector is located in the underground hall and 14 m. of soil and concrete filter low energy muons and electrons. Only muons with energy greater than 5 GeV can reach detector location. The energy of "parent" proton should be greater than 15 GeV to give birth to 5 GeV muon. These energies are extremely rare in SCR and if encounter lasting several minutes only. Therefore, in AMMM time series we are looking to very narrow peaks in coincidence with solar flares and GLEs detected by surface particle detectors sensitive to lower primary energies.

The 1- minute time series of the AMMM are presented in Figure 15. Enhancement of the count rate is seen at 10:12 10:14 UT. Unfortunately 14 from 45 channels of the AMMM detector were not operational at the time, therefore only 31 $m^2$ of muon detectors were in use to measure the high energy muon flux. The estimated mean count rate of the Galactic Cosmic Rays (GCR) as measured by the 31 $m^2$ of the AMMM detector during the 10:40 – 11:40 UT time span, excluding the enhanced interval from 10:12 to 11:14 UT, is 92040 particles per minute.

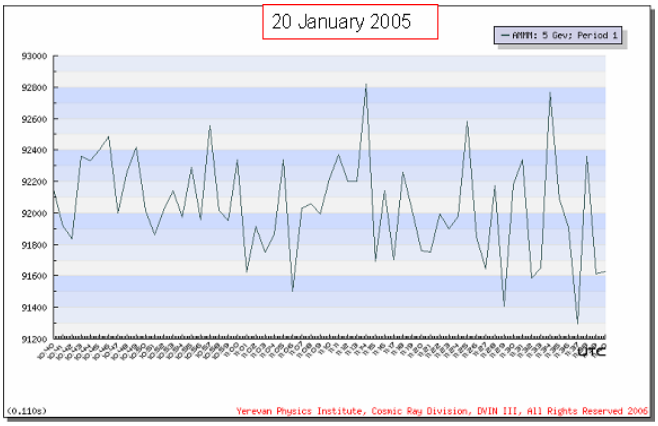


**Fig. 15 . Minutely data of AMMM.**

In the Table 1 are depicted the statistical parameters of one minute time series. To check significance of the GLE candidate we calculate the significance according to the Poisson distribution and standard Relative Mean Square Deviation (RMSD):

$$RMSD = \sqrt{\left(\frac{\sum_{i=1}^{i=N}(C_i - \bar{C})^2}{N-1}\right)} / \bar{C},$$

Where normalized residuals $X_i = \frac{C_i - \bar{C}}{S}$, $i = 1,60$, $C_{i,}$ are 1 minute count rates of the AMMM, $\bar{C}$ is hourly mean of the 1-minute time series and $\sqrt{\bar{C}}$ - is the hourly Poisson deviation of the count rates.

**Table 1 Characteristics of the AMMM detection of GLE candidate**

| | Max | Min | $\bar{C}$ | STD | RMSD | S |
|---|---|---|---|---|---|---|
| 1 min counts | 92821 | 91296 | 92040 | 315.45 | 0.34 | 0.33 |

Maximal value at 10:14 – 92821, enhancement (possible signal) is Δ =Max-Min =781. The relative enhancement $\Delta_r = \Delta / \bar{C} = 0.85\%$, correspondent to significance of $\Delta_r / \mathrm{RMSD} = 2.5\sigma$.

To emphasize the peak in the AMMM time series we group the 1 minute time series in the 3 minute time-intervals. In Figure 16 three different possibilities of regrouping of 1 minute time series in 3 are presented. All 3 demonstrates slightly different temporal pattern of time series. The particular time series started from the second element (10:41) provide biggest peak. In Figure 14 The 3-minute time series emphasized the peak, offset 2 provides maximal . However, the size of peak is not large enough to claim that AMMM detect the SCR and not only GCR fluctuation.

In the next steps of processing used offset 2 as a Time Series with a maximum Peak.

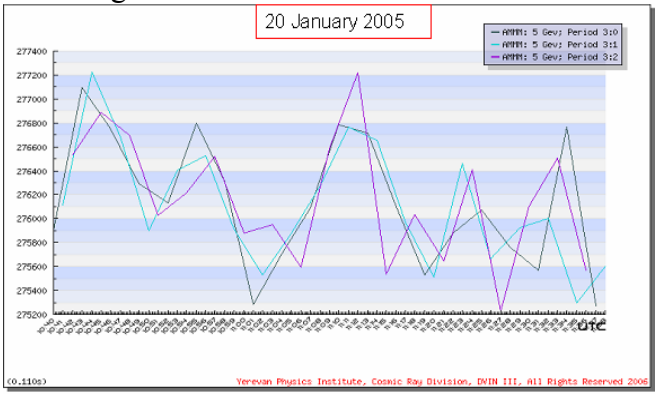


**Fig. 16. 3 Minutely data with all the offsets.**

For farther calculation we remove the Peak. To remove the peak we used “Up-Down Limit Cut” which replaces the points which are do not located in the given range with Periodic Median. At the Fig. 17 Presented two Time Series with and without Peak.

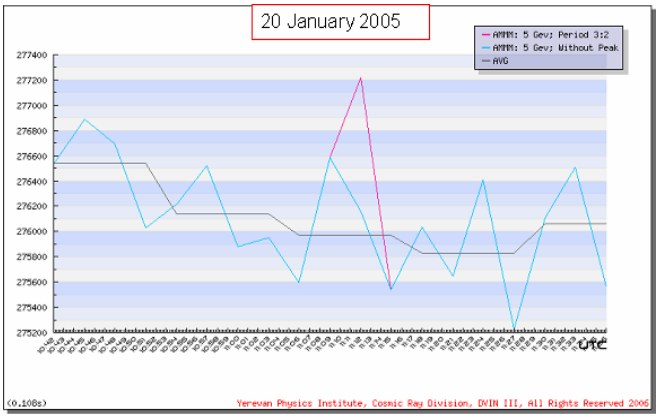


**Figure 17. AMMM: 5 Gev; Period 4:3 with and without peak and periodic AVG of the Time Series without Peak**

**At the following table presented statistical parameters of the time series with peak and without peak.**

| Name | Max | Min | Avg | STD | R.E.(100*STD/AVG) |
|---|---|---|---|---|---|
| AMMM: 5 Gev; Period 3:2 | 277219 | 275225 | 276165 | 497 | 0.178 |
| AMMM: 5 Gev; Period 3:2 without peak | 276892 | 275225 | 276109 | 434 | 0.159 |

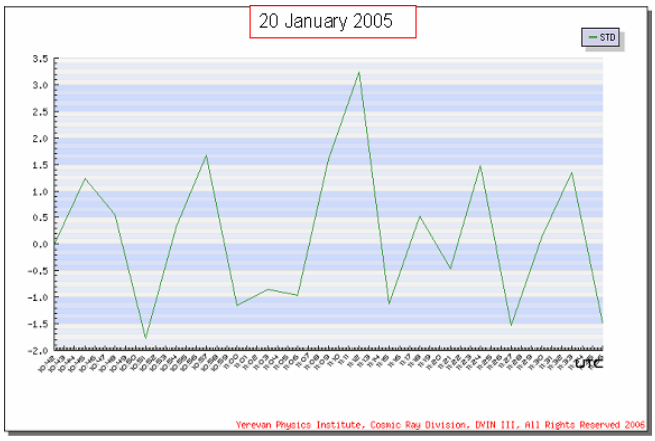


**Figure 18 Normalized residuals of AMMM 3 minute counts**

From the Picture 18 we can see that significance of the peak did not exceed 3.3; such enhancements we can detect several times during the day.

Therefore we can not reject the hypothesis that detected peak is background fluctuation only.

### 9.8 Correlation Analysis

Correlation Analysis is a new tool for the physical inference on multiple time series. Different ASEC monitors are sensitive to different populations of the primary protons and ions. If Neutron Monitors are detecting neutrons generated by primary protons with energies just after cuttof rigidity, the 5 GeV muons are generated by >15 GeV protons. Also different channels of the Solar Neutron Telescope (SNT) are selected slightly different energy populations of primaries. Therefore, measuring correlations between changing count rates of ASEC monitors we can get information about energy spectra of the solar cosmic rays (SCR), or about the nature of geomagnetic disturbance changing the actual value of the cutoff rigidity.

Time Series | Distribution | Correlation Matrix | Operations | Add Time Series | SQL | Wo

| | 1 | 2 | 3 | 4 | 5 |
|---|---|---|---|---|---|
| 1 NANM | 100 | 98 | 97 | 96 | 97 |
| 2 ArNM | 98 | 100 | 96 | 95 | 96 |
| 3 SNT: Threshold 120 Mev | 97 | 96 | 100 | 96 | 99 |
| 4 SNT: Threshold 290 Mev | 96 | 95 | 96 | 100 | 96 |
| 5 SNT: Charged particle monitor 5cm scintillators | 97 | 96 | 99 | 96 | 100 |

**Figure 19 Correlation matrix of 2003-10-29 in percents**

Time Series | Distribution | Correlation Matrix | Operations | Add Time Series | SC

| | 1 | 2 | 3 | 4 | 5 |
|---|---|---|---|---|---|
| 1 SNT: Threshold 120 Mev | 100 | 31 | 29 | 13 | 16 |
| 2 SNT: Threshold 290 Mev | 31 | 100 | 8 | 0 | 7 |
| 3 SNT: Charges Particles 5 cm Scintillators | 29 | 8 | 100 | 17 | 19 |
| 4 NANM | 13 | 0 | 17 | 100 | 13 |
| 5 ArNM | 16 | 7 | 19 | 13 | 100 |

**Figure 20 Correlation matrix of 2006-04-08 in percents**

In the Figure 19 and Figure 20 are depicted the correlation matrixes of two periods, 2003-10-29 which corresponds to the enormous Forbush decrease (correlations are very large, approaching ~1). At 2004-03-05 which corresponds to the calm phase of the Space Weather (no geomagnetic disturbances) there are no significant correlations detected.

### 9.9 Work Areas issue

Work Areas in DVIN defined as a set of Time Series which can are related to solar modulation effect and should be treated mutually. Saving work area gives users a very convenient feature for localizing the work, splitting the data analysis to several succeeding stages in time. Work areas allows producing temporary or so called middle stage time series. During work with data from Aragts monitors the number of different time series can rapidly grew and make the work with the DVIN very complicated. Therefore, we provide to user possibility to split the work (in programming this method called “Functional Programming” or “Procedural Programming”) to several sub stages and concentrate attention at small number of time series at a time.

### 9.10 Data Exchange between Users

Users of DVIN can interchange processed data and establish virtual collaboration. They interchange work areas using communication section. When user gets data from another user he can continue analyzing in the received work area or concatenate own work area with new one. In the figure 21 we illustrate this process by the “Communication” section of the DVIN.

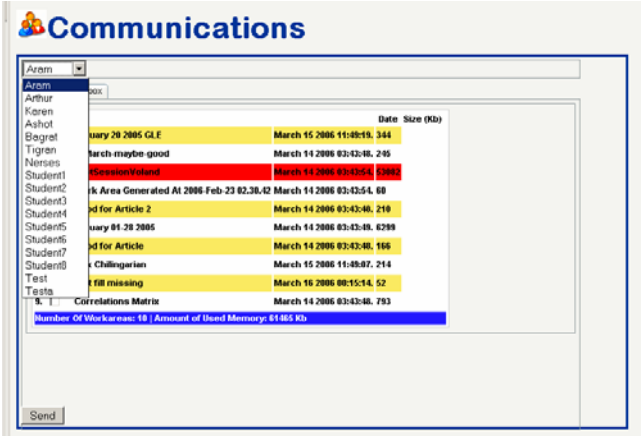


**Fig. 21 Communication Areas Subsection**

1. Drop down menu of Recipients ( DVIN Users )
2. Work Areas ready for delivery.

**Reference**

1. MySQL Reference Manual (URL:http://dev.mysql.com/doc/ )
2. PHP Manual (URL: http://www.php.net/docs.php )
3. MathWorld (URL: http://mathworld.wolfram.com/ )

## 10. Attachment 6: Official documents on creating of SEVAN network

INTERNATIONAL HELIOPHYSICAL YEAR
Secretariat American Geophysical Union

2000 Florida, Ave, NW Washington, DC 2009 USA

This is to confirm that Space Investigation Center, University of Costa Rica (CINESPA), will participate in the Instrument Development Program known as the United Nations Basic Space Sciences (UNBSS) for the International Heliophysical Year 2007 (IHY). The Cosmic Ray Division (CRD) of Yerevan Physics Institute will design and develop the basic hybrid SEVAN particle detector module and is responsible for all electronics and advanced data acquisition system (ADAS). CRD will fabricate and test SEVAN prototype module and provide free scintillator slabs and photomultipliers FEU-49 to be installed at the Irazu Solar Astrophysics Observatory (OASIZ) high altitude station. CRD performs detector response function calculation for the OASIZ location latitude and altitude.

The CINESPA is responsible for preparing steel frame of the detector, lead filter and scintillator housings, as well for providing scintillator slabs transportation from Armenia. Two groups of CRD experts will visit CINESPA observatory to mount the detector hardware, electronics and advanced data acquisition system. CINESPA provides travel expenses and leaving expenses for CRD experts inside Costa Rica. CINESPA is also responsible for preparing the detector site at Observatorio de Astrofísica Solar Irazú, Irazu research station, and providing uninterruptible Internet connection and electricity supply for the SEVAN detector.

The detector will be complete in 2008. After the installation of the SEVAN detector in CINESPA, CRD will provide software for data analysis and physical inference, developed for the SEVAN particle detectors network. CRD will host the staff from CINESPA with a short-term scholarship to familiarize them with the main facility of the SEVAN cosmic rays particle detectors network in Armenia; CRD will also support participation of Costa Rica in IHY and UNBSS events related to the cosmic rays field.

CRD will also organize yearly workshops for the network member countries to coordinate the network operation, discuss actual problems of solar physics and Space Weather and prepare joint scientific papers and conference publications.

CRD and CINESPA , as well as the IHY community, will have free access to all scientific data obtained by the new world wide SEVAN network of particle detectors.

Jorge Páez (CINESPA) Ashot Chilingarian (CRD) Nat Gopalaswamy (IHY)

UNIVERSIDAD DE COSTA RICA
CENTRO DE INVESTIGACIONES ESPACIALES
CINESPA

ՀԱՅԱՍՏԱՆԻ ՀԱՆՐԱՊԵՏՈՒԹՅՈՒՆ ԱՌԵՎՏՐԻ ԵՎ ՏՆՏԵՍԱԿԱՆ ԶԱՐԳԱՑՄԱՆ ՆԱԽԱՐԱՐՈՒԹՅՈՒՆ
Ա.Ի. ԱԼԻԽԱՆՅԱՆԻ անվան ԵՐԵՎԱՆԻ ՖԻԶԻԿԱՅԻ ԻՆՍՏԻՏՈՒՏ
ՊԵՏԱԿԱՆ ՈՉ ԱՌԵՎՏՐԱՅԻՆ ԿԱԶՄԱԿԵՐՊՈՒԹՅՈՒՆ

REPUBLIC OF ARMENIA
MINISTRY OF TRADE AND ECONOMICAL DEVELOPMENT
YEREVAN PHYSICS INSTITUTE After A.I. ALIKHANIAN
STATE NON COMMERCIAL ORGANIZATION

«12» 09 2007 № 01-14/256

№ _____

**Memorandum of Understanding**

This is to confirm that Institute for Nuclear Research and Nuclear Energy, Bulgarian Academy of Science (INRNE) will participate in the Instrument Development Program known as the United Nations Basic Space Sciences (UNBSS) for the International Heliophysical year (IHY).
The Cosmic Ray Division (CRD) of Yerevan Physics Institute will design and develop the basic hybrid SEVAN particle detector module and is responsible for all electronics and advanced data acquisition system (ADAS). CRD will fabricate and test SEVAN prototype module and provide free scintillator slabs and photomultipliers FEU-49 to be installed at the Musala high altitude research station of INRNE. CRD performs detector response function calculation for the Musala location latitude and altitude.

The INRNE is responsible for preparing steel frame of the detector, lead filter and scintillator housings, as well as provide scintillator slabs transportation from Armenia. Two groups of CRD experts will visit INRNE observatory for the mounting of the detector hardware, electronics and advanced data acquisition system. INRNE provides travel expenses and leaving expanses for CRD experts inside Bulgaria. INRNE also is responsible for preparing detector site at Musala research station, uninterruptible Internet connection and electricity supply for SEVAN detector.

CRD will prepare project to be submitted to funding agency for covering expanses of electronics and advanced data acquisition system as well as for transportation from Armenia to Bulgaria. The detector shall be complete by September 30, 2008. After installation of the SEVAN detector in INRNE, CRD will provide software for the data analysis and physical inference, specially developed for the SEVAN particle detectors network. Also CRD will organize yearly workshops for the network member countries for the coordination of the network operation, discussion of actual problems of the solar physics and Space Weather and for preparing joint scientific papers and conference publications.

CRD and INR as well as IHY community will have free access to all scientific data obtained by the new world wide SEVAN network of particle detectors.

Ashot Akhperjanyan (YerPhI) Ashot Chillingarian (CRD, YerPhI) Jordan Stamenov (INRNE)

**International Heliophysical Year**
Secretariat
Code 671
NASA GSFC
Greenbelt, MD 20771
USA

Ihy2007.org

**Memorandum of Understanding**

This is to confirm that Institute for Nuclear Research and Nuclear Energy, Bulgarian Academy of Science (INRNE) will participate in the Instrument Development Program known as the United Nations Basic Space Sciences (UNBSS) for the International Heliophysical year (IHY). The Cosmic Ray Division (CRD) of Yerevan Physics Institute will design and develop the basic hybrid SEVAN particle detector module and is responsible for all electronics and advanced data acquisition system (ADAS). CRD will fabricate and test SEVAN prototype module and provide free scintillator slabs and photomultipliers FEU-49 to be installed at the Musala high altitude research station of INRNE. CRD performs detector response function calculation for the Musala location latitude and altitude.

The INRNE is responsible for preparing steel frame of the detector, lead filter and scintillator housings, as well as provide scintillator slabs transportation from Armenia. Two groups of CRD experts will visit INRNE observatory for the mounting of the detector hardware, electronics and advanced data acquisition system. INRNE provides travel expenses and leaving expanses for CRD experts inside Bulgaria. INRNE also is responsible for preparing detector site at Musala research station, uninterruptible Internet connection and electricity supply for SEVAN detector.

CRD will prepare project to be submitted to funding agency for covering expanses of electronics and advanced data acquisition system as well as for transportation from Armenia to Bulgaria. The detector shall be complete by September 30, 2008. After installation of the SEVAN detector in INRNE, CRD will provide software for the data analysis and physical inference, specially developed for the SEVAN particle detectors network. Also CRD will organize yearly workshops for the network member countries for the coordination of the network operation, discussion of actual problems of the solar physics and Space Weather and for preparing joint scientific papers and conference publications.

CRD and INR as well as IHY community will have free access to all scientific data obtained by the new world wide SEVAN network of particle detectors.

Ashot Chillingarian (CRD) Jordan Stamenov (INRNE) Nat Gopalaswamy (IHY)

ՀԱՅԱՍՏԱՆԻ ՀԱՆՐԱՊԵՏՈՒԹՅՈՒՆ
ԱՌԵՎՏՐԻ ԵՎ
ՏՆՏԵՍԱԿԱՆ ԶԱՐԳԱՑՄԱՆ ՆԱԽԱՐԱՐՈՒԹՅՈՒՆ

Ա.Ի. ԱԼԻԽԱՆՅԱՆԻ ԱՆՎԱՆ
ԵՐԵՎԱՆԻ ՖԻԶԻԿԱՅԻ ԻՆՍՏԻՏՈՒՏ

ՊԵՏԱԿԱՆ ՈՉ ԱՌԵՎՏՐԱՅԻՆ
ԿԱԶՄԱԿԵՐՊՈՒԹՅՈՒՆ

REPUBLIC OF ARMENIA
MINISTRY OF TRADE AND ECONOMIC
DEVELOPMENT

YEREVAN PHYSICS INSTITUTE
After A.I ALIKHANIAN

STATE NON COMMERCIAL
ORGANIZATION

«28» 07 2007 №01-14/176

№

Astronomical Observatory
Astronomical Association of Zagreb
Opaticka 22, pp 943
Zagreb
10001 Zagreb
Croatia

28 June, 2007

**CERTIFICATE OF DONATION**

This is to certify that the following scientific equipment(s)

- 14 Plastic scintillator blocks of size 0.5 * 0.5 * 0.05 $m^3$ each with total value of 9,100$;
- 3 photomultipliers FEU-49 with total value of 550$;
- data acquisition electronics, 3 programmable Voltage power supplies, 8 – channel programmmable microcontroller board, cables, connectors, with total value of 1000 $.

**GRAND TOTAL VALUE (for customs purpose only) of 10,650 USD** is an outright donation, for scientific and educational purposes only, from Cosmic Ray Division (CRD), **Alikhanyan Physics Institute,** to

**Astronomical Observatory**
**Astronomical Association of Zagreb**
**Zagreb, Croatia**

The equipments will be used for scientific research and educational programs and it is not intended for sale or resale, nor for private use of any individual.

Ashot Akhperjanian
Deputy Director

375036 երևան, Ալիխանյան եղբայրների 2
Հեռ. 37410 341 500, ֆաքս. 398 392

2 Br. Alikhanyan str. Yerevan 375036
Tel (37410) 341 500 Fax (37410) 398 392